





# Journal of Experimental Biology and Agricultural Sciences

<http://www.jebas.org>

ISSN No. 2320 – 8694

## Unleashing the future: Exploring the transformative prospects of artificial intelligence in veterinary science

Khan Sharun<sup>1,2\*</sup> , S. Amitha Banu<sup>1</sup> , Merlin Mamachan<sup>1</sup> , Laith Abualigah<sup>3,4,5,6,7</sup> ,  
A. M. Pawde<sup>1</sup> , Kuldeep Dhama<sup>8\*</sup> 

<sup>1</sup>Division of Surgery, ICAR-Indian Veterinary Research Institute, Izatnagar, Bareilly, Uttar Pradesh, India

<sup>2</sup>Graduate Institute of Medicine, Yuan Ze University, Taoyuan 32003, Taiwan

<sup>3</sup>Computer Science Department, Al al-Bayt University, Mafraq 25113, Jordan.

<sup>4</sup>MEU Research Unit, Middle East University, Amman 11831, Jordan.

<sup>5</sup>Applied Science Research Center, Applied Science Private University, Amman 11931, Jordan.

<sup>6</sup>Jadara Research Center, Jadara University, Irbid 21110, Jordan

<sup>7</sup>Artificial Intelligence and Sensing Technologies (AIST) Research Center, University of Tabuk, Tabuk 71491, Saudi Arabia.

<sup>8</sup>Division of Pathology, ICAR-Indian Veterinary Research Institute, Izatnagar, Bareilly, Uttar Pradesh, India

Received – May 30, 2024; Revision – June 14, 2024; Accepted – June 27, 2024

Available Online – July 15, 2024

DOI: [http://dx.doi.org/10.18006/2024.12\(3\).297.317](http://dx.doi.org/10.18006/2024.12(3).297.317)

### KEYWORDS

Machine learning

Deep learning

Veterinary medicine

Telemedicine

Diagnostic radiology

Predictive medicine

### ABSTRACT

Artificial intelligence (AI) has emerged as a transformative paradigm, promising revolutionary advancements in animal healthcare. Leveraging AI's unparalleled capacity for rapid data analysis significantly enhances diagnostic precision and speed, thereby facilitating informed decision-making by veterinarians. Predictive medicine powered by AI not only anticipates disease outbreaks but also enables tracking zoonotic diseases and predicting individual health risks for animals. AI helps to generate personalized treatment plans by analyzing genetic, environmental, and historical data. Remote monitoring and telemedicine, empowered by AI, overcome geographical constraints and offer continuous care, enabling veterinarians to track vital signs and intervene promptly. However, as AI becomes integral to veterinary practice, ethical considerations surrounding data privacy, transparency, and responsible AI use are crucial. This review explores the scope of AI in enhancing research and drug development, highlighting its ability to improve the discovery process and contribute to novel therapeutic interventions. It emphasizes the necessity of maintaining a delicate balance between AI-driven automation and the expertise of veterinary professionals. As the veterinary community moves toward embracing

\* Corresponding author

E-mail: [sharunkhansk@gmail.com](mailto:sharunkhansk@gmail.com) (Khan Sharun);  
[kdhama@rediffmail.com](mailto:kdhama@rediffmail.com) (Kuldeep Dhama)

Peer review under responsibility of Journal of Experimental Biology and Agricultural Sciences.

Production and Hosting by Horizon Publisher India [HPI]  
(<http://www.horizonpublisherindia.in/>).  
All rights reserved.

All the articles published by [Journal of Experimental Biology and Agricultural Sciences](#) are licensed under a [Creative Commons Attribution-NonCommercial 4.0 International License](#) Based on a work at [www.jebas.org](http://www.jebas.org).



the transformative potential of AI, this comprehensive examination provides valuable insights into the current scenario. It discusses the challenges, opportunities, implications, and ethical considerations that shape the future of AI in veterinary science.

## 1 Introduction

The field of veterinary science has traditionally relied on empirical observations, clinical expertise, and diagnostic tests to diagnose and treat animal diseases (Perera et al. 2022). While these methods have served veterinarians well for centuries, the rapid progression of technology over the years has opened up new possibilities for enhancing veterinary care (Ogilvie and Kastelic 2022). One such technological advancement is artificial intelligence (AI), which utilizes various computational techniques enabling machines to replicate human cognitive functions such as decision-making and problem-solving (Sarker 2022). AI has already improved various sectors, including healthcare, entertainment, finance, and transportation (Davenport and Kalakota 2019).

In veterinary science, AI holds immense scope to revolutionize treatment and diagnostics modalities and overall patient care (Appleby and Basran 2022). With the world becoming progressively interconnected and reliant on data-driven processes, integrating AI technologies promises to unlock new insights, enhance efficiency, and improve outcomes in veterinary practice (Appleby and Basran 2022; Akinsulie et al. 2024). The application of AI in veterinary medicine includes a wide range of areas, including genetic analysis, treatment planning, drug discovery, and personalized medicine (Akinsulie et al. 2024). Machine learning (ML) algorithms, deep learning (DL) networks, natural language processing (NLP), and computer vision techniques are among the many AI tools that are being leveraged to analyze vast amounts of veterinary data, extract meaningful patterns, and generate actionable insights (Sarker 2021a, 2021b; Sharma et al. 2021).

While the potential benefits of integrating AI into veterinary medicine are considerable, numerous issues must be addressed to harness its full potential effectively (Akinsulie et al. 2024; Bellamy 2023). Data availability and quality stand out as primary challenges. While vast amounts of data are generated in veterinary practice, including patient records, diagnostic test results, and imaging studies, much remains fragmented, unstructured, or stored in incompatible formats (Cravero et al. 2022; Paynter et al. 2021). Additionally, variations in data quality and completeness can hinder the development and performance of AI algorithms, as they rely heavily on high-quality, standardized data for training and validation (Aldoseri et al. 2023). The cost of implementing AI technologies poses another significant barrier (Javaid et al. 2023; Neethirajan 2023). Developing and deploying AI-powered solutions in veterinary

practice requires substantial financial investment in hardware, software, training, and infrastructure, which may limit its access at the field level (Javaid et al. 2023).

Ethical considerations also loom large in integrating AI into veterinary medicine (Mennella et al. 2024). Data security, patient privacy, and informed consent concerns must be addressed to ensure that AI-driven systems adhere to ethical principles and respect the rights and welfare of animal patients and their owners (Gerke et al. 2020). Additionally, issues surrounding algorithmic bias, fairness, and accountability demand attention to prevent unintended consequences and ensure equitable access to veterinary care. Regulatory oversight is another critical aspect of AI integration in veterinary practice. Regulatory agencies must develop precise guidelines for validating and establishing AI technologies in veterinary medicine (Bellamy 2023; Mennella et al. 2024). These regulations should address data safety, privacy, and transparency to protect animal patients, their owners, and veterinary professionals (Mennella et al. 2024). Moreover, effective collaboration between veterinarians, data scientists, and technology developers is essential to overcome these challenges and tailor AI solutions to veterinary practice's unique needs and challenges (Bellamy 2023; Mennella et al. 2024). By fostering interdisciplinary partnerships and knowledge exchange, stakeholders can leverage their expertise to develop AI-driven tools and applications that address specific clinical needs and improve the overall quality of veterinary care (Yelne et al. 2023).

The rapid advancement of AI has permeated diverse sectors, and its transformative impact is increasingly evident in veterinary science (Appleby and Basran 2022). The integration of AI promises to revolutionize the field, offering innovative solutions, efficient diagnostics, and personalized treatments (Akinsulie et al. 2024; Appleby and Basran 2022). This paper explores the transformative prospects of AI in veterinary science, highlighting recent advancements and future directions in the field. By synthesizing the latest research findings and industry developments, this paper highlights the current scenario of AI-driven veterinary medicine and envisions the future trajectory of this rapidly evolving field.

## 2 Artificial intelligence, machine learning, and deep learning

AI represents a shift in computing where machines are endowed with capabilities traditionally associated with human intelligence (Xu et al. 2021). It involves various techniques and technologies to enable computers to perform tasks that usually require human intelligence (making decisions, identifying data patterns, and

experience-based learning (Najjar 2023; Xu et al. 2021). AI systems are classified into two main categories: Narrow AI, which performs specific tasks, and General AI, which exhibits human-like intelligence in different domains (Elahi et al. 2023). While General AI remains a theoretical concept, Narrow AI has widespread adoption in various applications, including virtual assistants, recommendation systems, and image recognition algorithms (Xu et al. 2021).

ML represents a subset of AI dedicated to crafting algorithms and statistical models. These models empower computers to obtain insights from data, making decisions autonomously without the need for programming (Sarker 2021b). ML algorithms learn from example data, known as training data, and iteratively improve performance through experience (Taye 2023). ML has found applications in diverse fields, including healthcare, finance, e-commerce, and autonomous vehicles (Jiang et al. 2020a).

DL concentrates on neural networks comprising numerous layers, known as deep neural networks (Najjar 2023). These DL algorithms can autonomously acquire hierarchical data representations from raw inputs, obviating the necessity for manual feature engineering (Taye 2023). CNNs, RNNs, and GANs are some of the most widely used architectures in DL (Alzubaidi et al. 2021). DL has attained notable success in various tasks, particularly in image recognition, NLP, speech recognition, and autonomous driving, surpassing human performance in certain domains (Alzubaidi et al. 2021; Sharma et al. 2021).

### 3 Diagnostics and disease prediction

AI-driven diagnostic tools represent a revolutionary advancement in veterinary science, leveraging the ability to process vast datasets encompassing diverse information such as medical records, diagnostic imaging, and genetic profiles (Akinsulie et al. 2024; Bellamy 2023). The integration of AI in diagnostics has noteworthy advantages beyond accelerating the diagnostic process (Bouhali et al. 2022; Hespel et al. 2022). AI algorithms excel in swiftly analyzing intricate datasets, providing veterinarians with near-instantaneous insights into the health status of animals. This is valuable in critical situations requiring quick decision-making (Akinsulie et al. 2024; Alowais et al. 2023). The precision achieved by AI-driven diagnostics is unparalleled. By scrutinizing numerous data points with high accuracy, these tools contribute to more nuanced and accurate diagnoses (Johnson et al. 2021). This heightened precision minimizes the margin of error in identifying health issues, enabling veterinarians to formulate precise treatment plans (Johnson et al. 2021; Najjar 2023). AI systems can seamlessly integrate various types of information, including medical histories, diagnostic images, and genetic data (Aldoseri et al. 2023). This holistic approach ensures that veterinarians

understand an animal's health comprehensively, allowing for more informed decisions regarding treatment and care.

AI detects subtle anomalies in diagnostic images and genetic markers, enhancing early disease detection capacity (Bouhali et al. 2022; Dumortier et al. 2022; Nyquist et al. 2024). This early identification is pivotal in initiating timely interventions, potentially preventing the progression of diseases or enabling more effective management strategies. AI-driven diagnostics identify health issues and contribute to personalized treatment recommendations (Johnson et al. 2021; Leary and Basran 2022). By considering individual variations in genetic makeup and response to therapies, these tools assist veterinarians in tailoring treatment plans that are more likely to yield positive outcomes (Nosrati and Nosrati 2023). One of the remarkable features of AI is its ability to continuously learn and improve its diagnostic capabilities (Hespel et al. 2022). As these systems encounter more cases and receive feedback from veterinary professionals, they become even more adept at identifying patterns and making accurate predictions (Schofield et al. 2021; Yoon et al. 2018). AI-driven diagnostics have the potential to enhance accessibility to advanced veterinary care (Alowais et al. 2023). By streamlining diagnostic processes, these tools can reduce cost, making advanced diagnostics more affordable and widely available, ultimately benefiting a larger population of animals.

The utilization of AI in diagnostic imaging is poised for significant growth, driven by the digitization of medical data and advancements in AI technology (Cohen and Gordon 2022). Clinical diagnostic imaging encompasses various technologies, including radiography, ultrasound, MRI, CT, and nuclear medicine (Bouhali et al. 2022; Pereira et al. 2023). With the widespread adoption of digital imaging technologies, vast amounts of digital data are generated from these modalities and their corresponding reports (Alhasan and Hasaneen 2021). Radiography, which involves using X-rays to generate internal structure images of the body, has transitioned from traditional film-based imaging to digital radiography (Bansal 2006). Digital radiography systems produce high-resolution images that is stored, transmitted, and analyzed using AI algorithms (Alhasan and Hasaneen 2021; Bansal 2006). Similarly, ultrasound imaging, which utilizes sound waves to visualize internal organs and tissues, has evolved with the development of digital ultrasound machines (Carovac et al. 2011). These machines generate digital images that can be processed and interpreted using AI-based image analysis algorithms (Figure 1 and 2) (Alhasan and Hasaneen 2021). CT and MRI are advanced imaging modalities that provide cross-sectional images of the internal structures (Paudyal et al. 2023). Digital CT and MRI scans produce volumetric datasets that contain a wealth of information about anatomical and pathological features (Bouhali et al. 2022; Paudyal et al. 2023). AI algorithms can analyze these datasets to assist radiologists in detecting abnormalities, quantifying disease

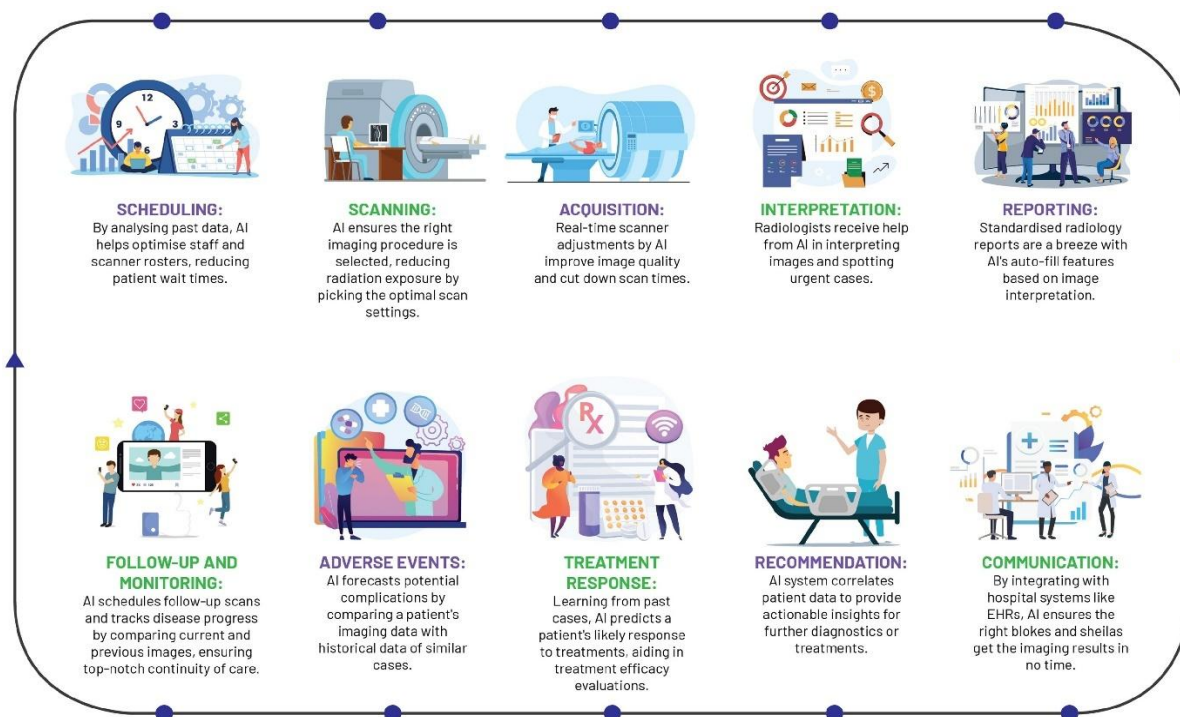


Figure 1 A schematic workflow diagram demonstrating the integration of AI into radiological practice. AI has catalyzed a transformative shift within radiology, reshaping conventional workflows and enhancing the role of radiologists. Reproduced from (Najjar, 2023) under CC BY license.

severity, and predicting treatment outcomes (Cohen and Gordon 2022). Nuclear medicine imaging techniques, such as SPECT and PET, involve using radioactive tracers to visualize metabolic processes and detect abnormalities at the molecular level. Digital nuclear medicine images can be processed and analyzed using AI algorithms to improve diagnostic accuracy and facilitate personalized treatment planning. The digitization of medical imaging data and reports has created opportunities for AI to enhance clinical diagnostic practices across various imaging modalities (Bouhali et al. 2022; Pereira et al. 2023). AI algorithms can automate image analysis tasks, identify specific patterns and issues in imaging data, and provide quantitative assessments of disease severity (Pereira et al. 2023).

The rapid progress in AI technology and computational capabilities has spurred the creation of a multitude of automated solutions for livestock monitoring (Jiang et al. 2020b; Siachos et al. 2024). Among these innovations are sophisticated systems employing AI algorithms explicitly designed to detect lameness in farm animals (Jiang et al. 2020b). To conduct comprehensive gait analysis, these cutting-edge systems utilize various tools and techniques, including accelerometers, radar sensors, body weight trackers, acoustic analysis, and advanced computer vision technology (Siachos et al. 2024). AI-driven diagnostic tools, powered by sophisticated algorithms, possess an unparalleled capacity to evaluate vast datasets, including diagnostic imaging records

(Pereira et al. 2023). Their excellence in identifying intricate patterns and trends goes beyond mere diagnostic acceleration, extending to predictive capabilities (Dumortier et al. 2022; Yoon et al. 2018). Through analyzing historical data and ongoing health trends, AI algorithms can predict and forecast potential disease outbreaks in animal populations (Cravero et al. 2022). This foresight allows veterinary professionals to implement vaccination campaigns or quarantine protocols to contain and mitigate the impact of infectious diseases (de Melo et al. 2020; Nyquist et al. 2024).

Zoonotic diseases pose significant public health risks (Elsohaby and Villa 2023). AI predictive models can track the spread of such diseases, identifying potential hotspots and vulnerable populations (Ganasegeran and Abdulrahman 2019). This information is invaluable for implementing proactive measures to prevent cross-species transmission and protect animal and human health. AI-driven tools can assess animal health risks based on various factors, including genetic predispositions, environmental exposures, and lifestyle (Ezanno et al. 2021; Kamel Boulos et al. 2019). This personalized approach enables veterinarians to anticipate potential health issues in specific animals, facilitating early interventions and tailored preventive care plans (Ezanno et al. 2021). The predictive capabilities empower veterinary professionals to adopt a proactive approach to animal healthcare (Alowais et al. 2023; Johnson et al. 2021). By anticipating health risks and potential



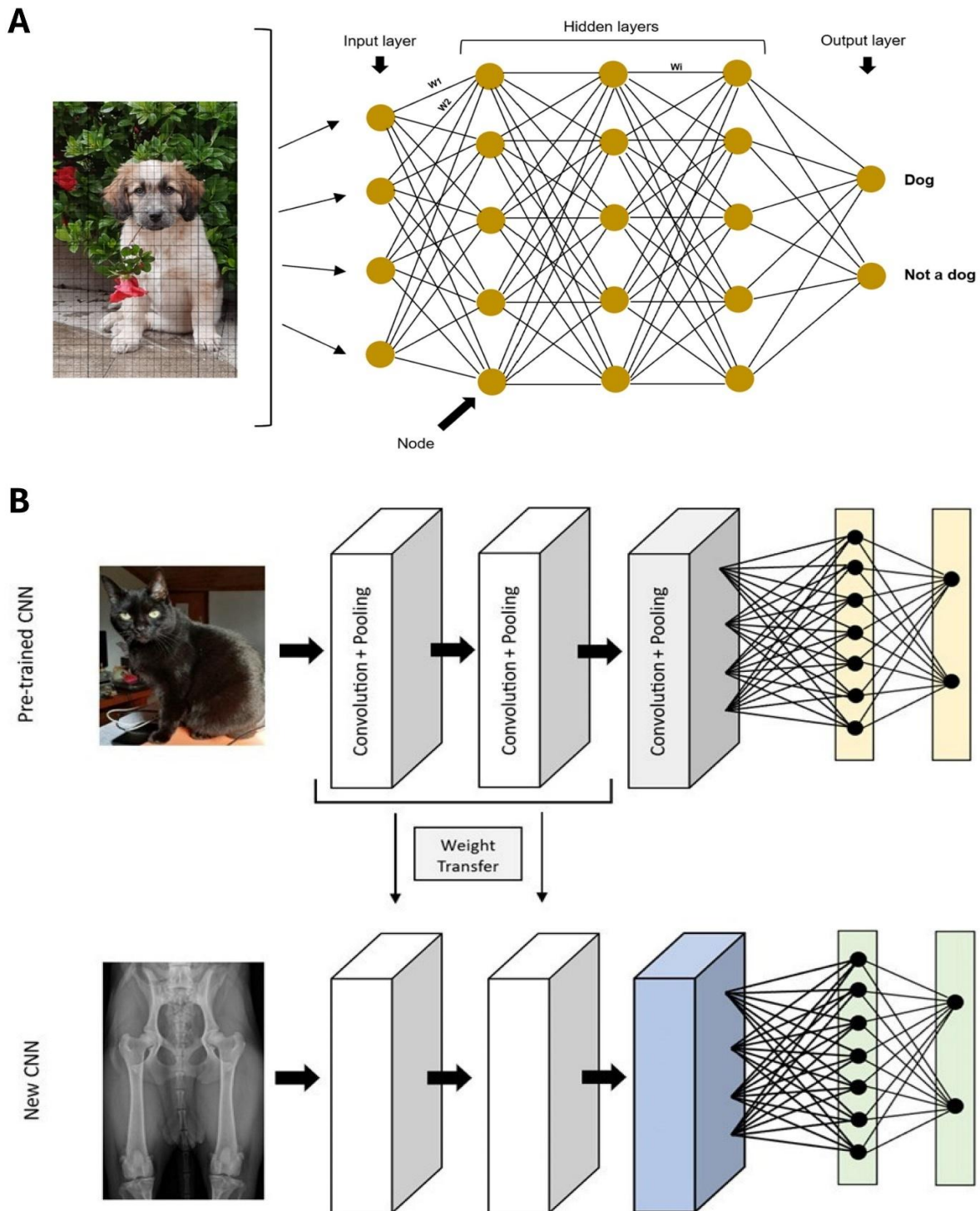


Figure 2 (A) Illustration depicting the artificial neural network architecture, with the pixels of a digital image of a dog serving as input. The network comprises four hidden layers and offers two potential outputs: "dog" or "not dog." Nodes are organized in layers and connected through connections, with weights denoted by the letter  $W$  ( $W_1$ ,  $W_2$ , and  $W_i$ ); (B) Depiction of the transfer learning process, where a portion of the weights from a CNN trained to analyze non-medical images is leveraged within a CNN tasked with classifying radiographs.

Reproduced from (Pereira et al., 2023) under CC BY license.

complications, veterinarians can implement preventive strategies, such as targeted screenings, dietary adjustments, and lifestyle modifications, to maintain and enhance the overall well-being of animals (Appleby and Basran 2022; Guitian et al. 2023). The University of Calgary has developed a specialized data extraction software called the UCDEP (Anholt et al. 2014). This software has been designed to extract and store electronic health records (HER) from veterinary practices participating in the program. The primary goal of UCDEP is to make these medical records readily available for disease surveillance and to facilitate knowledge generation for evidence-based practice in veterinary medicine (Anholt et al. 2014). AI predictive models can continuously monitor and analyze such databases in real-time.

The effectiveness of surveillance systems for animal and zoonotic diseases hinges on completing a wide array of tasks, many of which can benefit from applying ML algorithms. Similar to other domains, the utilization of ML in surveillance has experienced significant growth in the last decade (Guitian et al. 2023). This expansion is mainly attributable to datasets' availability, advancements in data analysis techniques, and increased computational capabilities. ML algorithms are now being employed to tackle previously unfeasible tasks, including identifying underlying patterns within extensive datasets derived from ongoing streams of abattoir condemnation records (Guitian et al. 2023). Furthermore, DL techniques facilitate the identification of lesions in images captured during the slaughtering process, while the analysis of free text within EHR from veterinary practices enables sentinel surveillance (Guitian et al. 2023). Beyond these novel applications, ML augments tasks traditionally reliant on statistical data analysis. While statistical models have traditionally been used to deduce relationships between predictors and diseases for risk-based surveillance, there is a growing trend toward employing ML algorithms for disease prediction and forecasting (Guitian et al. 2023). This shift toward ML-based prediction and forecasting enhances the precision and efficiency of surveillance efforts and enables more targeted interventions.

A system was developed to discern the presence of respiratory, gastrointestinal, or urinary pathology within necropsy reports (Bollig et al. 2020). Various ML algorithms, including DL were assessed for their performance in this task. This approach represents a novel ML application for syndromic surveillance utilizing necropsy reports (Bollig et al. 2020). The developed model was then applied to a dataset comprising over 33,000 necropsy reports spanning 14 years. This analysis revealed temporal and spatial patterns of diseases, providing valuable insights into epidemiological trends (Bollig et al. 2020). Notably, the model identified a potential cluster of gastrointestinal diseases from a single submitting producer in 2016, highlighting its utility in detecting and tracking disease outbreaks within veterinary populations (Bollig et al. 2020).

Confirmatory diagnosis of Cushing's syndrome (CS) can be challenging in dogs, necessitating exploring novel diagnostic approaches (Carotenuto et al. 2019). Four ML algorithms were employed to predict the likelihood of a future diagnosis of CS (Schofield et al. 2021). Utilizing structured clinical data from the VetCompass program in the UK, dogs flagged as suspected cases of CS were analyzed and categorized based on their final diagnosis in records (Schofield et al. 2021). The models incorporated clinical and demographic features available at initial suspicion by attending veterinarians. Remarkably, the ML methods demonstrated the ability to accurately classify recorded diagnoses of CS, exhibiting robust predictive performance (Schofield et al. 2021).

Significant efforts have been dedicated to developing computer-based decision support tools to aid veterinary clinicians across various aspects of patient care (Hennessey et al. 2022). Such applications enhance the accuracy of medical diagnoses and ultimately improve patient outcomes (La Perle 2019). While ample supporting evidence exists for the former assertion, the latter remains a more challenging endpoint to assess comprehensively (Awaysheh et al. 2019; La Perle 2019). As these tools become increasingly integrated into veterinary pathology, evidence-based outcome assessments will be possible, shedding further light on their true efficacy in clinical practice (Awaysheh et al. 2019; Zuraw and Aeffner 2022). Following the training of ML models, they function collaboratively with pathologists to enhance diagnostic outcomes (Zuraw and Aeffner 2022). By leveraging the vast amounts of data available, these models provide insights and support to pathologists during the diagnostic process (La Perle 2019). ML algorithms refine their predictions through continuous interaction and feedback loops, leading to accurate and reliable results (Awaysheh et al. 2019; La Perle 2019). Additionally, these models can assist in identifying subtle patterns not be apparent to human observers, thereby augmenting the diagnostic capabilities of pathologists (La Perle 2019).

In assessing tumor grading schemes, the manual count of mitotic figures holds significant importance, serving as a critical parameter in evaluating tumor aggressiveness (Ibrahim et al. 2022). However, the accuracy of this assessment can be influenced by the selection of the tumor region having the highest mitotic activity, which may vary due to the uneven distribution of mitotic figures (Aubreville et al. 2020). Three DL-based methods (indirect approach to predict mitotic figure segmentation map, directly estimating mitotic figures, and detecting mitotic figures as objects) were evaluated for their effectiveness in assessing the highest mitotic density. Surprisingly, the predictions made by all models surpassed those of expert pathologists on average (Aubreville et al. 2020). Particularly noteworthy was the two-stage object detector performance that consistently outperformed most human pathologists across the different tumor cases (Aubreville et al. 2020). This underscores the remarkable capabilities of DL algorithms in detecting the most

mitotically active regions within tumors (Aubreville et al. 2020). This suggests the potential for integrating these advanced technologies into clinical practice to enhance the efficiency and accuracy of tumor grading processes.

An AI-based software program (AISP) designed to detect dental issues in dogs and cats was evaluated compared to human evaluators (Nyquist et al. 2024). Pathologies were assessed, including periapical lucency, furcation bone loss, resorptive lesions, retained tooth roots, attachment loss, and tooth fractures. Inter-rater reliability showed good to excellent agreement among all parties, indicating the AISP's comparable performance to human evaluators in detecting specified pathologies (Nyquist et al. 2024). The sensitivity and specificity of the AISP were evaluated. The results showed low sensitivity and high specificity, indicating a tendency for false negatives. This raises concerns about its initial screening tool efficacy (Nyquist et al. 2024). However, the AISP demonstrated a low rate of false positives, indicating utility as a supplementary tool, enhancing diagnostic accuracy rather than serving as a standalone diagnostician (Nyquist et al. 2024). This technology could augment dental radiography utilization and diagnostic capabilities with proper understanding and integration into veterinary practice.

DL in veterinary science represents a promising avenue, mainly in computer-aided detection using CNNs. One such application focuses on detecting abnormalities from cat lateral thoracic radiographs (Dumortier et al. 2022). Thoracic radiography is a fundamental diagnostic tool in small animal medicine, offering valuable insights into pulmonary health through analyzing radiographic pulmonary patterns. Despite significant strides in DL for veterinary imaging, a notable gap remains in developing CNNs tailored to detect radiographic pulmonary patterns from thoracic radiograph images (Dumortier et al. 2022). This represents a crucial area of investigation, given the importance of accurate and timely diagnosis in veterinary medicine, particularly in identifying pulmonary abnormalities in veterinary patients (Dumortier et al. 2022). By leveraging CNNs, we can enhance diagnostic accuracy and efficiency, ultimately improving patient care and outcomes in veterinary practice.

In another study, three DL networks with multiple pretraining strategies aimed to predict different primary thoracic lesions in canine and feline patients from thoracic radiographs (Boissady et al. 2020). Lesions included left atrial enlargement, tracheal collapse, pneumothorax, alveolar patterns, and pulmonary masses. Following pretraining, the algorithms underwent specific training using over 22,000 thoracic veterinary radiographs, each accompanied by an expert veterinary radiologist's report as the standard (Boissady et al. 2020). Error rates for each observer were calculated for the 15 labels and subsequently compared. The network's overall error rate significantly outperformed unaided veterinarians and those aided by the network (10.7% vs 16.8% vs

17.2%, respectively) (Boissady et al. 2020). Notably, the network performed significantly better detecting cardiac enlargement and bronchial patterns. The evaluated network solely aids lesion detection and does not provide diagnostic conclusions (Boissady et al. 2020). Considering its commendable performance, this technology could serve as a valuable aid for general practitioners while awaiting a radiologist's report, potentially expediting diagnostic processes and improving patient care.

Researchers have also applied a DL and AI technique to analyze thoracic radiographs of dogs for diagnosing left atrial enlargement and compared it to the interpretations of veterinary radiologists (Li et al. 2020). A total of 792 radiographs were utilized to train and test a CNN algorithm (Li et al. 2020). The sensitivity and specificity were subsequently assessed with those determined by the experts. In comparison, sensitivity and specificity obtained by expert veterinary radiologists were identical, standing at 82.71%, 68.42%, and 87.09%, respectively (Li et al. 2020). While the accuracy of both the accuracy-driven CNN algorithm and radiologists was almost similar, their concordance reached an impressive 85.19%, indicating a higher agreement between the two approaches (Li et al. 2020).

Similarly, researchers examined the efficacy of an AI algorithm (Vetology AI<sup>®</sup>) for identifying pleural effusion in canine thoracic radiographs (Müller et al. 2022). The algorithm classified images into those with and without pleural effusion (Müller et al. 2022). The AI achieved an accuracy rate of 88.7% in detecting pleural effusion, with sensitivity and specificity levels at 90.2% and 81.8%, respectively (Müller et al. 2022). Utilizing this technology in evaluating radiographs presents promising prospects and merits additional exploration and validation through further investigation and testing. The effectiveness of Vetology AI<sup>®</sup> was also evaluated for identifying pulmonary nodules in canine thoracic radiography (Pomerantz et al. 2023). Positive cases were validated through CT, cytology, or histopathology, confirming pulmonary pathology. Among the confirmed cases, the AI software successfully detected pulmonary nodules or masses in 31 out of 56 instances (Pomerantz et al. 2023). Additionally, it accurately classified 30 out of 32 control cases. The AI model demonstrated an accuracy of 69.3%, balanced accuracy of 74.6%, sensitivity of 55.4%, and specificity of 93.75% (Pomerantz et al. 2023). These results indicate promising potential for the AI software in detecting pulmonary pathology, with notable sensitivity and specificity values.

Likewise, researchers assessed the accuracy of AI-powered software in diagnosing canine cardiogenic pulmonary oedema. Results revealed impressive metrics, with the AI-based software achieving 92.3% accuracy, 91.3% sensitivity, and 92.4% specificity compared to radiologist diagnoses (Kim et al. 2022). These findings advocate for integrating AI software screening in evaluating thoracic radiographs for dogs suspected of having cardiogenic pulmonary oedema. This approach is valuable in

aiding short-term decision-making, particularly when access to a radiologist is limited or unavailable (Kim et al. 2022). A computer-aided detection device employing CNNs was developed to identify cardiomegaly from right lateral chest radiographs in dogs (Burti et al. 2020). The diagnostic accuracy of four distinct CNN models in detecting cardiomegaly was assessed, revealing that all tested models exhibited high diagnostic accuracy (Burti et al. 2020). This suggests that CNNs have the potential to aid veterinarians in the detection of cardiomegaly in dogs from plain radiographs.

Another study has investigated the viability of BOF and CNN for computer-aided detection. It compared their efficacy to differentiate normal from abnormal thoracic radiographic findings of dogs (Yoon et al. 2018). Across testing sets, both models exhibited accuracy ranging from 79.6% to 96.9%. Notably, CNN demonstrated superior accuracy (92.9-96.9%) and sensitivity (92.1-100%) compared to BOF (accuracy: 79.6-96.9%, sensitivity: 74.1-94.8%) (Yoon et al., 2018). BOF and CNN promise to enhance work efficiency through double reading (Yoon et al. 2018). In another study, a deep CNN was trained to identify medial retropharyngeal lymph nodes using a small dataset comprising CT scans of canine heads (Schmid et al. 2022). The findings suggest that these architectures can effectively segment anatomical structures within complex and breed-specific regions like the head, potentially even with limited training sets (Schmid et al. 2022). However, veterinary radiologists exhibited a statistically lower error rate than CNNs (Adrien-Maxence et al. 2022). Some CNNs showed superiority over veterinary radiologists, indicating potential (Adrien-Maxence et al. 2022). This addresses several questions the current study raises to standardize AI and enhance patient care (Joslyn and Alexander 2022; Lungren and Wilson 2022).

In the context of time constraints physicians face during patient consultations, integrating automated systems can significantly expedite diagnostic processes while ensuring accuracy. Presently, many such systems rely on supervised DL methodologies. However, a significant drawback of these approaches is their reliance on extensive datasets with labeled data (Celniak et al. 2023). Acquiring such datasets is often challenging and resource-intensive in terms of time and financial investment. In response to this challenge, a recent study proposed a novel solution to improve classification accuracy while minimizing the dependency on large labelled datasets (Celniak et al. 2023). This methodology leverages knowledge transfer from self-supervised learning methods across species and pathologies. By harnessing inter-species self-supervised learning techniques, this approach facilitated the extraction of valuable insights from diverse datasets, thereby enhancing classification scores (Celniak et al. 2023). This innovative approach addresses the limitations associated with traditional supervised learning methods and offers a more efficient and cost-effective alternative for developing automated diagnostic

systems (Celniak et al. 2023). Through knowledge transfer from various sources, our solution has the potential to revolutionize diagnostic processes, enabling clinicians to make faster yet reliable diagnoses (Celniak et al. 2023).

AI algorithms, when applied to predictive modelling, can assist in optimizing treatment plans for individual animals (Zhang et al. 2024). By considering the predicted response to different therapeutic interventions based on historical data and case studies, veterinarians can tailor treatment approaches, improving efficacy and minimizing potential side effects (Lungren and Wilson 2022; Paudyal et al. 2023). AI's predictive modelling extends to population-level health management (Shaban-Nejad et al. 2018). Veterinary authorities can use these tools to assess and address the health needs of entire animal populations, guiding resource allocation, disease prevention strategies, and public health initiatives (Guitian et al. 2023; Olawade et al. 2023). AI-driven predictive models can also factor in environmental variables, assessing how climate or habitat changes may impact animal populations' health. This holistic approach enables a comprehensive understanding of the interconnected factors influencing animal health (Sarker 2022). As more data becomes available and the algorithms encounter new scenarios, they adapt and improve their predictive accuracy, ensuring that the models remain relevant over time (Aldoseri et al. 2023).

The adoption of AI within the realms of veterinary and human medicine are experiencing a swift and widespread surge. This expansion is evident in medical image analysis, where ML methodologies are frequently employed (Hennessey et al. 2022). Among these methodologies, CNNs are a prominent choice in DL classification and regression models, owing to their ability to process and interpret complex medical images effectively (Hespele et al. 2022). CNNs offer a sophisticated approach to analyzing medical images, allowing for detailed and nuanced assessments that contributing to accurate diagnoses and treatment planning. Furthermore, utilizing NLP techniques can streamline the generation of "truth-data," essential for training AI systems in radiation oncology applications (Hespele et al. 2022). By harnessing NLP, annotating and categorizing medical images becomes more efficient and precise, facilitating the development and refinement of AI-driven diagnostic and therapeutic tools (Hespele et al. 2022). As the integration of AI continues to evolve and expand within veterinary and human medicine, a comprehensive understanding of these methodologies, particularly CNNs and NLP, becomes increasingly crucial. Healthcare professionals can enhance their diagnostic capabilities, improve patient outcomes, and optimize care delivery across various medical specialties (Lungren and Wilson 2022).

Therefore, it is clear that the integration of AI into veterinary radiology is transforming diagnostic imaging practices, offering a wide array of advanced tools and techniques to enhance the interpretation and analysis of radiographic images for animals. One



significant application of AI in this field is image interpretation and diagnosis, where AI-powered algorithms analyze radiographic images, CT scans, MRI, and other diagnostic images to assist veterinarians in detecting abnormalities and diagnosing various conditions in animals. These algorithms can identify subtle changes in images that may indicate the presence of tumours, fractures, foreign bodies, or other health issues, thereby aiding in early detection and intervention. Moreover, AI algorithms automate the process of segmentation and annotation within radiographic images, facilitating the visualization and understanding of anatomical structures for precise diagnosis and treatment planning, particularly in complex cases where accurate anatomical localization is essential. Additionally, AI models trained on large datasets of veterinary imaging studies can classify different diseases and predict clinical outcomes based on radiographic findings, providing valuable insights for veterinarians in disease management and prognosis. Furthermore, AI-based techniques can help reduce noise, improve contrast, and reconstruct 3D images from 2D radiographs, offering veterinarians a comprehensive view of complex anatomical structures for surgical planning and intervention.

**4 Personalized treatment plans**

One area where AI excels is in the analysis of genetic data, which is important in tailoring personalized treatment plans (Johnson et

al. 2021). By leveraging AI algorithms to sift through vast genetic datasets, veterinarians can gain valuable insights into the genetic predispositions of animals to certain diseases and conditions (Johnson et al. 2021; Rezayi et al. 2022). Through genetic data analysis, AI can identify genetic markers associated with specific health risks or animal susceptibilities (Vilhekar and Rawekar 2024). This information allows veterinarians to proactively screen for potential health issues and design preventive measures tailored to each animal's unique genetic profile (Johnson et al. 2021; Vilhekar and Rawekar 2024). AI may recommend specific dietary adjustments to mitigate the risk of genetic diseases or enhance overall health and well-being (Johnson et al. 2021; Rezayi et al. 2022).

In addition to genetic data analysis, AI-powered systems can also consider environmental factors when tailoring treatment plans for individual animals (Johnson et al. 2021; Paudyal et al. 2023). Environmental factors such as diet, exercise levels, living conditions, and exposure to toxins or pollutants can significantly impact an animal's health and treatment outcomes. AI algorithms can analyze environmental data from various sources, including wearable sensors, environmental monitoring devices, and EHR (Figure 3)(Aldoseri et al. 2023; Shajari et al. 2023). By correlating environmental factors with health outcomes, AI can identify patterns and trends that may influence an animal's response to treatment. For example, AI may recommend changes in diet or exercise routines based on environmental factors to optimize

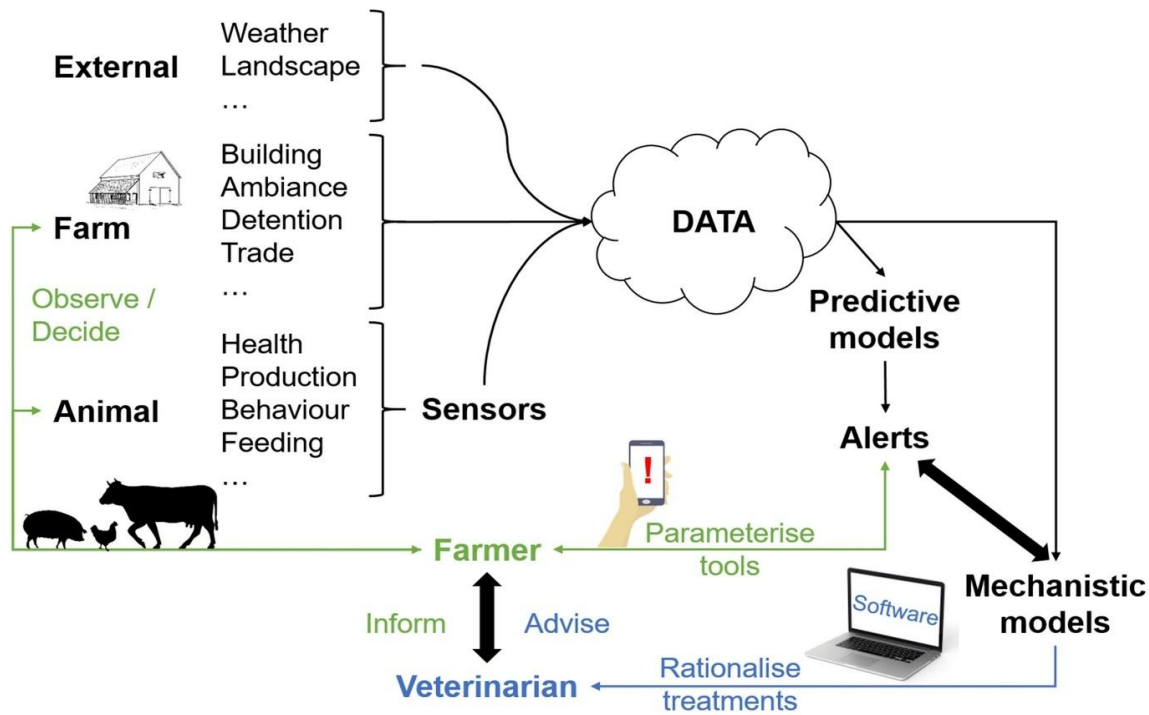


Figure 3 Enhancing animal health monitoring and treatment rationalization through data-driven approaches. Machine learning methods enable the identification of patterns and signals within extensive datasets, such as spatial data or time-series of disease cases. Reproduced from under CC BY license (Ezanno et al. 2021).

treatment efficacy and promote better health outcomes (Anholt et al. 2014).

AI can help to integrate historical data into the treatment planning process, allowing veterinarians to leverage past medical records and treatment outcomes to inform future decisions (Anholt et al. 2014; Paynter et al. 2021; Aldoseri et al. 2023). By analyzing historical data, AI can identify trends, patterns, and treatment responses that may guide personalized treatment strategies for individual animals (Paynter et al. 2021). Historical data integration enables veterinarians to track the progression of diseases over time, monitor the effectiveness of previous interventions, and identify factors associated with treatment success or failure (Cravero et al. 2022). This valuable information empowers veterinarians to make evidence-based decisions and adjust treatment plans in real-time based on each animal's unique medical history and response to therapy.

Using image registration, advanced contouring, and treatment optimization software is standard practice for clinical care in veterinary radiation oncology. However, significant progress has been made over the years due to developments in computing power and the rapid evolution of open-source software packages, neural networks, and data science. These developments have ushered in a new era of AI systems in radiation oncology, revolutionizing research and clinical applications (Bouhali et al. 2022; Leary and Basran 2022). Unlike conventional software, AI technologies exhibit greater complexity and can learn from representative and localized data. In human radiation oncology, these AI systems have already demonstrated their potential across various stages of patient care, including deformable registration, treatment simulation, adaptive radiotherapy, auto-segmentation, quality assurance, and modelling (Leary and Basran 2022).

While the veterinary field benefits significantly from these technologies in terms of time and cost savings, caution is warranted in their adoption due to the limited understanding of their full range of applications (Guitian et al. 2023). Nevertheless, several practical applications in veterinary radiation oncology are anticipated in the coming years, including deformable registration, automated segmentation, and adaptive radiotherapy (Leary and Basran 2022).

## 5 Remote monitoring and telemedicine

Remote monitoring, facilitated by AI technology, enables real-time tracking of an animal's health status (Shaik et al. 2023). By using wearable devices, sensors, and other monitoring tools, veterinarians can remotely monitor vital signs and activity levels (Shajari et al. 2023). AI algorithms analyze the data from such devices to detect abnormalities (Shaik et al. 2023; Shajari et al. 2023). Continuous health monitoring allows veterinarians to

identify signs of potential health issues, enabling timely interventions and preventive measures (Shaik et al. 2023). For example, AI algorithms can detect subtle changes in an animal's behavior or physiological parameters that may indicate pain, distress, or the onset of illness (Akinsulie et al. 2024; Shaik et al. 2023). Remote monitoring facilitates prompt diagnosis and treatment by alerting veterinarians to these changes, ultimately improving animal health outcomes (Jiang et al. 2024).

Telemedicine, powered by AI technology, extends the reach of veterinary care beyond traditional clinic settings, enabling remote consultations, diagnoses, and treatment planning (Rezaei et al. 2023). Through telemedicine platforms, veterinarians can communicate with pet owners, assess symptoms, review medical histories, and provide guidance on managing health concerns (Huang and Chueh 2021; Rezaei et al. 2023). AI-driven telemedicine applications leverage advanced algorithms to assist veterinarians in diagnosing and triaging cases remotely (Huang and Chueh 2021). For example, AI-based diagnostic tools can analyze medical images, laboratory results, and other diagnostic data to help veterinarians make accurate assessments and recommendations (Burrell 2023; Huang and Chueh 2021; Rezaei et al. 2023). Telemedicine also facilitates follow-up appointments and ongoing monitoring, allowing veterinarians to track treatment progress and adjust interventions as needed (Huang and Chueh 2021; Rezaei et al. 2023).

The key benefits of AI-enabled remote monitoring and telemedicine are overcoming geographical constraints and providing access to veterinary care in underserved or remote areas (Burrell 2023; Huang and Chueh 2021). By leveraging digital communication technologies, veterinarians can reach clients and patients in isolated regions where traditional veterinary services may be limited (Burrell 2023). AI-based telemedicine platforms enable virtual consultations and remote diagnostic evaluations, removing the need for pet owners to travel long distances to access veterinary care (Sharma et al. 2023). This improves convenience for pet owners and ensures that animals receive timely and appropriate medical attention, regardless of their location (Burrell 2023; Sharma et al. 2023). By breaking down geographical barriers, AI-driven telemedicine expands access to veterinary services, promoting the health and well-being of animals worldwide (Sharma et al. 2023).

## 6 AI in research and drug development

The advent of AI has revolutionized the pharmaceutical realm to a great extent. Conventional techniques in pharmaceutical research are limited by their dependence on trial-and-error experimentation and their difficulty in precisely predicting the behaviour of novel bioactive compounds (Xu et al. 2021). AI-based algorithms assist in identifying new targets for drug development, such as specific

biochemical or genetic pathways involved in diseases (You et al. 2019). ML precisely predicts small molecules' physical and chemical properties at a level comparable to quantum mechanics. AI is proficient in finding correlations between molecular representations and biological or toxicological activities (Aloawai et al. 2023). The synthetic pathways of new drug candidates are efficiently explored using AI-based algorithms. In conjunction with AI, robotics probes the chemical space for novel reactions through automated analysis of reaction feasibility. AI enables rapidly screening a virtual compound library containing billions of molecules within a few days (Álvarez-Machancoses and Fernández-Martínez 2019). Identifying preclinical candidates through an AI-based computational pipeline can be accomplished in a significantly shorter time. Moreover, DL algorithms are currently used to predict native protein folding and analyze protein structures quickly. It also contributes to the novel drug design from the databases of existing therapeutic compounds.

The drug discovery process is a complex, laborious, and time-consuming endeavour. It demands significant capital investments and, in some instances, ends up in failure in the final stages of drug development, leading to significant loss (Blanco-González et al. 2023). AI methodologies, such as ML and NLP, empower and accelerate drug discovery through highly accurate and efficient analysis of extensive databases. The effective application of DL accurately predicts drug compounds' efficacy. The drug discovery process consists of four phases: (i) identification and validation of targets, (ii) screening and refinement of compounds for lead optimization, (iii) preclinical investigations, and (iv) clinical trials (Chan et al. 2019). AI-driven methods are actively employed across various stages of the process to enhance efficiency in terms of time and cost. Real-time image-based cell sorting, cell classification, quantum mechanics calculations for compound properties, computer-aided organic synthesis, molecular design, and prediction of 3D structures for target proteins are the various platforms that utilize AI applications (Nitta et al. 2018; von Lilienfeld 2018). These procedures can be automated and optimized using AI to accelerate the research and development process for drug discovery significantly. AI is highly efficient in sorting and classifying cells based on image analysis, replacing traditional visual inspection due to its inefficiency in handling extensive datasets. The least-squares SVM method is an explicit AI-based approach to categorizing various cell types (Samui and Kothari 2011). Modern Image-Activated Cell Sorting devices depend on electrical, optical, and mechanical cell properties to automate cell sorting at scale. These devices achieve high-speed digital image processing and decision-making by implementing AI-based convoluted DNN algorithms (Ho et al. 2019). AI is pivotal in predicting the physical properties for effective drug design, particularly concerning bioavailability, toxicity, and bioactivity (Lynch et al. 2007).

The molecular representations employed in AI drug design algorithms encompass various inputs, such as molecular fingerprints, molecular graphs, simplified molecular-input line-entry system (SMILES) strings, potential energy measurements, Coulomb matrices, etc., undergoing a DNN training phase for accurate processing (Sanchez-Lengeling and Aspuru-Guzik 2018). The algorithm, such as molecular fingerprints and coulomb matrices, assesses biomolecules' physico-chemical and toxicological properties when selecting lead compounds. AI-based QSAR approaches, including linear discriminant analysis, random forest, and SVMs, are employed to identify potential drug candidates to expedite the process (Zhang et al. 2017). The prediction of drug-target binding affinity is crucial for anticipating drug-target interactions (Öztürk et al. 2018).

One notable area where AI has made significant advancements is in veterinary drug development (Blanco-González et al. 2023). AI-driven technologies are revolutionizing the process of discovering, designing, and developing new drugs for treating and managing various diseases in animals (Niazi 2023). AI offers various applications in veterinary drug development, revolutionizing traditional drug discovery and development processes (Paul et al. 2021). One significant application lies in virtual screening, where AI algorithms analyze extensive databases of chemical compounds to pinpoint potential drug candidates with therapeutic efficacy against particular diseases (Álvarez-Machancoses and Fernández-Martínez 2019; Han et al. 2023). AI-driven predictive modelling techniques, including ML and DL, empower the swift screening of millions of compounds, markedly expediting the drug discovery process (You et al. 2019). AI algorithms analyze complex biological data to identify molecular targets associated with animal disease pathways (Vora et al. 2023). By unraveling the fundamental mechanisms of diseases, AI plays a pivotal role in identifying novel drug targets and validating existing ones. This process paves the way for developing more precise and effective therapies, ultimately improving patient outcomes (Niazi 2023).

Furthermore, AI has a role in pharmacokinetic and pharmacodynamic modelling, optimizing dosing and predicting animal efficacy and safety profiles (Vora et al. 2023; Wu et al. 2024). AI-driven predictive modelling techniques analyze physiological and pharmacological data to simulate distribution, metabolism, and elimination processes in animal species, guiding the design of optimal drug formulations and dosing strategies (Wu et al. 2024). AI integration into veterinary drug development offers several benefits to researchers, pharmaceutical companies, veterinarians, and animal patients (Lungren and Wilson 2022). AI-driven virtual screening helps to identify potential drug candidates, saving time and cost compared to traditional high-throughput screening methods (Qureshi et al. 2023). Additionally, AI enhances the efficiency and accuracy of identification and

validation processes, leading to the development of targeted and personalized animal therapies (Akinsulie et al. 2024; Vora et al. 2023). By leveraging large-scale biological datasets and advanced computational algorithms, AI enables researchers to gain deeper insights into the molecular mechanisms of diseases, facilitating the discovery of innovative drug targets (Visan and Negut 2024; Vora et al. 2023). Moreover, AI-driven predictive modelling techniques improve the prediction of drug efficacy and safety profiles in animals, minimizing the risks associated with drug development. By optimizing dosing regimens and predicting adverse drug reactions (Paul et al. 2021), AI helps pharmaceutical companies streamline preclinical testing and accelerate the translation of promising drug candidates from the laboratory to clinical trials (Paul et al. 2021; Yang and Kar 2023).

AI is revolutionizing veterinary medicine by offering innovative solutions to address AMR. AI algorithms analyze vast proteomic, genomic, and metabolomic data datasets to identify potential drug targets for combating AMR. By deciphering complex microbial interactions and host-pathogen dynamics, AI aids in pinpointing vulnerabilities in pathogenic microorganisms, facilitating the development of targeted therapeutic interventions (Akinsulie et al. 2024). AI-driven approaches, such as ML and computational modelling, streamline the antibiotic discovery process by generating virtual libraries of candidates based on chemical structures and pharmacological properties. These candidates undergo further optimization and testing to identify promising leads for drug development (Akinsulie et al. 2024). Moreover, AI-powered decision support systems can help users optimize antibiotic use by analyzing patient data and microbial susceptibility patterns in real-time, enabling personalized treatment recommendations tailored to individual patients. AI models trained on large datasets predict the likelihood of AMR in clinical isolates, allowing for early detection of emerging resistance trends and proactive intervention strategies (Akinsulie et al. 2024). AI offers a transformative approach to accelerate drug discovery, optimize antibiotic use, and combat AMR, safeguarding animal and human health.

An NLP system can automate the extraction of essential data on proper antimicrobial use, including clinical indications, antimicrobial selection, dosage, and therapy duration. It analyzed over 4.4 million animal patient clinical records in Australia, focusing on consultations involving antimicrobial use (Hur et al. 2022). The primary objective was to gain insights into antibiotic usage patterns and the underlying reasons for their administration at a population level. However, the analysis revealed a significant limitation: only around 40% of the records contained comprehensive information regarding the rationale for prescribing antimicrobials, along with details on dosage and treatment duration (Hur et al. 2022). This gap poses a substantial challenge for data extraction, even with advanced NLP and DL techniques (Hur et al.

2022). While NLP and DL hold promise for overcoming such obstacles by extracting valuable insights from free-text clinical records, their efficacy depends on the availability of essential data within the records themselves. In cases where critical information is inadequately recorded, these technologies face limitations in fully capturing the nuances of antimicrobial prescribing practices. Thus, addressing the issue of incomplete data recording in clinical settings remains a crucial aspect to enable the effective utilization of advanced data extraction techniques in veterinary medicine (Hur et al. 2022).

Establishing MRLs for veterinary medicines is critical in safeguarding the human food supply (Pratiwi et al. 2023). Regulatory authorities provide guidelines for setting MRLs, which are adhered to by drug sponsors in each jurisdiction (Pratiwi et al. 2023; Zad et al. 2023). In the typical drug approval steps, residue limits are customized for particular species and matrices. Consequently, MRLs are often lacking for species other than those specifically targeted during approval. One of the study has evaluated the feasibility of predicting MRLs reliably for under-represented groups using ML techniques (Zad et al. 2023). By leveraging ML algorithms, we can accurately forecast and estimate MRLs even in cases where they have not been formally established. This has the potential to significantly reduce the necessity for live animal use, lower associated costs, and alleviate the overall research burden involved in determining new MRLs (Zad et al. 2023). The utilization of ML in predicting MRLs for diverse food commodity groups holds promise for streamlining regulatory processes, enhancing efficiency, and promoting more sustainable practices in veterinary medicine (Zad et al. 2023).

Despite several issues, the future of AI in veterinary drug development is promising (Zhang et al. 2017). Advances in AI technologies, coupled with the increasing availability of large-scale biological datasets and collaborative research initiatives, are poised to accelerate innovation in animal healthcare (Bohr and Memarzadeh 2020). By harnessing the power of AI-driven predictive modelling, virtual screening, and target identification techniques, researchers can develop safer, more efficacious, and personalized therapies for animals, addressing unmet medical needs and improving the quality of veterinary care worldwide (Chan et al. 2019; Pratiwi et al. 2023). As AI continues to evolve and integrate into veterinary drug development pipelines, it can revolutionize animal healthcare and transform the lives of countless animal patients.

## 7 Challenges and ethical considerations

Along with the potential benefits, several issues must be considered to realize the full potential of AI in veterinary practice (Lustgarten et al. 2020). One of the foremost challenges in leveraging AI in veterinary medicine is the quality of available



data (Anholt et al. 2014; Nie et al. 2018). Large and diverse datasets are required for training AI algorithms effectively (Lustgarten et al. 2020). Unlike human healthcare, where EHRs are more standardized and readily available, veterinary medical data are often fragmented, heterogeneous, and stored in various formats (Anholt et al. 2014; Santamaria and Zimmerman 2011). This lack of standardized data poses a significant obstacle to developing robust AI models that accurately predict and diagnose veterinary conditions. Veterinary patient records predominantly contain free-text entries lacking standardized clinical coding or fixed vocabulary (Anholt et al. 2014; Nie et al. 2018). Text-mining techniques enable the identification of pertinent cases within the unstructured data and facilitate the introduction of organization and structure to the records (Anholt et al. 2014). Text miners have previously demonstrated a sensitivity of 87.6% and a specificity of 99.3% in retrieving cases with enteric signs compared to the assessments made by human reviewers (Anholt et al. 2014). This indicates that the text-mining tool exhibited high accuracy in correctly identifying cases of enteric syndrome, with a low rate of false positives and negatives.

Moreover, the cost associated with developing and implementing AI-powered technologies presents another significant challenge for veterinary practices (Santamaria and Zimmerman 2011; Zhang et al. 2024). The initial investment required to acquire AI infrastructure, develop custom algorithms, and integrate AI systems into existing workflows can be substantial (Zhang et al. 2024). For many small and medium-sized veterinary clinics, the financial burden of adopting AI technology may be prohibitive, limiting access to advanced diagnostic and treatment capabilities. Ethical considerations also play a crucial role in adopting AI in veterinary medicine (Gerke et al. 2020; Cohen and Gordon 2022). As AI algorithms become highly influential in clinical decision-making, critical issues such as transparency and accountability come to the forefront of concern (Naik et al. 2022). Biases inherent in training data can result in discriminatory outcomes, potentially affecting the quality of care delivered to animal patients (Zhang et al. 2024).

Additionally, concerns have been raised about the displacement of veterinary professionals due to AI-based technologies, raising questions about the ethical implications of automation in the veterinary workforce (Bouchemla et al. 2023). Furthermore, the lack of regulatory systems and oversight mechanisms for AI in veterinary medicine presents a significant challenge. Unlike human healthcare, where regulatory bodies such as the FDA oversee the approval and monitoring of medical devices and AI algorithms, veterinary medicine lacks similar regulatory structures (Benjamens et al. 2020; Cohen and Gordon 2022). Without clear guidelines for AI systems in veterinary care, there is a risk of inadequate quality control, patient safety concerns, and legal liabilities (Hooper et al.

2023). Addressing such challenges requires collaboration between stakeholders, including veterinary professionals, researchers, policymakers, and industry leaders.

Initiatives to improve data sharing and interoperability, such as developing standardized veterinary medical ontologies and EHR systems, can help overcome data-related challenges and facilitate the development of AI-driven solutions (Lustgarten et al. 2020). Moreover, innovative financing models and partnerships between veterinary clinics, research institutions, and technology companies can help alleviate the financial barriers to AI adoption in veterinary practice (Hangl et al. 2023). By pooling resources and sharing costs, veterinary practices can access AI technologies and expertise that would otherwise be out of reach (Bouchemla et al. 2023; Hangl et al. 2023). Measures such as algorithmic auditing, bias detection, and explainable AI can help mitigate ethical risks and ensure that AI systems align with professional standards and ethical principles in veterinary care (de Manuel et al. 2023; Lungren and Wilson 2022). Lastly, establishing regulatory frameworks tailored to the unique needs and challenges of veterinary AI is essential for ensuring these technologies' safe and responsible use (Coleman and Moore 2024). Regulatory agencies, professional associations, and industry consortia should collaborate to develop guidelines, standards, and certification programs to govern AI systems' development, evaluation, and deployment in veterinary medicine (Hooper et al., 2023).

Our comprehension of the capabilities of AI models like ChatGPT in veterinary fields is currently in its infancy (Dave et al. 2023; Coleman and Moore 2024). We urgently need to deepen our understanding of these models to unlock their full potential, encourage responsible utilization, and ensure alignment with educational objectives (Abani et al. 2023; Jiang et al. 2024). One study assessed the knowledge and response consistency of ChatGPT by administering true/false and multiple-choice questions from fifteen courses of third-year veterinary students (Coleman and Moore 2024). The study revealed a lower overall performance score, indicating the need for caution among veterinarians when retrieving data from such AI-based platforms (Coleman and Moore 2024).

## 8 Balancing automation and professional expertise

Striking a balance between AI-driven automation and the expertise of veterinary professionals is crucial to ensuring the highest standards of care (Appleby and Basran 2022). This collaborative model acknowledges that while AI can enhance efficiency and accuracy in diagnosis and treatment, it cannot replace the nuanced judgment and clinical acumen of experienced veterinarians (Jiang et al. 2024). In this collaborative approach, AI will act as an essential tool that complements the skills and knowledge of veterinary professionals (Bouchemla et al. 2023). AI algorithms

can uncover patterns that may elude human observation, thereby aiding veterinarians in making well-informed decisions and delivering better patient care (Schofield et al. 2021; Alowais et al. 2023). For example, AI-powered diagnostic tools can help veterinarians interpret imaging studies, detect subtle changes in laboratory values, and predict disease outcomes (Burti et al. 2020; Celniak et al. 2023; Joslyn and Alexander 2022). However, it is necessary to recognize that AI algorithms are not infallible and may have limitations, particularly in complex and nuanced cases (Bouchemla et al. 2023). Therefore, the collaborative approach involves veterinarians working alongside AI systems, critically evaluating their recommendations, and providing context-specific insights that AI may lack. By combining the strengths of both humans and machines, veterinary professionals can ensure that patients receive the most accurate diagnoses and effective treatments (Bouchemla et al. 2023).

The concept of a veterinarian-AI partnership emphasizes the symbiotic relationship between veterinary professionals and AI technologies (Appleby and Basran 2022). In this partnership model, AI is not a replacement for veterinarians but rather a complementary tool that enhances their capabilities and extends their reach (Currie et al. 2023). The key benefit of the veterinarian-AI partnership is the potential to leverage AI's computational power to process extensive data quickly and efficiently (Currie et al. 2023). This enables veterinarians to make evidence-based decisions in real-time, resulting in accurate diagnoses and personalized treatment plans (Bouchemla et al. 2023). Moreover, AI algorithms learn and improve continuously, adapting to new information and refining their diagnostic accuracy. By incorporating feedback from veterinary professionals, AI systems can become increasingly sophisticated and effective in assisting with clinical decision-making (Currie et al. 2023). However, it is necessary to identify the limitations of AI and the importance of human oversight in the veterinarian-AI partnership. Veterinary professionals play a crucial role in validating AI-generated recommendations, ensuring their clinical relevance, and providing context-specific insights that AI may overlook (Currie et al. 2023). Additionally, veterinarians communicate effectively with clients, interpret AI-generated findings, and integrate them into comprehensive patient care plans.

As the integration of AI technologies advances, there is a pressing need to address regulatory and ethical issues to ensure the safe and effective use of AI systems in animal health (Bouchemla et al. 2023). One of the primary challenges is overcoming regulatory deficits that may hinder the widespread adoption of AI technologies in veterinary medicine (Bellamy 2023). Regulatory bodies should generate frameworks tailored explicitly to the use of AI systems in veterinary practice (Hooper et al. 2023). The potential for incorrect decisions by AI algorithms and the ambiguity surrounding liability for erroneous AI decisions raise

concerns within the veterinary community (Cohen and Gordon 2022). Veterinary professionals, policymakers, and legal experts must collaborate to establish clear guidelines for accountability and liability in cases involving AI systems in diagnostic or treatment decisions (Hooper et al. 2023). This may involve defining the responsibilities of veterinarians, AI developers, and pet owners in case of adverse outcomes resulting from AI-assisted procedures. Developing a robust regulatory structure for AI systems in veterinary practice is essential to ensure patient safety, uphold professional standards, and mitigate potential risks (Bellamy 2023).

Furthermore, the veterinary profession may need to revise its ethical guidelines for integrating AI technologies (Bellamy 2023). Ethical considerations surrounding issues such as patient autonomy, informed consent, and the veterinarian-client-patient relationship may need to be reexamined in AI-assisted veterinary care (Hooper et al. 2023). Veterinarians must uphold the highest ethical standards while leveraging AI technologies to enhance patient care (Marks 2024). In addition to regulatory and ethical considerations, education and training will prepare veterinary professionals to use AI systems in practice (Currie et al. 2023). Continuing education programs should incorporate training on AI technologies and critical appraisal of AI-generated recommendations to ensure veterinarians can access knowledge and skills to effectively integrate AI into their clinical workflows (Marks 2024).

## Conclusion and prospects

AI accelerates the pace of veterinary research and drug development. ML algorithms can analyze complex veterinary data and identify potential drug candidates. This expedites the discovery process and contributes to developing novel therapies for various veterinary conditions. The prospects of AI in veterinary science are undeniably transformative, redefining animal healthcare. AI offers a spectrum of benefits from rapid and precise diagnostics to personalized treatment plans and proactive disease management. However, embracing this future requires careful navigation of ethical considerations and a collaborative synergy between human expertise and AI capabilities.

AI-driven diagnostic tools can analyze massive datasets with unprecedented speed and accuracy. This accelerates the diagnostic process and enhances precision, allowing veterinarians to make informed decisions swiftly. AI algorithms excel at identifying patterns and trends. In veterinary science, predictive models can anticipate disease outbreaks, track zoonotic disease spread, and even predict individual health risks for animals. This proactive approach enables preventive measures and early interventions, ultimately improving animal health. Tailoring treatment plans to individual animals becomes more feasible with AI. AI can recommend personalized medications, dietary plans, and

rehabilitation strategies by analyzing genetic, environmental, and historical data. This individualized approach optimizes treatment outcomes and enhances the well-being of each animal. AI facilitates remote monitoring, allowing veterinarians to track animals' vital signs, detect anomalies, and provide timely interventions, even from a distance. AI-powered telemedicine enables consultations and follow-ups, overcoming geographical barriers and ensuring that animals receive continuous care.

Addressing regulatory deficits and ethical issues surrounding AI use in veterinary practice is essential while safeguarding animal health and welfare. By developing clear regulatory frameworks, fostering ethical discussions, and providing comprehensive education and training, the veterinary profession can embrace AI as an important tool in advancing veterinary care. AI can reform how we diagnose and treat animals, with applications ranging from analyzing medical images for faster and more accurate diagnoses to developing personalized treatment plans. AI-powered tools can also predict disease outbreaks, improve surgical precision through robotic assistance, and accelerate the discovery of new medications. These advancements promise significant benefits, including improved accuracy in veterinary care, earlier disease detection, and faster animal recovery times. However, challenges remain. Large datasets of veterinary medical data are required to train AI models effectively, and the cost of implementing these technologies can be a hurdle for veterinary practices. Ethical considerations surrounding bias in algorithms and potential job displacement for veterinarians need careful attention. Additionally, regulatory frameworks must be established for AI's ethical and safe use in animal healthcare. By acknowledging these issues and working towards solutions, we can tap the transformative potential of AI and ensure a future of improved animal health and well-being. As we unleash AI in veterinary science, a new era of compassionate, data-driven, and efficient animal care emerges, promising a healthier future for our animal companions.

#### Acknowledgments

The authors thank the Director, ICAR-Indian Veterinary Research Institute, Izatnagar, Bareilly, India, and the All-India Network Program on Diagnostic Imaging and Management of Surgical Conditions in Animals (AINP-DIMSCA) for providing the necessary facilities to carry out this work.

#### Ethical Approval

Not applicable.

#### CRedit authorship contribution statement

Khan Sharun: Writing – review & editing, Writing – original draft, Visualization, Methodology, Investigation, Formal analysis,

Conceptualization; S. Amitha Banu: Writing – review & editing, Writing – original draft; Merlin Mamachan: Writing – review & editing, Writing – original draft; Laith Abualigah: Writing – review & editing, Writing – original draft; A. M. Pawde: Writing – review & editing, Writing – original draft; Kuldeep Dhama: Writing – review & editing, Writing – original draft.

#### Funding

This compilation is a review article written, analyzed, and designed by its authors, and no substantial funding is required.

#### Declaration of Interest

All authors declare that no commercial or financial relationships exist that could, in any way, lead to a potential conflict of interest.

#### References

- Abani, S., Volk, H. A., De Decker, S., Fenn, J., Rusbridge, C., et al. (2023). ChatGPT and scientific papers in veterinary neurology; is the genie out of the bottle? *Frontiers in Veterinary Science*, *10*, 1272755. <https://doi.org/10.3389/fvets.2023.1272755>
- Adrien-Maxence, H., Emilie, B., Alois, D. L. C., Michelle, A., Kate, A., et al. (2022). Comparison of error rates between four pretrained DenseNet convolutional neural network models and 13 board-certified veterinary radiologists when evaluating 15 labels of canine thoracic radiographs. *Veterinary Radiology & Ultrasound: The Official Journal of the American College of Veterinary Radiology and the International Veterinary Radiology Association*, *63*(4), 456–468. <https://doi.org/10.1111/vru.13069>
- Akinsulie, O. C., Idris, I., Aliyu, V. A., Shahzad, S., Banwo, O. G., et al. (2024). The potential application of artificial intelligence in veterinary clinical practice and biomedical research. *Frontiers in Veterinary Science*, *11*, 1347550. <https://doi.org/10.3389/fvets.2024.1347550>
- Aldoseri, A., Al-Khalifa, K. N., & Hamouda, A. M. (2023). Rethinking data strategy and integration for artificial intelligence: Concepts, opportunities, and challenges. *Applied Sciences*, *13*(12), 7082.
- Alhasan, M., & Hasaneen, M. (2021). Digital imaging, technologies and artificial intelligence applications during COVID-19 pandemic. *Computerized Medical Imaging and Graphics*, *91*, 101933. <https://doi.org/10.1016/j.compmedimag.2021.101933>
- Alowais, S. A., Alghamdi, S. S., Alsuehaby, N., Alqahtani, T., Alshaya, A. I., et al. (2023). Revolutionizing healthcare: The role of artificial intelligence in clinical practice. *BMC Medical Education*, *23*(1), 689. <https://doi.org/10.1186/s12909-023-04698-z>

- Álvarez-Machancoses, Ó., & Fernández-Martínez, J. L. (2019). Using artificial intelligence methods to speed up drug discovery. *Expert Opinion on Drug Discovery*, 14(8), 769–777. <https://doi.org/10.1080/17460441.2019.1621284>
- Alzubaidi, L., Zhang, J., Humaidi, A. J., Al-Dujaili, A., Duan, Y., et al. (2021). Review of deep learning: Concepts, CNN architectures, challenges, applications, future directions. *Journal of Big Data*, 8(1), 53. <https://doi.org/10.1186/s40537-021-00444-8>
- Anholt, R. M., Berezowski, J., Maclean, K., Russell, M. L., Jamal, I., & Stephen, C. (2014). The application of medical informatics to the veterinary management programs at companion animal practices in Alberta, Canada: A case study. *Preventive Veterinary Medicine*, 113(2), 165–174. <https://doi.org/10.1016/j.prevetmed.2013.11.005>
- Appleby, R. B., & Basran, P. S. (2022). Artificial intelligence in veterinary medicine. *Journal of the American Veterinary Medical Association*, 260(8), 819–824. <https://doi.org/10.2460/javma.22.03.0093>
- Aubreville, M., Bertram, C. A., Marzahl, C., Gurtner, C., Dettwiler, M., et al. (2020). Deep learning algorithms out-perform veterinary pathologists in detecting the mitotically most active tumor region. *Scientific Reports*, 10(1), 16447. <https://doi.org/10.1038/s41598-020-73246-2>
- Alwaysheh, A., Wilcke, J., Elvinger, F., Rees, L., Fan, W., & Zimmerman, K. L. (2019). Review of Medical Decision Support and Machine-Learning Methods. *Veterinary Pathology*, 56(4), 512–525. <https://doi.org/10.1177/0300985819829524>
- Bansal, G. J. (2006). Digital radiography. A comparison with modern conventional imaging. *Postgraduate Medical Journal*, 82(969), 425–428. <https://doi.org/10.1136/pgmj.2005.038448>
- Bellamy, J. E. C. (2023). Artificial intelligence in veterinary medicine requires regulation. *The Canadian Veterinary Journal = La Revue Veterinaire Canadienne*, 64(10), 968–970.
- Benjamins, S., Dhunoo, P., & Meskó, B. (2020). The state of artificial intelligence-based FDA-approved medical devices and algorithms: An online database. *NPJ Digital Medicine*, 3, 118. <https://doi.org/10.1038/s41746-020-00324-0>
- Blanco-González, A., Cabezón, A., Seco-González, A., Conde-Torres, D., Antelo-Riveiro, P., Piñeiro, Á., & Garcia-Fandino, R. (2023). The Role of AI in Drug Discovery: Challenges, Opportunities, and Strategies. *Pharmaceuticals (Basel, Switzerland)*, 16(6), 891. <https://doi.org/10.3390/ph16060891>
- Bohr, A., & Memarzadeh, K. (2020). The rise of artificial intelligence in healthcare applications. *Artificial Intelligence in Healthcare*, 25–60. <https://doi.org/10.1016/B978-0-12-818438-7.00002-2>
- Boissady, E., de La Comble, A., Zhu, X., & Hespel, A.M. (2020). Artificial intelligence evaluating primary thoracic lesions has an overall lower error rate compared to veterinarians or veterinarians in conjunction with the artificial intelligence. *Veterinary Radiology & Ultrasound: The Official Journal of the American College of Veterinary Radiology and the International Veterinary Radiology Association*, 61(6), 619–627. <https://doi.org/10.1111/vru.12912>
- Bollig, N., Clarke, L., Elsmo, E., & Craven, M. (2020). Machine learning for syndromic surveillance using veterinary necropsy reports. *PLoS One*, 15(2), e0228105. <https://doi.org/10.1371/journal.pone.0228105>
- Bouchemla, F., Akchurin, S. V., Akchurina, I. V., Dyulger, G. P., Latynina, E. S., & Grecheneva, A. V. (2023). Artificial intelligence feasibility in veterinary medicine: A systematic review. *Veterinary World*, 16(10), 2143–2149. <https://doi.org/10.14202/vetworld.2023.2143-2149>
- Bouhali, O., Bensmail, H., Sheharyar, A., David, F., & Johnson, J. P. (2022). A Review of Radiomics and Artificial Intelligence and Their Application in Veterinary Diagnostic Imaging. *Veterinary Sciences*, 9(11), 620. <https://doi.org/10.3390/vetsci9110620>
- Burrell, D. N. (2023). Dynamic Evaluation Approaches to Telehealth Technologies and Artificial Intelligence (AI) Telemedicine Applications in Healthcare and Biotechnology Organizations. *Merits*, 3(4), Article 4. <https://doi.org/10.3390/merits3040042>
- Burti, S., Longhin Osti, V., Zotti, A., & Banzato, T. (2020). Use of deep learning to detect cardiomegaly on thoracic radiographs in dogs. *Veterinary Journal (London, England: 1997)*, 262, 105505. <https://doi.org/10.1016/j.tvjl.2020.105505>
- Carotenuto, G., Malerba, E., Dolfini, C., Brugnoli, F., Giannuzzi, P., Semprini, G., Tosolini, P., & Fracassi, F. (2019). Cushing's syndrome—an epidemiological study based on a canine population of 21,281 dogs. *Open Veterinary Journal*, 9(1), 27–32. <https://doi.org/10.4314/ovj.v9i1.5>
- Carovac, A., Smajlovic, F., & Junuzovic, D. (2011). Application of Ultrasound in Medicine. *Acta Informatica Medica*, 19(3), 168–171. <https://doi.org/10.5455/aim.2011.19.168-171>
- Celniak, W., Wodziński, M., Jurgas, A., Burti, S., Zotti, A., Atzori, M., Müller, H., & Banzato, T. (2023). Improving the classification of veterinary thoracic radiographs through inter-species and inter-pathology self-supervised pre-training of deep learning models.



- Scientific Reports*, 13(1), 19518. <https://doi.org/10.1038/s41598-023-46345-z>
- Chan, H. C. S., Shan, H., Dahoun, T., Vogel, H., & Yuan, S. (2019). Advancing Drug Discovery via Artificial Intelligence. *Trends in Pharmacological Sciences*, 40(8), 592–604. <https://doi.org/10.1016/j.tips.2019.06.004>
- Cohen, E. B., & Gordon, I. K. (2022). First, do no harm. Ethical and legal issues of artificial intelligence and machine learning in veterinary radiology and radiation oncology. *Veterinary Radiology & Ultrasound*, 63(Suppl 1), 840–850. <https://doi.org/10.1111/vru.13171>
- Coleman, M. C., & Moore, J. N. (2024). Two artificial intelligence models underperform on examinations in a veterinary curriculum. *Journal of the American Veterinary Medical Association*, 1–6. <https://doi.org/10.2460/javma.23.12.0666>
- Cravero, A., Pardo, S., Sepúlveda, S., & Muñoz, L. (2022). Challenges to Use Machine Learning in Agricultural Big Data: A Systematic Literature Review. *Agronomy*, 12(3), Article 3. <https://doi.org/10.3390/agronomy12030748>
- Currie, G., Hespel, A.M., & Carstens, A. (2023). Australian perspectives on artificial intelligence in veterinary practice. *Veterinary Radiology & Ultrasound: The Official Journal of the American College of Veterinary Radiology and the International Veterinary Radiology Association*, 64(3), 473–483. <https://doi.org/10.1111/vru.13234>
- Dave, T., Athaluri, S. A., & Singh, S. (2023). ChatGPT in medicine: An overview of its applications, advantages, limitations, future prospects, and ethical considerations. *Frontiers in Artificial Intelligence*, 6, 1169595. <https://doi.org/10.3389/frai.2023.1169595>
- Davenport, T., & Kalakota, R. (2019). The potential for artificial intelligence in healthcare. *Future Healthcare Journal*, 6(2), 94–98. <https://doi.org/10.7861/futurehosp.6-2-94>
- de Manuel, A., Delgado, J., Parra Jounou, I., Ausín, T., Casacuberta, D., et al. (2023). Ethical assessments and mitigation strategies for biases in AI-systems used during the COVID-19 pandemic. *Big Data & Society*, 10(1), 20539517231179199. <https://doi.org/10.1177/20539517231179199>
- de Melo, R. T., Rossi, D. A., Monteiro, G. P., & Fernandez, H. (2020). Veterinarians and One Health in the Fight Against Zoonoses Such as COVID-19. *Frontiers in Veterinary Science*, 7, 576262. <https://doi.org/10.3389/fvets.2020.576262>
- Dumortier, L., Guépin, F., Delignette-Muller, M.L., Boulocher, C., & Grenier, T. (2022). Deep learning in veterinary medicine, an approach based on CNN to detect pulmonary abnormalities from lateral thoracic radiographs in cats. *Scientific Reports*, 12(1), 11418. <https://doi.org/10.1038/s41598-022-14993-2>
- Elahi, M., Afolaranmi, S. O., Martinez Lastra, J. L., & Perez Garcia, J. A. (2023). A comprehensive literature review of the applications of AI techniques through the lifecycle of industrial equipment. *Discover Artificial Intelligence*, 3(1), 43. <https://doi.org/10.1007/s44163-023-00089-x>
- Elsohaby, I., & Villa, L. (2023). Zoonotic diseases: Understanding the risks and mitigating the threats. *BMC Veterinary Research*, 19(1), 186. <https://doi.org/10.1186/s12917-023-03736-8>
- Ezanno, P., Picault, S., Beaunée, G., Bailly, X., Muñoz, F., Duboz, R., Monod, H., & Guégan, J.F. (2021). Research perspectives on animal health in the era of artificial intelligence. *Veterinary Research*, 52(1), 40. <https://doi.org/10.1186/s13567-021-00902-4>
- Ganasegeran, K., & Abdulrahman, S. A. (2019). Artificial Intelligence Applications in Tracking Health Behaviors During Disease Epidemics. *Human Behaviour Analysis Using Intelligent Systems*, 6, 141–155. [https://doi.org/10.1007/978-3-030-35139-7\\_7](https://doi.org/10.1007/978-3-030-35139-7_7)
- Gerke, S., Minssen, T., & Cohen, G. (2020). Ethical and legal challenges of artificial intelligence-driven healthcare. *Artificial Intelligence in Healthcare*, 295–336. <https://doi.org/10.1016/B978-0-12-818438-7.00012-5>
- Guitian, J., Arnold, M., Chang, Y., & Snary, E. L. (2023). Applications of machine learning in animal and veterinary public health surveillance. *Revue Scientifique Et Technique (International Office of Epizootics)*, 42, 230–241. <https://doi.org/10.20506/rst.42.3366>
- Han, R., Yoon, H., Kim, G., Lee, H., & Lee, Y. (2023). Revolutionizing Medicinal Chemistry: The Application of Artificial Intelligence (AI) in Early Drug Discovery. *Pharmaceuticals (Basel, Switzerland)*, 16(9), 1259. <https://doi.org/10.3390/ph16091259>
- Hangl, J., Krause, S., & Behrens, V. J. (2023). Drivers, barriers and social considerations for AI adoption in SCM. *Technology in Society*, 74, 102299. <https://doi.org/10.1016/j.techsoc.2023.102299>
- Hennessey, E., DiFazio, M., Hennessey, R., & Cassel, N. (2022). Artificial intelligence in veterinary diagnostic imaging: A literature review. *Veterinary Radiology & Ultrasound: The Official Journal of the American College of Veterinary Radiology and the International Veterinary Radiology Association*, 63 Suppl 1, 851–870. <https://doi.org/10.1111/vru.13163>
- Hespel, A.M., Zhang, Y., & Basran, P. S. (2022). Artificial intelligence 101 for veterinary diagnostic imaging. *Veterinary*

- Radiology & Ultrasound: The Official Journal of the American College of Veterinary Radiology and the International Veterinary Radiology Association*, 63 Suppl 1, 817–827. <https://doi.org/10.1111/vru.13160>
- Ho, C. W. L., Soon, D., Caals, K., & Kapur, J. (2019). Governance of automated image analysis and artificial intelligence analytics in healthcare. *Clinical Radiology*, 74(5), 329–337. <https://doi.org/10.1016/j.crad.2019.02.005>
- Hooper, S. E., Hecker, K. G., & Artemiou, E. (2023). Using Machine Learning in Veterinary Medical Education: An Introduction for Veterinary Medicine Educators. *Veterinary Sciences*, 10(9), 537. <https://doi.org/10.3390/vetsci10090537>
- Huang, D.H., & Chueh, H.E. (2021). Chatbot usage intention analysis: Veterinary consultation. *Journal of Innovation & Knowledge*, 6(3), 135–144. <https://doi.org/10.1016/j.jik.2020.09.002>
- Hur, B., Hardefeldt, L. Y., Verspoor, K., Baldwin, T., & Gilkerson, J. R. (2022). Overcoming challenges in extracting prescribing habits from veterinary clinics using big data and deep learning. *Australian Veterinary Journal*, 100(5), 220–222. <https://doi.org/10.1111/avj.13145>
- Ibrahim, A., Lashen, A., Toss, M., Mihai, R., & Rakha, E. (2022). Assessment of mitotic activity in breast cancer: Revisited in the digital pathology era. *Journal of Clinical Pathology*, 75(6), 365–372. <https://doi.org/10.1136/jclinpath-2021-207742>
- Javaid, M., Haleem, A., Khan, I. H., & Suman, R. (2023). Understanding the potential applications of Artificial Intelligence in Agriculture Sector. *Advanced Agrochem*, 2(1), 15–30. <https://doi.org/10.1016/j.aac.2022.10.001>
- Jiang, B., Yin, X., & Song, H. (2020a). Single-stream long-term optical flow convolution network for action recognition of lameness dairy cow. *Computers and Electronics in Agriculture*, 175, 105536. <https://doi.org/10.1016/j.compag.2020.105536>
- Jiang, T., Gradus, J. L., & Rosellini, A. J. (2020b). Supervised Machine Learning: A Brief Primer. *Behavior Therapy*, 51(5), 675–687. <https://doi.org/10.1016/j.beth.2020.05.002>
- Jiang, Y., Irvin, J. A., Ng, A. Y., & Zou, J. (2024). VetLLM: Large Language Model for Predicting Diagnosis from Veterinary Notes. *Pacific Symposium on Biocomputing. Pacific Symposium on Biocomputing*, 29, 120–133.
- Johnson, K. B., Wei, W.Q., Weeraratne, D., Frisse, M. E., Misulis, K., Rhee, K., Zhao, J., & Snowdon, J. L. (2021). Precision Medicine, AI, and the Future of Personalized Health Care. *Clinical and Translational Science*, 14(1), 86–93. <https://doi.org/10.1111/cts.12884>
- Joslyn, S., & Alexander, K. (2022). Evaluating artificial intelligence algorithms for use in veterinary radiology. *Veterinary Radiology & Ultrasound: The Official Journal of the American College of Veterinary Radiology and the International Veterinary Radiology Association*, 63 Suppl 1, 871–879. <https://doi.org/10.1111/vru.13159>
- Kamel Boulos, M. N., Peng, G., & VoPham, T. (2019). An overview of GeoAI applications in health and healthcare. *International Journal of Health Geographics*, 18, 7. <https://doi.org/10.1186/s12942-019-0171-2>
- Kim, E., Fischetti, A. J., Sreetharan, P., Weltman, J. G., & Fox, P. R. (2022). Comparison of artificial intelligence to the veterinary radiologist's diagnosis of canine cardiogenic pulmonary edema. *Veterinary Radiology & Ultrasound: The Official Journal of the American College of Veterinary Radiology and the International Veterinary Radiology Association*, 63(3), 292–297. <https://doi.org/10.1111/vru.13062>
- La Perle, K. M. D. (2019). Machine Learning and Veterinary Pathology: Be Not Afraid! *Veterinary Pathology*, 56(4), 506–507. <https://doi.org/10.1177/0300985819848504>
- Leary, D., & Basran, P. S. (2022). The role of artificial intelligence in veterinary radiation oncology. *Veterinary Radiology & Ultrasound: The Official Journal of the American College of Veterinary Radiology and the International Veterinary Radiology Association*, 63 Suppl 1, 903–912. <https://doi.org/10.1111/vru.13162>
- Li, S., Wang, Z., Visser, L. C., Wisner, E. R., & Cheng, H. (2020). Pilot study: Application of artificial intelligence for detecting left atrial enlargement on canine thoracic radiographs. *Veterinary Radiology & Ultrasound: The Official Journal of the American College of Veterinary Radiology and the International Veterinary Radiology Association*, 61(6), 611–618. <https://doi.org/10.1111/vru.12901>
- Lungren, M. P., & Wilson, D. U. (2022). Artificial intelligence in veterinary care will be a major driving force behind ai advancements in healthcare. *Veterinary Radiology & Ultrasound: The Official Journal of the American College of Veterinary Radiology and the International Veterinary Radiology Association*, 63 Suppl 1, 913–915. <https://doi.org/10.1111/vru.13161>
- Lustgarten, J. L., Zehnder, A., Shipman, W., Ganchar, E., & Webb, T. L. (2020). Veterinary informatics: Forging the future between veterinary medicine, human medicine, and One Health initiatives—a joint paper by the Association for Veterinary Informatics (AVI) and the CTSA One Health Alliance (COHA). *JAMIA Open*, 3(2), 306–317. <https://doi.org/10.1093/jamiaopen/ooaa005>
- Lynch, S. R., Bothwell, T., & SUSTAIN Task Force on Iron Powders. (2007). A comparison of physical properties, screening

- procedures and a human efficacy trial for predicting the bioavailability of commercial elemental iron powders used for food fortification. *International Journal for Vitamin and Nutrition Research. Internationale Zeitschrift Fur Vitamin- Und Ernährungsforschung. Journal International De Vitaminologie Et De Nutrition*, 77(2), 107–124. <https://doi.org/10.1024/0300-9831.77.2.107>
- Marks, N. (2024). The Progressive Veterinary Practice. *The Veterinary Clinics of North America. Small Animal Practice*, 54(2), 265–276. <https://doi.org/10.1016/j.cvsm.2023.10.011>
- Mennella, C., Maniscalco, U., De Pietro, G., & Esposito, M. (2024). Ethical and regulatory challenges of AI technologies in healthcare: A narrative review. *Heliyon*, 10(4), e26297. <https://doi.org/10.1016/j.heliyon.2024.e26297>
- Müller, T. R., Solano, M., & Tsunemi, M. H. (2022). Accuracy of artificial intelligence software for the detection of confirmed pleural effusion in thoracic radiographs in dogs. *Veterinary Radiology & Ultrasound: The Official Journal of the American College of Veterinary Radiology and the International Veterinary Radiology Association*, 63(5), 573–579. <https://doi.org/10.1111/vru.13089>
- Naik, N., Hameed, B. M. Z., Shetty, D. K., Swain, D., Shah, M., et al. (2022). Legal and Ethical Consideration in Artificial Intelligence in Healthcare: Who Takes Responsibility? *Frontiers in Surgery*, 9, 862322. <https://doi.org/10.3389/fsurg.2022.862322>
- Najjar, R. (2023). Redefining Radiology: A Review of Artificial Intelligence Integration in Medical Imaging. *Diagnostics (Basel, Switzerland)*, 13(17), 2760. <https://doi.org/10.3390/diagnostics13172760>
- Neethirajan, S. (2023). Artificial Intelligence and Sensor Technologies in Dairy Livestock Export: Charting a Digital Transformation. *Sensors (Basel, Switzerland)*, 23(16), 7045. <https://doi.org/10.3390/s23167045>
- Niazi, S. K. (2023). The Coming of Age of AI/ML in Drug Discovery, Development, Clinical Testing, and Manufacturing: The FDA Perspectives. *Drug Design, Development and Therapy*, 17, 2691–2725. <https://doi.org/10.2147/DDDT.S424991>
- Nie, A., Zehnder, A., Page, R. L., Zhang, Y., Pineda, A. L., Rivas, M. A., Bustamante, C. D., & Zou, J. (2018). DeepTag: Inferring diagnoses from veterinary clinical notes. *NPJ Digital Medicine*, 1, 60. <https://doi.org/10.1038/s41746-018-0067-8>
- Nitta, N., Sugimura, T., Isozaki, A., Mikami, H., Hiraki, K., et al. (2018). Intelligent Image-Activated Cell Sorting. *Cell*, 175(1), 266–276.e13. <https://doi.org/10.1016/j.cell.2018.08.028>
- Nosrati, H., & Nosrati, M. (2023). Artificial Intelligence in Regenerative Medicine: Applications and Implications. *Biomimetics*, 8(5), Article 5. <https://doi.org/10.3390/biomimetics8050442>
- Nyquist, M. L., Fink, L. A., Mauldin, G. E., & Coffman, C. R. (2024). Evaluation of a Novel Veterinary Dental Radiography Artificial Intelligence Software Program. *Journal of Veterinary Dentistry*, 8987564231221071. <https://doi.org/10.1177/08987564231221071>
- Ogilvie, T., & Kastelic, J. (2022). Technology is rapidly changing our world, including veterinary medicine. *The Canadian Veterinary Journal = La Revue Veterinaire Canadienne*, 63(12), 1177–1178.
- Olawade, D. B., Wada, O. J., David-Olawade, A. C., Kunonga, E., Abaire, O., & Ling, J. (2023). Using artificial intelligence to improve public health: A narrative review. *Frontiers in Public Health*, 11, 1196397. <https://doi.org/10.3389/fpubh.2023.1196397>
- Öztürk, H., Özgür, A., & Ozkirimli, E. (2018). DeepDTA: Deep drug-target binding affinity prediction. *Bioinformatics (Oxford, England)*, 34(17), i821–i829. <https://doi.org/10.1093/bioinformatics/bty593>
- Paudyal, R., Shah, A. D., Akin, O., Do, R. K. G., Konar, A. S., Hatzoglou, V., Mahmood, U., Lee, N., Wong, R. J., Banerjee, S., Shin, J., Veeraghavan, H., & Shukla-Dave, A. (2023). Artificial Intelligence in CT and MR Imaging for Oncological Applications. *Cancers*, 15(9), 2573. <https://doi.org/10.3390/cancers15092573>
- Paul, D., Sanap, G., Shenoy, S., Kalyane, D., Kalia, K., & Tekade, R. K. (2021). Artificial intelligence in drug discovery and development. *Drug Discovery Today*, 26(1), 80–93. <https://doi.org/10.1016/j.drudis.2020.10.010>
- Paynter, A. N., Dunbar, M. D., Creevy, K. E., & Rupple, A. (2021). Veterinary Big Data: When Data Goes to the Dogs. *Animals: An Open Access Journal from MDPI*, 11(7), 1872. <https://doi.org/10.3390/ani11071872>
- Pereira, A. I., Franco-Gonçalo, P., Leite, P., Ribeiro, A., Alves-Pimenta, M. S., Colaço, B., et al. (2023). Artificial Intelligence in Veterinary Imaging: An Overview. *Veterinary Sciences*, 10(5), 320. <https://doi.org/10.3390/vetsci10050320>
- Perera, T. R. W., Skerrett-Byrne, D. A., Gibb, Z., Nixon, B., & Swegen, A. (2022). The Future of Biomarkers in Veterinary Medicine: Emerging Approaches and Associated Challenges. *Animals: An Open Access Journal from MDPI*, 12(17), 2194. <https://doi.org/10.3390/ani12172194>
- Pomerantz, L. K., Solano, M., & Kalosa-Kenyon, E. (2023). Performance of a commercially available artificial intelligence

- software for the detection of confirmed pulmonary nodules and masses in canine thoracic radiography. *Veterinary Radiology & Ultrasound: The Official Journal of the American College of Veterinary Radiology and the International Veterinary Radiology Association*, 64(5), 881–889. <https://doi.org/10.1111/vru.13287>
- Pratiwi, R., Ramadhanti, S. P., Amatulloh, A., Megantara, S., & Subra, L. (2023). Recent Advances in the Determination of Veterinary Drug Residues in Food. *Foods (Basel, Switzerland)*, 12(18), 3422. <https://doi.org/10.3390/foods12183422>
- Qureshi, R., Irfan, M., Gondal, T. M., Khan, S., Wu, J., et al. (2023). AI in drug discovery and its clinical relevance. *Heliyon*, 9(7), e17575. <https://doi.org/10.1016/j.heliyon.2023.e17575>
- Rezaei, T., Khouzani, P. J., Khouzani, S. J., Fard, A. M., Rashidi, S., et al. (2023). Integrating Artificial Intelligence into Telemedicine: Revolutionizing Healthcare Delivery. *Kindle*, 3(1), 1–161.
- Rezayi, S., Niakan Kalhori, S. R., & Saeedi, S. (2022). Effectiveness of Artificial Intelligence for Personalized Medicine in Neoplasms: A Systematic Review. *BioMed Research International*, 2022, 7842566. <https://doi.org/10.1155/2022/7842566>
- Samui, P., & Kothari, D. P. (2011). Utilization of a least square support vector machine (LSSVM) for slope stability analysis. *Scientia Iranica*, 18(1), 53–58. <https://doi.org/10.1016/j.scient.2011.03.007>
- Sanchez-Lengeling, B., & Aspuru-Guzik, A. (2018). Inverse molecular design using machine learning: Generative models for matter engineering. *Science (New York, N.Y.)*, 361(6400), 360–365. <https://doi.org/10.1126/science.aat2663>
- Santamaria, S. L., & Zimmerman, K. L. (2011). Uses of informatics to solve real world problems in veterinary medicine. *Journal of Veterinary Medical Education*, 38(2), 103–109. <https://doi.org/10.3138/jvme.38.2.103>
- Sarker, I. H. (2021a). Deep Learning: A Comprehensive Overview on Techniques, Taxonomy, Applications and Research Directions. *SN Computer Science*, 2(6), 420. <https://doi.org/10.1007/s42979-021-00815-1>
- Sarker, I. H. (2021b). Machine Learning: Algorithms, Real-World Applications and Research Directions. *SN Computer Science*, 2(3), 160. <https://doi.org/10.1007/s42979-021-00592-x>
- Sarker, I. H. (2022). AI-Based Modeling: Techniques, Applications and Research Issues Towards Automation, Intelligent and Smart Systems. *SN Computer Science*, 3(2), 158. <https://doi.org/10.1007/s42979-022-01043-x>
- Schmid, D., Scholz, V. B., Kircher, P. R., & Lautenschlaeger, I. E. (2022). Employing deep convolutional neural networks for segmenting the medial retropharyngeal lymph nodes in CT studies of dogs. *Veterinary Radiology & Ultrasound: The Official Journal of the American College of Veterinary Radiology and the International Veterinary Radiology Association*, 63(6), 763–770. <https://doi.org/10.1111/vru.13132>
- Schofield, I., Brodbelt, D. C., Kennedy, N., Niessen, S. J. M., Church, D. B., Geddes, R. F., & O'Neill, D. G. (2021). Machine-learning based prediction of Cushing's syndrome in dogs attending UK primary-care veterinary practice. *Scientific Reports*, 11(1), 9035. <https://doi.org/10.1038/s41598-021-88440-z>
- Shaban-Nejad, A., Michalowski, M., & Buckeridge, D. L. (2018). Health intelligence: How artificial intelligence transforms population and personalized health. *Npj Digital Medicine*, 1(1), 1–2. <https://doi.org/10.1038/s41746-018-0058-9>
- Shaik, T., Tao, X., Higgins, N., Li, L., Gururajan, R., Zhou, X., & Acharya, U. R. (2023). Remote patient monitoring using artificial intelligence: Current state, applications, and challenges. *WIREs Data Mining and Knowledge Discovery*, 13(2), e1485. <https://doi.org/10.1002/widm.1485>
- Shajari, S., Kuruvinashetti, K., Komeili, A., & Sundararaj, U. (2023). The Emergence of AI-Based Wearable Sensors for Digital Health Technology: A Review. *Sensors (Basel, Switzerland)*, 23(23), 9498. <https://doi.org/10.3390/s23239498>
- Sharma, N., Sharma, R., & Jindal, N. (2021). Machine Learning and Deep Learning Applications-A Vision. *Global Transitions Proceedings*, 2(1), 24–28. <https://doi.org/10.1016/j.gltp.2021.01.004>
- Sharma, S., Rawal, R., & Shah, D. (2023). Addressing the challenges of AI-based telemedicine: Best practices and lessons learned. *Journal of Education and Health Promotion*, 12, 338. [https://doi.org/10.4103/jehp.jehp\\_402\\_23](https://doi.org/10.4103/jehp.jehp_402_23)
- Siachos, N., Neary, J. M., Smith, R. F., & Oikonomou, G. (2024). Automated dairy cattle lameness detection utilizing the power of artificial intelligence; current status quo and future research opportunities. *The Veterinary Journal*, 304, 106091. <https://doi.org/10.1016/j.tvjl.2024.106091>
- Taye, M. M. (2023). Understanding of Machine Learning with Deep Learning: Architectures, Workflow, Applications and Future Directions. *Computers*, 12(5), Article 5. <https://doi.org/10.3390/computers12050091>
- Vilhekar, R. S., & Rawekar, A. (2024). Artificial Intelligence in Genetics. *Cureus*, 16(1), e52035. <https://doi.org/10.7759/cureus.52035>



- Visan, A. I., & Negut, I. (2024). Integrating Artificial Intelligence for Drug Discovery in the Context of Revolutionizing Drug Delivery. *Life*, *14*(2), Article 2. <https://doi.org/10.3390/life14020233>
- von Lilienfeld, O. A. (2018). Quantum Machine Learning in Chemical Compound Space. *Angewandte Chemie International Edition*, *57*(16), 4164–4169. <https://doi.org/10.1002/anie.201709686>
- Vora, L. K., Gholap, A. D., Jetha, K., Thakur, R. R. S., Solanki, H. K., & Chavda, V. P. (2023). Artificial Intelligence in Pharmaceutical Technology and Drug Delivery Design. *Pharmaceutics*, *15*(7), 1916. <https://doi.org/10.3390/pharmaceutics15071916>
- Wu, K., Li, X., Zhou, Z., Zhao, Y., Su, M., et al. (2024). Predicting pharmacodynamic effects through early drug discovery with artificial intelligence-physiologically based pharmacokinetic (AI-PBPK) modelling. *Frontiers in Pharmacology*, *15*. <https://doi.org/10.3389/fphar.2024.1330855>
- Xu, Y., Liu, X., Cao, X., Huang, C., Liu, E., et al. (2021). Artificial intelligence: A powerful paradigm for scientific research. *Innovation (Cambridge (Mass.))*, *2*(4), 100179. <https://doi.org/10.1016/j.xinn.2021.100179>
- Yang, S., & Kar, S. (2023). Application of artificial intelligence and machine learning in early detection of adverse drug reactions (ADRs) and drug-induced toxicity. *Artificial Intelligence Chemistry*, *1*(2), 100011. <https://doi.org/10.1016/j.aichem.2023.100011>
- Yelne, S., Chaudhary, M., Dod, K., Sayyad, A., & Sharma, R. (2023). Harnessing the Power of AI: A Comprehensive Review of Its Impact and Challenges in Nursing Science and Healthcare. *Cureus*, *15*(11), e49252. <https://doi.org/10.7759/cureus.49252>
- Yoon, Y., Hwang, T., & Lee, H. (2018). Prediction of radiographic abnormalities by the use of bag-of-features and convolutional neural networks. *Veterinary Journal (London, England: 1997)*, *237*, 43–48. <https://doi.org/10.1016/j.tvjl.2018.05.009>
- You, J., McLeod, R. D., & Hu, P. (2019). Predicting drug-target interaction network using deep learning model. *Computational Biology and Chemistry*, *80*, 90–101. <https://doi.org/10.1016/j.compbiolchem.2019.03.016>
- Zad, N., Tell, L. A., Ampadi Ramachandran, R., Xu, X., Riviere, J. E., et al. (2023). Development of machine learning algorithms to estimate maximum residue limits for veterinary medicines. *Food and Chemical Toxicology: An International Journal Published for the British Industrial Biological Research Association*, *179*, 113920. <https://doi.org/10.1016/j.fct.2023.113920>
- Zhang, L., Guo, W., Lv, C., Guo, M., Yang, M., Fu, Q., & Liu, X. (2024). Advancements in artificial intelligence technology for improving animal welfare: Current applications and research progress. *Animal Research and One Health*, *2*(1), 93–109. <https://doi.org/10.1002/aro2.44>
- Zhang, L., Tan, J., Han, D., & Zhu, H. (2017). From machine learning to deep learning: Progress in machine intelligence for rational drug discovery. *Drug Discovery Today*, *22*(11), 1680–1685. <https://doi.org/10.1016/j.drudis.2017.08.010>
- Zuraw, A., & Aeffner, F. (2022). Whole-slide imaging, tissue image analysis, and artificial intelligence in veterinary pathology: An updated introduction and review. *Veterinary Pathology*, *59*(1), 6–25. <https://doi.org/10.1177/03009858211040484>









## Journal of Experimental Biology and Agricultural Sciences

<http://www.jebas.org>

ISSN No. 2320 – 8694

### Biosynthesis of secondary metabolites in aromatic and medicinal plants in response to abiotic stresses: A review

J. Pradhan<sup>1</sup> , K. Pramanik<sup>2</sup> , A. Jaiswal<sup>1</sup> , G. Kumari<sup>1</sup> ,  
K. Prasad<sup>3</sup> , C. Jena<sup>2</sup> , Ashutosh K. Srivastava<sup>4\*</sup> 

<sup>1</sup>College of Basic Science & Humanities, Dr. Rajendra Prasad Central Agriculture University, Pusa, Samastipur, Bihar-848125, India

<sup>2</sup>M.S. Swaminathan School of Agriculture, Centurion University of Technology and Management, Paralakhemundi, Odisha-761211, India

<sup>3</sup>Tirhut College of Agriculture, Dr. Rajendra Prasad Central Agriculture University, Pusa, Samastipur, Bihar-848125, India

<sup>4</sup>Department of Basic Science, Rani Lakhmi Bai Central Agricultural University, Jhansi-284003, Uttar Pradesh, India

Received – May 31, 2024; Revision – June 01, 2024; Accepted – June 15, 2024

Available Online – July 15, 2024

DOI: [http://dx.doi.org/10.18006/2024.12\(3\).318.334](http://dx.doi.org/10.18006/2024.12(3).318.334)

#### KEYWORDS

Abiotic stress

Climate change

Secondary metabolites

MAPs

Medicine

#### ABSTRACT

Climate change has massive consequences on non-living factors in the environment, resulting in irregular precipitation, fluctuating atmospheric temperature, and variations in humidity. These changes cause biotic and abiotic stresses; plants must have defense mechanisms to survive. Therefore, plants divert some synthesized energy towards producing numerous plant secondary metabolites (PSMs), *viz.*, flavonoids, alkaloids, and essential oils. These compounds act as protections for the plants, helping them to survive under stressful conditions. Medicinal and aromatic plants (MAPs) are sessile organisms that are not immune to harmful consequences of various abiotic stresses in which the PSMs have an important role in acting against the adverse effects. In this regard, the MAPs have a coherent defense mechanism for abiotic stresses. The secondary metabolites produced by these plants are useful as medicines and aromatic products for humans. However, not all stresses produce high secondary metabolites, as their production is highly specific to certain stresses. This review provides a comprehensive understanding of secondary metabolite production under various stressful conditions, including extreme temperature, drought, water logging, salinity, harmful radiation, elevated levels of ozone and CO<sub>2</sub>, heavy metals, and agrochemicals on MAPs. Additionally, the production of these compounds can be modified by subjecting plants to various stressors. Many authors have reported on PSMs in MAPs, which need to be well documented and exploited for humankind.

\* Corresponding author

E-mail: [aksri\\_du@yahoo.com](mailto:aksri_du@yahoo.com) (Ashutosh K. Srivastava)

Peer review under responsibility of Journal of Experimental Biology and Agricultural Sciences.

Production and Hosting by Horizon Publisher India [HPI]  
(<http://www.horizonpublisherindia.in/>).  
All rights reserved.

All the articles published by [Journal of Experimental Biology and Agricultural Sciences](#) are licensed under a [Creative Commons Attribution-NonCommercial 4.0 International License](#) Based on a work at [www.jebas.org](http://www.jebas.org).



## 1 Introduction

Since time immemorial, plants have provided food, medicine and shelter for mankind. These generate a diverse kind of valuable primary and secondary metabolites. The primary metabolites have a vital role in the growth and development of plants, while the secondary metabolites participate in defense mechanisms against biotic and abiotic stresses. Climate change mainly, water stress, and heat stresses are found to affect plant morphology and physiology (Rodrigues et al. 2021), where the medicinal and aromatic plants are much more vulnerable to adverse conditions as per their biodiversity (Qaderi et al. 2023; Rahman et al. 2023). Human anthropogenic activities like rapid urbanization, industrialization, deforestation, automobiles, etc., lead to extreme changes in climatic conditions, resulting in the prevalence of unseasonal rainfall, extreme temperature, high wind, heavy snowfall, inundation of sea water, flood, drought, and rising pests population posing a significant risk for many plant species on earth including medicinal and aromatic plants (Figure 1). A defense response is evolved in plants by producing secondary metabolites (PSMs) to avoid cell and tissue injury (Yeshi et al. 2022). PSMs like terpenoids, alkaloids, and phenolic biochemicals form the major PSM group. It is reported that the medicinal and aromatic plants, as the sessile group of plants, are most evolved with the production of PSMs under even mild abiotic stresses without adversely impacting growth and development, while in some cases, the plant's performance may improve (Jampílek and Kráľová 2023). PSMs evolution may increase or decrease as per the intensity of environmental stresses (Liu et al. 2023). Secondary metabolite production was increased in *Thymus vulgaris*, *Rosmarinus officinalis*, and *Mentha pulégium* with the increase in temperature and water stress up to 50%, while further extreme

temperature and water pressure at 70% the levels of the compound depleted in plants (Laftouhi et al. 2023). The findings explained that the MAPs generate secondary metabolites (SMs) under non-living stresses to avoid interruption in the physiological process and damage to cells and tissues, though the extreme environment is quite detrimental. The growth and productivity of MAPs are strongly interrelated with the change in external climatic factors. Various researchers reported that plants have various responses like gene expression, physiological manipulation, architectural modification, and production of SMs to tackle the harmful effects of biotic and abiotic stresses (Mareri et al. 2022; Balfagón et al. 2022). The MAPs produce diverse secondary metabolites in low molecular weight such as alkaloids, flavonoids, phenolic compounds, steroids, terpenes, and anthocyanins, which are important for adaption, protection, and environment adjustment (Wink 2003). The production of these biochemical compounds is the main way they adapt to their environment (Figure 2) (Verma and Shukla 2015).

Medicinal and aromatic plants are cultivated for roots, leaves, bark, seeds, flowers, and stems, which are rich in secondary metabolites used for medicine, nutraceutical, perfumes, food flavour, soap, or cosmetics. As per the Food and Agriculture Organization (FAO), 60% of the world's population depends on these herbs for wellbeing and beauty (Mahajan et al. 2020), leading to huge exploitation. In addition, the alarming climate change has a dangerous impact on plant morphology and physiology of MAPs, which may cause their extinction. So, it is critical to study the impact of abiotic stressors on MAPs and to draw the attention of research personnel for its sustainable use in the future. This article elaborates on critical secondary metabolites in medicinal and aromatic plants and their synthesis under different abiotic stresses.

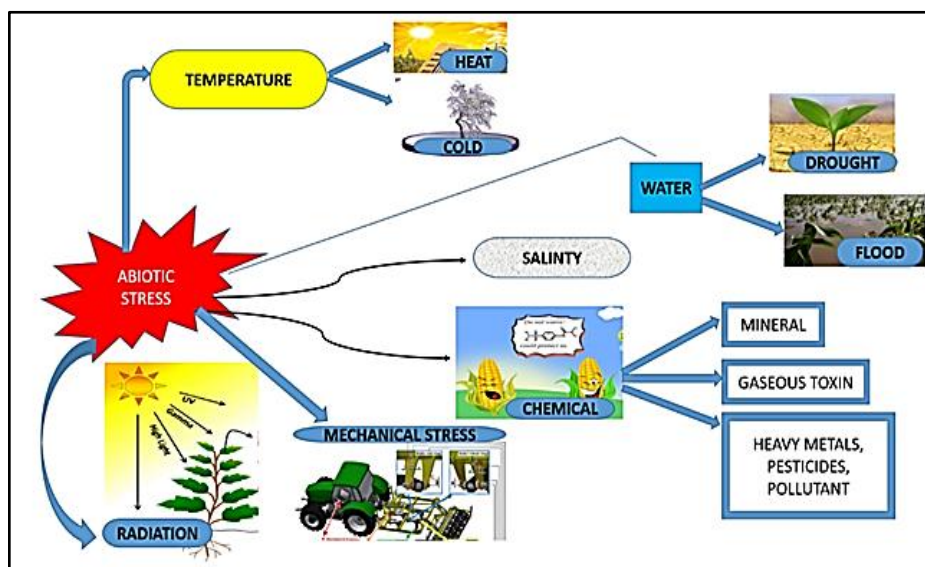


Figure 1 Various abiotic stresses affecting the growth and development of the plant

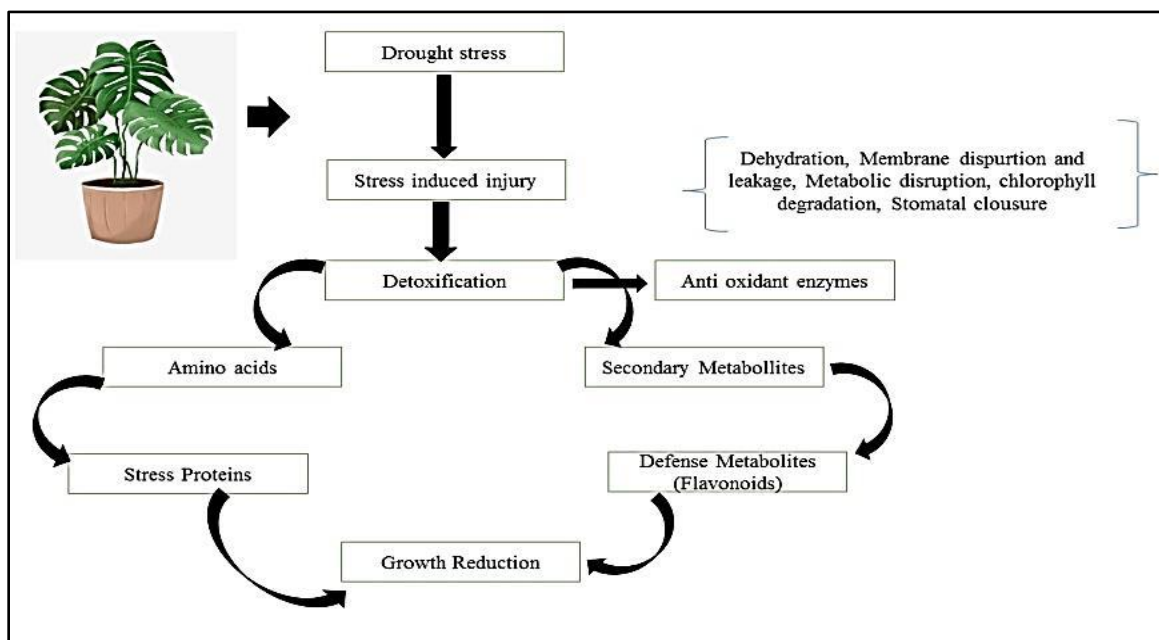


Figure 2 Illustrations of the effect of stress on plants growth and development

## 2 Secondary Metabolites and their Importance in Plants

Secondary metabolites (SMs) present in plants are among the most extensively studied chemicals due to their significant role in health, food, and beauty. The SMs have a direct correlation with morphological and physiological processes in plants. The plant is stunted under adverse conditions, which can be recovered by secondary metabolites generated in the plant body (Punetha et al. 2022). Several primary metabolites are produced in plants and can be easily extracted and crystallized, while the secondary metabolites are generated in extremely small quantities, and their extraction is complex and energy-intensive. Antibiotics and hormones are examples of secondary metabolites that are crucial for plant survival and growth. Plant secondary metabolites play more than one role in the plant metabolism process (Pagare et al. 2015). These metabolites impart a protection system when plants suffer biotic and abiotic stressors. Phenyl amides are formed, and polyamines are accumulated in beans and tobacco under abiotic stresses, explained the phytochemicals act as antioxidants to protect plants (Edreva et al. 2000). Likewise, accumulation of anthocyanin is observed in plants under the influence of drought, high light intensity, UV, wounds, disease attack, blue light expose, sugar and nutrient deficiencies (Winkel-Shirley 2001). The SMs are also crucial in plant pollination, chemical defense activities, molecule signaling, adaptation, seed dispersal, protection from insects, diseases, herbivores, and allelopathic injury (Pandita and Pandita 2021). The production and concentration of SMs are significantly affected by biotic factors, including insect and disease attacks (Taiz and Zeiger 2006). Plant secondary metabolites can also protect against various organisms, including fungi, bacteria,

viruses, nematodes, and insects (Tak and Kumar 2020). Examples of antimicrobial secondary metabolites plants use to defend against invaders include phytoalexins and phytoanticipins.

## 3 Use of SMs as medicine

In the present-day scenario, a large percentage of the global population still uses traditional medicine practices based on herbal medicines, which rely on the therapeutic qualities of plants (WHO 2013; Hosseinzadeh et al. 2015). Many plant-derived polyphenolic nutraceuticals or pharmaceuticals undergo initial transformations in the intestine via microbiota and enterocyte enzymes before being absorbed at the level of colonocyte and enterocyte. This process confers a broad range of consumer benefits, such as substantial protection against various pathogens, including bacteria and protozoa (Marin-Bruzos and Grayston 2019; Marin et al. 2015). This shows that the intricate relationship between secondary metabolites and human health underscores the continued importance of exploring their multifaceted roles in plant biology and therapeutic applications.

One of the untouched potent natural sources of antibacterial drugs is secondary plant metabolites. However, merely an insignificant fraction (< 1%) of tropical plant species on the planet has been subjected to phytochemical and pharmacological screening (Keita et al. 2022). Several bioactive secondary metabolites and their derivatives are produced by plants which have immense potential to be used as medications for the treatment of many disorders, such as cancer and neurological conditions, bacterial, fungal, and viral infections, and showed encouraging outcomes in the battle against



the spread of antibiotic-resistant bacteria (Lahlou 2013). Many of these metabolites have already been released onto the market or are currently being evaluated in clinical trials. Berberine, a natural compound obtained from plants, including *Rhizoma coptidis*, is effective against methicillin-resistant *Staphylococcus aureus* (MRSA) by preventing the formation of biofilms. Additionally, berberine has beneficial synergistic effects when taken with other antibiotics (Zuo et al. 2012; Chu et al. 2016; Zhang et al. 2020). Sulfur-containing allicin has been discovered to have wide antibacterial activity in contrast to gram +ve and -ve bacteria, *Streptococcus* sp., *E. coli*, MRSA, and *Salmonella enterica* (Barbieri et al. 2017). It is a derivative of raw garlic (*Allium sativum*). S-allylmercap to alteration of thiol-containing proteins by allicin reasons a reduction in glutathione levels, the progress of protein aggregation, and the deactivation of critical enzymes in bacteria (Wallock-Richards et al. 2014; Müller et al. 2016; Nakamoto et al. 2020). Piperine is an alkaloid found in the Piper species, such as *Piper longum* and *P. nigrum*, and has strong antimicrobial activity against both Gram+ve (*Bacillus subtilis* and *Staphylococcus aureus*) and Gram-ve bacteria (*Escherichia coli* and *Salmonella* sp.). It is an efflux pump inhibitor in *Staphylococcus aureus* when administered with ciprofloxacin (Hikal 2018). Ajoene, an organo-sulfur compound found in oil-macerated garlic, demonstrates antibacterial activity against various gram +ve and -ve bacteria (Bhatwalkar et al. 2021), and its mechanism of action is like allicin (Han et al. 2011). Eugenol, a hydroxyphenyl propene found in essential oils from the Lauraceae, Lamiaceae, Myristicaceae, and Myrtaceae families, exhibits various modes of action, such as disrupting the cell membrane of *Salmonella typhi*, inhibiting biofilm formation and enterotoxin production in *Streptococci*, and decreasing gene expression related to *S. aureus* contamination (Yadav et al. 2015). Moreover, eugenol hinders the synthesis of bacterial virulence agents like pyocyanin, violacein, and elastase (Marchese et al. 2017; Mak et al. 2019). Several plant species, including bananas, groundnuts, grapevines, pines, beans, pomegranates, and soybeans, contain resveratrol, a naturally occurring polyphenolic antioxidant with antibacterial properties against various Gram-negative and Gram-positive foodborne bacteria (Keita et al. 2022). Resveratrol inhibits toxin production, suppresses gene expression, impedes biofilm formation, interferes with motility, and disrupts quorum sensing in various fungal, bacterial, and viral species (Ma et al. 2018). Continued research into these natural compounds could lead to new treatments for infectious diseases and help address challenges posed by antimicrobial resistance.

#### 4 Influence of Abiotic Stresses on Secondary Metabolites (SMs) Production

The ability of plants to produce and aggregate (i.e., accumulate) phytochemicals is profoundly influenced by abiotic stresses such as temperature, soil, light intensity, and humidity (Radušienė et al.

2012). In addition, the production of plant secondary metabolites (SMs) can be influenced by minerals, radiation, heavy metals, and gaseous toxins (Akula and Ravishankar 2011). In order to adapt to varying environmental conditions, plants require acclimatization and adaptation, which leads to molecular, biochemical, physiological, and morphological responses. These responses may alter plant metabolic activity to decrease or repair damage caused by stress. This mechanism aims to safeguard the species' continual survival against certain growth conditions (Kapoor et al. 2020). In response to adverse environmental conditions, plants commonly produce reactive oxygen species (ROS), which are the final products of all stresses, such as superoxide ( $O_2^-$ ), hydroxyl radical (OH $\cdot$ ), and hydrogen peroxide ( $H_2O_2$ ) (Sharma et al. 2021). These can lead to cell damage by initiating an oxidative chain reaction called oxidative stress. As a countermeasure, plants employ secondary metabolism and other enzymatic and non-enzymatic processes to produce and store defensive chemicals. In nature, the intricate strategies employed by plants in response to environmental stresses highlight their remarkable capacity to adapt and survive through the synthesis and accumulation of protective phytochemicals.

Plants have limited mobility and a weak defense system, so they either change their orientation by moving or producing chemicals to defend themselves against environmental stress. When plants are under various environmental stresses, they typically produce and use more enzymes that help protect themselves, synthesizing secondary metabolite compounds. Chalcone synthase (CHS) and phenylalanine ammonia-lyase (PAL) are the enzymes that are essential in the synthesis of flavonoids. PAL (EC 4.1.3.5) plays a pivotal function in the defensive mechanisms of plants by producing phenol and lignin, while CHS (EC 2.3.1.74) is primarily responsible for the synthesis of flavonoids (Blanco-Ulate et al. 2015) (Figure 3).

Polyphenolic compounds, including flavonoids, proanthocyanidins, phenolic acids, and anthocyanins, can effectively reduce the harmful effects of salinity (Hichem and Mounir, 2009). This is because phenolic compounds possess antioxidant properties and function as ROS hunters. The production of these compounds typically occurs in response to biotic or abiotic stresses (D'Souza and Devaraj 2010). The synthesis and deposition of secondary metabolites are controlled by specific genes activated during the transcription stage. Certain transcription factors regulate the production and accumulation of these metabolites, with the total quantity depending on the expression of these genes. This process can produce numerous secondary metabolites through bioregulators and elicitors (Verma and Shukla 2015). This understanding enhances our knowledge of plant adaptation strategies and holds promise for applications in biotechnology and agriculture through controlled metabolite production (Table 1).

Table 1 Compilation of certain secondary metabolites and their respective roles

TERPENES		
Quinone	Helps in oxidation-reduction reaction	Yang et al. 2022
Pyrethroids	Highly toxic to insects	Meijar et al. 2024
$\beta$ - pinene, $\alpha$ -pinene, limonene and myrcene	Toxic to numerous insects and serious pests of conifers	Nikolić et al. 2024
Gossypol	Repellent to herbivores in cotton	Xie et al. 2024
Abscisic acid	A PGR, Stomatal closure, dormancy, abscission	Kumar et al. 2024
Abietic acid	Powerful new anticancer drug	Ahmad et al. 2024
Gibberellins	One of the major groups of phytohormones, role in seed germination	Hussain et al. 2024
Phorbol	Toxic to herbivorous mammal	Medina-Rodelo et al. 2024
Sterols	Components of cell membrane; Retard the permeability of small molecules by retarding the motion of fatty-acid chain	Samanta et al. 2024
Limonoids	Anti-herbivore compounds	Rzyska et al. 2024
Azadirachtin	Highly toxic to insects	Sarkar et al. 2024
Cardenolites	Used in the treatment of heart diseases	Akanmu et al. 2021
Saponins	Act as fungicide	Morcia et al. 2022
Yamogenin	Used in making birth control pills	Vishwakarma et al. 2022
Carotene and xanthophylls	Significant role in light-harvesting and shielding chlorophyll molecules against photo-oxidation	Sachdev et al. 2021
Rubber	It is a polyterpene from the latex of <i>Hevea brasiliensis</i>	Tran et al. 2023
PHENOLIC COMPOUNDS		
Protocatechuic acid and catechol	Protect onion bulbs against Smudge disease	Nag et al. 2024
Coumarins	Inhibit the growth of micro-organisms; with scopoletin are inhibitors of seed germination and cell elongation; stimulate the IAA oxidase	Wang et al. 2023
Lignin	Most abundant organic substance in plants, distributed in cell walls, tracheid, and vessels elements of the xylem, provides tensile strength and cementing of cell walls	Ghorbani et al. 2024
Anthocyanin	Get dissolved in the cell sap of epidermal cells and impart a bright color to flowers	Yoshida 2024
Quercetin	Bright yellow color of lemon juice	Tahosin et al. 2024
Flavonoids (flavones and flavanols)	Distributed in epidermal cells of green leaves and stems, they serve as UV-absorbing pigments, i.e., harmful to cells; legumes and nitrogen-fixing symbionts interact through substances excreted into the soil by legume roots	Guo et al. 2024
Tannins	A second large category of plant phenolics and astringent in taste, distributed in the cell sap, cell walls, barks, and leaves, accumulate in dead tissues; rich in unripe fruits; protect the plant against desiccation, decay, and injury by animals and microbes attack	Hameed et al. 2020
ALKALOIDS		
Anabasine	Synthesized in shoot of <i>Nicotiana glauca</i>	Zenkner et al. 2019
Ricine	Found in castor seeds	Yadav et al. 2022
Cocaine- atropine	Natural cocaine	Zamarripa et al. 2024
Reserpine	Collected from <i>Rauwolfia serpentina</i> and used for curing hypertension	Bankar et al. 2024
Strychnine	Obtained from <i>Strychnos nux-vomica</i> ; used as a poison for rats	Sadhunavar et al. 2015
Cinchonine and quinine	Extracted from the bark of Cinchona and used as a drug against malaria	Parveen et al. 2024
Colchicines	Inhibit the formation of spindle fiber formation during cell division; used in polyploidy formation	Ramirez-Castillo et al. 2024
Glycosinolates	Characteristic smell and taste of the members of the family Brassicaceae;	Raffo et al. 2024
Porphyrins	Constituent of chlorophyll and phytochrome	Ko et al. 2024

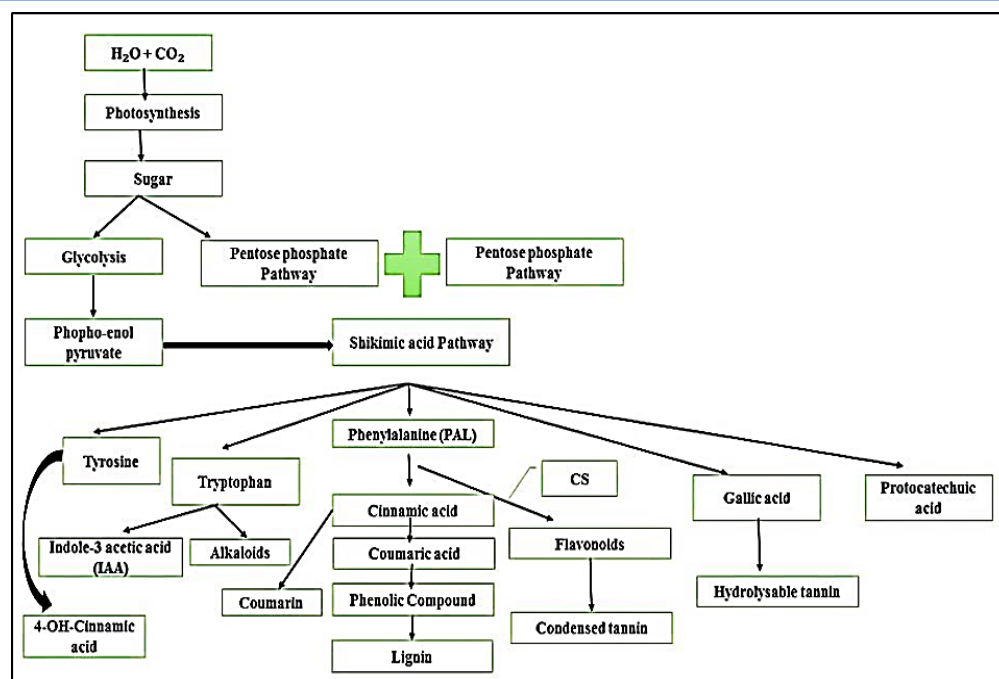


Figure 3 The concept of the Shikimic acid pathway

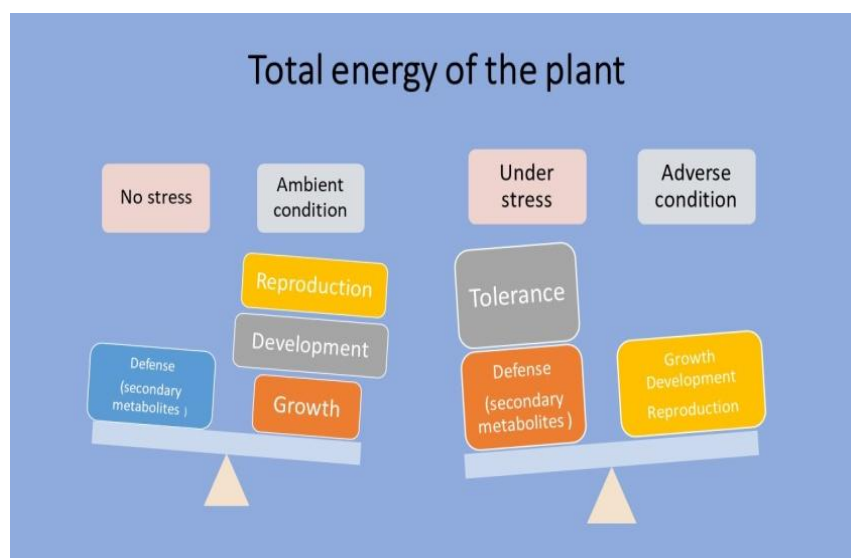


Figure 4 Secondary metabolites and the source sink balance hypothesis

#### 4.1 CO<sub>2</sub> concentration and its influence on SMs

The concentration of CO<sub>2</sub> in the air has a substantial influence on how plants utilize energy and develop. The equilibrium of carbon and nutrients, especially nitrogen, influences multiple growth, development, and differentiation processes. The alterations influence the relationship between the source-sink systems in the proportion of carbon allocated to growth, carbon-based secondary or structural components, and total non-structural carbohydrates (Figure 4). In the current climate change scenario, greenhouse

gases, mainly CO<sub>2</sub>, are rising sharply. Consequently, the C:N ratio is inappropriate, harming growth over time. Depiction of Figure 4 revealed that the allocation of resources between sources and sinks is influenced by the rise in CO<sub>2</sub> levels and the limited availability of nitrogen. Further, CO<sub>2</sub> influences source strength more than sink strength, while nutrient stress affects sink strength more. However, both are anticipated to boost the quantity of carbon-based secondary products in plant tissue. Some studies suggest that CO<sub>2</sub> can directly or indirectly influence *Taxus bacatta*, *H. perforatum*, and *Echinacea purpurea* to produce more secondary metabolites

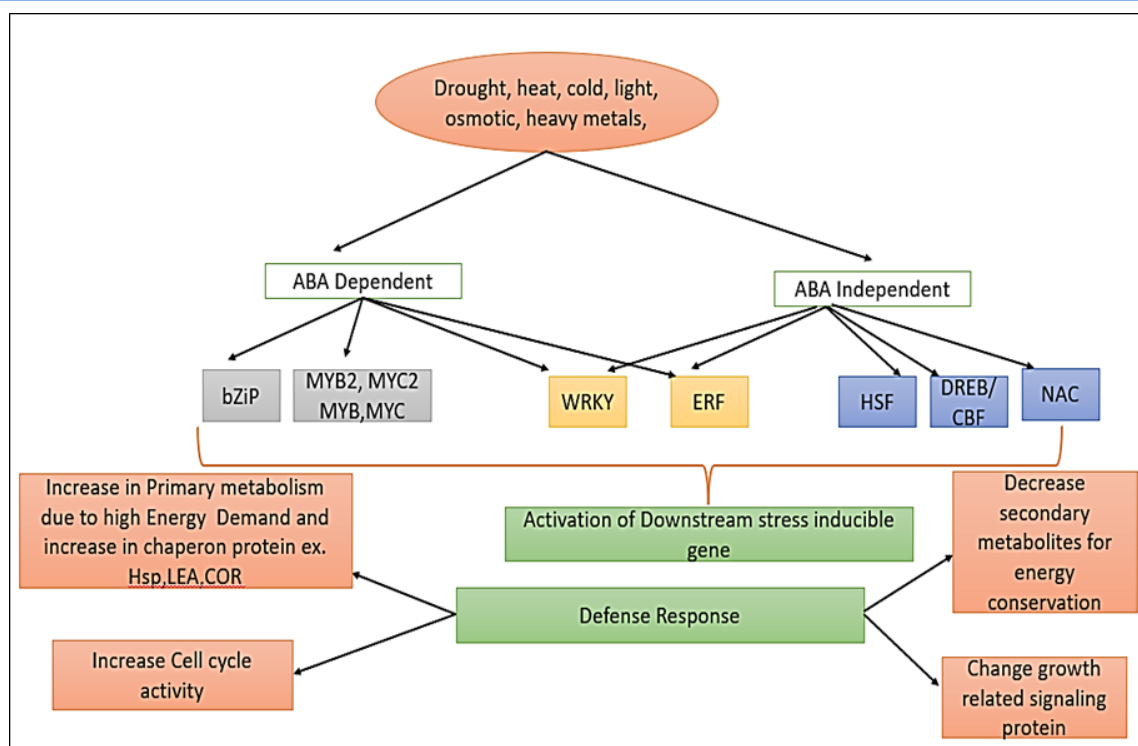


Figure 5 Effect of drought, heat, cold, light, osmotic, and heavy metal stress on secondary metabolite production

like phenols, flavonoids, lignins, nicotine, and coumarins (Savé et al. 2007). Further, Ibrahim et al. (2017) reported that elevated CO<sub>2</sub> levels increase phenol and flavonoid content in *Labisia pumila* plants. Similarly, lignins, nicotine, coumarins, and phenylpropanoids accumulate in tobacco plants after elevated CO<sub>2</sub> treatment (Li et al. 2018; Matros et al. 2006). Rising atmospheric CO<sub>2</sub> levels significantly influence how plants utilize energy and develop, impacting their carbon and nutrient balance. These changes highlight the intricate relationship between environmental shifts and plant biochemistry, with implications for ecological systems and agriculture.

#### 4.2 Impacts of Drought on SM Production

Plant morphology is directly affected by soil water content. A rain or soil water deficiency leads to drought stress, which decreases the plant's water potential and leaf turgidity. This, in turn, triggers or adjusts various biochemical and morpho-physiological components and wide-ranging genetic feedback based on the cultivar or species (Zhou et al. 2017). In order to survive, water-limited vegetation may postpone glucose accumulation and use carbon for secondary metabolism (Herms and Mattson 1992). Furthermore, drought increases the levels of isoprenoid abscisic acid in the leaf apoplastic area (Liu et al. 2005). Studies have shown that abscisic acid (ABA) treatment induces *Orthosiphon stamineus* to produce reactive oxygen species and secondary metabolites as a defence mechanism (Khan et al. 2011).

Plants generally produce bioactive chemicals such as phenolic compounds in response to water scarcity (Khan et al., 2011). Sampaio et al. (2016) found that water deprivation decreases the photosynthesis rate and increases ROS production and accumulation, resulting in increased phenolic compound production as a plant defence mechanism (Figure 5). Under mild water stress, *Labisia pumila* has more total flavonoids, anthocyanins, and phenolics than under severe stress (Jaafar et al. 2012). *Pisum sativum* cv. *meteor* under water deficit stress had higher anthocyanin and flavonoid content than well-watered controls (Nogués et al. 1998). Jaleel et al. (2007) observed that drought-induced oxidative stress enhanced the total alkaloid content in both the shoot and root of *Catharanthus roseus*. Further, drought stress also raised glycine betaine content in the *C. roseus* plant.

#### 4.3 Impacts of Salinity Stress on SMs Production

Salt stress causes plant ionic and osmotic stressors, which increase or reduce secondary metabolites. Antioxidant secondary metabolites help plants balance their oxidative state. Salt stress causes many metabolic changes in plants. Plants produce more suitable osmolytes (neutral, soluble organic compounds) to deal with salt stress (Nelson et al. 1998). Salinity stress raises sodium levels and causes cytoplasmic potassium imbalances. It creates ROS and inactivates and unsaturates numerous enzymes (Luo et al. 2005). Further, salt stress also increases proline aggregation



Table 2 Secondary Metabolite Production in Response to Salinity Stress in a Range of Species

S. N.	Plant species	Compounds	References
1.	<i>M. chamomilla</i>	Increase in phenolic acids, including chlorogenic, caffeic, and protocatechuic acid	Said-Al Ahl and Omer (2011); Abd El-Azim and Ahmed (2009)
2.	<i>Nigella sativa</i>	Increase in Phenols	Bourgou et al. (2008)
3.	<i>Mentha pulegium</i>	Increase in Phenols	Oueslati et al. (2010)
4.	<i>Matricaria reutita</i> <i>Satureja hartensis</i> <i>Salvia officinalis</i>	Increase in essential oil	Said-Al Ahl and Omer (2011)
5.	<i>Thymus maroccanus</i> <i>Origanum vulgare</i> <i>Mentha piperita</i> <i>Majorana hartensis</i> <i>Salvia officinalis</i> <i>M. chamomilla</i>	Decrease in essential oil	Said-Al Ahl and Omer (2011)
6.	<i>Plantago ovata</i>	Increase in proline, flavonoids, and saponins	Haghighi et al. (2012)

(Cardoso et al. 2019). Similarly, Akula and Ravishankar (2011) also suggested that salt stress can increase or reduce plant secondary metabolite levels through osmotic and ionic stress. Adaptation to stress involves alteration in proline metabolism. Proline dehydrogenase and 1-pyrroline-5-carboxylate dehydrogenase catalyze two dehydrogenation processes in proline catabolism. Mitochondrial matrix NAD<sup>+</sup>-dependent dehydrogenase raises NAD<sup>+</sup> PAL and converts this into polyphenols and antioxidants. Benjamin et al. (2019) found that NaCl increases flavonoids and other phenolic compounds in *S. brachiate* but decreases them in *S. portulacastrum*, which accumulates carotenoids, fighting ROS and aiding photosynthesis. Usually, shoots have more ricinine alkaloid content than roots and underground stems. Said-Al Ahl and Omer (2011) found that salt stress increases *Rouwolfia tetraphylla* reserpine and *Catharanthus roseus* shoot vincristine alkaloids. Numerous investigations are supported by current reviews and outlined in Table 2. Salt stress significantly impacts plant metabolism and secondary metabolite production through ionic and osmotic stress mechanisms. However, there remains a research gap in understanding the specific regulatory pathways and genetic mechanisms governing the differential responses of plants to salt stress, particularly to secondary metabolite synthesis under varying environmental conditions.

#### 4.4 Impact of Temperature on SMs Production

Global warming and disruptive seasonal events may reduce secondary metabolite production in medicinal and aromatic plants (MAPs), affecting livelihoods and biodiversity. Timely interventions are needed to avert biodiversity loss (Das et al. 2016). Low and high temperatures alter plant cell proteins, enzymes, and lipids, affecting membrane integrity. Thakur et al. (2019) suggested low and high temperatures affect plant secondary metabolite synthesis. Human activity has raised the average global

temperature by 0.74°C, and the temperature is anticipated to increase by 0.2°C each decade. As a supplementary defence against high temperatures, plants manufacture SMs (Isah 2019). Wahid and Close (2007) state that ROS from temperature stress harms plant cells.

Plants produce flavonoids and phenylpropanoids to deal with high temperatures. Table 3 illustrates the effects of elevated and reduced temperature stresses on producing various secondary metabolites in plants. Global warming and seasonal disruptions threaten secondary metabolite production in medicinal and aromatic plants (MAPs), impacting biodiversity and livelihoods. Extreme temperature alters plant cellular processes and membrane integrity, affecting secondary metabolite synthesis. As temperatures rise, plants increasingly rely on secondary metabolites like flavonoids and phenylpropanoids as a defence. However, further research is needed to fully understand and mitigate the effects of climate change on these vital plant compounds. Global warming and seasonal disruptions threaten secondary metabolite production in medicinal and aromatic plants (MAPs), impacting biodiversity and livelihoods. Extremes temperature may also alter plant cellular processes and membrane integrity, affecting secondary metabolite synthesis. As temperatures rise, plants increasingly rely on secondary metabolites like flavonoids and phenylpropanoids as a defence. However, further research is needed to fully understand and mitigate the effects of climate change on these vital plant compounds.

#### 4.5 Effect of Light Irradiation on SMs Production

Growth and metabolism in plants are significantly impacted by solar radiation. Research has shown that fluctuations in solar radiation levels can cause plants to produce and accumulate secondary metabolites to adapt to their environment (Yang et al. 2018). The length of the light period is one of the critical factors

Table 3 Secondary Metabolite Production in Response to Temperature Stress in a Range of Species

S. N.	Temperature	Plant species	Compounds	References
1	Low	<i>Melastoma malabathricum</i>	Anthocyanin	Chan et al. (2010)
2	Low	<i>Rhodiola crenulata</i>	Melatonin	Zhao et al. (2011)
3	High	<i>Ribes nigrum</i>	Delphinidin-3-O- glucoside, Delphinidin-3-O-rutinside, Myricetin-3-O-glucoside	Zheng et al. (2012)
4	Low	<i>Glycine max</i>	Genistein, Diazein, Genistin	Janas et al. (2002)
5	High	<i>C. accuminata</i>	10- hydroxycampothecin	Zu et al. (2003)
6	High	<i>Lupinus angustifolius</i>	Alkaloids	Jansen et al. (2009)
7	High	<i>C. roseus</i>	Vindoline, Catharanthine, Vinblastine	Guo et al. (2007)
8	High	<i>Picea abies</i>	Piperidine	Virjamo et al.(2014)
9	High	<i>Betula pendula</i> <i>Populus tremula</i>	Terpenoid	Ibrahim et al.(2010)

associated with irradiation that can impact the levels of secondary metabolites in plants. Studies have demonstrated that longer photoperiods can increase the levels of secondary metabolites, which can help plants resist the effects of light exposure. Conversely, shorter day-length conditions have been shown to reduce coumarin content in stems and leaves, while longer day-length periods have significantly increased coumarin content (de-Castro et al. 2007).

Light quality is a critical factor that significantly impacts the levels of secondary metabolites in plants. The escalation of ultraviolet radiation has been attributed to the diminution of the ozone layer, which had a detrimental effect on living organisms. Consequently, plant cells produce reactive oxygen species and accelerate the production of secondary metabolites that can absorb UV radiation (dos Santos Nascimento et al. 2015). Furthermore, it promotes antioxidant activity to minimize and correct oxidative harm (Takshak and Agrawal 2014). Park et al. (2007) demonstrated that the biosynthesis of anthocyanins is enhanced by the increased expression of genes responsible for producing proteins and enzymes, including dihydroflavonol reductase (DFR), flavanone 3-hydroxylase (F3H) and chalcone synthase. UV-B radiation leads to heightened activity of enzymes like cinnamyl alcohol dehydrogenase, phenylalanine ammonia-lyase (PAL), chalcone-flavanone isomerase, dihydroflavonol reductase (DFR), and 4-coumarate CoA ligase, along with increased levels of flavonoids, anthocyanins, and tannins in *Withania somnifera* (Takshak and Agrawal 2014). According to Ma et al. (2016), the effects of UV-B radiation on the phytochemical constituents of *Chrysanthemum* flowers, specifically chlorogenic acid and flavonoids, were investigated. These phytochemicals are the primary components that impart the healing properties of the flowers.

Solar radiation significantly influences plant metabolism and secondary metabolite production. Fluctuations in radiation levels

prompt plants to adjust secondary metabolite synthesis, with longer photoperiods enhancing their production. Additionally, UV radiation induces reactive oxygen species in plants, stimulating the biosynthesis of protective secondary metabolites like flavonoids and anthocyanins. Heavy metals such as chromium and cadmium disrupt plant metabolism, triggering oxidative stress and altering secondary metabolite profiles. Understanding these environmental impacts is crucial for optimizing plant-based bioactive compound production.

#### 4.6 Effect of Heavy Metal on SMs Production

The term "heavy metal" describes metallic elements with a high-density level that can inflict harm even at low concentrations. Heavy metals, including chromium, cadmium, iron, zinc, and manganese, can potentially elevate ROS generation, causing an imbalance between ROS generation and detoxification. These metals can have a detrimental impact on plants by either directly binding to proteins, owing to their affinities for histidyl-, thioyl-, and carboxyl-groups that mark catalytic, structural, or transport locations in cells or eliciting the production of reactive oxygen species, potentially leading to oxidative stress (Table 4) (Kaczor-Kamińska et al. 2020). In addition, the presence of heavy metals can affect plants by displacing essential cations from specific binding sites (Sharma and Dietz 2009). Kovacik and Klejdus (2008) found that varying copper doses, like 120 and 60  $\mu\text{M}$ , significantly boosted PAL activity, increasing lignin content and phenolic compound the day after treatment. This result reflects the response of the defence mechanism to metal entry. Reports are also available that higher artemisinin levels in *A. annua* were achieved by the application of arsenic-induced stress through two methods: converting dihydroartemisinic acid (monocarboxylic acid) to artemisinin via ROS breakage and promoting genes involved in artemisinin production (Rai et al. 2011a; Khare et al. 2020).

Table 4 Impact of heavy metal stress on the production of secondary metabolites by different species

S. N.	Heavy metal	Plant species	Compounds	References
1	AgNO <sub>3</sub>	<i>Perovskia abrotanoides</i>	Tanshinone	Zaker et al. (2015)
2	Ag	<i>Salvia castanea</i>	Tanshinone	Li et al. (2016)
3	AgNO <sub>3</sub>	<i>Datura metel</i>	Atropine	Shakeran et al. (2015)
4	Cd, Co, Ag	<i>Vitis vinifera</i>	Resveratrol	Cai et al. (2013)
5	Cu	<i>Bacopa monnieri</i>	Bacoside	Sharma et al. (2015)
6	Pb	<i>Mentha crispa</i>	Carvone	Sá et al. (2015)
7	Cu and Zn	<i>Mentha pulegium</i>	Pulegone Cineol Thymol	Lajayer et al. (2017)
8	Cd and Co	<i>Trigonella rogosum</i>	Diosgenin	De and De (2011)
9	Cr, Cd, Pb and Ni	<i>Ocimum basilicum</i>	Chavicol Cinalol	Prasad et al. (2011)
10	As	<i>Artemisia annua</i>	Artemisinin	Rai et al. (2011b)

The research gap lies in understanding the precise mechanisms by which different heavy metals individually and collectively influence secondary metabolite production in plants. Current studies often focus on specific metals like copper and arsenic, but comprehensive comparative analyses are limited across a broader spectrum of heavy metals. Additionally, there is a need to explore how varying concentrations and combinations of heavy metals affect different plant species' secondary metabolite profiles under realistic environmental conditions. This knowledge is crucial for developing strategies to mitigate heavy metal-induced stress and sustainably optimize plant-based bioactive compound production.

### Conclusion

Plant cells are recognized as a significant source of biochemical compounds, encompassing primary metabolites like sugars, fatty acids, and amino acids alongside a diverse array of secondary metabolites, including alkaloids, terpenoids, phenols, and sulfur-containing complexes. These secondary metabolites serve various functions, such as providing defence protection or engaging in offensive/invasive tactics in response to environmental factors, including microbes, insect pests, herbivorous predators, and insects. Various environmental factors, including sunlight, temperature, soil fertility, soil water, and acidity/salinity largely impact the generation and accumulation of secondary metabolites in plants. To cope with these conditions, plants adjust their metabolism towards producing numerous secondary metabolites. During environmental challenges, the orientation of secondary metabolism in plants involves complex signal transduction pathways. The current review presents comprehensive and reliable reasons for the variation in the composition of secondary metabolites in different ecological circumstances. Acquiring knowledge about secondary metabolism and its instability in plants may benefit both agriculturalists and geneticists. As advancements

in modern techniques continue to emerge, the significance of secondary metabolism in plant adaptation cannot be overstated. Furthermore, conducting extensive research into the physiological, molecular, and biochemical responses of plants and the primary genetic mechanisms involved can provide valuable insights and enhance adaptation to various environmental influences. By doing so, scientists may be able to strategically apply stress factors to increase the production of various secondary metabolites, ultimately benefiting humanity.

However, gaps remain in understanding the intricate signal transduction pathways and regulatory networks that govern secondary metabolism in response to diverse environmental challenges. Future research should unravel these complexities across various plant species and environmental conditions. Advancements in modern techniques, including omics technologies and gene editing tools, offer promising avenues to deepen our understanding of secondary metabolism. This knowledge could potentially enable agriculturalists and geneticists to manipulate plant metabolism strategically. By harnessing stress factors or enhancing genetic pathways, scientists may enhance the production of valuable secondary metabolites for medicinal, agricultural, and industrial applications, benefiting human health and sustainable agriculture practices.

### Conflict of interest

The authors declare no conflicts of interest

### References

- Abd EL-Azim, W. M., & Ahmed, S. T. (2009). Effect of salinity and cutting date on growth and chemical constituents of *Achillea fragratissima* Forssk, under Ras Sudr conditions. *Research Journal of Agriculture and Biological Sciences*, 5(6), 1121-1129

- Ahmad, B., Tian, C., Tang, J. X., Dumbuya, J. S., Li, W., & Lu, J. (2024). Anticancer activities of natural abietic acid. *Frontiers in Pharmacology*, *15*, 1392203. <https://doi.org/10.3389/fphar.2024.1392203>
- Akanmu, A. O., Yunus, H. H., Balogun, S. T., Sodipo, O. A., Paul, L. M., & Gulani, I. (2021). Antibacterial Activity of Aqueous and Ethanol Fruit Extracts of *Cucumis sativus* Linn. Against Selected Microorganisms at the University of Maiduguri Teaching Hospital, Maiduguri. *Sahel Journal of Veterinary Sciences*, *18*(2), 17-22. <https://doi.org/10.54058/saheljvs.v18i2.222>
- Akula, R., & Ravishankar, G. A. (2011). Influence of abiotic stress signals on secondary metabolites in plants. *Plant Signaling & Behavior*, *6*(11), 1720-1731. <https://doi.org/10.4161/psb.6.11.17613>
- Balfagón, D., Rambla, J. L., Granell, A., Arbona, V., & Gomez-Cadenas, A. (2022). Grafting improves tolerance to combined drought and heat stresses by modifying metabolism in citrus scion. *Environmental and Experimental Botany*, *195*, 104793.
- Bankar, J. S., Bondre, K. N., Wagh, P. P., Bhope, S. S., Pande, J. S., et al. (2024). Herbal Medicines for the Management of Diseases in the Heart, Circulation, and Blood. In A.K. Dhara, & S.C. Mandal (Eds.) *Role of Herbal Medicines: Management of Lifestyle Diseases* (pp. 129-144). Singapore: Springer Nature Singapore. [https://doi.org/10.1007/978-981-99-7703-1\\_7](https://doi.org/10.1007/978-981-99-7703-1_7)
- Barbieri, R., Coppo, E., Marchese, A., Daglia, M., Sobarzo-Sánchez, E., Nabavi, S. F., & Nabavi, S. M. (2017). Phytochemicals for human disease: An update on plant-derived compounds antibacterial activity. *Microbiological Research*, *196*, 44-68. <https://doi.org/10.1016/j.micres.2016.12.003>
- Benjamin, J. J., Lucini, L., Jothiramshekar, S., & Parida, A. (2019). Metabolomic insights into the mechanisms underlying tolerance to salinity in different halophytes. *Plant Physiology and Biochemistry*, *135*, 528-545. <https://doi.org/10.1016/j.plaphy.2018.11.006>
- Bhatwalkar, S. B., Mondal, R., Krishna, S. B. N., Adam, J. K., Govender, P., & Anupam, R. (2021). Antibacterial properties of organosulfur compounds of garlic (*Allium sativum*). *Frontiers in Microbiology*, *12*, 1869. <https://doi.org/10.3389/fmicb.2021.613077>
- Blanco-Ulate, B., Amrine, K. C., Collins, T. S., Rivero, R. M., Vicente, A. R., et al. (2015). Developmental and metabolic plasticity of white-skinned grape berries in response to *Botrytis cinerea* during noble rot. *Plant Physiology*, *169*(4), 2422-2443. <https://doi.org/10.1104/pp.15.00852>
- Bourgou, S., Ksouri R., Bellila, A., Skandarani, I., Falleh, H., Marzouk, B. (2008). Phenolic composition and biological activities of Tunisian *Nigella sativa* L. shoots and roots. *Journal Algérien des Régions Arides*, *33*(1), 48-55.
- Cai, Z., Kastell, A., Speiser, C., & Smetanska, I. (2013). Enhanced resveratrol production in *Vitis vinifera* cell suspension cultures by heavy metals without loss of cell viability. *Applied Biochemistry and Biotechnology*, *171*, 330-340. <https://doi.org/10.1007/s12010-013-0354-4>
- Cardoso, M.N., Araújo, A.G.D., Oliveira, L.A.R., Cardoso, B.T., Muniz, A.V.C.D.S., et al. (2019). Proline synthesis and physiological response of cassava genotypes under in vitro salinity. *Ciência Rural*, *Santa Maria*, *49*, (6), e20170175. <https://doi.org/10.1590/0103-8478cr20170175>
- Chan, L. K., Koay, S. S., Boey, P. L. & Bhatt A. (2010). Effects of abiotic stress on biomass and anthocyanin production in cell cultures of *Melastoma malabathricum*. *Biological Research*, *43*(1), 127-135. <http://dx.doi.org/10.4067/S0716-97602010000100014>
- Chu, M., Zhang, M. B., Liu, Y. C., Kang, J. R., Chu, Z. Y., et al. (2016). Role of Berberine in the Treatment of Methicillin-Resistant *Staphylococcus aureus* Infections. *Scientific reports*, *6*, 24748. <https://doi.org/10.1038/srep24748>
- D'Souza, M. R., & Devaraj, V. R. (2010). Biochemical responses of Hyacinth bean (*Lablab purpureus*) to salinity stress. *Acta Physiologiae Plantarum*, *32*, 341-353. <https://doi.org/10.1007/s11738-009-0412-2>
- Das, M., Jain, V., & Malhotra, S. K. (2016). Impact of climate change on medicinal and aromatic plants. *The Indian Journal of Agricultural Sciences*, *86*(11), 1375-82. <https://doi.org/10.56093/ijas.v86i11.62865>
- de Castro, E. M., Pinto, J. E. B. P., Bertolucci, S. K., Malta, M. R., Cardoso, M. D. G., & de MSilva, F. A. (2007). Coumarin contents in young *Mikania glomerata* plants (Guaco) under different radiation levels and photoperiod. *Acta Farmaceutica Bonaerense*, *25*(3), 387-392.
- De, D., & De, B. (2011). Elicitation of diosgenin production in *Trigonella foenum-graecum* L. seedlings by heavy metals and signaling molecules. *Acta physiologiae plantarum*, *33*, 1585-1590. <https://doi.org/10.1007/s11738-010-0691-7>
- dos Santos Nascimento, L. B., Leal-Costa, M. V., Menezes, E. A., Lopes, V. R., Muzitano, M. F., Costa, S. S., & Tavares, E. S. (2015). Ultraviolet-B radiation effects on phenolic profile and flavonoid content of *Kalanchoepinnata*. *Journal of Photochemistry and Photobiology B: Biology*, *148*, 73-81. <https://doi.org/10.1007/s11738-010-0691-7>
- Edreva A. M., Velikova, V., & Tsonev, T. (2000). Phenylamides in plants. *Russian Journal Plant Physiology*, *54*, 287-301. doi: 10.1134/S1021443707030016.



- Ghorbani, A., Emamverdian, A., Pehlivan, N., Zargar, M., Razavi, S. M., & Chen, M. (2024). Nano-enabled agrochemicals: mitigating heavy metal toxicity and enhancing crop adaptability for sustainable crop production. *Journal of Nanobiotechnology*, 22(1), 91. <https://doi.org/10.1186/s12951-024-02371-1>
- Guo, F., Danielski, R., Santhiravel, S., & Shahidi, F. (2024). Unlocking the Nutraceutical Potential of Legumes and Their By-Products: Paving the Way for the Circular Economy in the Agri-Food Industry. *Antioxidants*, 13(6), 636. <https://doi.org/10.3390/antiox13060636>
- Guo, X.R., Yang, L., Yu, J.H., Tang, Z. H., & Zu Y. G. (2007). Alkaloid variations in *Catharanthus roseus* seedlings treated by different temperatures in short term and long term. *Journal of Forestry Research*, 18(4), 313-315. <https://doi.org/10.1007/s11676-007-0063-3>
- Haghighi, Z., Karimi, N., Modarresi, M., & Mollayi, S. (2012). Enhancement of compatible solute and secondary metabolites production in *Plantago ovata* Forsk. by salinity stress. *Journal of Medicinal Plants Research*, 6(18), 3495-3500. <https://www.cabidigitallibrary.org/doi/full/10.5555/20123198771>
- Hameed, A., Hussain, S. A., & Suleria, H. A. R. (2020). "Coffee Bean-Related" agroecological factors affecting the coffee. In Méridon, JM., Ramawat, K. (eds) *Co-evolution of Secondary Metabolites* (pp. 641-705). Springer, Cham [https://doi.org/10.1007/978-3-319-96397-6\\_21](https://doi.org/10.1007/978-3-319-96397-6_21)
- Han, C.Y., Ki, S.H., Kim, Y.W., Noh, K., Lee, D.Y., et al. (2011). Ajoene, a stable garlic by-product, inhibits high fat diet-induced hepatic steatosis and oxidative injury through LKB1-dependent AMPK activation. *Antioxidants & Redox Signaling*, 14(2), pp.187-202. <https://doi.org/10.1089/ars.2010.3190>
- Herms, D. A., & Mattson, W. J. (1992). The dilemma of plants: to grow or defend. *The quarterly review of biology*, 67(3), 283-335.
- Hichem, H., & Mounir, D. (2009). Differential responses of two maize (*Zea mays* L.) varieties to salt stress: changes on polyphenols composition of foliage and oxidative damages. *Industrial crops and Products*, 30(1), 144-151.
- Hikal, D. M. (2018). Antibacterial activity of piperine and black pepper oil. *Biosciences Biotechnology Research Asia*, 15(4), 877.
- Hosseinzadeh, S., Jafarikukhdan, A., Hosseini, A., & Armand, R. (2015). The application of medicinal plants in traditional and modern medicine: a review of *Thymus vulgaris*. *International Journal of Clinical Medicine*, 6(09), 635-642. <http://doi.org/10.4236/ijcm.2015.69084>
- Hussain, S., Hafeez, M. B., Azam, R., Mehmood, K., Aziz, M., et al. (2024). Deciphering the role of phytohormones and osmolytes in plant tolerance against salt stress: Implications, possible cross-talk, and prospects. *Journal of Plant Growth Regulation*, 43(1), 38-59. <https://doi.org/10.1007/s00344-023-11070-4>
- Ibrahim, M. H., Jaafar, H. Z., & Zain, N. A. M. (2017). Impact of Elevated CO<sub>2</sub> on Leaf Gas Exchange, Carbohydrates and Secondary Metabolites Accumulation in *Labisia pumila* Benth. *Annual Research & Review in Biology*, 19(6), 1-16. <https://doi.org/10.9734/ARRB/2017/36673>
- Ibrahim, M.A., Mäenpää, M., Hassinen, V., Kontunen-Soppela, S., Malec, L., et al. (2010). Elevation of night-time temperature increases terpenoid emissions from *Betula pendula* and *Populus tremula*. *Journal of Experimental Botany*, 61(6), 1583-1595. <https://doi.org/10.1093/jxb/erq034>
- Isah, T. (2019). Stress and defense responses in plant secondary metabolites production. *Biological research*, 52, 39. <https://doi.org/10.1186/s40659-019-0246-3>
- Jaafar, H. Z., Ibrahim, M. H., & Fakri, N. F. M. (2012). Impact of soil field water capacity on secondary metabolites, phenylalanine ammonia-lyase (PAL), malondialdehyde (MDA) and photosynthetic responses of Malaysian Kacip Fatimah (*Labisia pumila* Benth). *Molecules*, 17(6), 7305-7322. <https://doi.org/10.3390/molecules17067305>
- Jaleel, C. A., Manivannan, P., Sankar, B., Kishorekumar, A., Gopi, R., Somasundaram, R., & Panneerselvam, R. (2007). Water deficit stress mitigation by calcium chloride in *Catharanthus roseus*: Effects on oxidative stress, proline metabolism and indole alkaloid accumulation. *Colloids and surfaces B: Biointerfaces*, 60(1), 110-116. <https://doi.org/10.1016/j.colsurfb.2007.06.006>
- Jampilek, J., & Kráľová, K. (2023). Impact of Abiotic Stresses on Production of Secondary Metabolites in Medicinal and Aromatic Plants. In T. Aftab (eds) *New Frontiers in Plant-Environment Interactions: Innovative Technologies and Developments* (pp. 169-252). Cham: Springer Nature Switzerland.
- Janas, K. M., Cvikrová, M., Pałagiewicz, A., Szafranska K., & Posmyk, M. M. (2002). Constitutive elevated accumulation of phenylpropanoids in soybean roots at low temperature. *Plant Science*, 163(2), 369-373. [https://doi.org/10.1016/S0168-9452\(02\)00136-X](https://doi.org/10.1016/S0168-9452(02)00136-X)
- Jansen, G., Jürgens, H. U., & Ordon, F. (2009). Effects of temperature on the alkaloid content of seeds of *Lupinus angustifolius* cultivars. *Journal of agronomy and crop science*, 195(3), 172-177. <https://doi.org/10.1111/j.1439-037X.2008.00356.x>
- Kaczor-Kamińska, M., Sura, P., & Wróbel, M. (2020). Multidirectional changes in parameters related to sulfur

- metabolism in frog tissues exposed to heavy metal-related stress. *Biomolecules*, *10*(4), 574. <https://doi.org/10.3390/biom10040574>
- Kapoor, D., Bhardwaj, S., Landi, M., Sharma, A., Ramakrishnan, M., & Sharma, A. (2020). The impact of drought in plant metabolism: How to exploit tolerance mechanisms to increase crop production. *Applied Sciences*, *10*(16), 5692. <https://doi.org/10.3390/app10165692>
- Keita, K., Darkoh, C., & Okafor, F. (2022). Secondary plant metabolites as potent drug candidates against antimicrobial-resistant pathogens. *SN Applied Sciences*, *4*(8), 209. <https://doi.org/10.1007/s42452-022-05084-y>
- Khan, T. A., Mazid M., & Mohammad, F. (2011). Status of secondary plant products under abiotic stress: an overview. *Journal of Stress Physiology & Biochemistry*, *7*(2), 75-98
- Khare, S., Singh, N. B., Singh, A., Hussain, I., Niharika, K. M., et al. (2020). Plant secondary metabolites synthesis and their regulations under biotic and abiotic constraints. *Journal of Plant Biology*, *63*, 203-216. <https://doi.org/10.1007/s12374-020-09245-7>
- Ko, Y. J., Lee, M. E., Cho, B. H., Kim, M., Hyeon, J. E., Han, J. H., & Han, S. O. (2024). Bioproduction of porphyrins, phycobilins, and their proteins using microbial cell factories: engineering, metabolic regulations, challenges, and perspectives. *Critical Reviews in Biotechnology*, *44*(3), 373-387. <https://doi.org/10.1080/07388551.2023.2168512>
- Kovacik, J. & Klejdus, B. (2008). Dynamics of phenolic acids and lignin accumulation in metal-treated *Matricaria chamomilla* roots. *Plant Cell Reports*, *27*(3) 605-615. <https://doi.org/10.1007/s00299-007-0490-9>
- Kumar, M., Sarvade, S., Kumar, R., & Kumar, A. (2024). Pre-Sowing Treatments on Seeds of Forest Tree Species to Overcome the Germination Problems. *Asian Journal of Environment & Ecology*, *23*(5), 1-18. <https://doi.org/10.9734/ajee/2024/v23i5543>
- Laftouhi, A., Eloutassi, N., Ech-Chihbi, E., Rais, Z., Abdellaoui, A., et al. (2023). The impact of environmental stress on the secondary metabolites and the chemical compositions of the essential oils from some medicinal plants used as food supplements. *Sustainability*, *15*(10), p.7842.
- Lahlou, M. (2013). The success of natural products in drug discovery, *Pharmacology and Pharmacy*, *4*, 17-31.
- Lajayer, H.A., Savaghebi, G., Hadian, J., Hatami, M., & Pezhmanmehr, M. (2017). Comparison of copper and zinc effects on growth, micro-and macronutrients status and essential oil constituents in pennyroyal (*Mentha pulegium* L.). *Brazilian Journal of Botany*, *40* (2) 379-388. <https://doi.org/10.1007/s40415-016-0353-0>
- Li, B., Wang, B., Li, H., Peng, L., Ru, M., Liang, Z., & Zhu, Y. (2016). Establishment of *Salvia castanea* Diels f. *tomentosa* Stib. hairy root cultures and the promotion of tanshinone accumulation and gene expression with Ag<sup>+</sup>, methyl jasmonate, and yeast extract elicitation. *Protoplasma*, *253*(1) 87-100. <https://doi.org/10.1007/s00709-015-0790-9>
- Li, X., Ahammed, G. J., Zhang, L., Yan, P., Zhang, L., & Han, W. Y. (2018). Elevated carbon dioxide-induced perturbations in metabolism of tea plants. In W. Y. Han, X. Li, G. Ahammed (eds) *Stress physiology of tea in the face of climate change* (pp. 135-155). Springer, Singapore. [https://doi.org/10.1007/978-981-13-2140-5\\_7](https://doi.org/10.1007/978-981-13-2140-5_7)
- Liu, F., Jensen, C.R., & Andersen, M.N. (2005). A review of drought adaptation in crop plants: changes in vegetative and reproductive physiology induced by ABA-based chemical signals, *Australian Journal of Agricultural Research*, *56*(11), 1245-1252. <https://doi.org/10.1071/AR05062>
- Liu, X., Li, Y., & Micallef, S. A. (2023). Natural variation and drought-induced differences in metabolite profiles of red oak-leaf and Romaine lettuce play a role in modulating the interaction with *Salmonella enterica*. *International Journal of Food Microbiology*, *385*, 109998.
- Luo, Q., Yu, B., & Liu, Y. (2005). Differential sensitivity to chloride and sodium ions in seedlings of *Glycine max* and *G. soja* under NaCl stress. *Journal of Plant Physiology*, *162*(9), 1003-1012. <https://doi.org/10.1016/j.jplph.2004.11.008>
- Ma, D.S., Tan, L.T.H., Chan, K.G., Yap, W.H., Pusparajah, P., Chuah, L.H., & Goh, B.H. (2018). Resveratrol—potential antibacterial agent against foodborne pathogens, *Frontiers in Pharmacology*, *9*, 102. <https://doi.org/10.3389/fphar.2018.00102>
- Ma, Q., Liu, Y., Zhan, R. & Chen, Y. (2016). A new is of lavanone from the trunk of *Horsfieldia pandurifolia*. *Natural Product Research*, *30*(2)131-137. <https://doi.org/10.1080/14786419.2015.1043554>
- Mahajan, M., Kuiry, R., & Pal, P. K. (2020). Understanding the consequence of environmental stress for accumulation of secondary metabolites in medicinal and aromatic plants. *Journal of Applied Research on Medicinal and Aromatic Plants*, *18*, 100255.
- Mak, K.K., Kamal, M., Ayuba, S., Sakirolla, R., Kang, Y. B., Mohandas, K., & Pichika, M. (2019). A comprehensive review on eugenol's antimicrobial properties and industry applications: A

- transformation from ethnomedicine to industry. *Pharmacognosy Reviews*, 13 (25) 1-9.
- Marchese, A., Barbieri, R., Coppo, E., Orhan, I.E., Daglia, M., et al. (2017). Antimicrobial activity of eugenol and essential oils containing eugenol: a mechanistic viewpoint. *Critical Reviews in Microbiology*, 43, 668–689. <https://doi.org/10.1080/1040841X.2017.1295225>
- Mareri, L., Parrotta, L., & Cai, G. (2022). Environmental stress and plants. *International Journal of Molecular Sciences*, 23(10), 5416.
- Marín, L., Miguélez, E. M., Villar, C. J., & Lombó, F. (2015). Bioavailability of dietary polyphenols and gut microbiota metabolism: antimicrobial properties. *BioMed research international*, 2015, 905215. <https://doi.org/10.1155/2015/905215>.
- Marin-Bruzos, M., & Grayston, S. J. (2019). Biological control of nematodes by plant growth promoting rhizobacteria: secondary metabolites involved and potential applications. In H. Singh, C. Keswani, M. Reddy, E. Sansinenea, & C. García-Estrada (Eds.) *Secondary Metabolites of Plant Growth Promoting Rhizomicroorganisms: Discovery and Applications* (pp. 253-264). Springer, Singapore. [https://doi.org/10.1007/978-981-13-5862-3\\_13](https://doi.org/10.1007/978-981-13-5862-3_13).
- Matros, A., Amme, S., Kettig, B., Buck-Sorlin, G. H., Sonnewald, U. W. E., & MOCK, H. P. (2006). Growth at elevated CO<sub>2</sub> concentrations leads to modified profiles of secondary metabolites in tobacco cv. Samsun NN and to increased resistance against infection with potato virus Y. *Plant, Cell & Environment*, 29(1), 126-137. <https://doi.org/10.1111/j.1365-3040.2005.01406.x>
- Medina-Rodelo, D. P., Quintana-Obregón, E. A., Gutiérrez-Dorado, R., Heredia, J. B., Puello-Cruz, A. C., & Angulo-Escalante, M. A. (2024). The effects of solid-state fermentation of the defatted *Jatropha platyphylla* meal on antinutritional factors, toxic compounds, and nutritional composition. *Journal of Food Measurement and Characterization*, 18(1), 664-675. <https://doi.org/10.1007/s11694-023-02191-1>
- Meijer, N., Zoet, L., Rijkers, D., Nijssen, R., Willemsen, M., Zomer, P., & van der Fels-Klerx, H. J. (2024). Toxicity, transfer and metabolization of the pyrethroid insecticides cypermethrin and deltamethrin by reared black soldier fly larvae. *Journal of Insects as Food and Feed*, 1(aop), 1-10. <https://doi.org/10.1163/23524588-00001167>
- Morcia, C., Piazza, I., Ghizzoni, R., Delbono, S., Felici, B., et al. (2022). In Search of Antifungals from the Plant World: The Potential of Saponins and Brassica Species against *Verticillium dahliae* Kleb. *Horticulturae*, 8(8), 729. <https://doi.org/10.3390/horticulturae8080729>
- Müller, A., Eller, J., Albrecht, F., Prochnow, P., Kuhlmann, K., Bandow, J.E., Slusarenko, A.J. & Leichert, L.I.O. (2016). Allicin induces thiol stress in bacteria through S-allylmercapto modification of protein cysteines. *Journal of Biological Chemistry*, 291 (22) 11477-11490. <https://doi.org/10.1074/jbc.M115.702308>
- Nag, S., Lone, R., Praharaju, M., Khan, P., & Hussain, A. (2024). Fungal Control Through Plant Phenolics: A Biotic Constraint. In R. Lone, S. Khan, A. M. Al-Sadi (Eds.) *Plant Phenolics in Biotic Stress Management* (pp. 339-365). Singapore: Springer Nature Singapore. [https://doi.org/10.1007/978-981-99-3334-1\\_14](https://doi.org/10.1007/978-981-99-3334-1_14)
- Nakamoto, M., Kunimura, K., Suzuki, J.I., & Kodera, Y. (2020). Antimicrobial properties of hydrophobic compounds in garlic: Allicin, vinylidithiin, ajoene and diallyl polysulfides. *Experimental and Therapeutic Medicine*, 19(2) 1550-1553. <https://doi.org/10.3892/etm.2019.8388>
- Nelson, D. E., Rammesmayer, G., & Bohnert, H. J. (1998). Regulation of cell-specific inositol metabolism and transport in plant salinity tolerance. *The Plant Cell*, 10(5), 753-764. <https://doi.org/10.1105/tpc.10.5.753>
- Nikolić, B. M., Ballian, D., & Mitić, Z. S. (2024). Autochthonous Conifers of Family Pinaceae in Europe: Broad Review of Morpho-Anatomical and Phytochemical Properties of Needles and Genetic Investigations. *Forests*, 15(6), 989. <https://doi.org/10.3390/f15060989>
- Nogués, S., Allen, D. J., Morison, J. I., & Baker, N. R. (1998). Ultraviolet-B radiation effects on water relations, leaf development, and photosynthesis in droughted pea plants. *Plant physiology*, 117(1), 173-181. <https://doi.org/10.1104/pp.117.1.173>
- Oueslati, S., Karray-Bouraoui, N., Attia, H., Rabhi, M., Ksouri, R., & Lachaal, M. (2010). Physiological and antioxidant responses of *Mentha pulegium* (Pennyroyal) to salt stress. *Acta Physiologiae Plantarum*, 32, 289-296. <https://doi.org/10.1007/s11738-009-0406-0>
- Pagare, S., Bhatia, M., Tripathi, N., Pagare, S., & Bansal, Y. K. (2015). Secondary metabolites of plants and their role: Overview. *Current trends in biotechnology and pharmacy*, 9(3), 293-304.
- Pandita, D., & Pandita, A. (2021). Secondary metabolites in medicinal and aromatic plants (MAPs): potent molecules in nature's arsenal to fight human diseases. In T. Aftab, K.R. Hakeem (Eds) *Medicinal and Aromatic Plants: Healthcare and Industrial Applications* (pp. 41-84). Springer, Cham. [https://doi.org/10.1007/978-3-030-58975-2\\_2](https://doi.org/10.1007/978-3-030-58975-2_2)

- Park, K.I., Ishikawa, N., Morita, Y., Choi, J.D., Hoshino, A. & Iida, S. (2007). A bHLH regulatory gene in the common morning glory, *Ipomoea purpurea*, controls anthocyanin biosynthesis in flowers, proanthocyanidin and phytomelanin pigmentation in seeds, and seed trichome formation', *The Plant Journal*, 49(4), 641-654. <https://doi.org/10.1111/j.1365-313X.2006.02988.x>
- Parveen, S., Maurya, N., Meena, A., & Luqman, S. (2024). Cinchonine: A Versatile Pharmacological Agent Derived from Natural Cinchona Alkaloids. *Current Topics in Medicinal Chemistry*, 24(4), 343-363. <https://doi.org/10.2174/0115680266270796231109171808>
- Prasad, A., Kumar, S., Khaliq, A. & Pandey, A. (2011). Heavy metals and arbuscular mycorrhizal (AM) fungi can alter the yield and chemical composition of volatile oil of sweet basil (*Ocimum basilicum* L.). *Biology and Fertility of Soils*, 47, 853-861. <https://doi.org/10.1007/s00374-011-0590-0>
- Punetha, A., Kumar, D., Suryavanshi, P., Padalia, R., & Kt, V. (2022). Environmental abiotic stress and secondary metabolites production in medicinal plants: a review. *Journal of Agricultural Sciences*, 28(3), 351-362. <https://doi.org/10.15832/ankutbd.999117>
- Qaderi, M. M., Martel, A. B., & Strugnell, C. A. (2023). Environmental factors regulate plant secondary metabolites. *Plants*, 12(3), 447.
- Radušienė, J., Karpavičienė, B. & Stanius, Ž. (2012). Effect of external and internal factors on secondary metabolites accumulation in St. John's worth. *Botanica Lithuanica*, 18(2), 101-108. <https://10.2478/v10279-012-0012-8>
- Raffo, A., Baiamonte, I., De Nicola, G. R., Melini, V., Moneta, E., et al. (2024). Sensory Attributes Driving Preference for Wild Rocket (*Diplotaxis tenuifolia*) Leaves Tasted as a Single Ingredient and as a Part of a Recipe. *Foods*, 13(11), 1699. <https://doi.org/10.3390/foods13111699>
- Rahman, S., Iqbal, M., & Husen, A. (2023). Medicinal plants and abiotic stress: an overview. In A. Husen, & M. Iqbal, (eds) *Medicinal Plants: Their Response to Abiotic Stress* (pp. 1-34), Springer, Singapore.
- Rai, R., Meena, R.P., Smita, S.S., Shukla, A., Rai, S.K. & Pandey-Rai, S. (2011a). UV-B and UV-C pre-treatments induce physiological changes and artemisinin biosynthesis in *Artemisia annua* L.—An antimalarial plant. *Journal of Photochemistry and Photobiology B: Biology*, 105(3), 216-225.
- Rai, R., Pandey, S., & Rai, S.P. (2011b). Arsenic-induced changes in morphological, physiological, and biochemical attributes and artemisinin biosynthesis in *Artemisia annua*, an antimalarial plant. *Ecotoxicology*, 20, 1900-1913. <https://doi.org/10.1007/s10646-011-0728-8>
- Ramirez-Castillo, R., Palma-Rojas, C., Seguel, P. J., Grusz, A. L., & Araya-Jaime, C. (2024). Unfurling an improved method for visualizing mitotic chromosomes in ferns. *Applications in Plant Sciences*, e11588. <https://doi.org/10.1002/aps3.11588>
- Rodrigues, A.M., Jorge, T., Osorio, S., Pott, D.M., Lidon, F.C., et al. (2021). Primary metabolite profile changes in *Coffea* spp. promoted by single and combined exposure to drought and elevated CO<sub>2</sub> concentration. *Metabolites*, 11(7), p.427.
- Rzyska, K., Stuper-Szablewska, K., & Kurasiak-Popowska, D. (2024). Diverse Approaches to Insect Control: Utilizing *Brassica carinata* (A.) Braun and *Camelina sativa* (L.) Crantz Oil as Modern Bioinsecticides. *Forests*, 15(1), 105. <https://doi.org/10.3390/f15010105>
- Sá, R.A., Sá, R.A., Alberton, O., Gazim, Z.C., Laverde Jr, A., et al. (2015). Phytoaccumulation and effect of lead on yield and chemical composition of *Mentha crispa* essential oil. *Desalination and Water Treatment*, 53(11), 3007-3017. <https://doi.org/10.1080/19443994.2013.874716>
- Sachdev, S., Ansari, S. A., Ansari, M. I., Fujita, M., & Hasanuzzaman, M. (2021). Abiotic stress and reactive oxygen species: Generation, signaling, and defense mechanisms. *Antioxidants*, 10, 277. <https://doi.org/10.3390/antiox10020277>
- Sadhunavar, B. C., Kolome, D. G., & Unger, B. S. (2015). Effect of Shodhana (Purification) on Convulsive Property of Kuppeelu (Strychnous Nuxvomica) Toxicity: An Experimental Study. *Indian Journal of Ancient Medicine and Yoga*, 8(1), 31.
- Said-Al Ahl, H.A.H., & Omer, E.A. (2011). Medicinal and aromatic plants production under salt stress A review. *Herba Polonica*, 57(1), 72-87.
- Samanta, S., Sarkar, T., & Chakraborty, R. (2024). Multifunctional applications of natural colorants: Preservative, functional ingredient, and sports supplements. *Biocatalysis and Agricultural Biotechnology*, 56, 103026. <https://doi.org/10.1016/j.bcab.2024.103026>
- Sampaio, B.L., Edrada-Ebel, R., & Da Costa, F.B. (2016). Effect of the environment on the secondary metabolic profile of *Tithonia diversifolia*: a model for environmental metabolomics of plants. *Scientific Reports*, 6(1), 29265. <https://doi.org/10.1038/srep29265>
- Sarkar, P., Dhara, K., & Guhathakurta, H. (2024). Azadirachtin in the aquatic environment: Fate and effects on non-target fauna. *Physical Sciences Reviews*, 9(2), 765-776. <https://doi.org/10.3390/f15010105>



- Savé i Montserrat, R., Herralde Traveria, F.D., Codina Mahrer, C., Sánchez Molino, F.J., & Biel Loscos, C. (2007). Effects of atmospheric carbon dioxide fertilization on biomass and secondary metabolites of some plant species with pharmacological interest under greenhouse conditions, *Afinidad*, 64(528), 237-241.
- Shakeran, Z., Keyhanfar, M., Asghari, G., & Ghanadian, M. (2015). Improvement of atropine production by different biotic and abiotic elicitors in hairy root cultures of *Datura metel*. *Turkish Journal of Biology*, 39(1), 111-118. <https://doi.org/10.3906/biy-1405-25>
- Sharma, M., Ahuja, A., Gupta, R. & Mallubhotla, S. (2015). Enhanced bacoside production in shoot cultures of *Bacopa monnieri* under the influence of abiotic elicitors. *Natural Product Research*, 29(8), 745-749. <https://doi.org/10.1080/14786419.2014.986657>
- Sharma, P., Jha, A. B., Dubey, R. S., & Pessarakli, M. (2021). Reactive oxygen species generation, hazards, and defense mechanisms in plants under environmental (abiotic and biotic) stress conditions. *Handbook of plant and crop physiology* (pp. 617-658). CRC Press, Boca Raton.
- Sharma, S. S., & Dietz, K. J. (2009). The relationship between metal toxicity and cellular redox imbalance. *Trends in Plant Science*, 14(1), 43-50. <https://doi.org/10.1016/j.tplants.2008.10.007>
- Tahosin, A., Halim, M. A., Khatun, H., Ove, T. A., Islam, M. A., et al. (2024). Production and evaluation of quality characteristics of ready-to-drink Aloe vera juice incorporation with ginger and lemon. *Food and Humanity*, 3, 100324. <https://doi.org/10.1016/j.foohum.2024.100324>
- Taiz, L. & Zeiger, E. (2006). *Plant Physiology Sinauer Associates*. Inc., Sunderland, MA.
- Tak, Y., & Kumar, M. (2020). Phenolics: a key defense secondary metabolite to counter biotic stress. *Plant Phenolics in Sustainable Agriculture*, 1, 309-329. [https://doi.org/10.1007/978-981-15-4890-1\\_13](https://doi.org/10.1007/978-981-15-4890-1_13)
- Takshak, S. & Agrawal, S.Á. (2014). Secondary metabolites and phenyl propanoid pathway enzymes as influenced under supplemental ultraviolet-B radiation in *Withania somnifera* Dunal, an indigenous medicinal plant. *Journal of Photochemistry and Photobiology B: Biology*, 140, 332-343. <https://doi.org/10.1016/j.jphotobiol.2014.08.011>
- Thakur, M., Bhattacharya, S., Khosla, P.K. & Puri, S. (2019). Improving production of plant secondary metabolites through biotic and abiotic elicitation. *Journal of Applied Research on Medicinal and Aromatic Plants*, 12, 1-12. <https://doi.org/10.1016/j.jarmap.2018.11.004>
- Tran, H. T. D., Nguyen, H. T. T., Huynh, T. B., Nguyen, H. N., Nguyen, L. T., et al. (2023). Functional characterization of a bark-specific monoterpene synthase potentially involved in wounding- and methyl jasmonate-induced linalool emission in rubber (*Hevea brasiliensis*). *Journal of Plant Physiology*, 282, 153942. <https://doi.org/10.1016/j.jplph.2023.153942>
- Verma, N. & Shukla, S. (2015). Impact of various factors responsible for fluctuation in plant secondary metabolites. *Journal of Applied Research on Medicinal and Aromatic Plants*, 2(4), 105-113. <https://doi.org/10.1016/j.jarmap.2015.09.002>
- Virjamo, V., Sutinen, S., & Julkunen-Tiitto, R. (2014). Combined effect of elevated UVB, elevated temperature and fertilization on growth, needle structure and phytochemistry of young Norway spruce (*Picea abies*) seedlings. *Global Change Biology*, 20(7), 2252-2260. <https://doi.org/10.1111/gcb.12464>
- Vishwakarma, H., Patel, S., Chouksey, S., Lodhi, S., Kurmi, R., & Nema, P. (2022). Herbal products for gynecological disorders. *Asian Journal of Dental and Health Sciences*, 2(2), 1-8. <http://dx.doi.org/10.22270/ajdhs.v2i2.15>
- Wahid, A., & Close, T. J. (2007). Expression of dehydrins under heat stress and their relationship with water relations of sugarcane leaves. *Biologia plantarum*, 51, 104-109. <https://doi.org/10.1007/s10535-007-0021-0>
- Wallock-Richards, D., Doherty, C.J., Doherty, L., Clarke, D.J., Place, M., Govan, J.R. & Campopiano, D.J. (2014). Garlic revisited: antimicrobial activity of allicin-containing garlic extracts against *Burkholderia cepacia* complex, *Plos ONE*, 9 (12), 1-8. <https://doi.org/10.1371/journal.pone.0112726>
- Wang, Y., Yang, L., Zhou, X., Wang, Y., Liang, Y., et al. (2023). Molecular mechanism of plant elicitor daphnetin-carboxymethyl chitosan nanoparticles against *Ralstonia solanacearum* by activating plant system resistance. *International Journal of Biological Macromolecules*, 241, 124580. <https://doi.org/10.1016/j.ijbiomac.2023.124580>
- WHO. (2013). WHO traditional medicine strategy 2014–2023. *Alternate Integr Med*: 1–78. Retrieved from [http://www.who.int/medicines/publications/traditional/trm\\_strategy14\\_23/en/](http://www.who.int/medicines/publications/traditional/trm_strategy14_23/en/).
- Wink, M. (2003). Evolution of secondary metabolites from an ecological and molecular phylogenetic perspective. *Phytochemistry*, 64(1), 3-19. [https://doi.org/10.1016/S0031-9422\(03\)00300-5](https://doi.org/10.1016/S0031-9422(03)00300-5)
- Winkel-Shirley, B. (2001). Flavonoid biosynthesis, A colorful model for genetics, biochemistry, cell biology, and biotechnology. *Plant Physiology*, 126, 485–93. <https://doi.org/10.1104/pp.126.2.485>

- Xie, X., Wang, Q., Deng, Z., Gu, S., Liang, G., & Li, X. (2024). Keap1 Negatively Regulates Transcription of Three Counter-Defense Genes and Susceptibility to Plant Toxin Gossypol in *Helicoverpa armigera*. *Insects*, *15*(5), 328. <https://doi.org/10.3390/insects15050328>
- Yadav, B., Singla, A., Gupta, P., & Rashid, S. (2022). Study of toxin' ricinine'present in *Ricinus communis* by tlc and gc-ms a forensic perspective. *Research Journal of Pharmacy and Technology*, *15*(3), 1018-1022. <https://doi.org/10.52711/0974-360X.2022.00170>
- Yadav, M.K., Chae, S.W., Im, G.J., Chung, J.W. & Song, J.J. (2015). Eugenol: a phyto-compound effective against methicillin-resistant and methicillin-sensitive *Staphylococcus aureus* clinical strain biofilms. *PLoS ONE*, *10*(3), 1-8. <https://doi.org/10.4172/2153-2435.1000367>
- Yang, L., Wen, K. S., Ruan, X., Zhao, Y. X., Wei, F., & Wang, Q. (2018). Response of plant secondary metabolites to environmental factors. *Molecules*, *23*(4), 762. <https://doi.org/10.3390/molecules23040762>
- Yang, P., Jiang, T., Cong, Z., Liu, G., Guo, Y., et al. (2022). Loss and increase of the electron exchange capacity of natural organic matter during its reduction and reoxidation: the role of quinone and nonquinone moieties. *Environmental Science & Technology*, *56*(10), 6744-6753. <https://doi.org/10.1021/acs.est.1c08927>
- Yeshi, K., Crayn, D., Ritmejeriyè, E., & Wangchuk, P. (2022). Plant secondary metabolites produced in response to abiotic stresses has potential application in pharmaceutical product development. *Molecules*, *27*(1), 313. <https://doi.org/10.3390/molecules27010313>
- Yoshida, K. (2024). Chemical and biological study of flavonoid-related plant pigment: current findings and beyond. *Bioscience, Biotechnology, and Biochemistry*, *88* (7), 705-718. <https://doi.org/10.1093/bbb/zbae048>
- Zaker, A., Sykora, C., Gössnitzer, F., Abrishamchi, P., Asili, J., Mousavi, S.H. & Wawrosch, C. (2015). Effects of some elicitors on tanshinone production in adventitious root cultures of *Perovskia abrotanoides* Karel. *Industrial Crops and Products*, *67*, 97-102. <https://doi.org/10.1016/j.indcrop.2015.01.015>
- Zamarripa, C. A., Huskinson, S. L., Townsend, E. A., Prisinzano, T. E., Blough, B. E., Rowlett, J. K., & Freeman, K. B. (2024). Contingent administration of typical and biased kappa opioid agonists reduces cocaine and oxycodone choice in a drug vs. food choice procedure in male rhesus monkeys. *Psychopharmacology*, *241*(2), 305-314. <https://doi.org/10.1007/s00213-023-06486-5>
- Zenkner, F. F., Margis-Pinheiro, M., & Cagliari, A. (2019). Nicotine biosynthesis in Nicotiana: a metabolic overview. *Tobacco Science*, *56*(1), 1-9. <https://doi.org/10.3381/18-063>
- Zhang, X., Sun, X., Wu, J., Wu, Y., Wang, Y., Hu, X. & Wang, X. (2020). Berberine damages the cell surface of methicillin-resistant *Staphylococcus aureus*. *Frontiers in Microbiology*, *11*, 621. <https://doi.org/10.3389/fmicb.2020.00621>
- Zhao, Y., Qi, L.W., Wang, W.M., Saxena, P.K., & Liu, C.Z. (2011). Melatonin improves the survival of cryopreserved callus of *Rhodiola crenulata*. *Journal of Pineal Research*, *50*(1), 83-88. <https://doi.org/10.1111/j.1600-079X.2010.00817.x>
- Zheng, J., Yang, B., Ruusunen, V., Laaksonen, O., Tahvonen, R., Hellsten, J. & Kallio, H. (2012). Compositional differences of phenolic compounds between black currant (*Ribes nigrum* L.) cultivars and their response to latitude and weather conditions. *Journal of Agricultural and Food Chemistry*, *60*(26), 6581-6593. <https://doi.org/10.1021/jf3012739>
- Zhou, R., Yu, X., Ottosen, C.O., Rosenqvist, E., Zhao, L., Wang, Y., Yu, W., Zhao, T. & Wu, Z. (2017). Drought stress had a predominant effect over heat stress on three tomato cultivars subjected to combined stress. *BMC plant biology*, *17*(1), 1-13. <https://doi.org/10.1186/s12870-017-0974-x>
- Zu, Y.G., Tang, Z.H., Yu, J.H., Liu, S.G., Wang, W. & Guo, X.R. (2003). Different responses of camptothecin and 10-hydroxycamptothecin to heat shock in *Camptotheca acuminata* seedlings. *Acta Botanica Sinica-Chinese Edition*, *45*(7), 809-814.
- Zuo, GY, Li, Y., Han, J., Wang, G.C., Zhang, Y.L., & Bian, Z.Q. (2012). Antibacterial and synergy of berberines with antibacterial agents against clinical multi-drug resistant isolates of methicillin-resistant *Staphylococcus aureus* (MRSA). *Molecules*, *17*(9), 10322-10330. <https://doi.org/10.3390/molecules170910322>






# Journal of Experimental Biology and Agricultural Sciences

<http://www.jebas.org>

ISSN No. 2320 – 8694

## Plant growth promotion activities of *Bacillus* spp. isolated from Jakrem hot water spring of Meghalaya, North East India

Amrit Kumar<sup>1,2</sup> , Jintu Rabha<sup>3</sup> , Kumananda Tayung<sup>1\*</sup> 

<sup>1</sup>Mycology and Plant Pathology Laboratory, Department of Botany, Gauhati University, Assam, 781014, India

<sup>2</sup>Department of Botany, Nowgong College (Autonomous), Nagaon, Assam, 782001, India

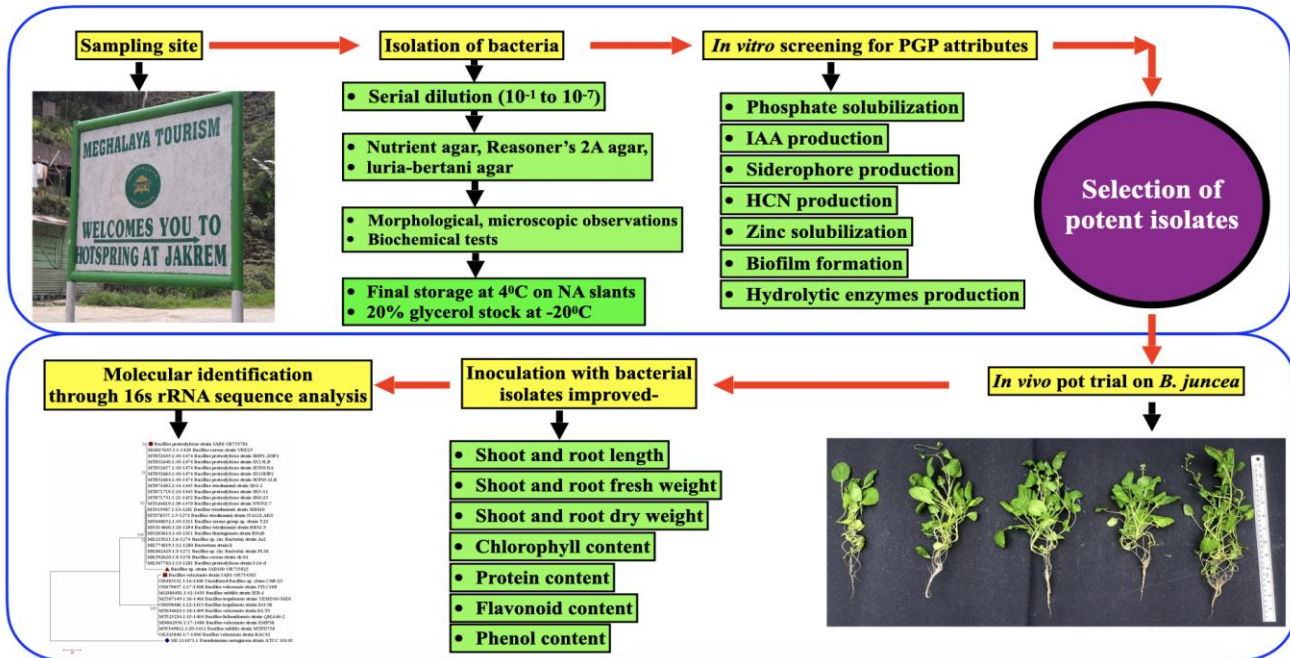
<sup>3</sup>Microbial Ecology Laboratory, Department of Botany, Gauhati University, Assam, 781014, India

Received – April 22, 2024; Revision – June 14, 2024; Accepted – June 28, 2024

Available Online – July 15, 2024

DOI: [http://dx.doi.org/10.18006/2024.12\(3\).335.353](http://dx.doi.org/10.18006/2024.12(3).335.353)

### GRAPHICAL ABSTRACT



\* Corresponding author

E-mail: [kumanand@gauhati.ac.in](mailto:kumanand@gauhati.ac.in) (Kumananda Tayung)

Peer review under responsibility of Journal of Experimental Biology and Agricultural Sciences.

All the articles published by [Journal of Experimental Biology and Agricultural Sciences](http://www.jebas.org) are licensed under a [Creative Commons Attribution-NonCommercial 4.0 International License](https://creativecommons.org/licenses/by/4.0/) Based on a work at [www.jebas.org](http://www.jebas.org).

Production and Hosting by Horizon Publisher India [HPI]  
(<http://www.horizonpublisherindia.in/>).  
All rights reserved.



## KEYWORDS

*Bacillus* spp.

Hot spring

Hydrolytic enzymes

IAA production

Growth promotion

## ABSTRACT

The study aims to investigate plant growth promotion (PGP) activities of thermophilic bacteria isolated from the Jakrem hot spring in Meghalaya, North-East India, and determine their effect on *Brassica juncea*'s growth. The bacteria were isolated by a culture-dependent approach following a serial dilution method in a nutrient agar medium. All the isolates were determined for PGP attributes such as indole acetic acid, phosphate solubilization, hydrolytic enzymes, and siderophore production. The potent bacterial isolates were characterized by 16S rDNA sequencing and phylogenetic analysis. Altogether, 53 bacterial isolates were obtained, most belonging to the genus *Bacillus*. Of the total isolates, 37.7% exhibited both PGP and hydrolytic enzyme activities. Three isolates, namely JAB1, JAB8, and JAB100, showed promising PGP and were identified as *Bacillus velezensis*, *B. proteolyticus*, and *Bacillus* sp., respectively. The PGP attributes of these isolates were determined *in vivo* on *B. juncea*, and their effects were measured in terms of shoot and root length biomass and biochemical contents. It was observed that combined inoculation of all three isolates significantly enhanced the growth and development of *B. juncea*, evident by increased shoot and root length, fresh and dry weight, and higher levels of protein, phenol, flavonoid, and chlorophyll content compared to the control. In conclusion, the study highlights the potential application of thermophilic *Bacillus* spp. from hot springs as bioinoculants to enhance crop productivity in sustainable agricultural practices.

## 1 Introduction

Substantial demand for food has increased in recent years due to limited land resources and the rise of the global population. Food production has increased significantly through chemical fertilizers in conventional agricultural systems to feed the growing population (Mishra and Dash 2014). However, indiscriminate and excessive use of chemical fertilizers to increase crop productivity has severely adverse effects on living organisms and the environment. Therefore, a sustainable agricultural system is urgently needed to overcome this problem and achieve food security for the growing global population (Glick 2018). Organic farming using beneficial microorganisms has gained tremendous attention as an alternative to agrochemicals. These microbes are used as bioinoculants to increase soil fertility and improve plant growth and soil health by increasing the supply of readily available nutrients or protecting them from biotic and abiotic stresses (Lugtenberg and Kamilova 2009).

Hot springs represent a unique ecological niche for microorganisms thriving under extreme environmental conditions. Recently, microbes, especially bacterial communities isolated from such environments, appeared to be of utmost importance due to producing industrially significant enzymes and secondary metabolites with multiple applications (Verma et al. 2018). Bacterial genera belonging to such extreme conditions have been reported to possess higher metabolic rates and stability when compared with their mesophilic counterpart (Verma et al. 2018). Moreover, enzymes produced by various bacterial genera, such as *Bacillus* sp. isolated from hot springs, remained stable and active at higher temperatures (Panda et al. 2013). Due to this property, thermophilic microorganisms have gained considerable attention

for large-scale production of enzymes, sugars, and a wide array of secondary metabolites (Satyanarayana et al. 2005; Lele and Deshmukh 2016; Mohammad et al. 2017). Besides, thermophilic microorganisms have also shown their ability to increase plant growth, resistance to salinity in crops of agricultural interest, and biocontrol against phytopathogens (Verma et al. 2018; Shilev 2020). Many instances have demonstrated that hot springs microorganisms, especially *Bacillus* spp., are potent agents for inducing the growth of plants through various plant growth-promoting attributes (Saharan and Verma, 2014; Verma et al. 2018). Production of different phytohormones viz. indole-3-acetic acid (IAA), cytokinins, gibberellins along with phosphate solubilization, iron chelation, production of 1-aminocyclopropane-1-carboxylate (ACC) deaminase and nitrogen-fixing properties that aid in plant growth promotion had also been previously reported from different species of *Bacillus* isolated from extreme environmental condition (Stein 2005; Yang et al. 2009; Arguelles-Arias et al. 2009; Rahman et al. 2016; Kaki et al. 2017; Verma et al. 2018; Kumar et al. 2021). Therefore, isolating beneficial microorganisms, particularly bacteria, from pristine environments, such as hot springs, would be paramount for bioinoculants for plant growth and health (Podile and Kishore 2006; Saharan and Nehra 2011).

Meghalaya is situated in India's North-Eastern Region (NER) and is rich in various natural resources. The state is endowed with several high-altitude lakes and hot springs. One such hot spring is Jakrem, which is less explored and located in one of the mega biodiversity-rich zones of the world in the Himalayan geothermal belt (Rakshak et al. 2013; Panda et al. 2016). Preliminary studies on microbial diversity of this hot spring by culture-independent approach had revealed a rich diversity of



microorganisms dominated by Firmicutes, Chloroflexi, unclassified bacteria, and a large number of sequences reads from bacterial taxa Arthronema which may represent novel species (Panda et al. 2016). However, a culture-dependent approach has not yet been undertaken to investigate the microbes for biotechnological applications. Therefore, the present study aimed to isolate and characterize the bacterial species from this hot spring by a culture-dependent approach, evaluate the isolates for plant growth promotion potential, and observe their effect on the growth and development of *B. juncea*, a commonly used leafy vegetable of North East India.

## 2 Materials and Methods

### 2.1 Study site and collection of sample

The hot spring of Jakrem is located in the West Khasi hill district of the Meghalaya state, which is situated at 25°24.463' N and 91°32.409' E and an altitude of 1439 m above mean sea level (MSL). Geographical positioning data and temperature of the water sample were recorded at the sampling site using a GPS locator system (Garmin eTrex 10) and portable thermometer (HICKS, Oval) respectively. The pH of the collected samples was recorded in the laboratory using a digital pH meter (Cyberscan, EUTECH). For collection of water samples, plastic containers (500 ml) were first cleaned with 20% sodium hypochlorite solution, washed thoroughly with several steps of sterile distilled water, and autoclaved at 121°C for 15 min. The containers were dried in a hot air oven at 50°C for 1 h and sterilized further under UV light in a laminar airflow cabinet for 1 h. Water samples were randomly collected in triplicates from hot springs in these plastic containers, stored in a dry ice box, and transported immediately to the laboratory (Kambura et al. 2016).

### 2.2 Isolation and identification of bacteria

Bacteria were isolated following serial dilution technique ( $10^{-1}$  to  $10^{-7}$ ) using three different growth mediums viz. nutrient agar (NA), Reasoner's 2A agar (R2A), and Luria-Bertani agar (LBA) medium. Briefly, 100 µl aliquot of each dilution was spread on growth media and sealed with paraffin strips. These plates were then incubated at 44±1°C for 72-96 h. After the incubation period, the dilution factor, at which the number of colonies ranged between 30-300, was further selected to calculate the colony format unit (CFU)/ml of the water sample. Distinct colonies on the growth medium were purified by repeated sub-culturing, and finally, purified bacterial isolates were stored at 4°C on NA slants and 20% glycerol stock at -20°C (Fasina et al. 2020; Kumar et al. 2021). Microscopic examinations were carried out at 1000X magnification using immersion oil in the compound microscope (LYNX, Lawrence & Mayo), and Cell morphology, viz. shape, size, elevation, pigmentation, and colour were recorded. Different

biochemical tests viz. catalase, oxidase, gram staining, and citrate utilization were carried out for identification up to genus level (Brenner et al. 2005; Yazdani et al. 2009; Kumar et al. 2012; Islam et al. 2017; Fasina et al. 2020; Tripathi and Sapra 2021).

### 2.2.1 Thermo-tolerance profile of isolated bacterial strains

The thermo-tolerant property of the bacterial isolates was determined by growing the isolates in freshly prepared NA medium and then incubating them at different temperatures: 30±1°C, 40±1°C, 50±1°C and 60±1°C for a period of 24 to 72 hours. The visible appearance of bacterial growth at specific thermal intervals was recorded as positive and was classified according to binary code viz. 0 (no growth) and 1 (appearance of growth on the medium), as suggested by Moreno et al. (2021) and López et al. (2021).

### 2.3 Physico-chemical analysis of water sample

Samples were analyzed for turbidity, Iron, chloride, fluoride, total hardness, calcium, magnesium, sulphate, nitrate, lead, nitrite, alkalinity, sodium, potassium, sulphide, cadmium, chromium, phosphorous, total organic carbon, total nitrogen, total suspended solids (TSS), volatile suspended solids (VSS) and total dissolved solids (TDS) as per the standard methodology (Indian Standard "IS 3025" 2009; APHA 2017; Kalsait et al. 2018; Agarwal et al. 2019).

### 2.4 Screening of the isolated bacterial isolates for plant growth-promoting traits

#### 2.4.1 Solubilization of phosphate

The isolated bacterial isolates were screened for their inorganic phosphate solubilization potential using Pikovskaya's agar medium. A loopful of bacterial culture was spot inoculated onto the agar plates and incubated at 30±1°C for 72-96 hours. The ability of the bacteria to solubilize inorganic phosphate was determined by forming a clear halo zone surrounding the bacterial colony, indicating phosphate solubilization activity (Syiemiong and Jha 2019). The diameter of the halo zone was measured to quantify the solubilization efficiency of each isolate. Phosphate solubilization was quantified in Pikovskaya's broth medium, which contained 0.5% tri-calcium phosphate as a sole source of inorganic phosphorous. The broth medium was inoculated with 100 µl of overnight grown bacterial strains ( $10^6$  cells/ml) and incubated in continuous shaking (120 rpm) for 144 h at 30±1°C. After incubation, a cell-free supernatant was obtained by centrifugation for 5 minutes at 10000 rpm. The obtained cell-free supernatant (0.5 ml) was mixed with 10% trichloroacetic acid (0.5 ml) and color reagent (4 ml) [1 (3M H<sub>2</sub>SO<sub>4</sub>): 1 (2.5% ammonium molybdate): 1 (10% ascorbic acid): 2 (distilled water)] (Syiemiong and Jha 2019). The resulting mixture was incubated at 30±1°C for 15 min, and absorbance of the resulting mixture was read at 820 nm



wavelength against control using a spectrophotometer. Solutions of  $\text{KH}_2\text{PO}_4$  was used at different concentrations to prepare the standard curve, and the amount of phosphorous solubilized by the bacterial isolates was calculated and expressed as  $\mu\text{g/ml}$  (Syiemiong and Jha 2019).

#### 2.4.2 Indole-3-acetic acid (IAA) production

IAA production was quantified by supplementing L-tryptophan (0.2%) as the precursor for IAA synthesis in the Luria Bertani broth medium. The broth medium was inoculated with overnight grown bacterial strains (100  $\mu\text{l}$ ;  $10^6$  cells/ml) and incubated at  $30\pm 1^\circ\text{C}$  for 96 h in shaking condition (120 rpm). Following incubation, cell-free supernatant (1 ml) was obtained by centrifugation at 10000 rpm for 10 min and mixed with Salkowsky reagent (3 ml). The reaction mixture was incubated in the dark for 15 min, and the absorbance of the developing color was read at 530 nm wavelength using a spectrophotometer against control (3 ml of Salkowsky reagent + 1 ml Luria-Bertani broth medium supplemented with 0.2% L-tryptophan). For estimation of IAA produced by bacterial strains, a standard curve was prepared from different concentrations viz. 5, 10, 20, 50 and 100  $\mu\text{g/ml}$  of pure IAA was used and expressed as  $\mu\text{g/ml}$  (Syiemiong and Jha 2019).

#### 2.4.3 Siderophore production

A qualitative assay for Iron chelating activity by the bacterial isolates was performed on CAS (Chrome azurol S) agar medium. For this assay, solution A (60.5 mg of CAS in 50 ml of sterile distilled water was mixed with 10 ml of 1 mM  $\text{FeCl}_3 \cdot 6\text{H}_2\text{O}$  prepared in 10 mM HCl) was mixed with solution B (72.9 mg of hexadecyl tri-methyl ammonium bromide in 40 ml of sterile distilled water) (Kumar et al. 2021). A solid agar medium (Kings medium B base; 42.23 gm/l) was prepared separately, and both the stock solution and the agar medium were autoclaved and allowed to cool inside the laminar airflow cabinet. When the temperature lowered to  $40\text{--}50^\circ\text{C}$ , both the solutions were mixed and poured onto petri plates and allowed to solidify. Bacterial strains were spot-inoculated onto petri plates and incubated for 96 h at  $30\pm 1^\circ\text{C}$ . The development of the orange-yellow zone surrounding the bacterial colony was recorded as positive for siderophore production (Kumar et al. 2021).

#### 2.4.4 Hydrogen cyanide (HCN) production

A qualitative assay for HCN production was carried out on Tryptic soy broth (30 g/l) amended with glycine (4.4 g/l). Briefly, overnight grown bacterial strains (100  $\mu\text{l}$ ,  $10^6$  cells/ml) were inoculated onto broth medium, and sterilized filter paper strips of uniform size (5 cm $\times$ 0.5 cm) soaked into a solution of 0.5 % picric acid in 2%  $\text{Na}_2\text{CO}_3$  was placed inside the tube in hanging position.

The tubes were air-tight with parafilm and incubated at  $30\pm 1^\circ\text{C}$  for 96 h. Following incubation, the filter paper was observed for color change from yellow to orange-brown for positive HCN production by the bacterial strains (Wani and Khan 2013).

#### 2.4.5 Zinc solubilization

Zinc solubilization was estimated qualitatively using zinc oxide (0.1%) amended in a minimal agar medium (MM9). A loopfull culture of bacterial isolate was spot inoculated onto the agar plates and incubated at  $30\pm 1^\circ\text{C}$  for 48 h. Following the incubation period, the development of a clear zone surrounding the colony was recorded as positive for zinc solubilization (Goteti et al. 2013).

#### 2.4.6 Biofilm formation

Quantitative detection of biofilm activity was carried out by inoculating bacterial strains (100  $\mu\text{l}$ ,  $10^6$  cells/ml) in a 5 ml broth medium. Following inoculation, the broth medium was incubated for 72 h at  $30\pm 1^\circ\text{C}$  under shaking conditions (120 rpm). After an incubation period, the cultured medium containing the bacterial cells was discarded completely and washed with phosphate buffer saline thrice (1X PBS pH 7.2) to remove adherent cells. The tubes were dried inside the laminar air flow cabinet and stained with crystal violet solution (0.2%) for 5 min. The tubes were again rinsed with phosphate buffer saline to remove excess stain, followed by air-drying. The absorbance of the stain adhered was read at 630nm wavelength by adding 2 ml of 95% ethanol in each tube against blank (Lotfi et al. 2014). The degree of adhesion was recorded as:

ODs < ODc: non-adherent

ODc < ODs < 2XODc: weakly-adherent

2x ODc < ODs < 4XODc: moderately-adherent

4xODc < ODs: strongly-adherent

Where ODc- control; ODs-sample, respectively.

### 2.5 Screening for the production of extracellular hydrolytic enzymes

#### 2.5.1 Cellulase

For this assay, bacterial isolates were spot inoculated onto solid agar plates amended with 0.1% carboxymethyl cellulose (CMC) as substrate. Following incubation, for 48 h at  $30\pm 1^\circ\text{C}$ , the solid agar plates were flooded with 0.1% congo red solution for 5 min and decanted. The plates were again flooded with 1M sodium chloride for 15 min. The development of a clear zone surrounding the bacterial colony was recorded as positive for extracellular cellulase activity (Kumar et al. 2021).

### 2.5.2 Amylase

For this assay, bacterial isolates were spot inoculated onto solid agar plates amended with 1% soluble starch as substrate. Following incubation, for 48 h at  $30\pm 1^{\circ}\text{C}$ , the plates were flooded with grams iodine solution for 5 min and decanted. Development of the clear zone surrounding the bacterial colony was recorded as positive for extracellular amylase activity (Kumar et al. 2021).

### 2.5.3 Lipase

For this assay, a loopfull culture of bacterial strain was spot inoculated onto Tributyrin agar (without Tributyrin) supplemented with Tributyrin (10 ml/ 1000 ml) as substrate and incubated at  $30\pm 1^{\circ}\text{C}$  for 48 h. Following incubation, the development of the clear zone surrounding the bacterial colony was recorded as positive for extracellular lipase activity (Berg 2009).

### 2.5.4 Protease

For the hydrolysis of protease, 10% skim milk was used as a substrate onto a solid agar medium (MM9). This medium was autoclaved and cooled to  $40\text{--}50^{\circ}\text{C}$ , then poured onto petri plates to solidify. Bacterial isolates were then spot-inoculated onto agar plates, following incubation at  $30\pm 1^{\circ}\text{C}$  for 48 h. The development of a clear zone surrounding the bacterial colony was recorded as positive for extracellular protease activity (Kumar et al. 2021).

### 2.5.5 Laccase

A solid agar medium was amended with 0.1% guaiacol as a substrate for laccase activity. Bacterial isolates were spot inoculated onto agar plates and incubated at  $30\pm 1^{\circ}\text{C}$  for 96 h. Following incubation, grams iodine was flooded onto petri plates for 5 min. Development of the clear zone surrounding the bacterial colony was recorded as positive for laccase activity (Kumar et al. 2021).

## 2.6 Mass multiplication of bacterial isolates

Based on the results from various *in-vitro* evaluations for plant growth promotion activities, the potent bacterial isolates were selected for *in-vivo* pot experimental trials. Mass multiplication of bacterial isolates was carried out by inoculating a loopfull culture of bacterial isolates in a 150 ml nutrient broth medium and incubating under continuous shaking conditions for 24 h at  $30\pm 1^{\circ}\text{C}$ . Following incubation, cells were harvested by centrifugation at 10000 rpm for 10 min and suspended in sterile distilled water. Bacterial density was further adjusted to  $10^6$  cells/ml using a haemocytometer count and stored at  $4^{\circ}\text{C}$  for field application (Kumar et al. 2021).

## 2.7 Pot experimental trial of potent bacterial isolates

A pot experimental trial on *B. juncea* evaluated the in-vivo plant growth-promoting potential of the potent bacterial isolates. Briefly, seeds of *B. juncea* were obtained from the National Bureau of Plant Genetic Resources (NBPGR), Umiam, Meghalaya, with cultivar number-IC 597866 and surface sterilized with a solution of sodium hypochlorite (2.5%) for 10 min. After surface sterilization, seeds were thoroughly washed with several steps of sterile distilled water (until traces of sodium hypochlorite was removed). The surface sterilized seeds were dried on sterile filter paper inside a laminar airflow cabinet (Gupta et al. 2020; Goswami and Deka 2020; Kumar et al. 2021). Ten seeds were transferred to each pot containing 200 g of double autoclaved sterilized soil and 20 ml of bacterial cell suspension ( $10^6$  cells/ml) was inoculated in pot with following sets of treatment: T1- Control (seeds without bacterial inoculation); T2 - seeds inoculated with bacterial isolate JAB1; T3 seeds inoculated with isolate JAB8; T4- seeds inoculated with isolate JAB100; T5- seeds inoculated with isolates JAB1+ JAB8; T6- seeds inoculated with isolates JAB8+ JAB100; T7- seeds inoculated with isolates JAB1+ JAB100; T8- seeds inoculated with isolates JAB1+ JAB8+ JAB100.

## 2.8 Growth and biochemical parameters studied

### 2.8.1 Evaluation of length (shoot and root), fresh weight and dry weight

After 45 days of seed sowing, different growth parameters, like shoot and root length, were determined using a standard scale. Fresh weight (root and shoot) was determined by harvesting the mustard plant and then washing it with running water to remove adhering particles. Excess moisture was removed using filter papers, and the fresh weight (root and shoot) was measured using an electronic weighing balance. Plant samples were then dried in an oven at  $70^{\circ}\text{C}$  and measured consecutively after 24 h until constant weight was attained for dry weight determination (Huang et al. 2017).

### 2.8.2 Chlorophyll content

The chlorophyll content was estimated in mustard leaves with 80% acetone. Briefly, mustard leaves (0.5 g) were finely ground using a mortar and pestle in 20 ml of acetone (80%). Supernatant from the resulting mixture was collected following centrifugation at 10000 rpm for 10 min, and the absorbance was recorded at 645 nm and 663 nm wavelength in a spectrophotometer against blank (only 80% acetone). Chlorophyll content was recorded as milligrams (mg) per gram (g) of fresh weight (FW) using the following formula (Arnon 1949; Sarkar and Kalita 2022).

Chlorophyll a (mg/g FW):  $\{12.7 \times (\text{Absorbance at } 663\text{nm}) - 2.69 \times (\text{Absorbance at } 645\text{nm})\} \times V/1000 \times W$

Chlorophyll b(mg/g FW):  $\{22.9 \times (\text{Absorbance at } 645\text{nm}) - 4.68 \times (\text{Absorbance at } 663\text{nm})\} \times V/1000 \times W$

Total chlorophyll (mg/g FW):  $\{20.2 \times (\text{Absorbance at } 645\text{nm}) + 8.02 \times (\text{Absorbance at } 663\text{nm})\} \times V/1000 \times W$

Where, V: Final volume of 80% acetone; W: Sample weight

### 2.8.3 Protein content

Estimating total protein content in leaves was conducted per the methodology described by Lowry et al. (1951) with some modifications. Briefly, fresh leaves (0.2 g) were crushed in 10 ml of 0.1M phosphate buffer using mortar and pestle. The resulting mixture was centrifuged for 10 min at 10000 rpm, and the obtained supernatant (1ml) was mixed with alkaline copper reagent (5 ml) [48 ml of 2%  $\text{Na}_2\text{CO}_3$  prepared in 0.1N NaOH (48 ml)+ 1%  $\text{KNaC}_4\text{H}_4\text{O}_6 \cdot 4\text{H}_2\text{O}$  (1 ml)+ 0.5%  $\text{CuSO}_4$  (1 ml)]. The final mixture was incubated for 15 min, and then 2N freshly prepared Folin-Ciocalteu reagent (1 ml) [Folin-Ciocalteu reagent (1): water (1)] was further added, followed by additional incubation in the dark for 30 min. After incubation, the absorbance of the developing mixture was read at 660 nm wavelength against control using a spectrophotometer. The amount of soluble protein was calculated from a bovine serum albumin (BSA) standard and expressed as mg BSAE/ g of fresh weight (Sarkar et al. 2020).

### 2.8.4 Phenol content

Total phenolic content was estimated according to the methodology described by Sarkar and Kalita (2022) with some modifications. Dried leaves (0.5g) were crushed using a mortar and pestle in chilled methanol and centrifuged at 10000 rpm for 10 min. Estimation of total phenol was carried out by adding 2.5 ml of Folin- Ciocalteu reagent (10% in water) and 2.5 ml of 7.5%  $\text{Na}_2\text{CO}_3$  to 500  $\mu\text{l}$  of the obtained supernatant, followed by incubation in the dark for 40 min at  $45 \pm 1^\circ\text{C}$ . The absorbance of the mixture was read at 765 nm wavelength using a spectrophotometer. The total phenol content in the sample was expressed as mg of gallic acid equivalent (GAE)  $\text{g}^{-1}$  DW using gallic acid as the standard.

### 2.8.5 Flavonoid content

Flavonoid content was estimated as per the methodology described by Sarkar and Kalita (2022). Briefly, supernatant extracted in methanol (100  $\mu\text{l}$ ) was mixed with distilled water (400  $\mu\text{l}$ ) and 5%  $\text{NaNO}_2$  (30  $\mu\text{l}$ ) and incubated for 5 min at  $30 \pm 1^\circ\text{C}$ . 10%  $\text{AlCl}_3$  (30  $\mu\text{l}$ ) was added to the mixture and incubated for 6 min at  $30 \pm 1^\circ\text{C}$ . After incubation, 1M NaOH (200  $\mu\text{l}$ ) was added to the mixture, and the final volume was adjusted to 1 ml with distilled water. The mixture was vortexed and incubated again for 5 min at  $30 \pm 1^\circ\text{C}$ . After incubation, the absorbance of the sample was read at 510 nm

wavelength using a spectrophotometer and expressed as mg of quercetin equivalent (QE)  $\text{g}^{-1}$  FW of the sample using quercetin as standard.

## 2.9 Molecular identification of potent bacterial isolates

Genomic DNA of the potent bacterial isolates was extracted using a Genomic DNA extraction kit as per manufacturer instructions. The extracted DNA was subjected to PCR amplification using universal primers 27F (5'-AGAGTTTGATCTGGCTCAG-3') and 1492R (5'-TACGGYTACCTTGTTACGACTT-3') in a thermal cycler. The reaction mixture contained dATP (0.2 mM), dCTP (0.2 mM), dGTP (0.2 mM), and dTTP (0.2 mM), 27F (1  $\mu\text{M}$ ), 1492R (1  $\mu\text{M}$ ),  $\text{MgCl}_2$  (2 mM), Taq DNA polymerase (1.25 U), genomic DNA (1  $\mu\text{l}$ ) with following reaction condition,  $95^\circ\text{C}$  (2 min), followed by 35 cycles of  $95^\circ\text{C}$  (30 s),  $53^\circ\text{C}$  (30 s) and  $72^\circ\text{C}$  (1.30 min) and final extension at  $72^\circ\text{C}$  (7 min). The amplified products were resolved through electrophoresis containing 1.2% agarose and were imaged in a gel documentation system. Purification and 16S rRNA gene sequencing of the amplified PCR products were performed at Unigenome (Unipath Specialty Laboratory). Using 16S rRNA gene sequences of the isolates, the phylogenetic tree was constructed using the neighbour-joining method to know their phylogenetic affiliations. The sequences were submitted to the GenBank NCBI database, and accession numbers were obtained (Agarwal et al. 2020; Kumar et al. 2021).

### 2.9.1 Statistical analysis

All the experiments were conducted in triplicates and expressed as a mean of three replicates with standard deviation. For data analysis of plant growth, ANOVA was conducted using R software (Version-1.2.1335) and significant differences were determined using the least significant differences test (LSD) at a significance level of  $P \leq 0.05^*$ .

## 3 Results and Discussion

### 3.1 Bacteria isolated from hot water spring

The pH of water samples obtained from the Jakrem hot spring was alkaline ( $8.54 \pm 0.02$ ) with a recorded temperature of  $44.96 \pm 0.2^\circ\text{C}$  at the sampling site. The temperature range of the hot water spring of Jakrem was classified as moderate thermophilic, and in many instances, the temperature of hot water springs located in different parts of India has also been reported to be moderately thermophilic (Yadav et al. 2015; Poddar and Das 2018; Narsing Rao et al. 2021). Our result corroborates with many previous studies where the pH of hot water springs was reportedly alkaline, and the temperature was often higher than  $40^\circ\text{C}$  (Mohammad et al. 2017; Sahay et al. 2017). Following serial dilutions, 53 distinct bacterial isolates were isolated in different media compositions. The water samples' colony forming unit (CFU) was  $1.36 \times 10^{-1}$  CFU/ml.

Based on morphological, microscopic and biochemical characterization, the isolates were rod-shaped and gram-positive bacteria belonging to the genus *Bacillus*. Worldwide geothermal sites are favourable habitats for thermophilic bacteria, which have developed unique survival strategies to adapt to such an environment. The dominant isolated bacteria belong to the genus *Bacillus* in the present study. The prevalence of the genus *Bacillus* and related genera as the dominant members have been previously reported from different hot springs (Adiguzel et al. 2009; Yadav et al. 2015; Priya et al. 2016). The occurrence of *Bacillus* species in different hot springs worldwide may be attributed to their high GC content and endospore formation, which might have favoured better adaptability for surviving in such extreme environmental conditions (Panda et al. 2013).

### 3.1.1 Thermo-tolerance profile of bacterial isolates

In the present study, thermo-tolerance profiles of the 53 bacterial isolates were determined at 4 different thermal intervals viz. 30, 40, 50 and 60°C. The results showed a score of 0 (no growth) for only 2 bacterial isolates at 30°C and 1 (visible growth) for 51 bacterial isolates at 30°C. In the present study, all 53 bacterial isolates were recorded positive and showed visible growth on NA medium with a score of 1 at 40 and 50°C. However, when the incubation temperature was increased to 60°C, only 29 bacterial isolates were recorded positive with a score of 1 (visible growth); therefore, these isolates can be considered thermophilic. The three potent bacterial isolates identified as *B. velezensis*, *B. proteolyticus*, and *Bacillus* sp. were thermophilic. Depending on the temperature range required for growth, bacteria can be classified as mesophilic, psychrophilic, thermophilic or thermotolerant (Moreno et al. 2021). Microorganisms that grow in wide temperature ranges offer better adaptability for survival in extreme environments (Kumar et al. 2013; Pandey et al. 2015; Khan et al. 2020). Isolation of thermo-tolerant strains of *Bacillus* and subsequent application as plant growth-promoting organic amendment have been cited in numerous literature (Kumar et al. 2013; Pandey et al. 2015; Khan et al. 2020). In this study, combined inoculation of the selected *Bacillus* species enhanced the growth and development of *B. juncea*. A similar result was observed in which inoculation with thermotolerant *Bacillus* sp. increased plant growth and development in soybean (Khan et al. 2020).

### 3.2 Physico-chemical properties of the water sample

The collected water sample was subjected to a comprehensive physico-chemical analysis. The physicochemical analysis of the water samples recorded 14 different mineral elements (Table 1).

The major elements consisted of sodium (20.76±1.45 mg/l), sulphate (14.53±0.35 mg/l) and chloride (14.47±0.67 mg/l). The chemical composition of hot water is predominantly influenced by

the interactions it undergoes with reservoir rocks and the minerals present in those rocks during its ascent, potentially leading to the spring water exhibiting either acidity or alkalinity (Chan et al. 2017). Notably, sodium content was found to be considerably low, which was agreed upon compared to a similar study on Jakrem conducted by Panda et al. (2016). Such low sodium content is often a characteristic of medium-low temperature geothermal systems (Mao et al. 2022). The physicochemical properties of the water samples followed the result obtained by Singh et al. (2018), who studied water samples from 9 different hot springs with increased concentrations of these elements. In this study, the sulphur content of the water sample was found to be high. Poddar and Das (2018) have also reported high sulphur content in water

Table 1 Physico-chemical properties of water samples from Jakrem hot spring

Parameter	Values
Temperature	44.96±0.2
pH	8.54±0.02
Turbidity (NTU)	0.49±0.37
Iron (mg/l)	0.02±0.005
Chloride (mg/l)	14.47±0.67
Fluoride (mg/l)	0.06±0.01
Calcium (mg/l)	4.73±1.44
Magnesium (mg/l)	0.51±0.16
Sulphate (mg/l)	14.53±0.35
Nitrate (mg/l)	10.73±0.15
Lead (mg/l)	0.003±0.001
Nitrite (mg/l)	0.001±0.0005
Alkalinity (mg/l)	8.56±1.25
Sodium (mg/l)	20.76±1.45
Potassium (mg/l)	2.83±0.65
Sulphide (mg/l)	0.004±0.001
Chromium (mg/l)	0.001±0.0005
Cadmium (mg/l)	Not Detected
Phosphorous (mg/l)	0.27±0.21
Total Organic Carbon (TOC) (mg/l)	0.42±0.03
Total nitrogen (mg/l)	0.04±0.011
Total hardness (mg/l)	16.9±6.45
Total Dissolved Solids (TDS) (mg/l)	141±27.22
Total Suspended Solids (TSS) (mg/l)	0.44±0.02
Volatile Suspended Solids (VSS) (mg/l)	0.85±0.54

Values are the mean of 3 replicates (n-3); ± standard deviation

samples of different hot springs in India. As suggested by earlier studies, the abundance of sulfate-reducing bacterial forms in the water sample could be the reason for this observation (Panda et al. 2016). In addition, trace amounts of heavy metals, specifically chromium ( $0.001\pm 0.0005$  mg/l) and lead ( $0.003\pm 0.001$  mg/l), were also detected, with their low concentrations unlikely to be toxic to the microbial population. Tekere et al. (2012) have also reported the presence of trace amounts of chromium and lead in water samples collected from different hot springs. Gram-positive bacteria identified in this study indicate a potential tolerance to the existing concentrations of these heavy metals, as they are generally more resilient to chromium than gram-negative counterparts (Fathima and Rao 2018). The sample also revealed  $141\pm 27.22$  mg/l of total dissolved solids (TDS),  $0.44\pm 0.02$  mg/l of total suspended solids (TSS) and  $0.85\pm 0.54$  mg/l of volatile suspended solids (VSS). A lower TDS level usually favors microbial growth, unlike a high TDS level, which can create a hostile environment for certain microbes, potentially affecting their survival and growth (Hanson et al. 2019). Similarly, the total dissolved solids (TDS) were in accordance with the water samples of different hot springs reported by many previous workers (Tekere et al. 2011; Kumar and Sharma 2019). Additionally, total organic carbon (TOC) and total nitrogen were found to be  $0.42\pm 0.03$  mg/l and  $0.04\pm 0.011$  mg/l, respectively, providing insights into the water's organic matter and nutrient content (Badhai et al. 2015). It was interesting to note that the local communities used the water sample of Jakrem hot spring for their curative properties against various skin ailments. This may be because sulphur from such natural hot springs has been known to alleviate the symptoms and have curative properties of an array of diseases, such as skin, high blood pressure and arthritis (Das et al. 2016; Jena et al. 2018). These results contributed to our understanding of the physico-chemical characteristics of Jakrem hot spring water and highlighted the potential implications for microbial communities in similar environments.

### 3.3 Plant growth promotion properties of the bacterial isolates

#### 3.3.1 production of extracellular hydrolytic enzymes

In the present study, out of 53 bacterial isolates, qualitative analysis revealed that isolate JAB100 showed 19 bacterial isolates positive for proteolytic activity and maximum activity. Similarly, 19 isolates showed positive results for cellulolytic activity and amongst the positive isolates, maximum halozone formation was shown by the isolate JAB1. Again, 20 isolates showed positive results for lipolytic activity with maximum halozone formation, as shown by the isolate JAK9. For amylolytic activity, 16 bacterial isolates showed positive results and maximum halozone formation was observed in the isolate JAK17. Screening for laccase enzyme also revealed 19 isolates with positive activity, and maximum halozone formation was shown by the isolate JK54 (Table 2). The

result indicated that thermophilic bacterial isolates could produce different hydrolytic enzymes. Similarly, Lele and Deshmukh (2016) reported that bacterial isolates isolated from Indian hot springs produced considerable hydrolytic enzymes. Production of different hydrolytic enzymes is considered an important attribute towards induction of plant growth promotion and biocontrol against numerous phytopathogens (Villarreal-Delgado et al. 2018; Morales-Cedeno et al. 2021). In addition, enzymes produced by thermophilic bacteria have an inherent ability to remain active at higher temperatures and can withstand harsh environments; therefore, they have potential industrial applications (Sahay et al. 2017). Since the isolates producing these enzymes are *Bacillus* species, the findings corroborate with Aanniz et al. (2015), who reported cellulase, amylase and protease enzyme production by thermophilic *Bacillus* spp. These enzymes have been known to play an important role in the biological transformation of wastes. Therefore, it can be assumed that producing hydrolytic enzymes by the thermophilic bacterial isolates might help decompose organic matter, thereby determining the physical and chemical properties of the hot springs water.

#### 3.3.2 Indole-3-acetic acid (IAA) production

Altogether, 20 isolates showed positive results for IAA activity in qualitative analysis both in the presence and absence of L-tryptophan (Table 3). Quantitative analysis revealed that the bacterial isolate JAB100 showed the highest IAA production. The isolate produced  $2.751\pm 0.078$   $\mu\text{g/ml}$  of IAA in the presence of L-tryptophan, followed by the isolates JAB1 and JAB8, which produced  $2.717\pm 0.138$   $\mu\text{g/ml}$  and  $1.916\pm 0.047$   $\mu\text{g/ml}$  of IAA respectively. However, in the absence of L-tryptophan, the highest IAA production was shown by the isolate JAB1, which produced  $1.849\pm 0.048$   $\mu\text{g/ml}$  of IAA, followed by the isolates JAB8 and JAB100 with IAA production of  $1.458\pm 0.074$   $\mu\text{g/ml}$  and  $1.097\pm 0.054$   $\mu\text{g/ml}$  respectively. Similarly, Verma et al. (2018) have also reported the production of IAA by thermophilic *Bacillus* strains isolated from the hot springs of the Leh and Ladakh regions of India. However, very few reports on the IAA production by thermophilic bacteria isolated from hot springs water are available. In recent years, global warming and climate change have severely affected the agricultural system, threatening food security. In this context, the production of IAA by thermophilic bacteria is of great significance, and such isolates are applicable as bioinoculants that withstand drought and abiotic stresses. Among various phytohormones, IAA is pivotal in enhancing cell division, yield, and plant growth (Verma et al. 2018). It was observed that the isolates could produce considerable IAA in the growth medium. However, adding L-tryptophan in the growth medium significantly enhanced IAA production. Ahmad et al. (2005) obtained a similar result and observed that *Azotobacter* and *Pseudomonas* enhanced IAA production when the medium was added with L-tryptophan as a precursor.



Table 2 Extracellular enzyme activities of the bacterial isolates isolated from Jakrem hot spring

Bacterial isolates	Enzymes activity (in mm)				
	Cellulase	Amylase	Lipase	Protease	Laccase
JAK1	9.2±0.36	7.32±0.3	20.79±1.7	25.13±0.82	10.26±0.58
JAK3	5.2±0.26	12.44±0.41	28.63±0.43	16.35±1.15	6.15±0.59
JAK6	19.98±1.25	11.68±0.69	14.16±0.3	11.33±0.55	7.64±1.08
JAK7	11.44±0.64	13.79±0.82	20.18±1.25	26.74±1.91	7.82±0.31
JAK9	26.26±1.15	14.61±0.53	39.92±1.66	22.08±0.91	10.02±0.72
JAK10	-	-	21.08±1.69	-	-
JAK17	16.77±1.81	15.72±0.43	27.3±1.95	26.42±1.33	8.55±0.26
JAK18	17.91±0.84	9.29±0.52	21.59±1.59	29.79±1.6	5.09±0.94
JAK22	13.2±1.4	10.42±0.56	28.22±1.91	26.35±1.18	8.34±0.46
JK24	27.13±1.66	18.06±0.3	16.18±1.29	23.52±1.12	15.03±0.16
JAK31	10.99±1.07	8.66±0.57	10.64±0.56	8.57±0.5	2.79±0.46
JK54	9.72±1.39	12.16±0.28	18.03±0.21	31.23±1.18	15.39±1.13
JAK251	16.71±0.43	7.45±0.38	21.04±1.74	27.39±0.91	13.84±0.95
JAW1	10.78±1.03	8.65±0.29	5.99±0.27	9.3±0.51	10.03±0.09
JAB1	38.63±0.88	-	14.91±0.5	20.21±1.01	8.91±0.18
JAB8	9.06±0.83	10.06±0.13	15.17±0.48	15.56±0.6	13.11±0.86
JAB9	11.81±0.81	15.31±0.48	13.16±0.99	20.64±1.49	10.16±0.2
JAB11	10.57±0.38	-	8.9±0.2	4.01±0.5	9.59±0.28
JAB12	12.96±0.76	4.88±0.45	16.09±0.87	9.51±0.69	3.66±0.38
JAB100	11.04±1.67	-	9.32±0.29	36.6±0.89	7.56±0.37

Values are the mean of 3 replicates (n-3); ± standard deviation

### 3.3.3 Solubilization of phosphate

The positive isolates for IAA production were further determined for qualitative and quantitative phosphate solubilization. Qualitative analysis showed 18 bacterial isolates as potential phosphate solubilizers that formed distinct halo zones surrounding bacterial colonies on Pikovskaya's agar medium (Table 3). The quantitative analysis of the strains revealed that the isolate JAB100 showed the highest Solubilization of inorganic phosphorous with a solubilization value of 19.4±0.73 µg/ml. The other isolates that showed considerable phosphate solubilization were JAB1 and JAB8, with a solubilization value of 14.28±0.65 µg/ml and 11.23±0.23 µg/ml, respectively. Amongst macro elements, phosphorus is essential for plant growth and health. However, this element is considered a limiting factor in plants as most available phosphorus is insoluble. In this context, the Solubilization of inorganic phosphorous by phosphate solubilizing bacteria would be beneficial in improving plant growth and soil health and the

maintenance of regular biogeochemical cycles (Gamalero and Glick 2011). In the present study, most bacterial isolates showed good phosphate solubilization activity. Similarly, different bacterial genera such as *Pseudomonas*, *Rhizobium*, *Burkholderia*, *Enterobacter* and several *Bacillus* species have been reported with phosphate solubilization activity increasing productivity in agricultural crops (Erman et al. 2010; Rajput et al. 2013; Pereira and Castro 2014). Studies conducted by Rodriguez and Fraga (1999) believed that applying phosphate-solubilizing bacteria could effectively reduce the application of synthetic phosphorous fertilizers by 50% without affecting crop productivity.

### 3.3.4 Siderophore, hydrogen cyanide, zinc solubilization and biofilm activities

The isolates that showed positive for phosphate solubilization were further determined to produce siderophore, hydrogen cyanide (HCN), Solubilization of zinc and biofilm activities. Out of the 18

Table 3 *In vitro* plant growth promoting (PGP) activities of bacterial isolates of Jakrem hot spring

Bacterial isolates	IAA production with Trp ( $\mu\text{g/ml}$ )	IAA production without Trp ( $\mu\text{g/ml}$ )	Phosphate solubilization ( $\mu\text{g/ml}$ )	Siderophore production	Zinc solubilization
JAK1	1.394 $\pm$ 0.054	0.745 $\pm$ 0.037	4.29 $\pm$ 0.07	-	-
JAK3	0.575 $\pm$ 0.032	0.494 $\pm$ 0.013	-	-	-
JAK6	0.85 $\pm$ 0.029	0.775 $\pm$ 0.026	4.38 $\pm$ 0.14	-	-
JAK7	1.319 $\pm$ 0.054	0.618 $\pm$ 0.040	-	-	-
JAK9	1.488 $\pm$ 0.051	0.55 $\pm$ 0.016	6.33 $\pm$ 0.15	-	-
JAK10	0.672 $\pm$ 0.009	0.485 $\pm$ 0.036	3.27 $\pm$ 0.09	-	+
JAK17	0.698 $\pm$ 0.032	0.683 $\pm$ 0.017	3.14 $\pm$ 0.11	-	-
JAK18	1.222 $\pm$ 0.064	0.605 $\pm$ 0.023	7.98 $\pm$ 0.15	-	+
JAK22	0.913 $\pm$ 0.036	0.88 $\pm$ 0.037	7.41 $\pm$ 0.08	-	-
JK24	1.147 $\pm$ 0.061	0.292 $\pm$ 0.013	2.73 $\pm$ 0.02	+	+
JAK31	1.336 $\pm$ 0.016	0.941 $\pm$ 0.038	4.005 $\pm$ 0.21	-	+
JK54	0.709 $\pm$ 0.042	0.532 $\pm$ 0.048	2.73 $\pm$ 0.02	+	+
JAK251	1.241 $\pm$ 0.003	1.04 $\pm$ 0.019	5.94 $\pm$ 0.17	-	+
JAW1	0.457 $\pm$ 0.006	0.253 $\pm$ 0.013	5.03 $\pm$ 0.08	-	-
JAB1	2.717 $\pm$ 0.138	1.849 $\pm$ 0.048	14.28 $\pm$ 0.65	+	+
JAB8	1.916 $\pm$ 0.047	1.458 $\pm$ 0.074	11.23 $\pm$ 0.23	+	+
JAB9	0.502 $\pm$ 0.038	0.406 $\pm$ 0.030	4.94 $\pm$ 0.14	+	+
JAB11	0.715 $\pm$ 0.019	0.588 $\pm$ 0.026	1.18 $\pm$ 0.08	-	-
JAB12	0.999 $\pm$ 0.023	0.61 $\pm$ 0.019	4.83 $\pm$ 0.05	-	-
JAB100	2.751 $\pm$ 0.078	1.097 $\pm$ 0.054	19.4 $\pm$ 0.73	+	+

Values are mean of 3 replicates (n=3);  $\pm$  standard deviation; + indicate positive activity; - indicate no activity; Trp- Tryptophan

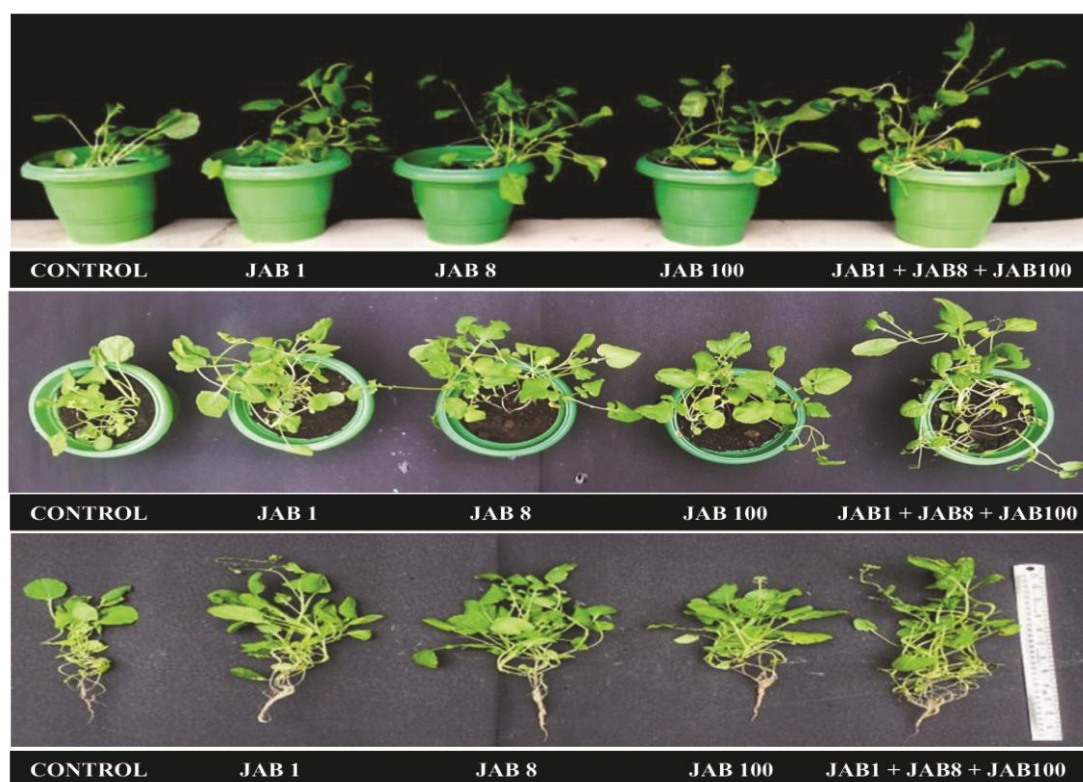
bacterial isolates, 6 were recorded positive for siderophore production, which was indicated by forming a distinct orange-yellow halo zone surrounding the bacterial colony on CAS blue agar medium. However, qualitative analysis revealed that all the bacterial isolates were negative for HCN production. Again, 10 bacterial isolates were recorded positive for the Solubilization of zinc and formed distinct halo zones surrounding the bacterial colonies under qualitative analysis. Only 11 bacterial isolates were recorded positive for biofilm-forming activity (Table 3). Plants require Iron as an important micronutrient for different metabolic processes, such as nitrogen fixation, respiration, photosynthesis, etc. (Slatni et al. 2008). However, the availability of Iron in the soil is generally much lower than required for the normal functioning of plants. Numerous bacteria of the genus *Bacillus* and *Pseudomonas* have been reported to maintain the bioavailability of Iron through the production of low molecular weight siderophore molecules, which chelate  $\text{Fe}^{3+}$  with high affinity and transport the labelled Iron, i.e. siderophore- $\text{Fe}^{3+}$  complex directly to the plants (Sudisha et al. 2006; Beneduzi et al. 2012; Gupta et al. 2015). In the present study, the bacterial

isolates have shown siderophore activity that might be useful for promoting plant growth and health. Yu et al. (2011) reported the biocontrol efficiency of siderophore-producing *B. subtilis* CAS15 on fusarium wilt disease. Further, increased plant growth with reduced disease intensity has been reported from rhizospheric bacteria *B. megaterium* mediated through siderophore production (Sivasakthi et al. 2014). Zinc is also an essential micronutrient for plant growth and health. Its deficiency affects various metabolic processes like nitrogen metabolism, photosynthesis, flowering, fruit formation and maturity, reducing crop plants' nutritional status and overall productivity (Kushwaha et al. 2021). In the present study, some bacterial isolates also showed zinc solubilization activity. Similarly, various workers have reported zinc solubilization and plant growth promotion of *Bacillus* spp. in numerous agricultural crops (Ramesh et al. 2014; Hussain et al. 2015; Khande et al. 2017; Zaheer et al. 2019). The bacterial isolates have also been reported to form biofilm in *in-vitro* studies. Biofilm formation enables the bacteria to survive in adverse environmental conditions mediated through quorum sensing by different bacterial species (Camele et al. 2019).

Table 4 Effect of potent bacterial isolates on growth and development of *B. juncea* under different treatments

Treatment	Shoot length (cm)	Root length (cm)	Shoot fresh weight (gm)	Shoot dry weight (gm)	Root fresh weight (gm)	Root dry weight (gm)
Control	18.8±0.65 <sup>h</sup>	8.46±0.15 <sup>g</sup>	5.56±0.43 <sup>f</sup>	0.542±0.03 <sup>fg</sup>	0.053±0.008 <sup>efg</sup>	0.035±0.003 <sup>de</sup>
JAB1	22.13±1.05 <sup>fg</sup>	10.9±0.2 <sup>ef</sup>	6.58±0.32 <sup>e</sup>	0.621±0.02 <sup>def</sup>	0.068±0.004 <sup>d</sup>	0.04±0.002 <sup>cd</sup>
JAB8	23.7±1.22 <sup>def</sup>	10.46±0.66 <sup>f</sup>	6.16±0.06 <sup>e</sup>	0.681±0.06 <sup>de</sup>	0.081±0.007 <sup>b</sup>	0.042±0.003 <sup>bc</sup>
JAB100	23.8±1.15 <sup>def</sup>	11.1±0.26 <sup>def</sup>	7.15±0.24 <sup>d</sup>	0.803±0.08 <sup>c</sup>	0.077±0.006 <sup>c</sup>	0.042±0.003 <sup>bc</sup>
JAB1+JAB8	25.3±1.32 <sup>bcd</sup>	11.63±0.61 <sup>cde</sup>	8.08±0.2 <sup>c</sup>	0.936±0.06 <sup>b</sup>	0.083±0.006 <sup>bc</sup>	0.062±0.001 <sup>a</sup>
JAB8+JAB100	26.16±0.9 <sup>bc</sup>	12.26±0.81 <sup>bc</sup>	8.15±0.21 <sup>c</sup>	0.822±0.03 <sup>c</sup>	0.09±0.009 <sup>bc</sup>	0.025±0.005 <sup>gh</sup>
JAB1+JAB100	24.23±1.59 <sup>cde</sup>	11.76±0.61 <sup>cd</sup>	8.83±0.2 <sup>b</sup>	0.938±0.06 <sup>b</sup>	0.084±0.006 <sup>bc</sup>	0.047±0.004 <sup>b</sup>
JAB1+JAB8+JAB100	31.3±1.8 <sup>a</sup>	13.76±0.45 <sup>a</sup>	10.87±0.47 <sup>a</sup>	1.131±0.12 <sup>a</sup>	0.116±0.007 <sup>a</sup>	0.064±0.005 <sup>a</sup>

Data were calculated after 45 days of inoculation and are mean of 3 replicates ± standard deviation; Different letters indicate significantly different values; \* $\leq 0.05$ ; LSD test

Figure 1 Root and shoot length of *B. juncea* after different treatments using potent bacterial isolates

### 3.4 Effect of bacterial isolates on growth promotion of *B. juncea*

#### 3.4.1 Plant length (shoot and root) and weight (fresh and dry)

Based on *in vitro* plant growth-promoting activities, 3 bacterial isolates, JAB1, JAB8 and JAB 100 were selected for *in vivo* pot experimental trials. The experiment was evaluated following inoculation of the bacterial isolate alone and in combination with

each other. After that, the growth promotion of the experimental plant was determined in terms of length, fresh weight, and dry weight. The result revealed that the highest shoots and root length were observed in the treatment sets where all three bacterial isolates (JAB1, JAB8 and JAB100) were co-inoculated in the rhizosphere region (Table 4, Figure 1). It was observed that the shoot length increased by 66.48%, whereas the root length increased by 62.64% as compared to the control (without bacterial inoculation). Similarly, fresh weight and dry weight were also

recorded as being highest in the same treatment set where shoot fresh weight increased by 95.5% and root fresh weight increased by 118.86% compared to control. Again, it was observed that the shoot dry weight increased by 108.67%, and the root dry weight increased by 82.85%. A similar study conducted by Sun et al. (2016) reported increased height, fresh weight, and dry weight of *B. napus* when co-inoculated with two strains of *B. subtilis* (LHS11 + FX2). In another study, the tomato's increased height and dry weight were observed after co-inoculation with *B. subtilis* (Singh et al. 2012). Therefore, our present study corroborates with many previous studies which showed that co-inoculation of bacterial isolates with plant growth-promoting activity indicated better enhancement in plant growth-promotion abilities, and such strains can be used as bioinoculants for application in crop productivity without the requirement of any chemicals.

### 3.4.2 Chlorophyll and protein content

Highest chlorophyll a, b, total chlorophyll and protein content were recorded in the treatment set with co-inoculation of all the selected bacterial isolates (JAB1+JAB8+JAB100) in the rhizospheric region (Table 5). It was observed that the treatment produced  $2.13 \pm 0.003$  mg/g FW of chlorophyll a,  $0.917 \pm 0.006$  mg/g FW of chlorophyll b, and  $3.04 \pm 0.006$  mg/g FW of total chlorophyll. There was also a gradual increase in total soluble protein content, which was  $76.62 \pm 4.11$   $\mu$ g/ml, as compared to the control, which showed only  $33.54 \pm 1.44$   $\mu$ g/ml of total soluble protein. Our study was similar to the findings of Cui et al. (2019), who reported increased chlorophyll a and b content in maize plants after treatment with *B. amyloliquefaciens* T B9601-Y2. The bio-based application of *Bacillus* for promoting plant growth with increased biochemical constituents has been cited in numerous literature (Goswami and Deka 2020; Kumar et al. 2021). The exogenous application of *B. methylotrophicus* KE2 as a plant growth promoter has been reported to increase protein content in lettuce leaves (Radhakrishnan and Lee 2016).

### 3.4.3 Phenol and flavonoid contents

The total phenolic (TPC) and flavonoid content were recorded highest again in the treatment set, which was co-inoculated with all the potent bacterial isolates (JAB1+JAB8+JAB100) (Table 5). The result showed that such a treatment set recorded  $1.25 \pm 0.005$  mgGAE/gram dried plant tissue compared to the control, which recorded  $0.71 \pm 0.048$  mg GAE/gram dried plant tissue. The flavonoid content was observed to be  $0.486 \pm 0.016$  QE/gm plant tissue in the combined inoculated set compared to the control, which showed  $0.265 \pm 0.009$  QE/gm plant tissue. These phenolic derivatives act as a precursor for lignin biosynthesis, and the fungi's toxic nature mediates the defense responses induction in plants and inhibits the growth of the fungal pathogen (Nakkeeran et al. 2006; Dutta et al. 2008). Increased flavonoid content after applying *B. subtilis* CBR05 has been reported in tomatoes (Chandrasekaran et al. 2019). Similarly, inoculation of maize plants with *B. thuringiensis* PM25 under salt stress has reported a 9.24% increase in total flavonoid content (Ali et al. 2022). Thus, the present study agreed with many previous reports on increased phenolic content in plant tissue upon inoculation with plant growth-promoting bacteria.

### 3.5 Molecular identification of potent bacterial isolates

The molecular identification of all three potent bacterial isolates (JAB1, JAB8 and JAB100) was confirmed by 16S rRNA gene sequences analysis (Figure 2). Based on the NCBI BLAST search, the isolate JAB1 showed the closest homology to *B. velezensis* (similarity 100%) with accession number ON679657, and the isolate JAB8 showed the closest homology with *B. proteolyticus* (similarity 100%) with accession number MT184819. The isolate JAB100 also showed homology with *Bacillus* sp.; however, the percentage of nucleotide sequence similarity was found to be less than 97%, which is below the minimum percentage similarity required for species-level identification (Drancourt et al. 2000).

Table 5 Effect of potent bacterial isolates on biochemical parameters of *Brassica juncea* under different treatments

Treatment	Protein content ( $\mu$ g/ml)	Phenol content (mg/gm DW)	Flavonoid content (mg/gm FW)	Chlorophyll a (mg/gm FW)	Chlorophyll b (mg/gm FW)	Total chlorophyll (mg/gm FW)
Control	$33.54 \pm 1.44$ <sup>j</sup>	$0.71 \pm 0.048$ <sup>k</sup>	$0.265 \pm 0.009$ <sup>cd</sup>	$1.36 \pm 0.007$ <sup>k</sup>	$0.591 \pm 0.004$ <sup>i</sup>	$1.95 \pm 0.003$ <sup>m</sup>
JAB1	$58.46 \pm 3.25$ <sup>de</sup>	$0.9 \pm 0.009$ <sup>ij</sup>	$0.297 \pm 0.009$ <sup>c</sup>	$1.89 \pm 0.011$ <sup>c</sup>	$0.781 \pm 0.007$ <sup>d</sup>	$2.67 \pm 0.008$ <sup>d</sup>
JAB8	$53.79 \pm 0.94$ <sup>ef</sup>	$0.91 \pm 0.015$ <sup>ij</sup>	$0.281 \pm 0.009$ <sup>cd</sup>	$1.81 \pm 0.015$ <sup>f</sup>	$0.671 \pm 0.008$ <sup>f</sup>	$2.48 \pm 0.011$ <sup>h</sup>
JAB100	$59.79 \pm 0.38$ <sup>d</sup>	$0.93 \pm 0.006$ <sup>hi</sup>	$0.303 \pm 0.024$ <sup>c</sup>	$1.45 \pm 0.006$ <sup>j</sup>	$0.586 \pm 0.006$ <sup>i</sup>	$2.03 \pm 0.013$ <sup>l</sup>
JAB1+JAB8	$66.37 \pm 0.14$ <sup>bc</sup>	$0.95 \pm 0.005$ <sup>h</sup>	$0.297 \pm 0.008$ <sup>c</sup>	$1.68 \pm 0.025$ <sup>e</sup>	$0.84 \pm 0.005$ <sup>b</sup>	$2.52 \pm 0.027$ <sup>g</sup>
JAB8+JAB100	$70.37 \pm 4.75$ <sup>b</sup>	$1.18 \pm 0.04$ <sup>f</sup>	$0.382 \pm 0.022$ <sup>b</sup>	$1.85 \pm 0.006$ <sup>d</sup>	$0.741 \pm 0.004$ <sup>e</sup>	$2.59 \pm 0.003$ <sup>f</sup>
JAB1+JAB100	$62.46 \pm 8.59$ <sup>cd</sup>	$0.89 \pm 0.01$ <sup>j</sup>	$0.378 \pm 0.018$ <sup>b</sup>	$1.89 \pm 0.008$ <sup>c</sup>	$0.812 \pm 0.009$ <sup>c</sup>	$2.7 \pm 0.019$ <sup>c</sup>
JAB1+JAB8+JAB100	$76.62 \pm 4.11$ <sup>a</sup>	$1.25 \pm 0.005$ <sup>e</sup>	$0.486 \pm 0.016$ <sup>a</sup>	$2.13 \pm 0.003$ <sup>a</sup>	$0.917 \pm 0.006$ <sup>a</sup>	$3.04 \pm 0.006$ <sup>a</sup>

Data were calculated after 45 days of inoculation and are mean of 3 replicates  $\pm$  standard deviation. Different letters indicate significantly different values; \* $\leq 0.05$ ; LSD test).

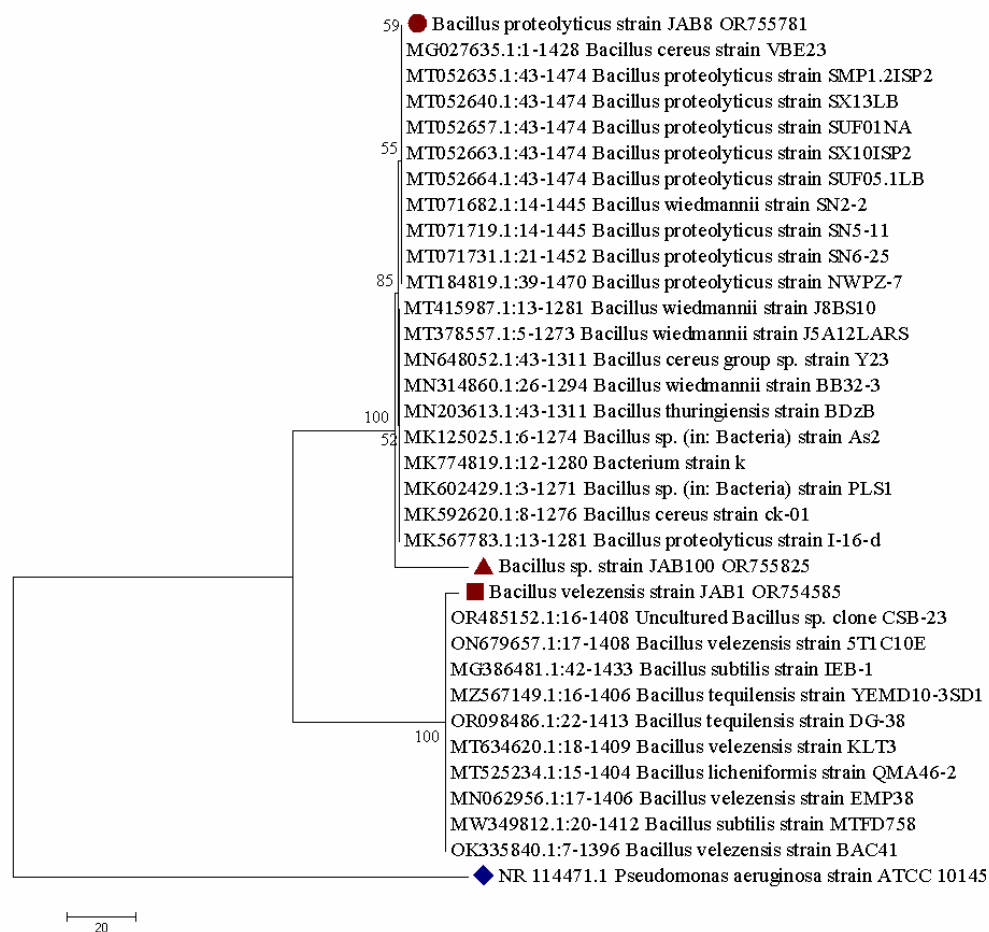


Figure 2 Phylogenetic trees showing the evolutionary relationship of three potent bacterial isolates (JAB1, JAB8 and JAB100) inferred using the Neighbour-joining method considering 16S rDNA sequences.

Therefore, JAB100 could not be conclusively identified at the species level and requires further analysis for accurate taxonomic classification. The phylogenetic tree generated by the neighbor-joining method also validated the identity of the bacterial isolates. The sequences of the isolates JAB1, JAB8 and JAB100 were deposited in NCBI, GenBank database with accession numbers OR754585, OR755781 and OR755825, respectively. Many previous workers have reported the occurrence and dominance of *Bacillus* species in various hot springs (Adiguzel et al. 2009; Nazari and Mehrabi 2019). The isolation of *B. velezensis* strain MRC 5958f has recently been reported from the Bakra hot spring (Sarangthem et al. 2023). Such findings indicated that members of the genus *Bacillus* might be common inhabitants and well-adapted to survive in extreme environments like hot springs.

## Conclusion

The study revealed that Jakrem hot water springs are a rich source of thermophilic bacteria that are dominant by *Bacillus* spp., capable of producing hydrolytic enzymes, and possess plant

growth-promoting potential. Characterization of the potent *Bacillus* isolates by morphological, biochemical and 16S rRNA sequencing identified the isolates as *B. velezensis*, *B. proteolyticus*, and *Bacillus* sp. Combined inoculation of these *Bacillus* strains demonstrated significant improvements in plant growth parameters and biochemical constituents of *B. juncea* in *in-vivo* experiments. The findings highlight the ecological significance and biotechnological potential of hot spring bacteria for application as bioinoculants for sustainable agriculture. Harnessing their capabilities can offer promising solutions to mitigate agricultural challenges, promote soil health, and contribute to enhanced crop productivity in the face of evolving climate change and environmental degradation.

## Acknowledgement

The authors would like to express their deepest gratitude to (L) Prof. Dhruva Kumar Jha, Former Professor, Department of Botany, Gauhati University for his immense guidance and tireless support while completing the work. The authors are also thankful to



Department of Botany (UGC-DRS I and DST-FIST), Gauhati University, for providing the necessary facilities to successfully complete research work. The authors are also thankful to National Bureau of Plant Genetic Resources (NBPGR), Umiam, Meghalaya for providing mustard seeds used in the present study. AK would like to thank Council of Scientific and Industrial Research (CSIR) for the financial support received under CSIR-UGC NET JRF scheme (F.No. 16-9 (June 2019)/2019(NET/CSIR); UGC-Ref. No.:598/ (CSIR-UGC NET JUNE 2019).

#### Authors contribution

All the authors contributed to research conception, data analysis and interpretation. AK Collected the sample, performed the experiment and drafting. JR-Participated in the drafting and critical revisions of the article. KT- Writing, review, editing, supervision and validation. All the authors consented and approved to submit the work in the present journal.

#### Funding by external sources

This work was supported by funding received under CSIR-UGC NET JRF scheme, Government of India.

#### Conflict of interest

The authors have no conflict of interest.

#### References

- Aanniz, T., Ouadghiri, M., Melloul, M., Swings, J., Elfahime, E., Ibjibijen, J., Ismaili, M., & Amar, M. (2015). Thermophilic bacteria in Moroccan hot springs, salt marshes and desert soils. *Brazilian Journal of Microbiology*, 46(2), 443–453. <https://doi.org/10.1590/S1517-838246220140219>
- Adiguzel, A., Ozkan, H., Baris, O., Inan, K., Gulluce, M., & Sahin, F. (2009). Identification and characterization of thermophilic bacteria isolated from hot springs in Turkey. *Journal of Microbiological Methods*, 79, 321–328. <https://doi.org/10.1016/j.mimet.2009.09.026>
- Agarwal, M., Singh, M. & Hussain, J. (2019). Assessment of groundwater quality with special emphasis on nitrate contamination in parts of Gautam Budh Nagar district, Uttar Pradesh, India. *Acta Geochim*, 38, 703–717. <https://doi.org/10.1007/s11631-018-00311-z>
- Agarwal, H., Dowarah, B., Baruah, P.M., Bordoloi, K.S., Krishnatreya, D.B., & Agarwala, N. (2020). Endophytes from *Gnetum gnemon* L. can protect seedlings against the infection of phytopathogenic bacterium *Ralstonia solanacearum* as well as promote plant growth in tomato. *Microbiological Research*, 238, 126503. <https://doi.org/10.1016/j.micres.2020.126503>
- Ahmad, F., Ahmad, I., & Khan, M.S. (2005). Indole acetic acid production by the indigenous isolates of *Azotobacter* and *Flourescent pseudomonas* in the presence and absence of tryptophan. *Turkish Journal of Biology*, 29, 29–34.
- Ali, B., Hafeez, A., Ahmad, S., Javed, M.A., Sumaira, Afridi, M.S., et al. (2022). *Bacillus thuringiensis* PM25 ameliorates oxidative damage of salinity stress in maize via regulating growth, leaf pigments, antioxidant defense system, and stress responsive gene expression. *Frontiers in Plant Science*, 13, 921668. <https://doi.org/10.3389/fpls.2022.921668>
- APHA. (2017). Standard Methods for the Examination of Water and Wastewater, 23rd ed.; American Public Health Association: Washington, DC, USA.
- Arguelles-Arias, A., Ongena, M., Halimi, B., Lara, Y., Brans, A., Joris, B., & Fickers, P. (2009). *Bacillus amyloliquefaciens* GA1 as a source of potent antibiotics and other secondary metabolites for biocontrol of plant pathogens. *Microbial Cell Factories*, 8, 63. <https://doi.org/10.1186/1475-2859-8-63>
- Arnon, D.I. (1949). Copper enzymes in isolated chloroplasts. Polyphenoloxidase in *Beta vulgaris*. *Plant Physiology*, 24, 1–15.
- Badhai, J., Ghosh, T.S., & Das, S.K. (2015). Taxonomic and functional characteristics of microbial communities and their correlation with physicochemical properties of four geothermal springs in Odisha, India. *Frontiers in Microbiology*, 6, 1166. <https://doi.org/10.3389/fmicb.2015.01166>
- Beneduzi, A., Ambrosini, A., & Passaglia, L.M. (2012). Plant growth-promoting rhizobacteria (PGPR): their potential as antagonists and biocontrol agents. *Genetics and Molecular Biology*, 35(4), 1044–1051. <https://doi.org/10.1590/s1415-47572012000600020>
- Berg, G. (2009). Plant-microbe interactions promoting plant growth and health: perspectives for controlled use of microorganisms in agriculture. *Applied Microbiology and Biotechnology*, 84 (1), 11–18.
- Brenner, D.J., Krieg, N.R., Staley, J.T., & Garrity, G.M. (2005). *Bergey's Manual of Determinative Bacteriology*, Volume 2, Parts A-C, Springer Science Business Media, Inc., New York, NY, USA, 2nd edition. <https://doi.org/10.1007/0-387-28021-9>
- Camele, I., Elshafie, H.S., Caputo, L., Sakr, S.H., & De Feo, V. (2019). *Bacillus mojavensis*: biofilm formation and biochemical investigation of its bioactive metabolites. *Journal of Biological Research-Bollettino Della Società Italiana Di Biologia Sperimentale*, 92, 39–45. <https://doi.org/10.4081/jbr.2019.8296>

- Chan, C.S., Chan, K.G., Ee, R., Hong, K.W., Urbietta, M.S., Donati, E.R., Shamsir, M.S., & Goh, K.M. (2017). Effects of Physiochemical Factors on Prokaryotic Biodiversity in Malaysian Circumneutral Hot Springs. *Frontiers in Microbiology*, 8, 1252.
- Chandrasekaran, M., Chun, S.C., Oh, J.W., Paramasivan, M., Saini, R.K., & Sahayarayan, J.J. (2019). *Bacillus subtilis* CBR05 for Tomato (*Solanum lycopersicum*) Fruits in South Korea as a Novel Plant Probiotic Bacterium (PPB): Implications from Total Phenolics, Flavonoids, and Carotenoids Content for Fruit Quality. *Agronomy*, 9, 838. <https://doi.org/10.3390/agronomy9120838>
- Cui, W., He, P., Munir, S., He, P., Li, X., Li, Y., Wu, J., Wu, Y., Yang, L., & He, Y. (2019). Efficacy of plant growth promoting bacteria *Bacillus amyloliquefaciens* B9601-Y2 for biocontrol of southern corn leaf blight. *Biological Control*, 139, 104080. <https://doi.org/10.1016/j.biocontrol.2019.104080>
- Das, S., Najar, I., Sherpa, M.T., & Thakur, N. (2016). Hot springs of Sikkim: biotechnological and sociological importance. In S. Das, I. Najar, M.T. Sherpa, N. Thakur (Eds.) *Research on Biotechnology in India: some initiatives and accomplishments*. New India Publishing Agency, New Delhi, 149–181.
- Drancourt, M., Bollet, C., Carlioz, A., Martelin, R., Gayral, J. P., & Raoult, D. (2000). 16S ribosomal DNA sequence analysis of a large collection of environmental and clinical unidentifiable bacterial isolates. *Journal of clinical microbiology*, 38(10), 3623–3630.
- Dutta, S., Mishra, A.K., & Kumar, B.D. (2008). Induction of systemic resistance against Fusarial wilt in pigeon pea through interaction of plant growth promoting rhizobacteria and rhizobia. *Soil Biology and Biochemistry*, 40 (2), 452–461. <https://doi.org/10.1016/j.soilbio.2007.09.009>.
- Erman, M., Kotan, R., Cakmakci, R., Cig, F., Karagoz, F., & Sezen, M. (2010). Effect of nitrogen fixing and phosphate-solubilizing Rhizobacteria isolated from Van Lake Basin on the growth and quality properties in wheat and sugar beet. Paper presented at: Proceedings of the Turkey IV Organic Farming Symposium, Erzurum, Turkey.
- Fasina, K.A., Adesetan, T.O., Oseghale, F., Egberongbe, H.O., Aghughu, O.O., & Akpobome, F.A. (2020). Bacteriological and Phytochemical Assessment of *Ficus asperifolia* Linn. Infusion. *BioMed Research International*, 2020, 9762639. <https://doi.org/10.1155/2020/9762639>
- Fathima, A., & Rao, J.R. (2018). Is Cr(III) toxic to bacteria: toxicity studies using *Bacillus subtilis* and *Escherichia coli* as modelorganism. *Archives of Microbiology*, 200, 453–462.
- Gamalero, E., & Glick, B.R. (2011). Mechanisms used by plant growth-promoting bacteria. In DK Maheshwari (Ed.) *Bacteria in Agrobiology: Plant Nutrient Management* (pp. 17–46). Springer: Berlin/Heidelberg, Germany. [https://doi.org/10.1007/978-3-642-21061-7\\_2](https://doi.org/10.1007/978-3-642-21061-7_2)
- Goswami, M., & Deka, S. (2020). Isolation of a novel rhizobacteria having multiple plant growth promoting traits and antifungal activity against certain phytopathogens. *Microbiological Research*, 240, 1–17. <https://doi.org/10.1016/j.micres.2020.126516>
- Goteti, P.K., Emmanuel, L.D.A., Desai, S., & Shaik, M.H.A. (2013). Prospective zinc solubilizing bacteria for enhanced nutrient uptake and growth promotion in maize (*Zea mays* L.). *International Journal of Microbiology*, 1–7. <https://doi.org/10.1155/2013/869697>
- Glick, B.R. (2018). Soil microbes and sustainable agriculture. *Pedosphere*, 28, 167–169.
- Gupta, G., Parihar, S.S., Ahirwar, N.K., Snehi, S.K., & Singh, V. (2015). Plant growth-promoting rhizobacteria (PGPR): Current and prospects for the development of sustainable agriculture. *Journal of Microbial & Biochemical Technology*, 7, 96–102.
- Gupta, P., Kumar, V., Usmani, Z., Rani, R., Chandra, A., & Gupta, V.K. (2020). Implications of plant growth promoting *Klebsiella* sp. CPSB4 and *Enterobacter* sp. CPSB49 in luxuriant growth of tomato plants under chromium stress. *Chemosphere*, 240, 124944. <https://doi.org/10.1016/j.chemosphere.2019.124944>
- Hanson, A.J., Luek, J.L., Tummings, S.S., McLaughlin, M.C., Blotvogel, J., & Mouser, P.J. (2019). High total dissolved solids in shale gas wastewater inhibit biodegradation of alkyl and nonylphenol ethoxylate surfactants. *Science of The Total Environment*, 668, 1094–1103.
- Huang, P., de-Bashan, L., Crocker, T., Kloepper, J.W., & Bashan, Y. (2017). Evidence that fresh weight measurement is imprecise for reporting the effect of plant growth-promoting (rhizo) bacteria on growth promotion of crop plants. *Biology and Fertility of Soils*, 53, 199–208. <https://doi.org/10.1007/s00374-016-1160-2>
- Hussain, A., Arshad, M., Zahir, Z.A., & Asghar, M. (2015). Prospects of zinc solubilizing bacteria for enhancing growth of maize. *Pakistan Journal of Agricultural Sciences*, 52, 915–922.
- Indian Standard (IS: 3025).(2009). Methods of sampling and test (physical and chemical) for water used in industry. Bureau of Indian Standard, New Delhi.
- Islam, F., Islam, M.S., Islam, M., Sikdar, B., Khalekuzzaman, M., & Islam, M.A. (2017). Detection of bacterial wilt disease of

- banana through biochemical approaches and its biological control. *Plant Environment Development*, 6(2), 19-23.
- Jena, R., Pradhan, B., & Abdollahi, A. (2018). Curable Properties of Hot Water Springs in Odisha Related to Eastern Ghats Minerals: A Review. *Scenario of Environmental Research and Development*, 94-100.
- Kaki, A.A., Ali, M.K., Milet, A., Moula, N., Thonart, P., & Chaouche, N.K. (2017). In vitro control and biofertilization features study of a *Bacillus amyloliquefaciens*(4RH) strain isolated from a hot spring soil in Algeria. *African Journal of Microbiology Research*, 11(43), 1564-1572. <http://dx.doi.org/10.5897/AJMR2017.8745>
- Kalsait, R.P., Dehariya, N.K., Nagdev, S.A., & Umekar, M.J. (2018). Comparative Quality : A Quantitative Approach For Safe Drinking Water. *Research Pharmaceutica*, 2(2), 07-10.
- Kambura, A.K., Mwirichia, R.K., Kasili, R.W., Karanja, E.N., Makonde, H.M., & Boga, H.I. (2016). Bacteria and Archaea diversity within the hot springs of Lake Magadi and Little Magadi in Kenya. *BMC Microbiology*, 16, 136. <https://doi.org/10.1186/s12866-016-0748-x>
- Khan, M.A., Asaf, S., Khan, A.L., Jan, R., Kang, S.M., Kim, K.M., & Lee, I.J. (2020). Thermotolerance effect of plant growth-promoting *Bacillus cereus* SA1 on soybean during heat stress. *BMC Microbiology*, 20, 175.
- Khande, R., Sharma, S.K., Ramesh, A., & Sharma, M.P. (2017). Zinc solubilizing *Bacillus* strains that modulate growth, yield and zinc biofortification of soybean and wheat. *Rhizosphere*, 4, 126–138. <https://doi.org/10.1016/j.rhisph.2017.09.002>
- Kumar, A., Kumar, A., Thakur, P., Patil, S., Payal, C., Kumar, A., & Sharma, P. (2012). Antibacterial activity of green tea (*Camellia sinensis*) extracts against various bacteria isolated from environmental sources. *Recent Research in Science and Technology*, 4, 19–23.
- Kumar, M., Prasanna, R., Bidyarani, N., Babu, S., Mishra, B.K., et al. (2013). Evaluating the plant growth promoting ability of thermotolerant bacteria and cyanobacteria and their interactions with seed spice crops. *Scientia Horticulturae*, 164, 94–101.
- Kumar, R., & Sharma, R.C. (2019). Microbial diversity and physico-chemical attributes of two hot water springs in the Garhwal Himalaya, India. *Journal of Microbiology, Biotechnology and Food Sciences*, 8, 1249–1253.
- Kumar, A., Rabha, J., & Jha, D.K. (2021). Antagonistic activity of lipopeptide-biosurfactant producing *Bacillus subtilis* AKP, against *Colletotrichum capsici*, the causal organism of anthracnose disease of chilli. *Biocatalysis and Agricultural Biotechnology*, 36, 102133. <https://doi.org/10.1016/j.bcab.2021.102133>
- Kushwaha, P., Srivastava, R., Pandiyan, K., Singh, A., Chakdar, H., et al. (2021). Enhancement in plant growth and zinc biofortification of chickpea (*Cicer arietinum* L.) by *Bacillus altitudinis*. *Journal of Soil Science and Plant Nutrition*, 21, 922–935. <https://doi.org/10.1007/s42729-021-00411-5>
- Lele, O.H., & Deshmukh, P.V. (2016). Isolation and characterization of thermophilic *Bacillus* sp. with extracellular enzymatic activities from hot spring of Ganeshpuri, Maharashtra, India. *International Journal of Applied Research*, 2, 427–430.
- López, M.J., Jurado, M.M., López-González, J.A., Estrella-González, M.J., Martínez-Gallardo, M.R., Toribio, A., & Suárez-Estrella, F. (2021). Characterization of Thermophilic Lignocellulolytic Microorganisms in Composting. *Frontiers in Microbiology*, 12, 697480.
- Lotfi, G., Hassaine, H., Klouche, N., Khadir, A., Aissaoui, N., Nas, F., & Zingg, W. (2014). Detection of biofilm formation of a collection of fifty strains of *Staphylococcus aureus* isolated in Algeria at the University Hospital of Tlemcen. *Journal of bacteriology research*, 6, 1–6.
- Lowry, O.H., Rosebrough, N.J., Farr, A.L., & Randall, R.J. (1951). Protein measurement with the Folin phenol reagent. *Journal of Biological Chemistry*, 193, 265-275.
- Lugtenberg, B., & Kamilova, F. (2009). Plant-growth-promoting rhizobacteria. *Annual Review of Microbiology*, 63, 541–556.
- Mao, X., Ye, J., Shi, Z., & Dong, Y. (2022). The Possible Source of Abnormally High Sodium Content in Low-Salinity Geothermal Water. *Groundwater*, 61(4), 517-531.
- Mishra, P., & Dash, D. (2014). Rejuvenation of biofertilizer for sustainable agriculture and economic development. *Consilience: The Journal of Sustainable Development*, 11 (1), 41–61.
- Mohammad, B.T., Al Daghistani, H.I., Jaouani, A., Abdel-Latif, S., & Kennes, C. (2017). Isolation and characterization of thermophilic bacteria from Jordanian hot springs: *Bacillus licheniformis* and *Thermomonas hydrothermalis* isolates as potential producers of thermostable enzymes. *International Journal of Microbiology*, 2017, 6943952. <https://doi.org/10.1155/2017/6943952>
- Morales-Cedeño, L.R., Orozco-Mosqueda, M.D.C., Loeza-Lara, P.D., Parra-Cota, F.I., de los Santos-Villalobos, S., & Santoyo, G. (2021). Plant growth-promoting bacterial endophytes as biocontrol agents of pre- and post-harvest diseases: fundamentals, methods of application and future perspectives. *Microbiological Research*, 242, 126612. <https://doi.org/10.1016/j.micres.2020.126612>

- Moreno, J., López-González, J.A., Arcos-Nievas, M.A., Suárez-Estrella, F., Jurado, M.M., Estrella-González, M.J., et al. (2021). Revisiting the succession of microbial populations throughout composting: a matter of thermotolerance. *Science of The Total Environment*, *773*, 145587.
- Nakkeeran, S., Kavitha, K., Chandrasekar, G., Renukadevi, P., & Fernando, W.G.D. (2006). Induction of plant defense compounds by *Pseudomonas chlororaphis* PA23 and *Bacillus subtilis* BSCBE4 in controlling damping-off of hot pepper caused by *Pythium aphanidermatum*. *Biocontrol Science and Technology*, *16*, 403–416.
- Narsing Rao, M.P., Dong, Z.-Y., Luo, Z.-H., Li, M.M., Liu, B.B., Guo, S.X., Hozzein, W.N., Xiao, M., & Li, W.J. (2021). Physicochemical and Microbial Diversity Analyses of Indian Hot Springs. *Frontiers in Microbiology*, *12*, 627200. <https://doi.org/10.3389/fmicb.2021.627200>
- Nazari, L., & Mehrabi, M. (2019). Purification and characterization of an extracellular thermotolerant alkaliphilic serine protease secreted from newly isolated *Bacillus* sp. DEM07 from a hot spring in Dehloran, Iran. *Biocatalysis and Agricultural Biotechnology*, *18*, 101053. <https://doi.org/10.1016/j.bcab.2019.101053>
- Panda, M.K., Sahu, M.K., & Tayung, K. (2013). Isolation and characterization of a thermophilic *Bacillus* sp. with protease activity isolated from hot spring of Tarabalo, Odisha, India. *Iranian Journal of Microbiology*, *5*, 159.
- Panda, A.K., Bisht, S.S., De Mandal, S., & Kumar, N.S. (2016). Bacterial and archeal community composition in hot springs from Indo-Burma region, North-east India. *AMB Express*, *6*, 111. <https://doi.org/10.1186/s13568-016-0284-y>
- Pandey, A., Dhakar, K., Sharma, A. et al. (2015). Thermophilic bacteria that tolerate a wide temperature and pH range colonize the Soldhar (95 °C) and Ringigad (80 °C) hot springs of Uttarakhand, India. *Annals of Microbiology*, *65*, 809–816. <https://doi.org/10.1007/s13213-014-0921-0>
- Pereira, S.I., & Castro, P.M. (2014). Phosphate solubilizing rhizobacteria enhance *Zea mays* growth in agricultural P-deficient soils. *Ecological Engineering*, *73*, 526–535. <https://doi.org/10.1016/j.ecoleng.2014.09.060>
- Podile, A.R., & Kishore, G.K. (2006). Plant growth-promoting rhizobacteria. In S.S. Gnanamanickam (Ed.) *Plant-Associated Bacteria* (pp. 195-230). Springer; Netherlands, 195–230.
- Poddar, A., & Das, S.K. (2018). Microbiological Studies of Hot Springs in India: A Review. *Archives of Microbiology*, *200*, 1–18. <https://doi.org/10.1007/s00203-017-1429-3>
- Priya, I., Dhar, M.K., Bajaj, B.K., Koul, S., & Vakhlu, J. (2016). Cellulolytic activity of thermophilic bacilli isolated from Tattapani hot spring sediment in north west Himalayas. *Indian Journal of Microbiology*, *56*, 228–231. <https://doi.org/10.1007/s12088-016-0578-4>
- Radhakrishnan, R., & Lee, I.J. (2016). Gibberellins producing *Bacillus methylotrophicus* KE2 supports plant growth and enhances nutritional metabolites and food values of lettuce. *Plant Physiology and Biochemistry*, *109*, 181–189. <https://doi.org/10.1016/J.PLAPHY.2016.09.018>
- Rahman, M.M.E., Hossain, D.M., Suzuki, K., Shiiya, A., Suzuki, K., Dey, T.K., Nonaka, M., & Harada, N. (2016). Suppressive effects of *Bacillus* spp. on mycelia, apothecia and sclerotia formation of *Sclerotinia sclerotiorum* and potential as biological control of white mold on mustard. *Australasian Plant Pathology*, *45*, 103–117. <https://doi.org/10.1007/s13313-016-0397-4>
- Rakshak, K., Ravinder, K., Nupur., Srinivas, T.N.R., & Kumar, P.A. (2013). *Caldimonasmeghalayensis* sp. nov., a novel thermophilic betaproteobacterium isolated from a hot spring of Meghalaya in northeast India. *Antonie van Leeuwenhoek*, *104*, 1217–1225. <https://doi.org/10.1007/s10482-013-0043-x>
- Rajput, L., Imran, A., Mubeen, F., & Hafeez, F.Y. (2013). Salt tolerant PGPR strain *Planococcus rifietoensis* promotes the growth and yield of wheat (*Triticum aestivum* L.) cultivated in saline soil. *Pakistan Journal of Botany*, *45*, 1955–1962.
- Ramesh, A., Sharma, S.K., Sharma, M.P., Yadav, N., & Joshi, O.P. (2014). Inoculation of zinc solubilizing *Bacillus aryabhata* strains for improved growth, mobilization and biofortification of zinc in soybean and wheat cultivated in Vertisols of central India. *Applied Soil Ecology*, *73*, 87–96. <https://doi.org/10.1016/j.apsoil.2013.08.009>
- Rodriguez, H., & Fraga, R. (1999). Phosphate solubilizing bacteria and their role in plant growth promotion. *Biotechnology Advances*, *17*, 319–339.
- Saharan, B.S., & Nehra, V. (2011). Plant growth promoting rhizobacteria: A critical review. *Life Sciences and Medicine Research*, *21*, 1–30.
- Saharan, BS, & Verma, S. (2014). Potential plant growth promoting activity of *Bacillus licheniformis* UHI(II)7. *International Journal of Microbial Resource Technology*, *2*(3), 22-27.
- Sahay, H., Yadav, A.N., Singh, A.K., Singh, S., Kaushik, R., & Saxena, A.K. (2017). Hot springs of Indian Himalayas: potential sources of microbial diversity and thermostable hydrolytic enzymes. *3 Biotech*, *7*, 118.



- Sarkar, S., Mondal, M., Ghosh, P., Saha, M., & Chatterjee, S. (2020). Quantification of total protein content from some traditionally used edible plant leaves: a comparative study. *Journal of Medicinal Plant Studies*, 8(4), 166-170. <https://doi.org/10.22271/plants.2020.v8.i4c.1164>
- Sarangthem, I., Rajkumari, L., Ngashangva, N., Nandeibam, J., Yendrembam, R.B.S., & Mukherjee, P.K. (2023). Isolation and Characterization of Bacteria from Natural Hot Spring and Insights into the Thermophilic Cellulase Production. *Current Microbiology*, 80, 64. <https://doi.org/10.1007/s00284-022-03168-x>
- Sarkar, R.D., & Kalita, M.C. (2022). Green Synthesized Se Nanoparticle-mediated Alleviation of Salt Stress in Field Mustard TS-36 Variety. *Journal of Biotechnology*, 359, 95-107. <https://doi.org/10.1016/j.jbiotec.2022.09.013>
- Satyanarayana, T., Raghukumar, C., & Shivaji, S. (2005). Extremophilic microbes: diversity and perspectives. *Current Science*, 89, 78-90.
- Shilev, S. (2020). Plant-growth-promoting bacteria mitigating soil salinity stress in plants. *Applied Sciences*, 10, 7326.
- Singh, D., Yadav, D.K., Sinha, S., & Upadhyay, B.K. (2012). Utilization of plant growth promoting *Bacillus subtilis* isolates for the management of bacterial wilt incidence in tomato caused by *Ralstonia solanacearum* race 1 biovar 3. *Indian Phytopathology*, 65(1), 18-24. <https://epubs.icar.org.in/index.php/IPPI/article/view/16082>
- Singh, Y., Gulati, A., Singh, D.P., & Khattar, J.I.S. (2018). Cyanobacterial community structure in hot water springs of Indian North-Western Himalayas: a morphological, molecular and ecological approach. *Algal Research*, 29, 179-192. <https://doi.org/10.1016/j.algal.2017.11.023>
- Sivasakthi, S., Usharani, G., & Saranraj, P. (2014). Biocontrol potentiality of plant growth promoting bacteria (PGPR)-*Pseudomonas fluorescens* and *Bacillus subtilis*: A review. *African Journal of Agricultural Research*, 9, 1265-1277.
- Slatni, T., Kroma, A., Aydi, S., Gouia, C., & Abdelly, C.H. (2008). Growth nitrogen fixation and ammonium assimilation in common bean subjected to iron deficiency. *Plant and Soil*, 312, 49-57.
- Stein, T. (2005). *Bacillus subtilis* antibiotics: structures, syntheses and specific functions. *Molecular Microbiology*, 56, 845-857. <https://doi.org/10.1111/j.1365-2958.2005.04587.x>
- Sun, G., Yao, T., Feng, C., Chen, L., Li, J., & Wang, L. (2016). Identification and biocontrol potential of antagonistic bacteria strains against *Sclerotinia sclerotiorum* and their growth-promoting effects on *Brassica napus*. *Biological Control*, 104, 35-43. <http://dx.doi.org/10.1016/j.biocontrol.2016.10.008>
- Sudisha, J., Niranjana, S.R., Umesha, S., Prakash, H.S., & Shekar Shetty, H. (2006). Transmission of seed-borne infection of muskmelon by Didymellabryoniae and effect of seed treatments on disease incidence and fruit yield. *Biological Control*, 37, 196-205.
- Syiemiong, D., & Jha, D.K. (2019). Search for plant growth promoting actinobacteria from a limestone mining spoil soil in Meghalaya. *Research Journal of Life Sciences, Bioinformatics, Pharmaceutical and Chemical Sciences*, 5, 1024-36.
- Tekere, M., Lötter, A., Olivier, J., Jonker, N., & Venter, S. (2011). Metagenomic analysis of bacterial diversity of Siloam hot water spring, Limpopo, South Africa. *African Journal of Biotechnology*, 10, 18005-18012. <https://doi.org/10.5897/AJB11.899>
- Tekere, M., Prinsloo, A., Olivier, J., Jonker, N., & Venter, S. (2012). An evaluation of the bacterial diversity at Tshipise, Mphephu and Sagole hot water springs, Limpopo Province, South Africa. *African Journal of Microbiology Research*, 6, 4993-5004. <https://doi.org/10.5897/AJMR12.250>
- Tripathi, N., & Sapra, A. (2021). Gram Staining. In: Statpearls. Treasure Island (FL: StatPearls Publishing).
- Verma, J.P., Jaiswal, D.K., Krishna, R., Prakash, S., Yadav, J., & Singh, V. (2018). Characterization and Screening of Thermophilic *Bacillus* Strains for Developing Plant Growth Promoting Consortium From Hot Spring of Leh and Ladakh Region of India. *Frontiers in Microbiology*, 9, 1293. <https://doi.org/10.3389/fmicb.2018.01293>
- Villarreal-Delgado, M.F., Villa-Rodríguez, E.D., Cira-Chávez, L.A., Estrada-Alvarado, M.I., Parra-Cota, F.I., & Santos-Villalobos, S.D.L. (2018). The genus *Bacillus* as a biological control agent and its implications in the agricultural biosecurity. *Revista Mexicana de Fitopatología*, 36, 95-130. <https://doi.org/10.18781/r.mex.fit.1706-5>
- Wani, P.A., & Khan, M.S. (2013). Nickel Detoxification and Plant Growth Promotion by Multi Metal Resistant Plant Growth Promoting *Rhizobium* Species RL9. *Bulletin of Environmental Contamination and Toxicology*, 91, 117-124. <https://doi.org/10.1007/s00128-013-1002-y>
- Yadav, A.N., Verma, P., Kumar, M., Pal, K.K., Dey, R., et al. (2015). Diversity and phylogenetic profiling of niche-specific Bacilli from extreme environments of India. *Annals of Microbiology*, 65, 611-629. <https://doi.org/10.1007/s13213-014-0897-9>
- Yang, D., Wang, B., Wang, J., Chen, Y., & Zhou, M. (2009). Activity and efficacy of *Bacillus subtilis* strain NJ-18 against rice



- sheath blight and Sclerotinia stem rot of rape. *Biological Control*, 51, 61–65. <https://doi.org/10.1016/j.biocontrol.2009.05.021>
- Yazdani, M., Naderi-Manesh, H., Khajeh, K., Soudi, M.R., Asghari, S.M., & Sharifzadeh, M. (2009). Isolation and characterization of a novel gamma-radiation-resistant bacterium from hot spring in Iran. *Journal of Basic Microbiology*, 49, 119–127. <https://doi.org/10.1002/jobm.200800177>
- Yu, X., Ai, C., Xin, L., & Zhou, G. (2011). The siderophore-producing bacterium, *Bacillus subtilis* CAS15, has a biocontrol effect on *Fusarium* wilt and promotes the growth of pepper. *European Journal of Soil Biology*, 47, 138–145. <https://doi.org/10.1016/j.ejsobi.2010.11.001>
- Zaheer, A., Malik, A., Sher, A., Qaisrani, M.M., Mehmood, A., et al. (2019). Isolation, characterization, and effect of phosphate-zinc-solubilizing bacterial strains on chickpea (*Cicer arietinum* L.) growth. *Saudi Journal of Biological Sciences*, 26, 1061–1067. <https://doi.org/10.1016/j.sjbs.2019.04.004>






# Journal of Experimental Biology and Agricultural Sciences

<http://www.jebas.org>

ISSN No. 2320 – 8694

## Role of Probiotic Microorganisms in the Brain Plasticity Development

Murugan Mukilan \* , Rameshbabu Adithya , Senthilkumar Pruthivi 

Department of Biotechnology, Sri Ramakrishna College of Arts & Science, Coimbatore 641 006, Tamil Nadu, India

Received – February 27, 2024; Revision – June 03, 2024; Accepted – July 03, 2024

Available Online – July 15, 2024

DOI: [http://dx.doi.org/10.18006/2024.12\(3\).354.365](http://dx.doi.org/10.18006/2024.12(3).354.365)

### KEYWORDS

Cognition

Synaptic Plasticity

Probiotics

Reward-based learning  
paradigm

### ABSTRACT

Probiotics are defined as beneficial microorganisms that are responsible for the maintenance of homeostasis mechanisms within the host system, especially in humans. Other than homeostasis, it is also used to improve a host system's cognition, immune functions, and antioxidant levels. Over the past decades, probiotic microorganisms have been used most commonly as traditional fermented foods in our country and some parts of southeast asia. These fermented food products majorly consist of *Lactobacillus* species, including *Lactobacillus acidophilus*, *L. fermentum*, and *L. plantarum*. The present study explored the potential role of three different lactobacillus strains (*L. acidophilus*, *L. fermentum*, and *L. Plantarum*) in forming brain plasticity changes (BPC) with the help of a cue-based learning paradigm (CBLP). Two staged behavioral studies were conducted for all behavioral analysis groups (BAG) before (without probiotic infusions - WiPI) and after probiotic infusions (with probiotic infusions - WPI) in RBLP. Behavioral responses of the WiPI & WPI phases showed the effect of a stress-free habituated environment in developing BPC and strengthening of BPC by oral infusions of probiotic microorganisms (PM). WiPI and WPI behavioral analysis were used in this study to validate BPC in a laboratory-controlled environment. Infusion of probiotic microorganisms through oral passage may have a more significant impact on the synthesis, production, and transmission of neurotransmitter precursor compounds (NPC) from the gut to the central nervous system (CNS) through the blood-brain barrier (BBB). Increased transmission of the NPC strengthens the formed plasticity changes, which results in the formation of cognitive memory functions. Thus, the present study proved that probiotic microorganisms may play a major role in cognition development through the BPC.

\* Corresponding author

E-mail: [mukilan@srcas.ac.in](mailto:mukilan@srcas.ac.in) (Murugan Mukilan)

Peer review under responsibility of Journal of Experimental Biology and Agricultural Sciences.

Production and Hosting by Horizon Publisher India [HPI]  
(<http://www.horizonpublisherindia.in/>).  
All rights reserved.

All the articles published by [Journal of Experimental Biology and Agricultural Sciences](#) are licensed under a [Creative Commons Attribution-NonCommercial 4.0 International License](#) Based on a work at [www.jebas.org](http://www.jebas.org).



## 1 Introduction

Synaptic plasticity is a unique adaptive feature of our central nervous system that uses activity-dependent mechanisms to restructure/alter the strength of neuronal connections based on stimulus exposure (Chaudhury et al. 2016; Kim et al. 2018; Abraham et al. 2019; Appelbaum et al. 2023; Mukilan et al. 2024a). It was already reported that synaptic plasticity plays an unavoidable role in incorporating beneficial/harmful experiences in the form of long-lasting information in different brain regions during the formation of learning and memory (LM) (Ramirez and Arbuckle 2016; Appelbaum et al. 2023; Mukilan 2023). This formed LM follows two distinct molecular mechanisms for the acquaintance and retrieval of learned information in the brain. These two molecular mechanisms result in the formation of short-term (ST) memory and long-term (LT) memory. ST and LT memory use existing proteins and RNA-dependent-protein synthesis mechanisms to form memory. Formed ST and LT memory will last for 2-6 hours (ST) until the end of life (LT). However, the time needed to form LTM is high compared to STM (Norris 2017; Abraham et al. 2019; Ashok et al. 2019; Evans et al. 2021; Luis and Ryan 2022; Mukilan et al. 2024b). For memory formation, LTM uses specific neuronal signaling pathways like cAMP response element binding protein (CREB)-mediated neuronal signaling pathway (MNSP). This CREB-MNSP is initiated by releasing specific neurotransmitters like 5-HT from the presynaptic neuron into the synaptic cleft (SC). In the SC, released neurotransmitter binds to the specific postsynaptic neuronal receptors (PNR)(Ganesh et al. 2010; Ganesh et al. 2012; Mukilan et al. 2015; Ortega-Martínez 2015; Rajan 2021). Binding neurotransmitters with the PNR results in calcium influx (CI) induction. CI influx later activates adenylyl cyclase (AC), cyclic adenosine monophosphate (cAMP), protein kinase A (PKA), and enzyme-regulated kinase - 1 (ERK - 1). Upregulation of AC, cAMP, PKA, and ERK - 1 later results in the activation and phosphorylation of CREB, which induces immediate-early genes (IEG) and postsynaptic density (PSD) protein expressions. Reliable expressions of these neuronal signaling molecules are involved in the formation of LT memory in the different brain regions (Peng et al. 2010; Mukilan et al. 2018a, 2018b; Bai and Suzuki 2020; Lin et al. 2021; Mukilan 2022; Mukilan 2023).

Reported research findings showed that oral/gut-beneficial microflora are responsible for the maintenance of the brain homeostasis mechanisms of a host (Appleton 2018; Gentile and Weir 2018; Suganya and Koo 2020). In a healthy state, some oral/gut bacterial strains are unavoidable in synthesizing and producing neurotransmitter precursor compounds (NPCs) in the gut. Produced NPCs are transported from the gut to the CNS through the BBB (Misiak et al. 2020; Mukilan 2023). Transmitted NPCs are involved in the production of a wide range of neurotransmitters [serotonin (5-HT),  $\gamma$ -aminobutyric acid (GABA),

dopamine (DA), and noradrenaline (NA)] from the presynaptic neurons for the induction of neuronal signaling pathways (NSP) (Chen et al. 2017; O'Donnell et al. 2020; Sengupta 2020; Dicks 2022). Induction of NSP forms the cognitive memory in the olfactory bulb, hippocampus, and amygdala. Thus, the formed cognitive memory inter-relates the oral-gut-brain axis with the CNS. It also proved that oral/gut-beneficial flora are important in forming cognitive functions (Mukilan et al. 2018a; Salami and Soheili 2022; Mukilan 2023). In normal conditions, existing beneficial flora is affected by various conditions like food habits, alcohol consumption, changes in circadian rhythm, alcohol consumption, diet, smoking, and other environmental conditions. To overcome the depletion of beneficial flora, nowadays's varying range of probiotic microorganisms are taken along with the diet to maintain oral/gut probiotic health (Hillemacher et al. 2018; Savin et al. 2018; Yang et al. 2020; Kumar et al. 2024). In the present work, we tried to elucidate the importance of probiotic microorganisms in strengthening brain plasticity changes during cognitive learning and memory formation with the help of a cue-based learning paradigm (CBLP).

## 2 Materials and Methods

### 2.1 Experimental Fishes

Commercially available adult goldfish (*Carassius auratus*) with body lengths (6-8 cm) and weights (8 – 15 g) were obtained from a local market. Obtained fishes were maintained with their respective groups (n = 6/group) in the home aquarium throughout the experimental period. Rectangular glass tanks, 42 X 30 X 21 (length, breadth, and height - LBH) inches, served as home aquariums. In the home aquarium, continuous air circulation, photoperiod (12 hours of light:12 hours of dark), and a standard temperature of  $26 \pm 2$  °C were provided for all experimental fishes. Commercial dry food pellets (Taiyo Pet Products India Pvt. Ltd) were provided thrice a day @ 8.00, 14.00, and 19.00 hours to meet the energy needs of all experimental animals. The home tank was adequately cleaned and replaced with fresh water on alternative days to maintain a debris-free environment. Experimental design follows the institutional ethical regulatory guidelines of Sri Ramakrishna Institutions, Coimbatore, Tamil Nadu, India.

### 2.2 Experimental Design

A rectangular glass tank (RGT) having an LBH of 42 X 30 X 21 inches was custom-designed and used in the behavioral analysis. The designed RGT was divided into three different compartments based on the study's needs. These three chambers include two feeding compartments (FC) and one central compartment (CC). FCs and CC vary in their LBH of 6 X 30 X 21 and 30 X 30 X 21 inches. In the two FCs, one FC acts as a positive reward chamber with blue colored cues, and another one acts as a negative chamber

with red colored cues. Both the FCs have a central opening for fish movement from CC to FCs.

### 2.3 Infusion Mixture Preparation

All three probiotic strains *L. acidophilus* (MTCC No. 10307), *L. fermentum* (MTCC No. 9748), and *L. plantarum* (MTCC No. 12921) were acquired from the MTCC (Microbial Type Culture Collection and Gene Bank), IMTECH (Institute of Microbial Technology), Sector 39, Chandigarh, Punjab, India. Acquired probiotic strains were streaked on *Lactobacillus* MRS Agar to confirm their purity. After purity confirmation, acquired probiotic cultures were used to prepare an oral probiotic mixture in the ratio of 50:50 (as a single dose in a pure form), and 20:20:20:40 (as a single dose in mixed form). Prepared oral mixtures were used for the oral administrations into specific experimental groups after the primary phase of behavioral analysis (PPBA).

### 2.4 Behavioral Analysis

#### 2.4.1 Experimental Groups

Fishes were randomly separated into four different groups. These are Group -1 (infused with *L. acidophilus*), Group - 2 (infused with *L. fermentum*), Group - 3 (infused with *L. plantarum*), and Group - 4 (infused with *L. acidophilus*, *L. fermentum*, and *L. Plantarum*).

#### 2.4.2 Cue-based Learning Paradigm

The cue-based learning paradigm (CBLP) was used to understand the effect of a controlled environment and probiotic infusions on learning and memory formation (LMF). During LMF, two different color cues (blue, and red) were used for the behavioral studies in the FCs of the experimental apparatus. Blue and red colored cues act as positive and negative rewards with/ without food rewards. Behavioral responses were calculated based on the amount of time spent in the left chamber (LC), central chamber (CC), and right chamber (RC).

#### 2.4.3 Predator Exposure Test

A predator exposure test (PET) was performed to identify whether probiotic oral infusions develop stress or not. In this PET, RGT has a size of 42 X 30 X 21 inches (LBH) and was used as an exposure chamber (EC). The EC was divided into three equal-sized zones (LBH of 14 X 10 X 21 inches), including a no-fear zone (NFZ), mid-fear zone (MFZ), and complete-fear zone (CFZ) with the help of two transparent plexi sheets with central openings. During PET, goldfish (*C. auratus*) and its predator (bluegills) were introduced into NFZ, & isolated chamber in CFZ for 15 minutes. Behavioral responses of all experimental groups were recorded in terms of time spent in NFZ, MFZ, and CFZ.

#### 2.4.4 Open Field Test

Followed by PET, an open field test (OFT) is employed in this study to identify the presence/absence of anxiety-like behavior. OFT was carried out in RGT, which was 42 X 30 X 21 inches (LBH) and had 36 square boxes (5 X 5 cm/each). All 36 square boxes were divided into two different zones, i.e. the outer and inner zones. The outer and inner zone consists of 18 square boxes. Behavioural responses of experimental groups were analyzed in terms of time spent in an inner compartment (TSI) and time spent in an outer compartment (TSO).

### 2.5 Statistical Representation

Behavioral responses of all three behavioral tests were plotted as a bar diagram with the help of a Microsoft Excel program. An online tool (MedCalc statistical software) was used to calculate the p-value with the help of mean average values and standard error.

## 3 Results

### 3.1 Role of stress-free assimilated environment in the formation of cognitive functions

The current study initially uses the primary phase of behavioral analysis (PPBA) to understand the effect of a stress-free assimilated environment on cognitive memory formation using a CBLP in a controlled environment. Initially, animals of all experimental groups underwent learning and memory retention tests in the experimental apparatus after completing the assimilation and exploration phases. During the assimilation process, animals were maintained in the home tank for five days (Days 1-5) for their adaptations to the laboratory-controlled conditions. Following the habituation process, all experimental animals were allowed to explore the experimental apparatus without the color cue in FCs during the exploration phase (Days 6-8). Behavioral responses showed that initially, animals spent more time in CC than LC and RC. Later, time spent in CC was reduced in the subsequent days, showing that animals explored the FCs on the opposite sides of CC. After the exploration, all experimental groups were trained on CBLP based on color cues with/without food rewards between days 9-11. During the training phase, all experimental animals learned about the positive/negative stimuli based on food reward learning. Every visit to RC was awarded a food pellet, and vice versa, in LC. Obtained behavioral scores showed that the initial day (day 9) had fewer visits to RC than other days (days 10 and 11). It showed that animals spend more time in LC and CC on the first training day than in RC. Only a few animals grasped the information on the first day and were rewarded for their effort. Later, all animals gradually increased their visits to RC in the subsequent days due to training (Figure 1).

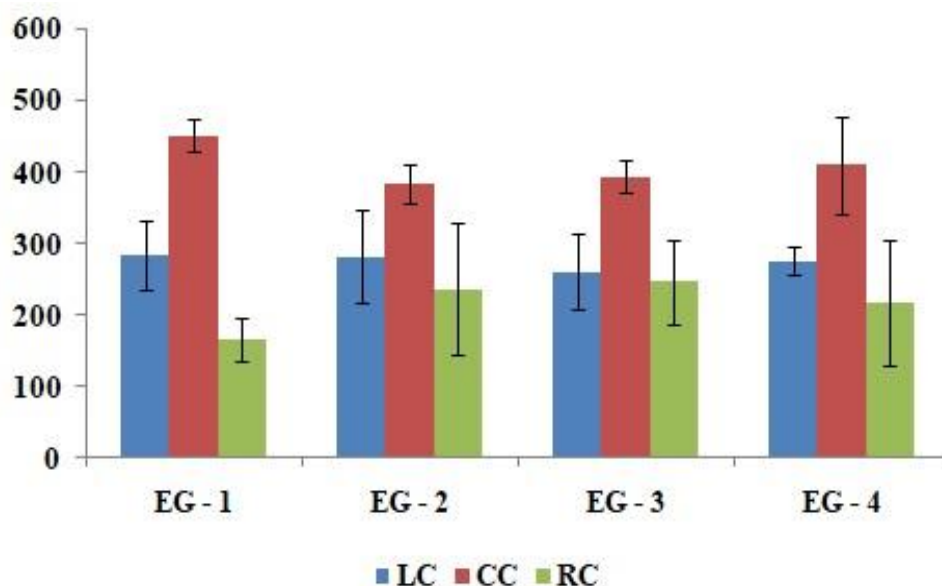


Figure 1 The first phase of behavioral training (without probiotic infusions - WiPI) showed that all experimental animals were trained in the experimental setup with the help of color cues based on reward learning. Initially, the number of visits to the right chamber (RC) was low on day 9 and gradually increased on days 10, and 11 which showed the animal's learning ability was associated with a reward. (Y axis denotes time in seconds; EG – experimental group; LC- left chamber; RC – right chamber; CC – central chamber).

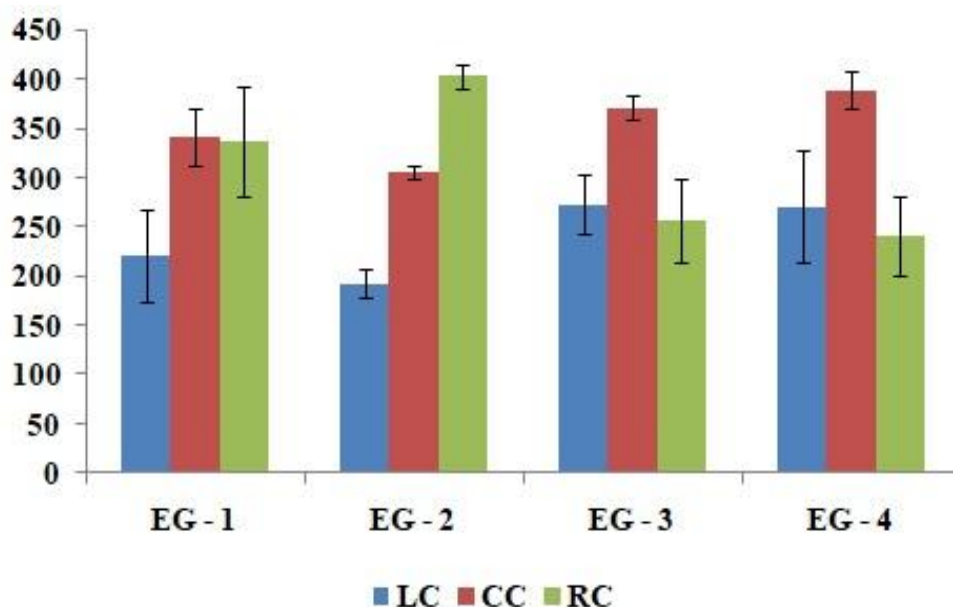


Figure 2 The first phase of behavioral testing (without probiotic infusions - WiPI) proved that experimental groups acquired information about the positive/negative reward with efficient retrieval of learned information. (Y axis denotes the time in seconds; EG – experimental group; LC- left chamber; RC – right chamber; CC – central chamber).

Following training, a five-day time gap (days 12-16) was given to consolidate learned information in the brain. Formed consolidated memory was tested for all experimental groups between days 17-20 in the experimental apparatus using positive and negative color cues. Behavioral scores proved that the training phase is important in retrieving learned information with an increased response to the

positive chamber in the CBLP (Figure 2). Consolidated behavioral scores showed that a habituated stress-free controlled environment may involved in the formation of cognitive memory through the enrichment of formed neuronal plasticity (Figure 3). After completion of PPBA, all experimental groups are maintained in the home aquarium between days 21-23 for memory reconsolidation.



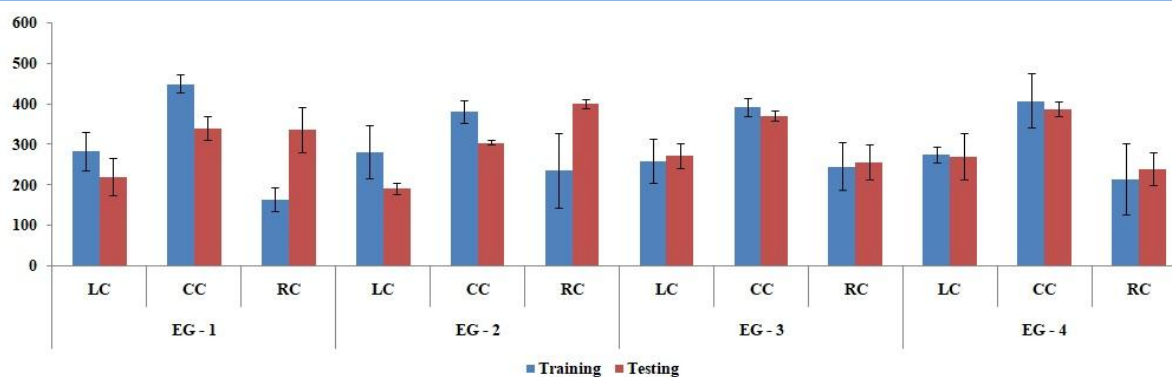


Figure 3 Comparative analysis of the primary phase of behavioral training and testing (without probiotic infusions - WiPI) showed that all four experimental groups learned about the provided positive/negative color stimuli during the process of training and retrieved stored information in an increased manner during the testing phase (Days 21 – 23). (Y axis denotes time in seconds; EG – experimental group; LC- left chamber; RC – right chamber; CC – central chamber).

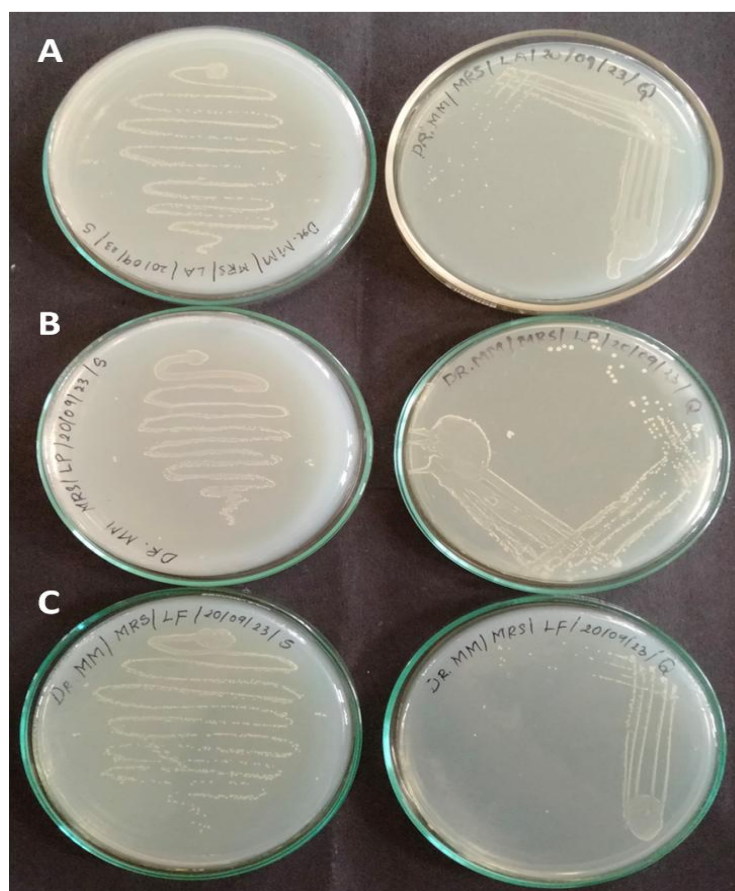


Figure 4 Representative plate pictures (A – *Lactobacillus acidophilus*, B - *Lactobacillus Plantarum*, and C - *Lactobacillus fermentum*) showing the purity confirmation of acquired *Lactobacillus* cultures with the help of the quadrant streak plate method.

### 3.2 Efficiency of probiotic infusions in the strengthening of developed cognitive functions

Following PPBA, the purity of acquired *Lactobacillus* cultures was identified using the quadrant streak plate method (Figure 4).

Obtained individual colonies of all three probiotic microorganisms were inoculated in 5 ml of *Lactobacillus* MRS broth medium and incubated at 37 °C for 24-36 hours. The prepared overnight culture was used for the preparation of the oral microbial mixture along with phosphate buffer saline (PBS) in a ratio of 50:50 (pure form)

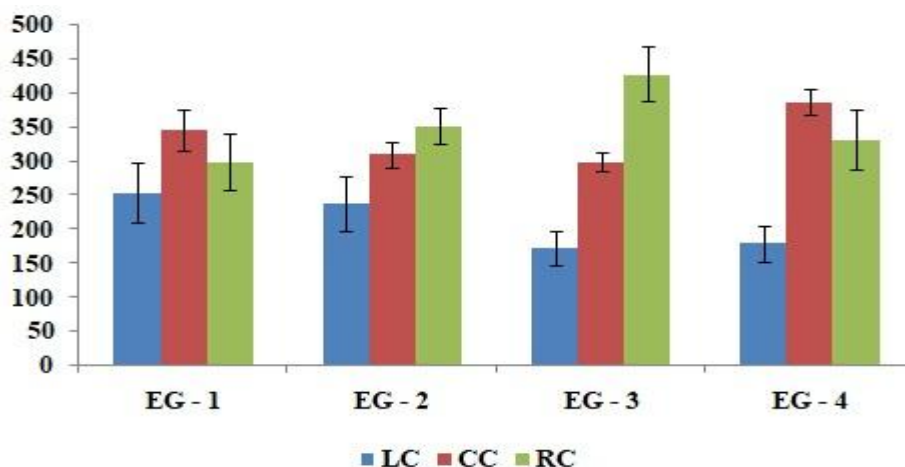


Figure 5 Behavioral scores of second phase training showed that probiotic oral infusions may take part in the strengthening of formed synaptic plasticity during the first phase of behavioral training. (Y axis denotes time in seconds; EG – experimental group; LC- left chamber; RC – right chamber; CC – central chamber).

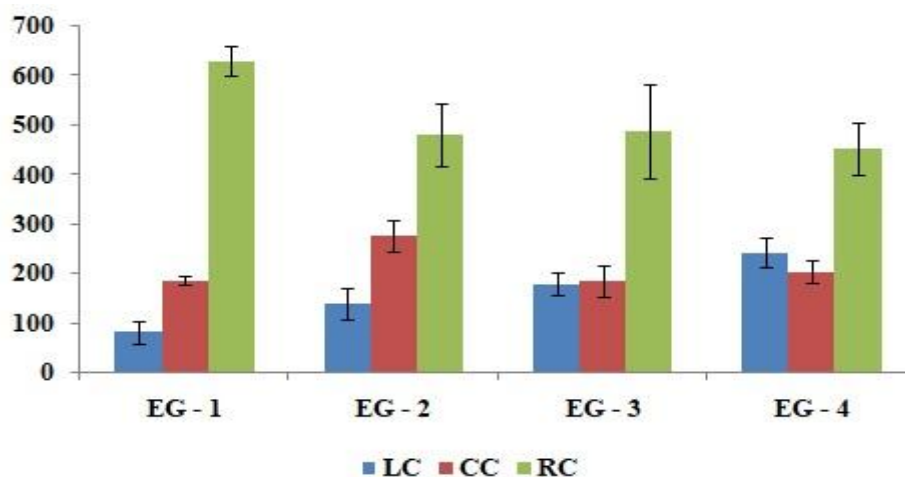


Figure 6 Behavioral scores of the second phase of testing showed that probiotic oral infusions also enhanced information retrieval compared to the first phase of behavioral testing. (Y axis denotes time in seconds; EG – experimental group; LC- left chamber; RC – right chamber; CC – central chamber).

and 20:20:20:40 (mixed form). According to the study, the prepared infused mixtures were infused into experimental groups in pure and mixed doses. Before the secondary phase of behavioral analysis (SPBA), experimental groups – 1, 2, and 3 (received pure oral infusions) and experimental group – 4 are infused with mixed probiotic cultures. Prepared oral infusion mixtures were orally administrated into the experimental groups on day 24. Following the three-day time intervals (days 25-27), the SPBA training phase was carried out to identify the impact of probiotic oral microbial infusions (POMI) on strengthening synaptic connections during learning and memory formation. The training and testing phases were carried out between two different time intervals. In SPBA, training was carried out for three days between days 28-30. Behavioral responses of the SPBA training phase showed that all experimental groups actively learned about the reward provided in

the RC compared to the FPBA training phase (Figure 5). SPBA training scores also showed that POMI may induce increased secretion of NPCs and neurotransmitters responsible for increased information acquisition. Followed by training, testing was carried out after 72 hours (3 days) of SPBA training on days 34-36. Testing behavioral scores showed that all animals spent more time/a higher number of visits to the positive-reward chamber than other chambers (Figure 6). Comparative analysis of training and testing phases proved that POMI played a major role in strengthening formed plasticity changes in the brain (Figure 7).

Comparative analysis of two different training phases, PPBA (without probiotic infusions – WiPI) and SPBA (with probiotic infusions – WPI), proved that a controlled habituated laboratory environment plays an unavoidable role in the formation of stress-free cognitive memory

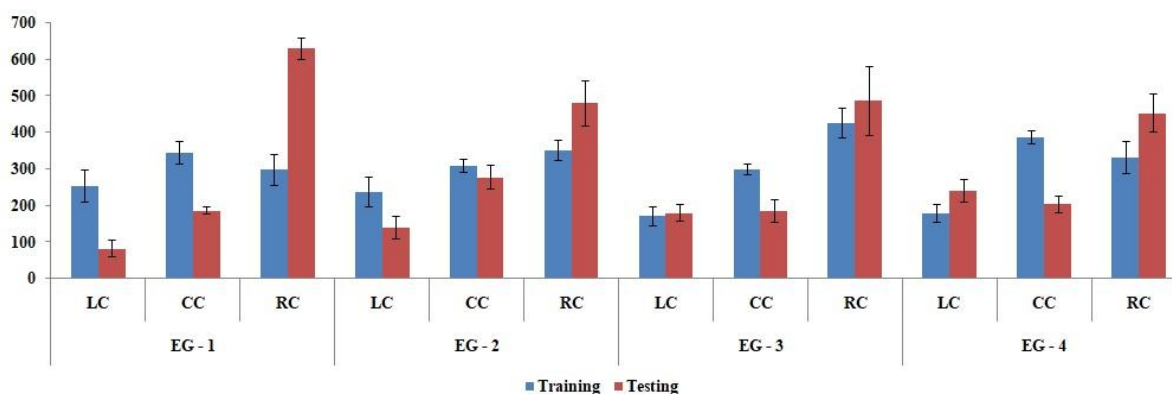


Figure 7 Comparative analysis of behavioral training and testing (with probiotic infusions) showed that all four experimental groups showed enhanced learning abilities during the process of training and efficient retrieval of stored information compared to the without probiotic infusive training and testing. (Y axis denotes time in seconds; EG – experimental group; LC- left chamber; RC – right chamber; CC – central chamber).

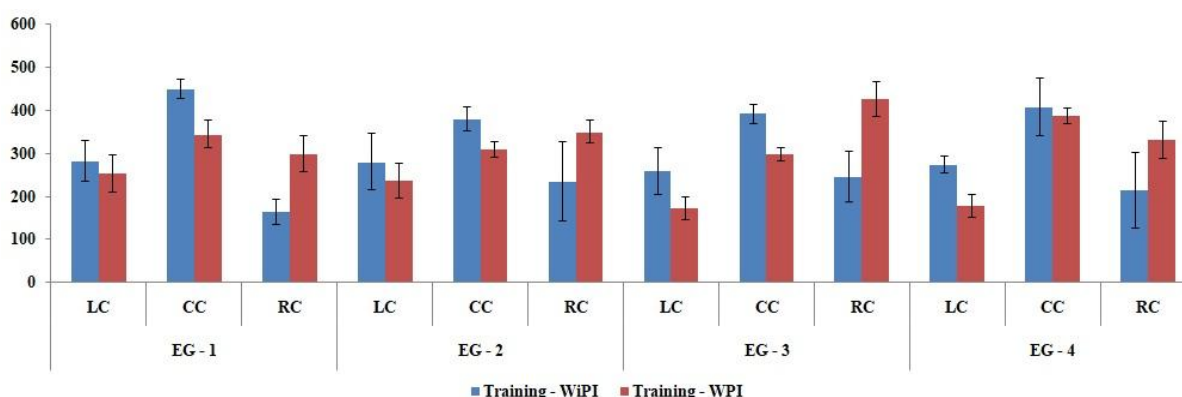


Figure 8 Comparative analysis of behavioral training (without probiotic infusions – WiPI Vs with probiotic infusions – WPI) showed that probiotic oral infusions played a major role in the development of synaptic plasticity (enhanced learning ability) compared to non-infusive training. (Y axis denotes time in seconds; EG – experimental group; LC- left chamber; RC – right chamber; CC – central chamber).

through the formation of neuronal/synaptic plasticity changes. Formed neuronal plasticity was further strengthened during the training phase after probiotic infusions. Thus, the obtained results showed that formed plasticity changes can be strengthened with the help of probiotic intake (Figure 8). Besides enhancing learning ability, probiotic oral infusions also enhance the efficient retrieval of learned information during testing after infusions. Thus, the comparative testing analysis proved that probiotic microorganisms play a pivotal role in strengthening formed neuronal connections with their intake in pure and mixed form (Figure 9).

### 3.3 Effect of probiotic oral microbial infusions on the development of stress-free cognitive functions

To prove the effect of probiotic oral microbial infusions on stress-free memory development, we used predator exposure test (PET) and open field test (OFT) in this study. All experimental animals performed PET and OFT to detect the absence of anxiety-like behavior, and fear memory formation in the infused groups. Scores

of PET showed that probiotic oral microbial infusions were never involved in the formation of anxiety-like behavior in infused groups. The animals spent more time in the stress-free zone (inner compartments) than the stressed zone (outer compartments) in the experimental setup. It also proved that probiotic oral microbial infusions never induce anxiety-like behavior against pure and mixed doses of infusions (Figure 10). Followed by PET, OFT was performed to prove that probiotic oral infusions may prevent the formation of fear memory when experimental groups are exposed to their predators. Behavioral responses of the experimental groups showed that all animals spent more time near their predator, which showed that probiotic oral infusions might limit the production of cortisol through the hypothalamic-pituitary-adrenal (HPA) axis. Reduced amount of cortisol production may result in the prevention of stress formation (Figure 11). Statistical analysis showed no significant differences among the CBLP, PET, and OFT experimental groups. Nonsignificant differences were calculated by the observed p values with the help of mean average values and standard errors.

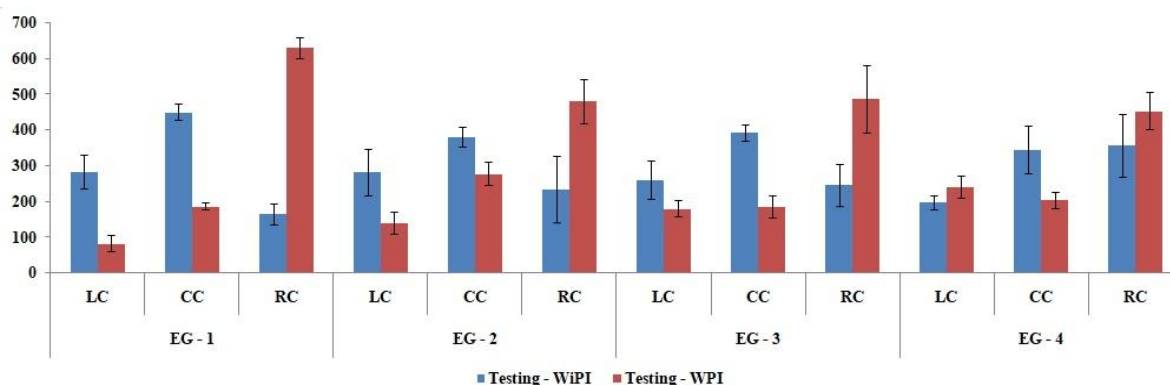


Figure 9 Comparative analysis of behavioral testing (without probiotic infusions – WiPI Vs with probiotic infusions – WPI) showed that probiotic oral infusions played an unavoidable role in the retrieval of learned information along with the development of synaptic plasticity during the testing phase. (Y axis denotes time in seconds; EG – experimental group; LC- left chamber; RC – right chamber; CC – central chamber).

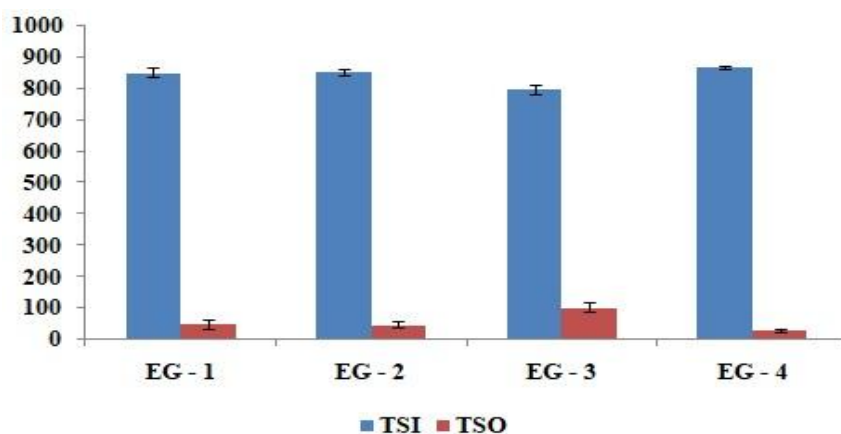


Figure 10 Behavioral responses of open field test (OFT) showed that infused experimental groups with probiotics in pure (EG – 1, 2, and 3) and mixed form (EG – 4) did not show any anxiety-like behavior development as animals spent more amount of time in the inner compartment (TSI) compared to the outer compartment (TSO). (Y axis denotes time in seconds; EG – experimental group; LC- left chamber; RC – right chamber; CC – central chamber).

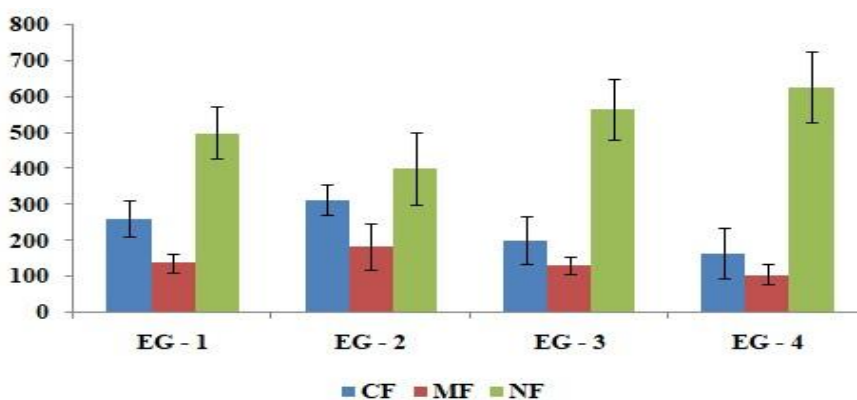


Figure 11 Behavioral scores of the predator exposure test (PET) proved that probiotic oral infusions do not show any fear memory development in the experimental groups. Responses showed that all experimental animals spend most of the time near the predator [No fear zone (NF)] other than mid fear zone (MF), and complete fear zone (CFZ). Thus observed result supports the role of probiotics in the alleviation of stress formation. (Y axis denotes time in seconds; EG – experimental group; LC- left chamber; RC – right chamber; CC – central chamber).

#### 4 Discussion

In recent scenarios, oral and gut microflora research has become a prominent research area in the oral-gut-brain (OGB) axis. This OGB axis shows close interconnection between the oral cavity, brain, and gastrointestinal tract (GI) (Narengaowa et al. 2021; Paudel et al. 2022; Chaudhry et al. 2023; Mukilan et al. 2024b). Emerging clinical evidence shows that this oral and gut microbiota may contain many bacterial communities, including beneficial and harmful flora. In a healthy condition, these beneficial flora play a relevant role in the maintenance of the homeostasis mechanism in the GI, which results in the production and transmission of neurotransmitter precursor compounds (NPCs) from the gut to the CNS (Zheng et al. 2020; Chen et al. 2021; Varela-Trinidad et al. 2022; Ji et al. 2023). The BBB carried out transmission of NPCs through the vagus nerve in a direct/indirect way. Transmitted NPCs produce brain neurotransmitters and the subsequent activation of neuronal signaling molecules involved in cognitive memory formation (Alajangi et al. 2022; Sarubbo et al. 2022; Mukilan 2023). Dysbiosis of oral/gut microflora further plays a major role in forming immune dysfunction, lung diseases, and reduced cognitive functions within a host. Few reports showed that ageing, food habit alterations, pathogenic infections, and poor oral hygiene play an unavoidable role in the development of cognitive dysfunctions through oral-gut dysbiosis (Kandpal et al. 2022; Malik et al. 2023; Mitra et al. 2023). Formed oral-gut dysbiosis consequently results in the causation of gastritis and other systematic disorders. This formed dysbiosis state can be reversed by the intake of probiotic microorganisms along with diet for the maintenance of probiotic flora within the oral cavity and gut (Sandhu et al. 2017; Den et al. 2020; Zhu et al. 2021; Liu et al. 2023).

The present study strived to explore the role of probiotic microorganisms in developing and strengthening synaptic plasticity with the help of a cue-based learning paradigm. Recent reports have proved that pathogenic microbial colonization plays a significant role in developing cognitive dysfunctions during dysbiosis. In healthy conditions, this pathogenic microbial colonization may controlled by the action of native flora with its mutual relationship with the barrier immunity of the existing host immune system (Sarkar et al. 2021; Dash et al. 2022; Ahmed et al. 2024; Pitchaikani et al. 2024). To prevent the colonization of pathogens, probiotic intake has become an alternative way to safeguard the host from oral and gut microflora disturbances. Based on the information availed from the recent reports, the current study tried to traverse through the beneficial effect of probiotics in the strengthening of brain neuronal plasticity changes (Han et al. 2021; Wang et al. 2021; Dahiya and Nigam 2022; Gebrayel et al. 2022). Obtained results showed that probiotic oral infusions had a major role in regulating neurotransmitter

production and its associated signaling molecules for the development of proper cognitive memory. Formed cognitive memory showed the proper production and transmission of NPCs from the gut to the brain via the BBB. Transported NPCs resulted in synthesizing neurotransmitters (serotonin) in the presynaptic neurons and their release into the SC. Once released into the SC, serotonin binds with 5-HT receptors, increasing calcium influx inside postsynaptic neurons. Increased calcium influx further activates neuronal signaling molecules needed for the maintenance of proper cognitive health (Chen et al. 2021; Dicks 2022; Miri et al. 2023; Margoob et al. 2024). This probiotic strain may also prevent stress formation by regulating the production of cortisol in the hypothalamic-pituitary-adrenal (HPA) axis (Freimer et al. 2022; Sabit et al. 2023). Thus, the present study revealed that probiotics are responsible for cognitive memory formation in the brain and alleviating stress formation in a host system.

#### Conclusion

The eventual upshots of the present study manifest the effect of probiotic infusions on the formation of cognitive memory. Recently, it was shown that pathogenic microbial colonization or conversion of normal flora into opportunistic pathogens may result in cognitive impairment through oral/gut dysbiosis. It was also reported that formed oral/gut dysbiosis can be reversed with the oral intake of probiotic microorganisms to reverse the formed cognitive impairment. In the current study, the ramifications of probiotics on the formation and strengthening of neuronal connections were studied in a controlled, habituated, serene environment. The studies showed that probiotic's impact on enhancing brain plasticity development was studied using a reward-based learning paradigm in a laboratory. Experimental behavioral responses showed that entering live probiotic microorganisms into the oral passage might prevent pathogenic colonization in the oral cavity and gut and positively impact cognitive health. Development of cognitive health results in the proper neurotransmitter production by transmitting the needed amount of neurotransmitter precursor compounds from the gut through the BBB. Formation of the needed quantity of neurotransmission results in the development of RNA/Protein mediated LT memory formation by regulating neuronal signaling molecules, microRNAs, and negative regulators of cognitive memory formation. It also proved that probiotics may control the synthesis and production of stress hormones like cortisol in the HPA axis other than enhanced neuronal plasticity changes. For the first time, the current study opened up the dual role of probiotic microorganisms in controlling stress formation and its effect on developing and strengthening existing neuronal connections to maintain proper cognitive health. The present study also revealed that probiotics can be stress relievers to control endocrine hormone production.



### Authors Contributions

MM performed the conceptualization, research design, funding acquisition, original investigation, draft preparation, revision, and editing of this manuscript. RA and SP performed the experimentation and data collection.

### Funding

MM thanks the Department of Science and Technology – Fund for Improvement of S&T Infrastructure in Universities and Higher Educational Institutions (DST-FIST), Government of India for the financial support under PG College Level – A Program (SR/FST/COLLEGE-/2022/1203).

### Conflict of Interest

Authors report no conflicts of interest in this work

### Data Availability

Research data is available with the authors and shall be provided upon request.

### References

- Abraham, W.C., Jones, O.D., & Glanzman, D.L. (2019). Is plasticity of synapses the mechanism of long-term memory storage? *Npj Science of Learning*, 4, 9.
- Ahmed, G.K., Ramadan, H.K., Elbeh, K., & Haridy, N.A. (2024). Bridging the gap: associations between gut microbiota and psychiatric disorders. *Middle East Current Psychiatry*, 31, 2.
- Alajangi, H.K., Kaur, M., Sharma, A., Rana, S., et al. (2022). Blood-brain barrier: emerging trends on transport models and new-age strategies for therapeutics intervention against neurological disorders. *Molecular Brain*, 15, 49.
- Appelbaum, L.G., Shenasa, M.A., Stolz, L., & Daskalakis, Z. (2023). Synaptic plasticity and mental health: methods, challenges and opportunities. *Neuropsychopharmacology*, 48, 113-120.
- Appleton, J. (2018). The Gut-brain Axis: Influence of Microbiota on Mood and Mental Health. *Integrative Medicine*, 17, 28-32.
- Ashok, A., Leroy, F., Rayman, J.B., & Kandel, E.R. (2019). Molecular Mechanisms of the Memory Trace. *Trends in Neuroscience*, 42, 14-22.
- Bai, Y., & Suzuki, T. (2020). Activity-Dependent Synaptic Plasticity in *Drosophila melanogaster*. *Frontiers in physiology*, 11, 161.
- Chaudhry, T.S., Senapati, S.G., Gadam, S., Mannam, H.P.S.S., et al. (2023). The Impact of Microbiota on the Gut-brain Axis: Examining the complex Interplay and Implications. *Journal of Clinical Medicine*, 12, 5231.
- Chaudhury, S., Sharma, V., Kumar, V., Nag, T.C., & Wadhwa, S. (2016). Activity-dependent synaptic plasticity modulates the critical phase of brain development. *Brain & Development*, 38, 355-363.
- Chen, D., Yang, X., Yang, J., Lai, G., et al. (2017). Prebiotic effect of fructooligosaccharides from *Morinda officinalis* on alzheimer's disease in rodent models by targeting the microbiota-gut-brain axis. *Frontiers in Aging Neuroscience*, 9, 403.
- Chen, Y., Xu, J., & Chen, Y. (2021). Regulation of Neurotransmitters by the Gut Microbiota and Effects on Cognition in Neurological Disorders. *Nutrients*, 13, 2099.
- Dahiya, D., & Nigam, P.S. (2022). The Gut Microbiota Influenced by the Intake of Probiotics and Functional Foods with Prebiotics Can Sustain Wellness and Alleviate Certain Ailments like Gut-Inflammation and Colon-Cancer. *Microorganisms*, 10, 665.
- Dash, S., Syed, Y.A., & Khan, M.R. (2022). Understanding the Role of the Gut Microbiome in Brain Development and Its Association With Neurodevelopmental Psychiatric Disorders. *Frontiers in Cell and Developmental Biology*, 10, 880544.
- Den, H., Dong, X., Chen, M., & Zhou, Z. (2020). Efficacy of probiotics on cognition, and biomarkers of inflammation and oxidative stress in adults with Alzheimer's disease or mild cognitive impairment – a meta-analysis of randomized controlled trials. *Aging*, 12, 4010-4039.
- Dicks, L.M.T. (2022). Gut Bacteria and Neurotransmitters. *Microorganisms*, 10, 1838.
- Evans, H.T., Blackmore, D., Götz, J., & Bodea, L. (2021). De novo proteomic methods for examining the molecular mechanisms underpinning long-term memory. *Brain Research Bulletin*, 169, 94-103.
- Freimer, D., Yang, T.T., Ho, T.C., Tymofiyeva, O., & Leung, C. (2022). The gut microbiota, HPA axis, and brain in adolescent-onset depression: Probiotics as a novel treatment. *Brain, Behaviour, & Immunity*, 26, 100541.
- Ganesh, A., Bogdanowicz, W., Balamurugan, K., Varman, D.R., & Rajan, K.E. (2012). Egr-1 antisense oligodeoxynucleotide administration into the olfactory bulb impairs olfactory learning in the greater short-nosed fruit bat *Cynopterus sphinx*. *Brain Research*, 1471, 33-45.
- Ganesh, A., Bogdanowicz, W., Haupt, M., Marimuthu, G., & Rajan, K.E. (2010). Role of olfactory bulb serotonin in olfactory

- learning in the greater short-nosed fruit bat, *Cynopterus sphinx* (Chiroptera: Pteropodidae). *Brain Research*, 1352, 108-117.
- Gebreyel, P., Nicco, C., Khodor, A.A., Bilinski, J., et al. (2022). Microbiota medicine: towards clinical revolution. *Journal of Translational Medicine*, 20, 111.
- Gentile, C.L., & Weir, T.L. (2018). The gut microbiota at the intersection of diet and human health. *Science*, 362, 776-780.
- Han, S., Lu, Y., Xie, J., Fei, Y., et al. (2021). Probiotic Gastrointestinal Transit and Colonization After Oral Administration: A Long Journey. *Frontiers in Cellular and Infection Microbiology*, 11, 609722.
- Hillemacher, T., Bachmann, O., Kahl, K.G., & Frieling, H. (2018). Alcohol, microbiome, and their effect on psychiatric disorders. *Progress in Neuropsychopharmacology and Biological Psychiatry*, 85, 105-115.
- Ji, J., Jin, W., Liu, S., Jiao, Z., & Li, X. (2023). Probiotics, probiotics, and postbiotics in health and disease. *MedComm*, 4, e420.
- Kandpal, M., Indari, O., Baral, B., Jakhmola, S., et al. (2022). Dysbiosis of Gut Microbiota from the Perspective of the Gut-Brain Axis: Role in the Provocation of Neurological Disorders. *Metabolites*, 12, 1064.
- Kim, S., Kim, H., & Um, J.W. (2018). Synapse development organized by neuronal activity-regulated immediate-early genes. *Experimental & Molecular Medicine*, 50, 1-7.
- Kumar, A., Sivamaruthi, B.S., Dey, S., Kumar, Y., Malviya, R., Prajapati, B.G., & Chaiyasut, C. (2024). Probiotics as modulators of gut-brain axis for cognitive development. *Frontiers in Pharmacology*, 15, 1348297.
- Lin, H., Chen, C., de Belle, J.S., & Chiang, A. (2021). CREBA and CREBB in two identified neurons gate long-term memory formation in *Drosophila*. *Proceedings of the National Academy of the United States of America*, 118, e2100624118.
- Liu, N., Yang, D., Sun, J., & Li, Y. (2023). Probiotic supplements are effective in people with cognitive impairment: a meta-analysis of randomized controlled trials. *Nutrition Reviews*, 81, 1091-1104.
- Luis, C.O.S., & Ryan, T.J. (2022). Understanding the physical basis of memory: Molecular mechanisms of the engram. *Journal of Biological Chemistry*, 298, 101866.
- Malik, J.A., Zafar, M.A., Lamba, T., Nanda, S., et al. (2023). The impact of aging-induced gut microbiome dysbiosis on dendritic cells and lung diseases. *Gut Microbes*, 15, 2290643.
- Margoob, M., Kouser, S., & Jan, N. (2024). Serotonin: The Link between Gut Microbiome and Brain. In K.F. Shad (Ed), Serotonin – Neurotransmitter and Hormone of Brain. IntechOpen. DOI:10.5772/intechopen.1003826.
- Miri, S., Yeo, J., Abubaker, S., & Hammami, R. (2023). Neuromicrobiology, an emerging neurometabolic facet of the gut microbiome? *Frontiers in Microbiology*, 14, 1098412.
- Misiak, B., Łoniewski, I., Marlicz, W., Freydeca, W., et al. (2020). The HPA axis dysregulation in severe mental illness: can we shift the blame to gut microbiota. *Progress in Neuro Psychopharmacology and Biological Psychiatry*, 102, 109951.
- Mitra, S., Dash, R., Nishan, A.A., Habiba, S.U., & Moon, I.S. (2023). Brain modulation by the gut microbiota: From disease to therapy. *Journal of Advanced Research*, 53, 153-173.
- Mukilan, M., Elakkiya, V., Darshini, M., & Varshini, M. (2024a). Exploring the Potential Role of *Lactobacillus plantarum* in the Reversal of Induced Cognitive Long-term Memory Impairment. *Journal of Experimental Biology and Agricultural Sciences*, 12, 175-187.
- Mukilan, M., Antony Mathew, M.T., Yaswanth, S., & Mallikarjun, V. (2024b). Role of Probiotic Strain *Lactobacillus acidophilus* in the Reversal of Gut Dysbiosis Induced Brain Cognitive Decline. *Journal of Experimental Biology and Agricultural Sciences*, 12, 36-48.
- Mukilan, M. (2023). Impact of *Pseudomonas aeruginosa*, *Bacillus subtilis*, *Staphylococcus aureus*, and *Escherichia coli* Oral Infusions on Cognitive Memory Decline in Mild Cognitive Impairment. *Journal of Experimental Biology and Agricultural Sciences*, 11, 581-592.
- Mukilan, M. (2022). Effects of Probiotics, Prebiotics and Synbiotic Supplementation on Cognitive Impairment: A Review. *Journal of Experimental Biology and Agricultural Sciences*, 10, 1-11.
- Mukilan, M., Bogdanowicz, W., Marimuthu, G., & Rajan, K.E. (2018a). Odour discrimination learning in the Indian greater short-nosed fruit bat (*Cynopterus sphinx*): differential expression of Egr-1, C-fos and PP-1 in the olfactory bulb, amygdala and hippocampus. *Journal of Experimental Biology*, 221, jeb175364.
- Mukilan, M., Rajathej, D.M., Jeyaraj, E., Kayalvizhi, N., & Rajan, K.E. (2018b). MiR-132 regulated olfactory bulb proteins linked to olfactory learning in greater short-nosed fruit bat *Cynopterus sphinx*. *Gene*, 671, 10-20.
- Mukilan, M., Varman, D.R., Sudhakar, S., & Rajan, K.E. (2015). Activity-dependent expression of miR-132 regulates immediate

- early gene induction during olfactory learning in the greater short-nosed fruit bat, *Cynopterus sphinx*. *Neurobiology of Learning and Memory*, *120*, 41-51.
- Narengaowa, Kong, W., Lan, F., Awan, U.F., et al. (2021). The Oral-Gut-Brain AXIS: The Influence of Microbes in Alzheimer's Disease. *Frontiers in Cellular Neuroscience*, *15*, 633735.
- Norris, D. (2017). Short-Term Memory and Long-Term Memory are Still Different. *Psychological Bulletin*, *143*(9), 992-1009.
- O'Donnell, M.P., Fox, B.W., Chao, P., Schroder, F.C., & Sengupta, P. (2020). A neurotransmitter produced by gut bacteria modulates host sensory behaviour. *Nature*, *583*, 415-420.
- Ortega-Martínez, S. (2015). A new perspective on the role of the CREB family of transcription factors in memory consolidation via adult hippocampal neurogenesis. *Frontiers in Molecular Neuroscience*, *8*, 46.
- Paudel, D., Uehara, O., Giri, S., Yoshida, K., et al. (2022). Effect of psychological stress on the oral-gut microbiota and the potential oral-gut-brain axis. *Japanese Dental Science Review*, *58*, 365-375.
- Peng, S., Zhang, Y., Zhang, J., Wang, H., & Ren, B. (2010). ERK in learning and memory: a review of recent research. *International Journal of Molecular Sciences*, *11*, 222-232.
- Pitchaikani, S., Mukilan, M., Govindan, P., Kathiravan G., Shakila H. (2024). Highlighting the Importance of Matrix Metalloproteinase 1, 8, and 9 Expression during the Progression of *Mycobacterium tuberculosis* Infection. *Journal of Experimental Biology and Agricultural Sciences*, *12*, 49-59.
- Rajan, K.E. (2021). Olfactory learning and memory in the greater short-nosed fruit bat *Cynopterus sphinx*: the influence of conspecifics distress calls. *Journal of Comparative physiology. A, Neuroethology, Sensory, Neural, and Behavioral Physiology*, *207*, 667-679.
- Ramirez, A., & Arbuckle, M.R. (2016). Synaptic Plasticity: The Role of Learning and Unlearning in Addiction and Beyond. *Biological Psychiatry*, *80*(9), e73-e75.
- Sabit, H., Kassab, A., Alaa, D., Mohamed, D., et al. (2023). The Effect of Probiotic Supplementation on the Gut-Brain Axis in Psychiatric Patients. *Current Issues in Molecular Biology*, *45*, 4080-4099.
- Salami, M., & Soheili, M. (2022). The microbiota-gut-hippocampus axis. *Frontiers in Neuroscience*, *16*, 1065995.
- Sandhu, K.V., Sherwin, E., Schellekens, H., Stanton, C., et al. (2017). Feeding the microbiota-gut-brain axis: diet, microbiome, and neuropsychiatry. *Translational Research*, *179*, 223-244.
- Sarkar, A., Yoo, J.Y., Dutra, S.V.O., Morgan, K.H., & Groer, M. (2021). The Association between Early-Life Gut Microbiota and Long-Term Health and Diseases. *Journal of Clinical Medicine*, *10*, 459.
- Sarubbo, F., Cavallucci, V., & Pani, G. (2022). The Influence of Gut Microbiota on Neurogenesis: Evidence and Hopes. *Cells*, *11*, 382.
- Savin, Z., Kivity, S., Yonath, H., & Yehuda, S. (2018). Smoking and the intestinal microbiome. *Archives of Microbiology*, *200*, 677-684.
- Sengupta, P. (2020). A neurotransmitter produced by gut bacteria modulates host sensory behaviour. *Nature*, *583*, 415-420.
- Suganya, K., & Koo, B. (2020). Gut-Brain Axis: Role of Gut Microbiota on Neurological Disorders and How Probiotics/Prebiotics Beneficially Modulate Microbial and Immune Pathways to Improve Brain Functions. *International Journal of Molecular Sciences*, *21*, 7551.
- Varela-Trinidad, G.U., Domínguez-Díaz, C., Solórzano-Castanedo, K., Íñiguez-Gutiérrez, L., et al. (2022). Probiotics: Protecting Our Health from the Gut. *Microorganisms*, *10*, 1428.
- Wang, X., Zhang, P., & Zhang, X. (2021). Probiotics Regulate Gut Microbiota: An Effective Method to Improve Immunity. *Molecules*, *26*, 6076.
- Yang, X., Yu, D., Xue, L., Li, H., et al. (2020). Probiotics modulate the microbiota-gut-brain axis and improve memory deficits in aged SAMP8 mice. *Acta Pharmaceutica Sinica B*, *10*, 475-87.
- Zheng, D., Liwinski, T., & Elinay, E. (2020). Interaction between microbiota and immunity in health and disease. *Cell Research*, *30*, 492-506.
- Zhu, G., Zhao, J., Zhang, H., Chen, W., & Wang, G. (2021). Probiotics for Mild Cognitive Impairment and Alzheimer's Disease: A Systematic Review and Meta-Analysis. *Foods*, *10*, 1672.










# Journal of Experimental Biology and Agricultural Sciences

<http://www.jebas.org>

ISSN No. 2320 – 8694

## Hematite Nanoparticle Mediated Enhancement of *Chlorella minutissima* Lipid Productivity for Sustainable Biodiesel Production

Richa Pahariya<sup>1</sup> , Abhishek Chauhan<sup>2\*</sup> , Anuj Ranjan<sup>2</sup> , Rupesh Kumar Basniwal<sup>3</sup> ,  
 Sumant Upadhyay<sup>4</sup> , Smile Kataria<sup>4</sup> , Hardeep Singh Tuli<sup>5</sup> , Moyad Shahwan<sup>6,7</sup> ,  
 Vinay Mohan Pathak<sup>8</sup> , Tanu Jindal<sup>2\*</sup> 

<sup>1</sup>Amity Institute of Environmental Sciences, Amity University, Noida, U.P., India

<sup>2</sup>Amity Institute of Environmental Toxicology Safety and Management, Amity University, Noida, U.P., India

<sup>3</sup>Amity Institute of Advanced Research and Studies (M&D), Amity University, Noida, U.P., India

<sup>4</sup>Amity Institute of Nanotechnology, Amity University, Noida U.P., India

<sup>5</sup>Department of Biotechnology, Maharishi Markandeshwar (Deemed to be University), Mullana, Ambala 12 133207, Haryana, India

<sup>6</sup>Department of Clinical Sciences, College of Pharmacy and Health Sciences, Ajman University, Ajman 346, United Arab Emirates

<sup>7</sup>Centre of Medical and Bio-Allied Health Sciences Research, Ajman University, Ajman 346, United Arab Emirates

<sup>8</sup>Pritam International Private Ltd, Roorkee, Uttarakhand, India

Received – April 17, 2024; Revision – June 26, 2024; Accepted – July 06, 2024

Available Online – July 15, 2024

DOI: [http://dx.doi.org/10.18006/2024.12\(3\).366.378](http://dx.doi.org/10.18006/2024.12(3).366.378)

### KEYWORDS

Hematite nanoparticles

Microalgal growth

Lipid productivity

Biodiesel production

Iron oxide nanoparticles

Biofuel Enhancement

### ABSTRACT

This study aims to enhance lipid and biofuel productivity from *Chlorella minutissima* with hematite ( $\alpha$ -Fe<sub>2</sub>O<sub>3</sub>) nanoparticles (IONPs) as a growth stimulant. The IONPs were synthesized using chemical method and characterized using X-ray diffraction (XRD), Scanning Electron Microscopy (SEM), and Energy Dispersive X-ray (EDX) analysis to confirm their structure and composition. The experimental setup involved inoculating various concentrations of IONPs (10, 20, and 30 mg·L<sup>-1</sup>) into the microalgal BG-11 growth medium to evaluate their impact on microalgal growth and biodiesel production. Results of this study showed that a concentration of 10 mg·L<sup>-1</sup> of IONPs significantly increased the biomass concentration to 508.1 mg·L<sup>-1</sup> over a 20-day cultivation period, achieving the highest biomass production rate of 31.7 mg·L<sup>-1</sup>·d<sup>-1</sup> at this concentration. The lipid extracted from the microalgal biomass was subsequently transesterified into biodiesel. Key biodiesel properties, such as cetane number, calorific value, density, and viscosity, were measured to assess fuel quality. The findings demonstrate that incorporating hematite nanoparticles into the microalgal growth medium can significantly

\* Corresponding author

E-mail: akchauhan@amity.edu (Abhishek Chauhan), tjindal@amity.edu (Tanu Jindal)

Peer review under responsibility of Journal of Experimental Biology and Agricultural Sciences.

Production and Hosting by Horizon Publisher India [HPI]  
 (<http://www.horizonpublisherindia.in/>).  
 All rights reserved.

All the articles published by [Journal of Experimental Biology and Agricultural Sciences](#) are licensed under a [Creative Commons Attribution-NonCommercial 4.0 International License](#) Based on a work at [www.jebas.org](http://www.jebas.org).



boost both lipid content and overall growth, thereby improving biodiesel production. This study suggests that the use of  $\alpha$ -Fe<sub>2</sub>O<sub>3</sub> nanoparticles presents a promising approach for scalable and sustainable biofuel production from microalgae.

## 1 Introduction

The development of microalgal biomass to produce carbon-neutral and renewable biofuel is essential for environmental sustainability, national economy, and energy security (Vasistha et al. 2021; Zhao et al. 2024a). Biodiesel, which is classified as an alkyl monoester of long-chain fatty acids, is a sustainable fuel that is extensively utilized in diesel engines across several nations (Yaşar 2020; Moschona et al. 2024). It has been proposed that biofuels such as biodiesel and bioethanol present captivating alternatives to renewable energy sources. Microalgae have been thoroughly investigated as a source for generating biofuels. The main components present in microalgal biomass are lipids, proteins, and polysaccharides. The lipid component is used as the primary material for biodiesel production. Some oleaginous species such as *Chlorella* (Saxena et al. 2020), *Nitzschia* (Huang et al. 2022), and *Scenedesmus obliquus* (He et al. 2017) are the most widely researched species in biodiesel production (Ma et al. 2022). The intensive part of producing biofuel from microalgae is extracting biomass from the diluted culture broth (Muhammad et al. 2021). Consequently, one of the main obstacles to the commercialization and large-scale production of microalgae is the low cell concentration and lipid content. Thus, the methods to enhance the growth of microalgae with comparatively greater biomass concentration and lipid accumulations are significant requirements in biofuel production (Kaushik et al. 2009; Ganesh Saratale et al. 2022). Adding nanoparticles throughout the cultivation and harvesting phases is one of the many methods that may be employed to improve microalgae development (Vasistha et al. 2021). The application of NPs during the microalgal growth phase can increase the amount of CO<sub>2</sub> that is absorbed from the atmosphere and even improve the photobioreactor's ability to convert light efficiently, which accelerates the growth of the microalgae (Pahariya et al. 2023). While incorporating nano-additives into microalgae cultures, it is important to consider both the characteristics and concentration of the NPs carefully. However, the impact of NPs on the growth and biochemical composition of microalgae depends closely on their unique physical characteristics (Saxena et al. 2020). It is reported that the lipid content of *Chlorella fusca* LEB 111 increased by 10.9% and 16.7% when grown outdoors with 0.3 and 0.5 g L<sup>-1</sup> of nanofibers, respectively. These nanofibers are composed of polymeric nanofibers (10% w/v) made from polyacrylonitrile (PAN) dissolved in dimethylformamide (DMF) with the addition of 4% (w/v) Fe<sub>2</sub>O<sub>3</sub>NPs. When exposed to uncoated nano-zero-valent iron (nZVI), *Tetraselmis suecica* showed a lipid augmentation of 41.90% in the study on the effects of nZVI on various microalgae species. Additionally, they noticed that adding inorganically coated nZVI powder to *Pavlova lutheri* resulted in a 46.34% increase in

lipid levels (Kadar et al. 2012). The biodiesel yield in *Spirulina* was enhanced up to 81% by Fe<sub>2</sub>O<sub>3</sub> nanoparticles, which were synthesized using a green procedure involving extracts from *Hibiscus rosa-sinensis* (Banerjee et al. 2019). Similarly, it was found that the addition of a 100 mg. L<sup>-1</sup> dose of nZVI enhances the biomass concentration in *Isochrysis galbana* by 18.75%, accompanied by a 3.57% increase in lipid accumulation (Kadar et al. 2012). Similarly, the lipid content was increased by 16.7% in *Chlorella fusca* when nZVI was added at 0.5 g L<sup>-1</sup> (Da Silva Vaz et al. 2020). The impact of nanoparticles on the growth and biochemical composition of microalgae is contingent upon their physical characteristics (Khan et al. 2018). *Candida rugosa* lipase was employed for the transesterification of algal lipids after being immobilized on graphene oxides magnetized with NiFe<sub>2</sub>O<sub>4</sub> nanoparticles (NiFe<sub>2</sub>O<sub>4</sub>-GO). This nanocomposite proved to be an outstanding nano biocatalyst for efficient biodiesel generation, with biodiesel production efficiency three times better than that of free enzymes (Aghabeigi et al. 2023). The increase in lipid content is attributed to the use of NPs, which positively impact cellular activity. For example, iron (Fe) serves as a crucial micronutrient for microalgae, playing a vital role in essential cellular functions such as photosynthesis and respiration. The availability of iron regulates their productivity, community structure, and overall ecosystem functioning (Cheng et al. 2020). In contrast, Fe<sub>2</sub>O<sub>3</sub> nanoparticles showed toxicity towards *C. sorokiniana* even at the low dose of 2 mg. L<sup>-1</sup>, whereas the dose of 20 and 30 mg. L<sup>-1</sup> in *C. pyrenoidosa* increased biomass productivity and lipid content (Rana et al. 2020). The effects of copper and selenium nano aqua chelate carboxylated with citric acid on biomass accumulation in *C. vulgaris* were also investigated. The inoculation of 0.67–4 mg. L<sup>-1</sup> of Cu nano carboxylates resulted in an approximately 20% increase in *Chlorella* biomass. However, concentrations of 20–40 mg. L<sup>-1</sup> significantly inhibited algal development after the 12<sup>th</sup> day of incubation. Se nanocarboxylates at concentrations of 0.4–4 mg. L<sup>-1</sup> also fostered the growth of *C. vulgaris*, leading to a 40–45% rise in biomass (Mykhaylenko and Zolotareva 2017).

Previous research has shown that NPs concentration can significantly impact microalgae growth; the specific effects vary depending on several factors. Such factors include the type of NPs, the microalgae species itself, and environmental conditions like culture media and pH. Among microalgae, *C. minutissima* is a particularly promising strain for biofuel production. It is also known to be less sensitive to Fe NPs compared to other types, such as nZVI and Fe<sub>3</sub>O<sub>4</sub>. However, the impact of IONPs on *C. minutissima*'s growth and its potential for biofuel production remains unclear.



Therefore, the present research aims to investigate the effect of IONPs on both the growth and lipid accumulation of *C. minutissima*. It involved testing various concentrations of IONPs in BG11 media and measuring parameters like cell density and lipid accumulation within *C. minutissima*. By examining these factors, this research will provide valuable insights into the potential use of IONPs in *C. minutissima* cultivation for biofuel production. The findings will help us understand if specific IONPs concentrations can promote both microalgae growth and lipid accumulation, making them a viable tool for this purpose.

## 2 Materials and Methods

### 2.1 Microalgal species

The oleaginous microalga *C. minutissima* MCC 27 was obtained from the Centre for Blue Green Algae, Indian Agricultural Research Institute (IARI), New Delhi, India. A sterile culture BG 11 medium was prepared for the inoculation, and pH was maintained at 7.1.

### 2.2 Chemical synthesis of Fe<sub>2</sub>O<sub>3</sub> nanoparticles

IONPs termed "Hematite" were synthesized using the sol-gel process as per the method described by Paulson and Jothibas (2021). In the experiment, 100 mL of distilled water was used to dissolve the 0.3 M of Ferric chloride hexahydrate, which was maintained by vigorous stirring at 300 rpm for 15 minutes. Following that, a reagent solution made up of 10 mL of NH<sub>3</sub>-ammonia solution and 10 mL of distilled water was combined. The produced reagent solution was then carefully added to the ferric chloride anhydrous solution, and it was stirred vigorously (400 ± 20 rpm) for one hour at 80 °C. The gel was put into a petri dish once the initial cleaning was finished and kept in the oven at 80 °C for 24 hours. The resultant nano-powder sample was then stored for subsequent characterizations after being calcined at 400 °C for 3 hours in an open environment.

### 2.3 Materials Characterization

#### 2.3.1 X-ray diffraction (XRD)

The X-ray diffraction was performed using a Philips XRD 3100 diffractometer (Philips Electronics Co., Eindhoven, Netherlands) with a medium scan rate of 0.3 degrees per second over a 2θ range of 20-70°.

#### 2.3.2 Scanning Electron Microscopy (SEM)

The SEM and EDX study was performed using TESCAN Magna 200 eV-30 KV along with cross-sectional, morphology, and elemental analysis for Fe & O.

### 2.4 Evaluation of microalgal growth

Initial studies were carried out in 250 mL Erlenmeyer flasks with 100 mL of BG 11 medium to examine the biomass potential and growth profiles. 10% (v/v) of freshly grown *C. minutissima* was added to the medium containing flasks and incubated in a microalgae growth chamber at 25 ± 2 °C. All the experiments were carried out in triplicates. The flasks were kept under LED light (about 2500 Lux) for an 18:6 light and dark period (18-hour light-dark cycle 6 hours) for 20 days. Throughout 20 days, the optical density of the microalgae was measured at 680 nm utilizing an Agilent Technologies Cary 60 UV-Vis Spectrophotometer.

To measure the effect of iron nanoparticles, *C. minutissima* was cultured in 100 mL of BG11 media supplemented with different concentrations of nanoparticles (0, 10, 20, and 30 mg·L<sup>-1</sup>). The cultures were maintained under the controlled conditions mentioned above. The growth of the microalgae was measured by sampling the culture every two days for 20 days. After 20 days, the microalgal biomass was harvested by centrifugation and washed with double distilled water to remove impurities. After centrifugation, the pellets were dried in an oven at 60 °C until they reached a consistent weight. After drying, the biomass was placed in desiccators to estimate the accumulation of lipids and biodiesel. Biomass concentration, biomass yield, and biomass productivity were calculated using corresponding equations (1), (2), and (3).

$$\text{Biomass concentration} = \text{Weight (mg)} / \text{volume of culture (L)} \quad (1)$$

$$B = X_f - X_0 \quad (2)$$

Where B= biomass yield (g·L<sup>-1</sup>)

X<sub>f</sub>= final biomass concentration

X<sub>0</sub> = initial biomass concentration

$$P_b = (X_2 - X_1) / (t_1 - t_0) \quad (3)$$

Where P<sub>0</sub>= biomass productivity

X<sub>2</sub> and X<sub>1</sub>= biomass concentrations

### 2.5 Calculation of Chlorophyll a

Chlorophyll-a (chl-a) was estimated using the colorimetry method (Porra et al. 1989). In summary, a 1.5 mL Eppendorf tube containing an aliquot (1 mL) of microalgae culture was centrifuged at room temperature for 10 minutes at 6000 rpm. The sample was then rinsed three times with deionized water to remove the impurities. The pellets were again suspended in 1 millilitre of methanol after the supernatant was disposed off. The tubes were tightly sealed with parafilm and immersed in a water bath heated to

60 °C for 30 minutes to extract chlorophyll-a. Following cooling to room temperature, absorbance readings were taken at wavelengths of 652 nm, 665.2 nm, and 750 nm. Porra's equation was then used to estimate the concentration of chl-a in  $\mu\text{g}\cdot\text{mL}^{-1}$ .

$$\text{Chl - a} = 16.29 (A_{665.2} - A_{750}) - 8.54 (A_{652} - A_{750}) \quad (4)$$

## 2.6 Lipid extraction from harvested microalgae

The lipids from microalgae were extracted using the modified Bligh and Dyer (1959) method. Then, dried and powdered microalgal biomass was dispersed in distilled water. After microwaving at 540 W, the microalgal cells were disrupted, and the suspension was allowed to cool to room temperature. Subsequently, chloroform and methanol were introduced into the microalgal suspension. The mixture was vigorously shaken manually and left at room temperature for 4 hours. Following this, water was added to aid in the separation of phases. The mixture was subsequently left undisturbed until the organic layer settled and the upper phase became clear (Lee et al. 2010). The organic phase, containing chloroform and lipids, was carefully extracted, and its volume was recorded, and the lipid content was calculated using the following equation:

$$\text{Lipid content (\%)} = \frac{\text{Mass of lipid (in grams)} \times 100}{\text{Mass of algae culture (in grams)}}$$

## 2.7 Fatty Acid Methyl Ester (FAME) formation

FAME formation was carried out by Transesterification (Mishra et al. 2014). Briefly, in this process, methanol was added to sodium hydroxide into the glass blender. The mixture of methanol and sodium hydroxide was appropriately mixed with the help of a magnetic stirrer after dissolving NaOH in methanol. Then, the extracted oil was transferred into a glass blender for 30 minutes.

Following that, the mixture was put into a sterile container. The mixture is divided into two layers after two to three hours. The first layer was biodiesel, and the second was glycerine. The biodiesel was then washed multiple times with distilled water to remove traces of alcohol, catalyst and glycerol.

### 2.7.1 FT-IR Analysis

A Bruker Vertex 70 FTIR spectrophotometer with a Platinum ATR (attenuated total reflection) module was used to conduct the spectral study. FT-IR spectra were produced at 400–4000  $\text{cm}^{-1}$  (Portaccio et al. 2023). The Origin software (version 5.0, 2007) was then used to evaluate these spectra.

## 2.8 Assessment of biodiesel fuel properties

The biodiesel obtained from *C. minutissima* grown in BG 11 was subjected to testing for its physical characteristics, including specific density (Prabakaran et al. 2021), viscosity (Al-Ansari et al. 2023), calorific value (Boopathi et al. 2023), cetane number (Tesfa et al. 2013), iodine value, and oxidative stability (Geng et al. 2023). These tests were conducted according to the protocols outlined by ASTM D6751 and EN 14214 fuel standards.

## 3 Results

### 3.1 Morphology of *C. minutissima*

Under the scanning microscope, *C. minutissima* has a unicellular structure, yellow-green color, and a spherical shape with a diameter ranging from 5 to 15  $\mu\text{m}$ . The cells appear spherical or ellipsoidal under a scanning electron microscope, and their walls either have smooth surfaces or uneven coastal portions, as shown in Figure 1. The cells exist in either a unicellular state or in the palmella stage.

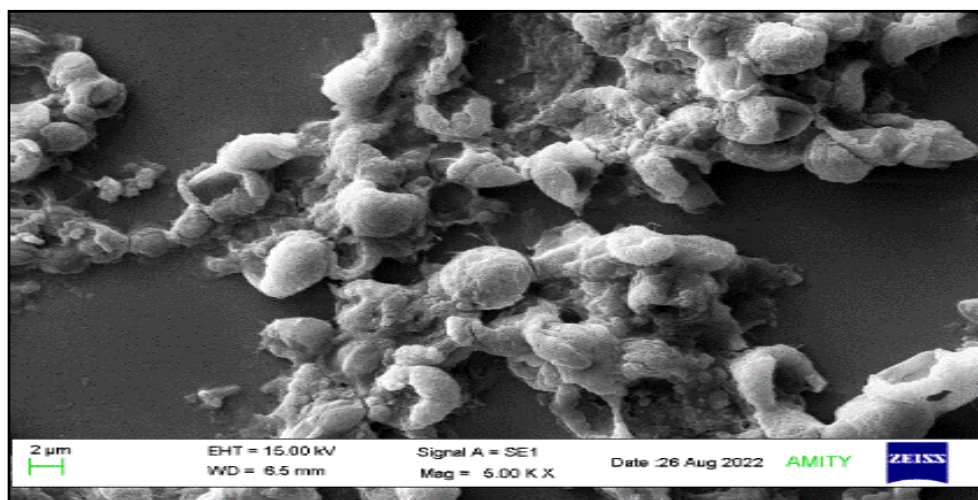


Figure 1 Scanning microscopic image of *C. minutissima*

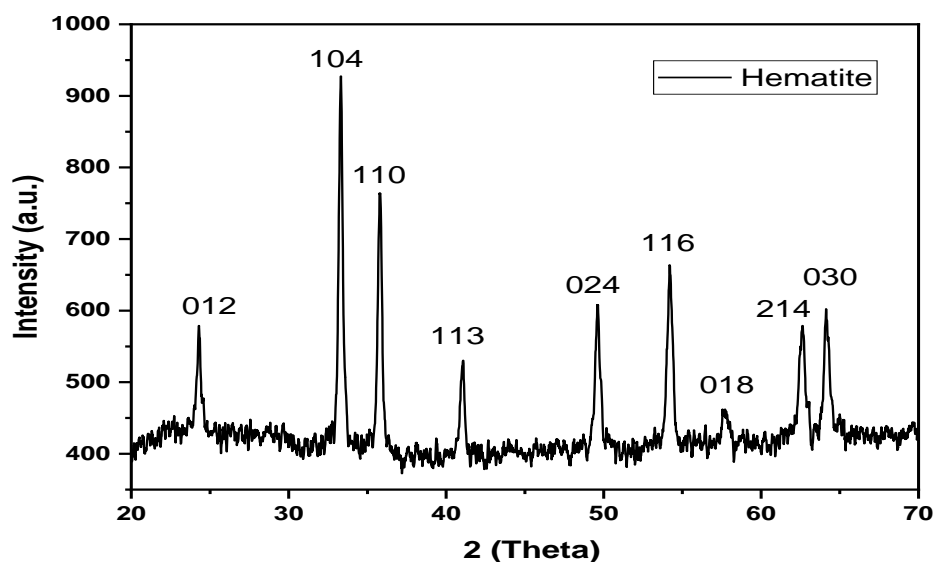


Figure 2 X-ray diffraction (XRD) pattern of synthesized nanoparticles of iron oxide ( $\alpha$ -Fe<sub>2</sub>O<sub>3</sub>)

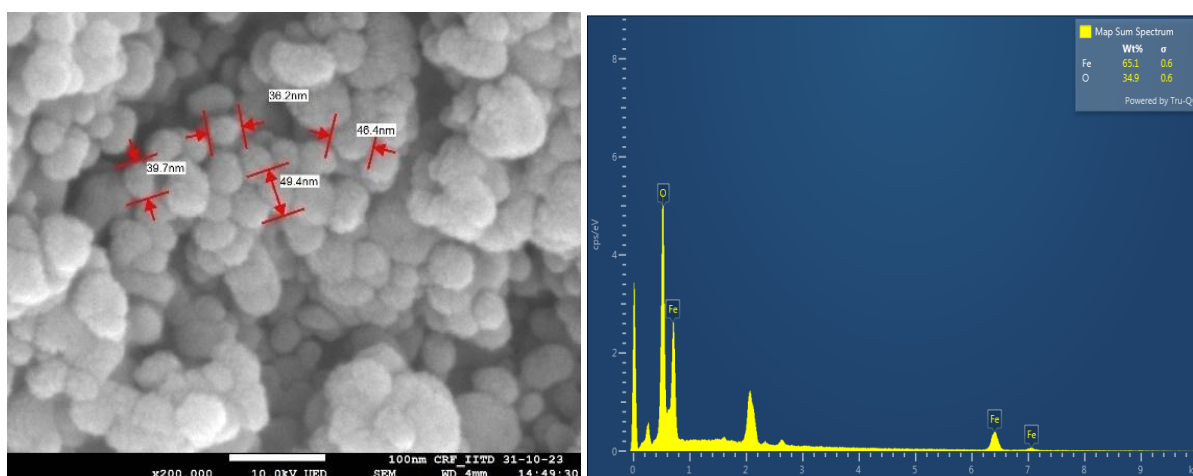


Figure 3 (a) SEM (b) EDX image of synthesized Fe<sub>2</sub>O<sub>3</sub> ( $\alpha$ -Fe<sub>2</sub>O<sub>3</sub>) nanoparticles

### 3.2 XRD analysis

Figure 2 shows the X-ray diffraction pattern for iron oxide ( $\alpha$ -Fe<sub>2</sub>O<sub>3</sub>). The X-ray diffraction study for  $\alpha$ -Fe<sub>2</sub>O<sub>3</sub> shows the characteristic peaks for the 104 plane corresponding to the 2 $\theta$  angle of 33.29, implying the formation of  $\alpha$ -Fe<sub>2</sub>O<sub>3</sub>. The referred X-ray diffractions are from the JCPDS Card No. 86-0550. The crystallite size was determined using the Debye-Scherrer's equation:  $D = K\lambda / \beta \cos\theta$

Where the wavelength of Cu-K $\alpha$  radiation utilized is  $\lambda = 1.5418 \text{ \AA}$ , the form factor is  $k = 0.9$ , the full-width half maximum (FWHM) is expressed in radians ( $\beta$ ), the crystallite's diameter is  $D$ , and Bragg's angle is  $\theta$  (Sun et al. 2006). The crystallite size for the  $\alpha$ -Fe<sub>2</sub>O<sub>3</sub> was calculated to be 40 nm from FWHM of the most intense (104) diffraction peak using Debye-Scherrer's equation.

### 3.3 SEM analysis

Figure 3 (a, b) shows the FE-SEM micrograph for the  $\alpha$ -Fe<sub>2</sub>O<sub>3</sub> at a scale of 100nm, along with the elemental X-ray electron energy and their elemental mapping. The particle size calculated for sample  $\alpha$ -Fe<sub>2</sub>O<sub>3</sub> was ~46 nm using SEM, which is in good agreement with the size calculated using XRD data.

### 3.4 Assessment of growth parameters in *C. minutissima*

*C. minutissima* is the fastest-growing strain. After 20 days of incubation, microalgal cells were subjected to further analysis. To access the growth parameters, the strain was cultured in a BG 11 medium. Figure 4 shows that the OD of samples increased and reached the maximum in 14 days. The absorbance ( $A_{680}$ ) of the culture microalgae strain was recorded using a spectrophotometer

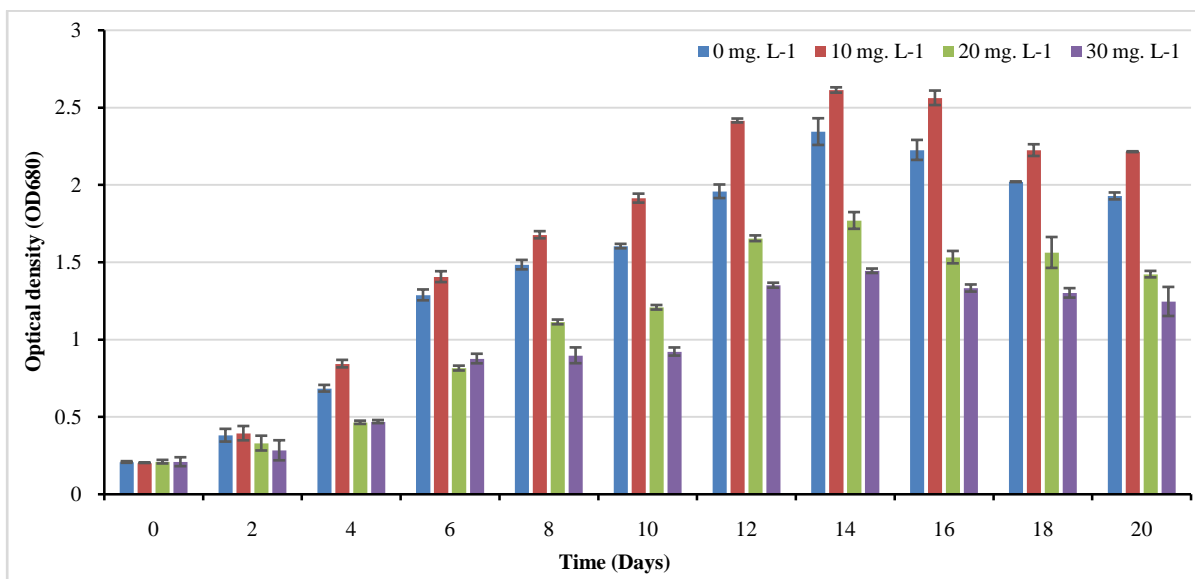


Figure 4 Graphical representation of optical density on various IONPs concentrations on *C. minutissima*

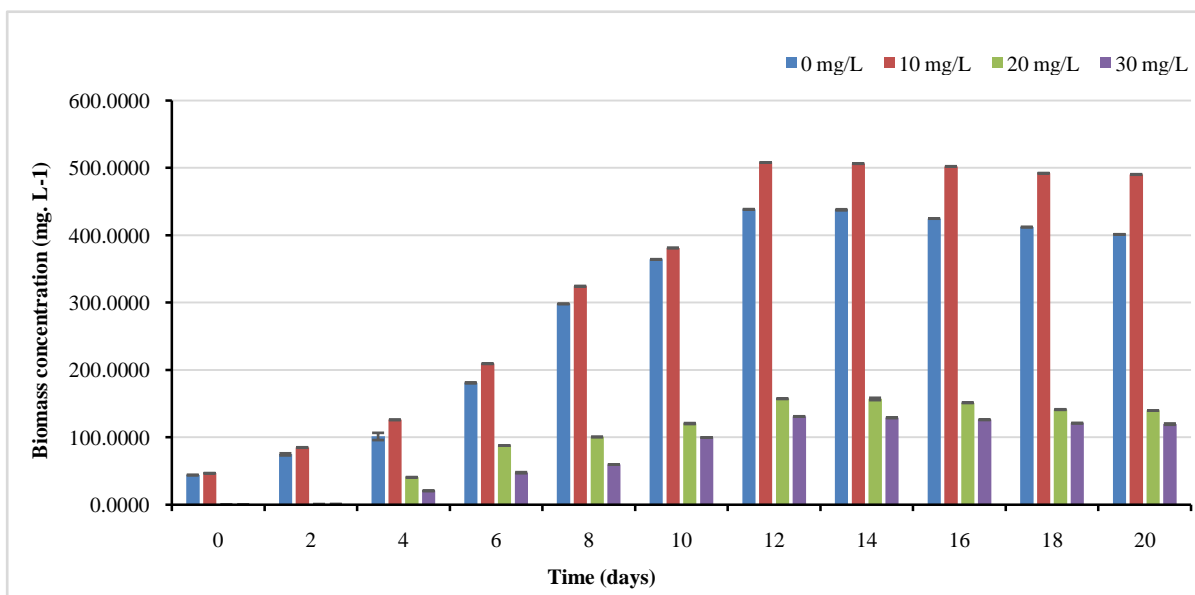


Figure 5 Graphical representation of biomass concentration on various IONPs concentration on *C. minutissima*

(Agilent Technologies Cary 60 UV-Vis). According to Figure 4, the optical density is at 0 mg. L<sup>-1</sup> observed 2.34 for *C. minutissima*. Further, the highest *C. minutissima* optical density of  $2.61 \pm 0.08$  was exhibited at a 10 mg·L<sup>-1</sup> IONPs dose, while 20 and 30 mg·L<sup>-1</sup> showed  $1.76 \pm 0.05$  and  $1.44 \pm 0.01$  on 14<sup>th</sup> day of inoculation respectively (Figure 4).

### 3.4.1 Estimation of biomass concentration on *C. minutissima*

After 20 days of the batch study, a gradual exponential growth phase extended until the 14<sup>th</sup> day (Figure 5). Biomass concentration was calculated based on the dry cell weight (DCW).

The highest biomass concentration ( $438.533 \pm 0.35$  mg. L<sup>-1</sup>) was reported for the control sample (0 mg. L<sup>-1</sup>).

### 3.4.2 Estimation of biomass concentration on *C. minutissima* on different concentrations of synthesized Fe<sub>2</sub>O<sub>3</sub>

The growth pattern of biomass for *C. minutissima* is illustrated in Figure 5. Until the 8<sup>th</sup> day, there were no significant changes reported in various concentrations of IONPs in the culture medium, and the highest concentration of 508.1 mg·L<sup>-1</sup> was reported in 10 mg·L<sup>-1</sup>. Whereas 157.53 and 131.3 mg. L<sup>-1</sup> recorded in 20 and 30 mg. L<sup>-1</sup> dose of IONPs

### 3.4.3 Estimation of Chlorophyll-a in *C. minutissima*

During the growth, chlorophyll-a content also increased in correspondence to optical density. The results of the study revealed a concentration of  $12.00 \pm 0.5689 \mu\text{g}\cdot\text{mL}^{-1}$  Chlorophyll-a in *C. minutissima* up to the 12<sup>th</sup> day. However, after the 12<sup>th</sup> day, chlorophyll-a concentration starts decreasing gradually (Figure 6).

### 3.4.4 Estimation of Chlorophyll-a in *C. minutissima* on different concentrations of synthesized $\text{Fe}_2\text{O}_3$

Exposure to various concentrations of IONPs ranging from 10 to 30  $\text{mg L}^{-1}$  resulted in different levels of Chlorophyll-a in *C. minutissima* cultures (Figure 6). Further, Chlorophyll-a concentration was higher ( $17.11 \pm 1.29 \mu\text{g}\cdot\text{mL}^{-1}$ ) at 10  $\text{mg L}^{-1}$  IONPs dose until the 12<sup>th</sup> day of cultivation while at 30 and 20  $\text{mg L}^{-1}$  dose of IONPs chl-a concentrations were 6.3 and 9.073

$\mu\text{g}\cdot\text{mL}^{-1}$ , respectively. However, impairment in chl-a concentration was noted at all IONPs doses starting on the 14<sup>th</sup> day.

### 3.4.5 Estimation of biomass productivity and yield on *C. minutissima*

Once inoculated into BG 11 media, *C. minutissima* exhibited exponential growth. The biomass productivity at 0  $\text{mg L}^{-1}$  was recorded  $26.66 \text{ mg}\cdot\text{L}^{-1}\cdot\text{d}^{-1}$  and the final biomass yield was recorded  $357.003 \text{ mg}\cdot\text{L}^{-1}$

### 3.4.6 Estimation of biomass productivity and yield on *C. minutissima* on different concentrations of synthesized $\text{Fe}_2\text{O}_3$

As shown in Figure 7, biomass productivity was recorded  $31.74 \text{ mg}\cdot\text{L}^{-1}\cdot\text{d}^{-1}$  at 10  $\text{mg L}^{-1}$  while 9.69 and 8.1  $\text{mg}\cdot\text{L}^{-1}\cdot\text{d}^{-1}$  was observed at 20 and 30  $\text{mg L}^{-1}$ , respectively. Similarly, At 10  $\text{mg}\cdot\text{L}^{-1}$  IONPs

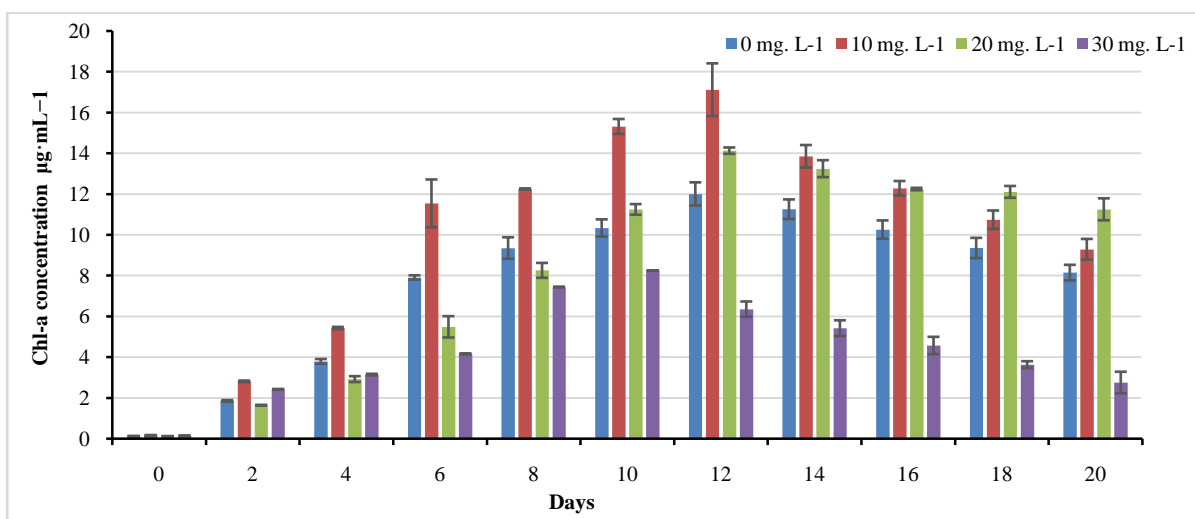


Figure 6 Graphical representation of Chl-a on various IONPs concentration on *C. minutissima*

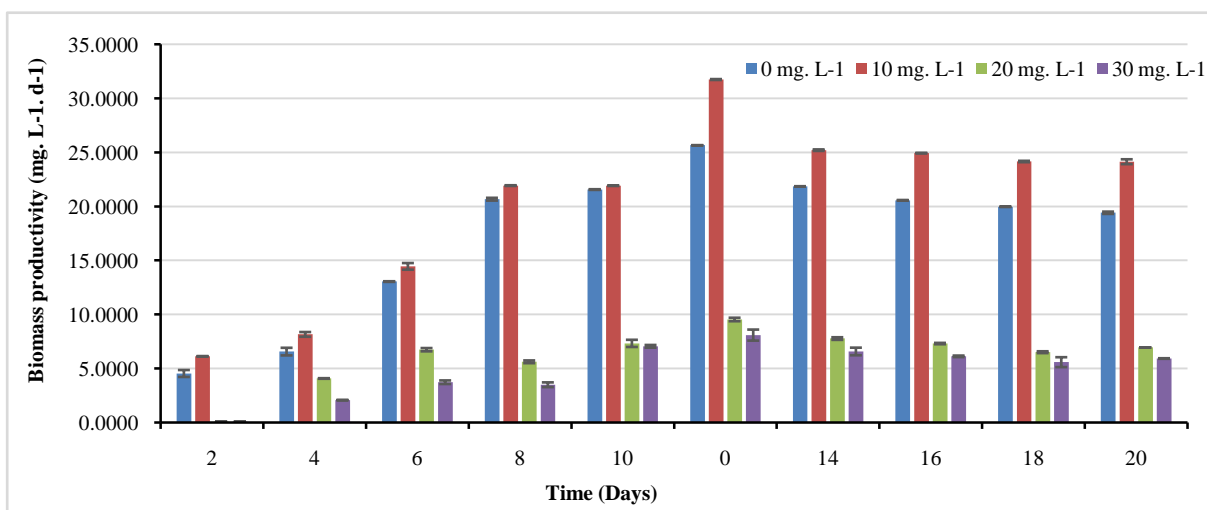


Figure 7 Graphical representation of biomass productivity on various IONPs concentrations on *C. minutissima*



dose, *C. minutissima* demonstrated the highest biomass yield of 443.167 mg.L<sup>-1</sup>, whereas at 20 mg.L<sup>-1</sup> and 30 mg.L<sup>-1</sup>, the yields were 139.86 mg.L<sup>-1</sup> and 119.75 mg.L<sup>-1</sup>, respectively. At 10 mg.L<sup>-1</sup> biomass yield is 24% higher in comparison to other doses.

### 3.5 Lipid productivity

In this study, the assessment of the total lipid content or productivity of *C. minutissima* was conducted following the harvesting process. Among the different doses of IONPs, the highest lipid production (29.52%) was reported at 10 mg.L<sup>-1</sup>, which was 28.52 % higher than control. The observed changes in growth and lipid production suggest the absorption of NPs and their potential effects. This phenomenon is intricately linked to the specific nanoparticles used and the choice of microalgal strain. The interaction between these factors plays a crucial role in shaping the outcomes, emphasizing the need for a detailed understanding of the interplay between IONPs, nanoparticles, and microalgal strains to optimize and tailor the effects for desired outcomes in applications such as biomass and lipid production.

#### 3.5.1 FTIR

The FTIR spectra of the microalgal oil are displayed in Figure 8. The region indicates the presence of lipids in the sample in

the spectra between 3100 and 2800 cm<sup>-1</sup>, which arises due to the vibrations of both symmetric and asymmetric stretching of the -CH<sub>2</sub>- groups. These -CH<sub>2</sub>- groups serve as the foundational structure of lipids and demonstrate absorption, especially at 2923 and 2865 cm<sup>-1</sup>. The algal oil's FTIR spectra revealed well-absorbed areas between 3500 and 3000 cm<sup>-1</sup>, 1747 and 1172 cm<sup>-1</sup>, and 800 and 700 cm<sup>-1</sup>. The regular peaks at 2923 and 2860 cm<sup>-1</sup> result from the -CH<sub>2</sub>- groups' symmetric and asymmetric stretching vibrations. The spectra of algal oil also showed peaks at 3005 cm<sup>-1</sup> from double bond stretching and 1300–1100 cm<sup>-1</sup> from the C–O bond (axial stretching). There were also observed absorption peaks at 722 cm<sup>-1</sup> attributed to the -CH<sub>2</sub>- bending out of the plane and at 1365–1377 and 1465 cm<sup>-1</sup> attributed to the -CH<sub>3</sub> bond. The existence of these peaks signifies the transformation of oil into biodiesel.

Table 1 compiles the different fuel qualities of *C. minutissima* biodiesel produced under ideal circumstances. The biodiesel showed a density of 0.86 g/cm<sup>3</sup>, a viscosity of 3.24 mm<sup>2</sup>/s and an iodine value of 124 g I<sub>2</sub>/100 g, which abided by the fuel standards. All the tested parameters were found to be closely aligned with the American Society for Testing and Materials (ASTM) D6751 and EN 14214 fuel standards, respectively.

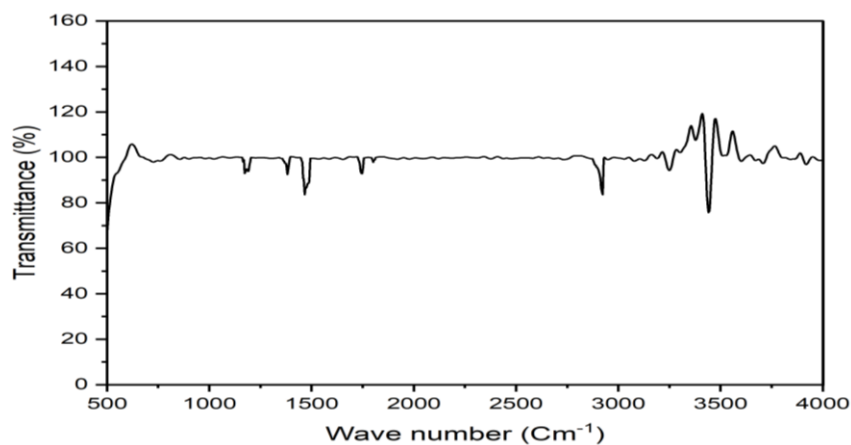


Figure 8 FTIR spectrum of *C. minutissima* algal oil

Table 1 Comparison of *C. minutissima* biodiesel with various biodiesel standards

Parameters	Present study	ASTM standards	EN 14214
Density (g cm <sup>-3</sup> )	0.86	-	0.86-0.90
Viscosity (mm <sup>2</sup> /s)	3.5	1.9-6.0	3.5-5.0
Calorific value (MJ Kg <sup>-1</sup> )	35.58	-	-
Iodine value (g I <sub>2</sub> /100 g)	124	-	<120
Cetane number	50.34	>47	>51
Degree of unsaturation (%)	70.15	-	-
Oxidative stability	6	-	>6

#### 4 Discussion

Fe<sub>2</sub>O<sub>3</sub> nanoparticles were chosen for the microalgae due to their demonstrated highest efficiency in harvesting in this research. Surface characterization was analyzed through XRD, as depicted in Figure 2. The pattern in the figure indicates the crystalline nature of Fe<sub>2</sub>O<sub>3</sub> nanoparticles. The observed peaks are corresponding to pure Fe<sub>2</sub>O<sub>3</sub> nanoparticles. The presence of narrow and sharp peaks suggests that the hematite products exhibit high crystallinity (Lassoued et al. 2017). The average grain size of the synthesized  $\alpha$ -Fe<sub>2</sub>O<sub>3</sub> was determined by SEM to be less than 100 nm. SEM analysis of the synthesized nanoparticles revealed the formation of spherical particles in shape and uniform distribution (Qayoom et al. 2020). Additionally, the elemental composition of Fe<sub>2</sub>O<sub>3</sub> nanoparticles was examined through energy dispersive spectroscopy, as depicted in Figure 3(b). The analysis revealed the presence of peaks corresponding to Fe and O, indicating the absence of impurities.

The addition of IONPs demonstrated positive outcomes regarding the growth, biomass concentration, biomass productivity and biomass yield of *C. minutissima*. According to the current findings, *C. minutissima* and NPs doses of 10, 20, and 30 mg·L<sup>-1</sup> were chosen for subsequent investigations and the growth of *C. minutissima* was analyzed at OD<sub>680</sub>. A similar result was reported by Attre et al. (2018), who cultured *C. minutissima* strain on glycine medium. Overall, the highest biomass concentration of 508.1 mg·L<sup>-1</sup> was achieved at 10 mg·L<sup>-1</sup>. In contrast, biomass concentrations for NPs doses of 20 and 30 mg·L<sup>-1</sup> were recorded as 157.33 ± 0.32 and 131.3 ± 0.26 mg·L<sup>-1</sup>, respectively. It was noted that in the low-concentration range of nanoparticles, the biomass of algal cells initially increased but then declined with higher concentrations of Fe<sub>3</sub>O<sub>4</sub> NPs (Wang et al. 2021). Results of Kaliampurthi et al. (2019) are contradictory to the findings of the present study, where no aggregation was reported at a lower concentration of 50 mg·L<sup>-1</sup> for ZnO nanoparticles, but higher microalgae accumulation was noted at 100 mg·L<sup>-1</sup> (Kaliampurthi et al. 2019). Further, carbon nanotubes inhibit cell growth in freshwater microalgae *Scenedesmus obliquus*, while nano Fe<sub>2</sub>O<sub>3</sub> promotes growth in the same species (He et al. 2017). Up to the 14<sup>th</sup> day, there was a notable distinction in biomass productivity among various doses of NPs. In the current study, biomass productivity is measured in the NP-treated samples, and higher biomass (31.74 mg·L<sup>-1</sup>·d<sup>-1</sup>) was observed at 10 mg·L<sup>-1</sup> IONPs, while at higher concentrations, it decreased. The biomass productivity, in the context of using MIL-100(Fe), a type of metal-organic framework incorporating iron, was measured in *Arthrospira* sp., and it was determined to be 0.61 g·L<sup>-1</sup> (Cheng et al. 2020). Biomass yield was 24.12% at 10 mg·L<sup>-1</sup>, which is higher than that of the control. The stimulation of algal proliferation may be linked to the dissociation of minute iron nanoparticles (Marsalek et al. 2012). Due to its association with the

photosynthetic electron transport chain, iron may be required for both growth and metabolic alterations, as suggested by the enhanced growth of microalgal biomass; this supports the hypothesis. However, the rise in NPs concentrations is adversely correlated with the notable reduction in growth. The growth of marine phytoplankton *Skeletonema costatum* and *Nitzschia closterium* is inhibited by metal salt (Cu<sup>2+</sup>), nano-metal (nano-Cu), and nano-metal oxide (nano-CuO). Cu<sup>2+</sup> and nano-Cu EC50 values, which range from 0.356 to 0.991 mg·L<sup>-1</sup> and 0.663 to 2.455 mg·L<sup>-1</sup>, have been shown to have an impact on the extracellular polymeric compounds and amino acids secreted by *S. costatum* and *N. closterium* microalgae (Huang et al. 2022). Further, Chl-a concentrations also decreased at all IONPs doses starting on the 14th day. The highest chl-a was recorded (17.11 ± 0.09 µg·mL<sup>-1</sup>) at 10 mg·L<sup>-1</sup>. Moreover, the concentration of 30 mg·L<sup>-1</sup> exhibited the lowest number of Chl-a. Studies have indicated that titanium oxide nanoparticles notably hindered the growth and biomass (including dry weight, chlorophyll A, and total chlorophyll) of *Chlorella vulgaris* due to their surface adsorption on the algal cell, which promotes growth inhibition (Roy et al. 2018). On the contrary, when Fe<sub>2</sub>WO<sub>6</sub> NPs inoculated at different concentrations in the culture medium of *Dunaliella salina*, the cell density, chlorophyll a and b, increased at lower 20 ppm concentrations (Hassanpour et al. 2020).

As per a recent study, in *Scenedesmus obliquus*, lower concentrations of CNTs and Fe<sub>2</sub>O<sub>3</sub> increased the chlorophyll content, while higher concentrations repressed photosynthesis (He et al. 2017). Iron is essential for photosynthesis, cell respiration, and the creation of phytohormones and chlorophyll (Zhao et al. 2024b). From the current observations, it was hypothesized that the lower dose of NPs functions as a source of iron for the growth of microalgae. In general, NPs demonstrated favourable effects on *C. minutissima*, leading to increased biomass growth and chlorophyll-a concentration at 10 mg·L<sup>-1</sup> NPs dose. In contrast, recent research signifies a significant advancement in the field. Cultivation of *C. minutissima* not only remained viable but also demonstrated an enhanced growth rate in NP-supplemented media. This opens up new possibilities for employing NPs in large-scale cultivation of targeted microalgae, leading to increased biomass production. The highest lipid production of 29.52% was observed at 10 mg·L<sup>-1</sup> NPs dose, which was 28.52 % higher than that of control (15.98%). The change in growth and lipid production is a sign of metal oxide absorption and its consequences. Using Carbon Nano Tubes, Fe<sub>2</sub>O<sub>3</sub>, and MgO nanoparticles, increases in lipid production were reported at 8.9%, 39.6%, and 18.5%, respectively (He et al. 2017). The treatment with 50 mg/L of ZnO-NP increased the synthesis of neutral lipids (6.08-fold) and triacylglycerol (8.21-fold) without causing complete growth inhibition (Kaliampurthi et al. 2019). The rise in lipid synthesis indicates a change in cellular metabolism. Likewise, Chandra et al. (2019) observed 37.24 mg·L<sup>-1</sup>·d<sup>-1</sup> a lipid content in *C.*

*minutissima* at a concentration of 50 mg. L<sup>-1</sup>. In contrast, a slight decrease in lipid (23.07 %) was also observed at NPs doses of 20 mg.L<sup>-1</sup>. At this concentration, the relatively low lipid percentage partially suggests the absorption of NPs and the generation of reactive oxygen species (Shi et al. 2017). Hence, the gradual uptake of NPs at an optimal dose could help balance oxidative stress and enhance lipid productivity. Previous research indicates that in cultures containing NPs, microalgal biomass typically has only a few nanoparticles adhering to the cell surface (Taghizadeh et al. 2022). Nanomaterials can stimulate the generation of reactive oxygen species (ROS), initiating the cellular mechanism of oxidative stress (Wang et al. 2021). However, a significant decline in biomass growth represents a considerable constraint in conditions of nutrient scarcity. However, the NPs that were examined for this study did not exhibit any restrictions on the growth of microalgae. Overall, 10 mg. L<sup>-1</sup> NPs dose was shown to be optimal for *C. minutissima* development and growth with improved lipid accumulation based on the acquired biomass potential and lipid yields. The region indicates the presence of lipids in the sample in the spectra between 3100 and 2800 cm<sup>-1</sup>, which is caused by the symmetric and asymmetric stretching vibrations of the symmetric CH<sub>2</sub> and asymmetric CH<sub>3</sub> and CH<sub>2</sub> stretching (Wallach et al. 1979). These -CH<sub>2</sub>- groups serve as the lipids' structural backbone and exhibit absorption, especially at 2923 and 2865 cm<sup>-1</sup> (Portaccio et al. 2023). The algal oil's FTIR spectra revealed well-absorbed areas between 3500 and 3000 cm<sup>-1</sup>, 1747 and 1172 cm<sup>-1</sup>, and 800 and 700 cm<sup>-1</sup>. The normal peaks at 2923 and 2860 cm<sup>-1</sup> result from the -CH<sub>2</sub>- groups' symmetric and asymmetric stretching vibrations (Arif et al. 2021). The spectra of algal oil also showed peaks at 3005 cm<sup>-1</sup> from double bond stretching and 1300–1100 cm<sup>-1</sup> from the C–O bond (axial stretching). There were also observed absorption peaks at 722 cm<sup>-1</sup> attributed to the -CH<sub>2</sub>- bending out of the plane and at 1365–1377 and 1465 cm<sup>-1</sup> attributed to the -CH<sub>3</sub> bond (Nematian et al. 2020). The existence of these peaks signifies the transformation of oil into biodiesel. The characteristics of biodiesel predominantly depend on its fatty acid esters (Mondal et al. 2021). In a study, Mallick et al. (2012) found that the calorific value of *C. minutissima* is comparable to *C. vulgaris*. Further, the Iodine value in *C. minutissima* shows a high oxidative value, which means the presence of a mixture of fatty acids; it is found within the range according to ASTM and EN 14214 (Thirugnanasambandham 2018). Density plays a significant role in airless combustion systems as it directly impacts the efficiency of fuel atomization. Density was recorded at 0.86 g cm<sup>-3</sup> in *C. minutissima*, which is also in synchronization with ASTM and EN standards. The above results show that *C. minutissima* fuel properties are aligned well with commercial biodiesel.

## Conclusion

The utilization of hematite (α-Fe<sub>2</sub>O<sub>3</sub>) nanoparticles demonstrates a promising approach to enhance lipid and biofuel productivity in microalgal cultivation. Characterization studies confirm the

suitability of these nanoparticles for the effective conversion of microalgal lipids into biodiesel. Particularly, at 10 mg.L<sup>-1</sup> concentration, iron oxide nanoparticles significantly boost biomass concentration and growth rates in *Chlorella minutissima* cultures. The findings highlight the feasibility of integrating hematite nanoparticles into microalgal media for sustainable biofuel production.

## References

- Aghabeigi, F., Nikkhah, H., Zilouei, H., & Bazarganipour, M. (2023). Immobilization of lipase on the graphene oxides magnetized with NiFe<sub>2</sub>O<sub>4</sub> nanoparticles for biodiesel production from microalgae lipids. *Process Biochemistry*, 126, 171–185. <https://doi.org/10.1016/j.procbio.2023.01.012>
- Al-Ansari, M. M., Al-Humaid, L., Al-Dahmash, N. D., & Aldawsari, M. (2023). Assessing the benefits of *Chlorella vulgaris* microalgal biodiesel for internal combustion engines: Energy and exergy analyses. *Fuel*, 344, 128055. <https://doi.org/10.1016/j.fuel.2023.128055>
- Arif, M., Li, Y., El-Dalatony, M. M., Zhang, C., Li, X., & Salama, E.S. (2021). A complete characterization of microalgal biomass through FTIR/TGA/CHNS analysis: An approach for biofuel generation and nutrients removal. *Renewable Energy*, 163, 1973–1982. <https://doi.org/10.1016/j.renene.2020.10.066>
- Attre, T., Roy, A., & Bharadvaja, N. (2018). Influence of various Carbon and Nitrogen sources on Lipid productivity of *Chlorella minutissima* and *Scenedesmus* sp. and their FAME analysis. *Journal of Algal Biomass Utilization*, 9(1): 72–85. [https://doi.org/10.1016/0304-4157\(79\)90001-14](https://doi.org/10.1016/0304-4157(79)90001-14)
- Banerjee, S., Rout, S., Banerjee, S., Atta, A., & Das, D. (2019). Fe<sub>2</sub>O<sub>3</sub> nanocatalyst aided transesterification for biodiesel production from lipid-intact wet microalgal biomass: A biorefinery approach. *Energy Conversion and Management*, 195, 844–853. <https://doi.org/10.1016/j.enconman.2019.05.060>
- Bligh, E. G., & Dyer, W. J. (1959). A rapid method of total lipid extraction and purification. *Canadian Journal of Biochemistry and Physiology*, 37(8), 911–917. <https://doi.org/10.1139/o59-099>
- Boopathi, M., Sathiskumar, S., Manideep, B., Jayakrishnan, S., Praveen, S. B., Gokul, V., Sakthi Ganesh, P., & Gokulraj, V. (2023). Experimental investigation on performance and emission characteristics of algae oil biodiesel with methanol additive in CI engine. *Materials Today: Proceedings*, S2214785323014529. <https://doi.org/10.1016/j.matpr.2023.03.405>
- Chandra, R., Amit, & Ghosh, U. K. (2019). Effects of various abiotic factors on biomass growth and lipid yield of *Chlorella minutissima* for sustainable biodiesel production. *Environmental*

- Science and Pollution Research*, 26(4), 3848–3861. <https://doi.org/10.1007/s11356-018-3696-1>
- Cheng, J., Zhu, Y., Li, K., Lu, H., & Shi, Z. (2020). Calcinated MIL-100(Fe) as a CO<sub>2</sub> adsorbent to promote biomass productivity of *Arthrospira platensis* cells. *Science of the Total Environment*, 699, 134375. <https://doi.org/10.1016/j.scitotenv.2019.134375>
- Da Silva Vaz, B., Alberto Vieira Costa, J., & Greque De Morais, M. (2020). Physical and biological fixation of CO<sub>2</sub> with polymeric nanofibers in outdoor cultivations of *Chlorella fusca* LEB 111. *International Journal of Biological Macromolecules*, 151, 1332–1339. <https://doi.org/10.1016/j.ijbiomac.2019.10.179>
- Ganesh Saratale, R., Ponnusamy, V. K., Jeyakumar, R. B., Sirohi, R., Piechota, G., et al. (2022). Microalgae cultivation strategies using cost-effective nutrient sources: Recent updates and progress towards biofuel production. *Bioresource Technology*, 361, 127691. <https://doi.org/10.1016/j.biortech.2022.127691>
- Geng, L., Zhou, W., Qu, X., Sa, R., Liang, J., Wang, X., & Sun, M. (2023). Iodine values, peroxide values and acid values of Bohai algae oil compared with other oils during the cooking. *Heliyon*, 9(4), e15088. <https://doi.org/10.1016/j.heliyon.2023.e15088>
- Hassanpour, M., Hosseini Tafreshi, S. A., Amiri, O., Hamadianian, M., & Salavati-Niasari, M. (2020). Toxic effects of Fe<sub>2</sub>WO<sub>6</sub> nanoparticles towards microalga *Dunaliella salina*: Sonochemical synthesis nanoparticles and investigate its impact on the growth. *Chemosphere*, 258, 127348. <https://doi.org/10.1016/j.chemosphere.2020.127348>
- He, M., Yan, Y., Pei, F., Wu, M., Gebreluel, T., Zou, S., & Wang, C. (2017). Improvement on lipid production by *Scenedesmus obliquus* triggered by low dose exposure to nanoparticles. *Scientific Reports*, 7(1), 15526. <https://doi.org/10.1038/s41598-017-15667-0>
- Huang, W., Zhou, Y., Zhao, T., Tan, L., & Wang, J. (2022). The effects of copper ions and copper nanomaterials on the output of amino acids from marine microalgae. *Environmental Science and Pollution Research*, 29(7), 9780–9791. <https://doi.org/10.1007/s11356-021-16347-3>
- Kadar, E., Rooks, P., Lakey, C., & White, D. A. (2012). The effect of engineered iron nanoparticles on growth and metabolic status of marine microalgae cultures. *Science of the Total Environment*, 439, 8–17. <https://doi.org/10.1016/j.scitotenv.2012.09.010>
- Kaliamurthi, S., Selvaraj, G., Cakmak, Z. E., Korkmaz, A. D., & Cakmak, T. (2019). The relationship between *Chlorella* sp. and zinc oxide nanoparticles: Changes in biochemical, oxygen evolution, and lipid production ability. *Process Biochemistry*, 85, 43–50. <https://doi.org/10.1016/j.procbio.2019.06.005>
- Kaushik, P., Garima, G., Abhishek Chauhan, A. C., & Pankaj Goyal, P. G. (2009). Screening of *Lyngbya majuscula* for potential antibacterial activity and HPTLC analysis of active methanolic extract. *Journal of Pure and Applied Microbiology*, 3 (1), 169–174.
- Khan, M. I., Shin, J. H., & Kim, J. D. (2018). The promising future of microalgae: Current status, challenges, and optimization of a sustainable and renewable industry for biofuels, feed, and other products. *Microbial Cell Factories*, 17(1), 36. <https://doi.org/10.1186/s12934-018-0879-x>
- Lassoued, A., Dkhil, B., Gadri, A., & Ammar, S. (2017). Control of the shape and size of iron oxide (A-Fe<sub>2</sub>O<sub>3</sub>) nanoparticles synthesized through the chemical precipitation method. *Results in Physics*, 7, 3007–3015. <https://doi.org/10.1016/j.rinp.2017.07.066>
- Lee, J.Y., Yoo, C., Jun, S.Y., Ahn, C.Y., & Oh, H.M. (2010). Comparison of several methods for effective lipid extraction from microalgae. *Bioresource Technology*, 101(1), S75–S77. <https://doi.org/10.1016/j.biortech.2009.03.058>
- Ma, X., Mi, Y., Zhao, C., & Wei, Q. (2022). A comprehensive review on carbon source effect of microalgae lipid accumulation for biofuel production. *Science of the Total Environment*, 806, 151387. <https://doi.org/10.1016/j.scitotenv.2021.151387>
- Mallick, N., Mandal, S., Singh, A. K., Bishai, M., & Dash, A. (2012). Green microalga *Chlorella vulgaris* as a potential feedstock for biodiesel. *Journal of Chemical Technology & Biotechnology*, 87(1), 137–145. <https://doi.org/10.1002/jctb.2694>
- Marsalek, B., Jancula, D., Marsalkova, E., Mashlan, M., Safarova, K., Tucek, J., & Zboril, R. (2012). Multimodal action and selective toxicity of zerovalent iron nanoparticles against cyanobacteria. *Environmental Science & Technology*, 46(4), 2316–2323. <https://doi.org/10.1021/es2031483>
- Mishra, S. R., Mohanty, M. K., Das, S. P., & Pattanaik, A. K. (2014). Optimization of base-catalyzed transesterification of *Simarouba glauca* oil for biodiesel production. *International Journal of Sustainable Energy*, 33(6), 1033–1040. <https://doi.org/10.1080/14786451.2013.796942>
- Mondal, M., Khan, A. A., & Halder, G. (2021). Estimation of biodiesel properties based on fatty acid profiles of *Chlamydomonas* sp. BTA 9032 and *Chlorella* sp. BTA 9031 obtained under mixotrophic cultivation conditions. *Biofuels*, 12(10), 1175–1181. <https://doi.org/10.1080/17597269.2019.1600453>
- Moschona, A., Spanou, A., Pavlidis, I. V., Karabelas, A. J., & Patsios, S. I. (2024). Optimization of Enzymatic Transesterification of Acid Oil for Biodiesel Production Using a Low-Cost Lipase: The Effect of Transesterification Conditions and

- the Synergy of Lipases with Different Regioselectivity. *Applied biochemistry and biotechnology*, 10.1007/s12010-024-04941-3.
- Muhammad, G., Alam, M. A., Mofijur, M., Jahirul, M. I., Lv, Y., Xiong, W., Ong, H. C., & Xu, J. (2021). Modern developmental aspects in the field of economical harvesting and biodiesel production from microalgae biomass. *Renewable and Sustainable Energy Reviews*, 135, 110209. <https://doi.org/10.1016/j.rser.2020.110209>
- Mykhaylenko, N. F., & Zolotareva, E. K. (2017). The effect of copper and selenium nanocarboxylates on biomass accumulation and photosynthetic energy transduction efficiency of the green algae *Clorella vulgaris*. *Nanoscale Research Letters*, 12(1), 147. <https://doi.org/10.1186/s11671-017-1914-2>
- Nematian, T., Salehi, Z., & Shakeri, A. (2020). Conversion of bio-oil extracted from *Chlorella vulgaris* micro algae to biodiesel via modified superparamagnetic nano-biocatalyst. *Renewable Energy*, 146, 1796–1804. <https://doi.org/10.1016/j.renene.2019.08.048>
- Pahariya, R., Chauhan, A., Ranjan, A., Basniwal, R. K., Upadhyay, S., Thakur, S. K., & Jindal, T. (2023). A critical review on the efficacy and mechanism of nanoparticle-based flocculants for biodiesel feedstock production from microalgae. *BioEnergy Research*, 17(2), 1065–1079. <https://doi.org/10.1007/s12155-023-10672-w>
- Paulson, E., & Jothibas, M. (2021). Significance of thermal interfacial in hematite (A-fe2o3) nanoparticles synthesized by sol-gel method and its characteristics properties. *Surfaces and Interfaces*, 26, 101432. <https://doi.org/10.1016/j.surfin.2021.101432>
- Porra, R. J., Thompson, W. A., & Kriedemann, P. E. (1989). Determination of accurate extinction coefficients and simultaneous equations for assaying chlorophylls a and b extracted with four different solvents: Verification of the concentration of chlorophyll standards by atomic absorption spectroscopy. *Biochimica et Biophysica Acta (BBA) - Bioenergetics*, 975(3), 384–394. [https://doi.org/10.1016/S0005-2728\(89\)80347-0](https://doi.org/10.1016/S0005-2728(89)80347-0)
- Portaccio, M., Famarzi, B., & Lepore, M. (2023). Probing biochemical differences in lipid components of human cells by means of atr-ftir spectroscopy. *Biophysica*, 3(3), 524–538. <https://doi.org/10.3390/biophysica3030035>
- Prabakaran, S., Manimaran, R., Mohanraj, T., & Ravikumar, M. (2021). Performance analysis and emission characteristics of VCR diesel engine fuelled with algae biodiesel blends. *Materials Today: Proceedings*, 45, 2784–2788. <https://doi.org/10.1016/j.matpr.2020.11.742>
- Qayoom, M., Shah, K. A., Pandit, A. H., Firdous, A., & Dar, G. N. (2020). Dielectric and electrical studies on iron oxide (A-fe2o3) nanoparticles synthesized by modified solution combustion reaction for microwave applications. *Journal of Electroceramics*, 45(1), 7–14. <https://doi.org/10.1007/s10832-020-00219-2>
- Rana, M. S., Bhushan, S., Sudhakar, D. R., & Prajapati, S. K. (2020). Effect of iron oxide nanoparticles on growth and biofuel potential of *Chlorella* spp. *Algal Research*, 49, 101942. <https://doi.org/10.1016/j.algal.2020.101942>
- Roy, B., Chandrasekaran, H., Palamadai Krishnan, S., Chandrasekaran, N., & Mukherjee, A. (2018). UVA pre-irradiation to P25 titanium dioxide nanoparticles enhanced its toxicity towards freshwater algae *Scenedesmus obliquus*. *Environmental Science and Pollution Research*, 25(17), 16729–16742. <https://doi.org/10.1007/s11356-018-1860-2>
- Saxena, P., Sangela, V., Ranjan, S., Dutta, V., Dasgupta, N., Phulwaria, M., Rathore, D. S., & Harish. (2020). Aquatic nanotoxicology: Impact of carbon nanomaterials on algal flora. *Energy, Ecology and Environment*, 5(4), 240–252. <https://doi.org/10.1007/s40974-020-00151-9>
- Shi, K., Gao, Z., Shi, T. Q., Song, P., Ren, L. J., Huang, H., & Ji, X. J. (2017). Reactive oxygen species-mediated cellular stress response and lipid accumulation in oleaginous microorganisms: the state of the art and future perspectives. *Frontiers in microbiology*, 8, 793.
- Sun, YP, Li, X., Cao, J., Zhang, W., & Wang, H. P. (2006). Characterization of zero-valent iron nanoparticles. *Advances in Colloid and Interface Science*, 120(1–3), 47–56. <https://doi.org/10.1016/j.cis.2006.03.001>
- Taghizadeh, S. M., Ebrahiminezhad, A., Raei, M. J., Ramezani, H., Berenjian, A., & Ghasemi, Y. (2022). A study of l-lysine-stabilized iron oxide nanoparticles (IONPs) on microalgae biofilm formation of *Chlorella vulgaris*. *Molecular Biotechnology*, 64(6), 702–710.
- Tesfa, B., Mishra, R., Zhang, C., Gu, F., & Ball, A. D. (2013). Combustion and performance characteristics of CI (Compression ignition) engine running with biodiesel. *Energy*, 51, 101–115. <https://doi.org/10.1016/j.energy.2013.01.010>
- Thirugnanasambandham, K. (2018). Biodiesel production from *Chlorella minutissima* microalgae: Kinetic and mathematical modeling. *Energy Sources, Part A: Recovery, Utilization, and Environmental Effects*, 40(12), 1461–1468. <https://doi.org/10.1080/15567036.2018.1477872>
- Vasistha, S., Khanra, A., Clifford, M., & Rai, M. P. (2021). Current advances in microalgae harvesting and lipid extraction processes



- for improved biodiesel production: A review. *Renewable and Sustainable Energy Reviews*, 137, 110498. <https://doi.org/10.1016/j.rser.2020.110498>
- Wallach, D. F. H., Verma, S. P., & Fookson, J. (1979). Application of laser raman and infrared spectroscopy to the analysis of Membrane structure. *Biochimica et Biophysica Acta (BBA) - Reviews on Biomembranes*, 559(2–3), 153–208. [https://doi.org/10.1016/0304-4157\(79\)90001-7](https://doi.org/10.1016/0304-4157(79)90001-7)
- Wang, F., Liu, T., Guan, W., Xu, L., Huo, S., Ma, A., Zhuang, G., & Terry, N. (2021). Development of a strategy for enhancing the biomass growth and lipid accumulation of *Chlorella* sp. Uj-3 using magnetic Fe<sub>3</sub>O<sub>4</sub> nanoparticles. *Nanomaterials*, 11(11), 2802. <https://doi.org/10.3390/nano11112802>
- Yaşar, F. (2020). Comparison of fuel properties of biodiesel fuels produced from different oils to determine the most suitable feedstock type. *Fuel*, 264, 116817.
- Zhao, Q., Han, F., You, Z., Huang, Y., She, X., Shi, X., & Han, P. (2024a). Evaluation of microalgae biodiesel for carbon neutrality based on the waste treatment by the autotrophic and heterotrophic combination. *Energy*, 291, 130314.
- Zhao, Y., Chen, Z., Li, W., Liu, F., Sun, L., Wu, M., Zhang, P., Hou, L., Li, M., & Xu, J. (2024b). Revealing the molecular basis regulating the iron deficiency response in quinoa seedlings by physio-biochemical and gene expression profiling analyses. *Plant and Soil*, 495(1–2), 77–97. <https://doi.org/10.1007/s11104-023-06094-4>



## Journal of Experimental Biology and Agricultural Sciences

<http://www.jebas.org>

ISSN No. 2320 – 8694

### Isolation and characterization of polygalacturonase producing thermophilic *Aspergillus niger* isolated from decayed tomato fruits

Gebiru Sinshaw<sup>1,5</sup> , Jeyaramraja P R<sup>2\*</sup> , Sasikumar J M<sup>3</sup> , Abate Ayele<sup>4,5</sup> 

<sup>1</sup>Department of Biotechnology, Debre Berhan University, Ethiopia

<sup>2</sup>PG and Research Department of Botany, PSG College of Arts & Science, Avinashi Road, Civil Aerodrome Post, Coimbatore - 641 014, Tamil Nadu, India

<sup>3</sup>Department of Microbiology, Karpagam Academy of Higher Education, Pollachi Main Road, Eachanari Post, Coimbatore - 641 021, Tamil Nadu, India

<sup>4</sup>Department of Biotechnology, Addis Ababa Science and Technology University, Addis Ababa, Ethiopia

<sup>5</sup>Center of Excellence for Biotechnology and Bioprocess, Addis Ababa Science and Technology University, Addis Ababa, Ethiopia

Received – May 17, 2024; Revision – June 23, 2024; Accepted – July 13, 2024

Available Online – July 15, 2024

DOI: [http://dx.doi.org/10.18006/2024.12\(3\).379.389](http://dx.doi.org/10.18006/2024.12(3).379.389)

#### KEYWORDS

*Aspergillus niger*

Column chromatography

Polygalacturonase

Solid-state fermentation

#### ABSTRACT

This study aimed to isolate a fungal strain capable of producing acidophilic and thermostable polygalacturonase. In this study, the fungal isolate was isolated from decaying tomatoes. Based on the colony characteristics, microscopic and morphological observations, the isolated fungal pathogen has been identified as *Aspergillus niger*. The isolated fungus was used in solid-state fermentation to produce an acidic polygalacturonase enzyme. The enzyme was then purified using ammonium sulphate precipitation and column chromatography, and its activity was assayed by measuring the releasing sugar group from citrus pectin using a 3, 5-dinitrosalicylic acid (DNSA) reagent assay. The crude extract obtained from solid-state fermentation had an activity of 94.6 U/mL. Ammonium sulphate precipitation increased the enzyme's specific activity from 6.89 U/mg to 12.42 U/mg. Sephadex G-200 was used to purify the enzyme 3.58 times, and its specific activity was determined to be 24.66 U/mg. The Sephacryl S-100 column achieved a final fold purification of 9.93 times and a specific activity of 68.41 U/mg. The purified enzyme performed best when polygalacturonic acid was used as a substrate. The enzyme's optimum temperature and pH were 55°C and 5, respectively. CaCl<sub>2</sub> was found to be the best chelating ion for the enzyme. This enzyme is recommended for use in a variety of industrial applications as the enzyme was found to be stable at acidic pH and high temperature.

\* Corresponding author

E-mail: [jeyaramrajapr@psgcas.ac.in](mailto:jeyaramrajapr@psgcas.ac.in) (Jeyaramraja P R)

Peer review under responsibility of Journal of Experimental Biology and Agricultural Sciences.

Production and Hosting by Horizon Publisher India [HPI]  
(<http://www.horizonpublisherindia.in/>).  
All rights reserved.

All the articles published by [Journal of Experimental Biology and Agricultural Sciences](#) are licensed under a [Creative Commons Attribution-NonCommercial 4.0 International License](#) Based on a work at [www.jebas.org](http://www.jebas.org).



## 1 Introduction

Enzymes are now the cornerstone of several industries worldwide, including pharmaceuticals, brewing, fabric, and most processed foods. As a result, the demand for enzymes has risen dramatically (Li et al. 2012; Cocok et al. 2017; Raveendran et al. 2018; Ramesh et al. 2020). Pectinases are a class of pectinolytic enzymes that catalyse the depolymerisation and degradation of pectinaceous materials using hydrolases, lyases (depolymerisation reaction), or esterases (de-esterification reaction) (Zhang et al. 2021). Pectinase can also hydrolyze the  $\alpha$ -1, 4 glycosidic linkages between galacturonic acid residues and sugar (Rahman et al. 2019). Polygalacturonases, pectin lyases, and pectin methyl esterases are enzymes that hydrolyze the glycosidic bonds in pectic substances (Jayani et al. 2010; Khatri et al. 2015; Wang et al. 2015). Polygalacturonase is a depolymerizing enzyme that catalyses the  $\alpha$ -1,4 glycosidic linkage in the pectin chain, resulting in galacturonic acid units (Ahmed et al. 2021). The biotechnological potential of polygalacturonase is expanding due to increasing applications in the food and feed industries. It belongs to the pectinase enzyme family, which accounts for 25% of all industrial enzymes worldwide (Munir et al. 2019). Polygalacturonases are the most exhaustively studied pectinolytic enzyme family (Jayani et al. 2005).

Microorganisms account for the majority of industrial demand for enzymes. Microorganisms are preferred in the industry for enzyme production due to their high growth capability, short life span, and ease of genetic manipulation (Haile and Ayele 2022). Microbial pectinolytic enzymes, produced mainly by fungi, are used in various large-scale industrial processes (Soares et al. 2012). Filamentous fungi are the primary sources of hydrolases because they produce multienzyme complexes composed of endo- and exo-enzymes that degrade polymers such as cellulose, hemicellulose, and pectin (Ramos-Ibarra et al. 2017). Commercial pectinases are primarily derived from *Aspergillus* (Ravi and Raghu 2017). *Aspergillus* sp. *pectinases* are widely used in industry because this strain has GRAS (Generally Recognized As Safe) status, which means that the metabolites produced by this strain can be used safely. This fungus produces pectinases such as polymethylgalacturonase, polygalacturonase, and pectin esterase (Reddy and Sreeramulu 2012). Adding commercial pectinolytic enzyme preparations greatly improves the juice yield (Ribeiro et al. 2010). Thermophilic fungi are eukaryotes that have an exceptional ability to grow at high temperatures of 50°-60°C and can survive in a wide range of extreme environments (Majumdar et al. 2018). Furthermore, the maximum activation temperature of fungi-produced polygalacturonase enzymes is between 35 and 60°C (Thakur et al. 2010; Anand et al. 2016).

The most common methods for producing enzymes are submerged and solid-state fermentation, but solid-state fermentation is more

productive than the others (Karimi et al. 2021). Solid-state fermentation has several advantages, such as high productivity, extended product stability, and low production costs (Yoon et al. 2014). Rice bran, sugar cane bagasse, orange bagasse, sugar beet pulp, wheat bran, and other food processing waste are all suitable substrates for pectinase production via solid-state fermentation (Alavi et al. 2020). The primary objective of this study was to identify an efficient fungal strain capable of producing polygalacturonase. To achieve this objective, comparatively less explored fruit sources such as tomatoes were investigated. Various endophytic and pathogenic fungi were reported to be present in tomato fruits (Paolo et al. 2018). Some endophytic fungi (Kaur et al. 2004) and pathogenic fungi (Samal et al. 2023) have been reported to produce a variety of industrially important enzymes. The diversity and interactions of endophytic and pathogenic fungi within tomato fruits present a fascinating area of research with the potential to uncover novel strategies for producing industrially important enzymes (Ikram et al. 2020). This study aimed to isolate and characterize the polygalacturonase-isolated enzyme from the thermophilic *Aspergillus niger* fungal pathogen found in decayed tomato fruits.

## 2 Materials And Methods

### 2.1 Sample collection

The ripened fruits of tomatoes were collected from a local fruit market in Ethiopia. These ripened fruits were transferred to the laboratory in sterilized polythene bags for further processing. These fruits were allowed to decay in the laboratory (Figure 1).



Figure 1 Decayed tomato fruits used in this study

### 2.2 Isolation of fungi and primary screening

The fruit samples were immersed in sterilised distilled water to prepare a stock solution. Each stock was serially diluted twice and aseptically poured into plates containing mineral salt agar media (0.2g NaNO<sub>3</sub>, 0.05g KCl, 0.05g MgSO<sub>4</sub>, 0.02g K<sub>2</sub>HPO<sub>4</sub>, 0.01g FeSO<sub>4</sub>, 1g pectin, and 2g agar/100mL). Plates were incubated at 50°C for five to seven days. Following incubation, plates were poured with a potassium iodide-iodine solution (1.5g potassium

iodide and 0.3g iodine/100mL) to examine the pectin lysis zones on plates for primary screening of fungal isolates with minor modifications (Munir et al. 2019).

### 2.3 Secondary screening

Solid-state fermentation was used for secondary screening for polygalacturonase estimation. Bagasse from sugarcane was extracted and dried to make powder. This powdered extract was then used as a carbon source in a fermentation medium prepared according to Acuña-Argüelles et al. (1995). The fermentation medium (250 ml) was inoculated aseptically with spore inoculum (2 ml). The inoculated fermentation medium was incubated at 50°C for 4-5 days. Furthermore, the fermented media was extracted with 30 mL of distilled water. The flasks were vigorously shaken for 1 hour before being filtered through cheesecloth. The crude enzyme was extracted by adding 100 mL of citrate buffer to each flask (0.1 M, pH 5.0). The extract was centrifuged at 4°C for 15 min at 10,000 rpm, and the supernatant was sieved using Whatman No. 1 filter paper to remove all spores. The obtained supernatant (crude enzyme) was used to estimate polygalacturonase activity as per the method of Adedayo et al. (2021).

### 2.4 Identification of polygalacturonase-producing isolate

The fungus with the highest polygalacturonic acid hydrolysis value was identified by observing hyphal characteristics colony characteristics such as colour, texture, and spore structure following the methodology of Shamly et al. (2014). The conventional lactophenol cotton blue technique (LPCB) was used to study the fungal morphology.

### 2.5 Enzyme Purification

The culture filtrate was centrifuged at 10,000 rpm for 20 minutes at room temperature. The salting-out procedure was carried out following the method of Siddiqui et al. (2012). To achieve 20% saturation, solid ammonium sulphate was added slowly to the crude enzyme preparation in an ice bath with continuous stirring and then stored overnight at 4°C. The precipitated protein was removed by centrifugation at 4°C for 30 minutes at 10,000 rpm. After that, ammonium sulphate was added to the supernatant to reach 80% saturation. Again, centrifugation at 4°C for 30 min at 10,000 rpm separated the precipitated protein, which was then dissolved in sodium acetate buffer (0.1 M; pH 5.0). The crude enzyme was then loaded onto a Sephadex G-200 (150 cm) column pre-equilibrated with sodium acetate buffer (0.1 M; pH 5.0). At a flow rate of 24 ml/h, 3 mL volume fractions were collected. The eluted fractions were monitored using a spectrophotometer at 280 nm for protein and enzyme activity. The fractions with the highest polygalacturonase activity were loaded onto pre-equilibrated

Sephacryl S-100 columns (1.6 cm X 60 cm) at a flow rate of 20 ml/h. Fractions (1.5 ml) were collected and examined regularly for protein and polygalacturonase activity.

### 2.6 Enzyme assay

Polygalacturonase activity was determined by measuring the releasing sugar group from citrus pectin using DNSA reagent assay, according to Adedayo et al. (2021). In a test tube, 2 ml of crude enzyme and 2 ml of citrus pectin were mixed in phosphate buffer and incubated at 50°C for 30 minutes. After incubation, the mixture was filtered, and 2 mL of DNSA reagent was added to 2 mL of the filtrate to stop the reaction and the mixture was kept in a boiling water bath at 100°C for 10 minutes until yellow colour developed. The tubes were then cooled with running water. A spectrophotometer was used to measure the optical density of the resulting coloured solution at 540 nm. The amount of enzyme that released 1 mol of galacturonic acid per minute was defined as one unit of pectinase activity (U).

### 2.7 Protein estimation

The protein concentration was determined as described by Lowry et al. (1951) using bovine serum albumin (BSA) as standard, and absorbance was read at 660 nm using a UV-Vis spectrophotometer.

### 2.8 Characterization of the enzyme

#### 2.8.1 Substrate specificity

Purified polygalacturonase was evaluated for substrate specificity against polygalacturonic acid, pectin, xylan, galactose, and cellulose at 0.1% (w/v) (Thakur et al. 2010). The substrates were incubated with the purified enzyme for 4 hours in 50 mM citrate buffer (pH 4.4). Polygalacturonase activity was determined for each substrate, with pectin serving as control.

#### 2.8.2 Effect of temperature

The enzyme activity was determined by incubating the reaction mixture (as described in the enzyme assay method) at different temperatures from 30 to 60°C. The optimum temperature for polygalacturonase activity was calculated by plotting enzyme activity against temperatures.

#### 2.8.3 Effect of pH

The effect of reaction pH on polygalacturonase activity was assessed using citrate buffer (pH 2.0–4.0) and potassium-phosphate buffer (pH 5.0–8.0) following the method of Bentouhami et al. (2024). The reaction mixture was incubated for 4 hr at 50°C. Finally, the enzyme activity was determined to evaluate its stability in varying ionic strengths.

### 2.8.4 Effect of divalent cations on enzyme activity

The divalent cations tested include  $\text{CaCl}_2$ ,  $\text{MgCl}_2$ ,  $\text{MnSO}_4$ , and  $\text{FeCl}_2$ . To study the effect of various divalent cations on enzyme activity, 2 ml of crude enzyme and 2 ml of citrus pectin were mixed in phosphate buffer containing divalent cations to a final concentration of 10 mM and incubated at 50°C for 30 minutes. After incubation, the mixture was filtered, and 2 mL of DNSA reagent was added to 2 mL of the filtrate to stop the reaction. The remaining steps were performed as given in section 2.6.

### 2.9 Statistical analysis

The experiments were conducted following a completely randomized block design. Each experiment was repeated three times to get triplicate data subjected to statistical analysis using the SPSS tool to compute mean and standard error (SE) values.

## 3 Results and Discussion

### 3.1 Isolation of fungi producing polygalacturonase

Fungi secrete various enzymes that can degrade complex plant-derived polysaccharides, such as cellulose and pectin (Badhan et al. 2018). Among the pectinolytic enzymes, polygalacturonase plays a crucial role in the degradation of polygalacturonic acid, the main component of pectin (Pedrolli et al. 2009). The activity of polygalacturonase can lead to the formation of clear zones in nutrient media, a widely used phenotypic characteristic for identifying and screening fungal isolates (Balabanova et al. 2018). The present study isolated twenty-five fungal strains from infected tomato fruits. Pure cultures of isolated fungal strains were sub-cultured onto pectin agar media and kept for enzymatic studies and identification. Among these twenty-five pure cultured fungal strains, ten strains that were able to grow on a medium containing polygalacturonic acid as the sole carbon source were isolated. At pH 5.6, these ten strains were tested for polygalacturonic acid hydrolysis using a plate assay. Polygalacturonase activity of a strain was indicated by a clear zone in the media (Figure 2). When a fungal strain presented at least 23 mm clear zones around colonies, the strains were classified as very good producers of pectin depolymerizing enzymes, while if the zones were at least of

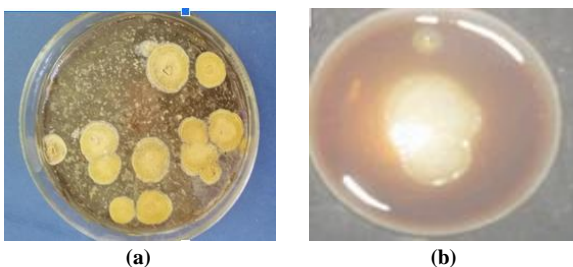


Figure 2 (a) Fungal isolate culture, (b) Secondary screening for potential fungal isolate (Zone of polygalacturonic acid hydrolysis).

Table 1 Polygalacturonase activity of different isolated fungal strains

S.N.	Polygalacturonase isolates	Zone of Inhibition in mm
1.	AT <sub>1</sub>	20
2.	AT <sub>3</sub>	23
3.	AT <sub>5</sub>	19
4.	AT <sub>7</sub>	17
5.	AT <sub>11</sub>	21
6.	AT <sub>14</sub>	25
7.	AT <sub>16</sub>	30
8.	AT <sub>20</sub>	20
9.	AT <sub>22</sub>	15
10.	AT <sub>24</sub>	18

18 mm and 15 mm these strains were considered as good producers and weak producers, respectively. Finally, the strain was considered poor producers when no polygalacturonase activity and clear zones were observed (Table 1). The strain with the most extensive zone (approximately 30 mm) was used for further parameter evaluation and to produce enzymes in liquid media.

### 3.2 Secondary screening

Solid-state fermentation has emerged as a promising approach for producing various enzymes, including polygalacturonase, a key enzyme involved in pectin degradation (Madamwar et al. 1989). Sugarcane bagasse, a readily available agricultural waste, has been extensively investigated as a carbon-rich substrate for solid-state fermentation due to its lignocellulosic composition (Garcia et al. 2018; Lamounier et al. 2018). The present study aims to explore the potential of utilizing sugarcane bagasse as a renewable and cost-effective carbon source for producing polygalacturonase by fungi in a solid-state fermentation system. The secondary screening was performed on the selected pectinolytic fungal strains AT<sub>3</sub>, 14, and 16 (Table 2). Among these, a fungal strain AT<sub>16</sub> isolated from the tomato samples collected from Arba Minch had the highest polygalacturonase production ( $25.67 \pm 0.10$  U/ml/min) and protein content (13.74 mg/ml), with production carried out using sugarcane bagasse dried powder as substrate.

Table 2 Secondary screening of polygalacturonase fungal isolates for polygalacturonase production

S.N.	Polygalacturonase isolates	Polygalacturonase activity (U/ml/Min)
1	AT <sub>3</sub>	$19.83 \pm 0.18$
2	AT <sub>14</sub>	$16.57 \pm 0.36$
3	AT <sub>16</sub>	$25.67 \pm 0.10$

Values are mean of triplicates followed by  $\pm$ SE



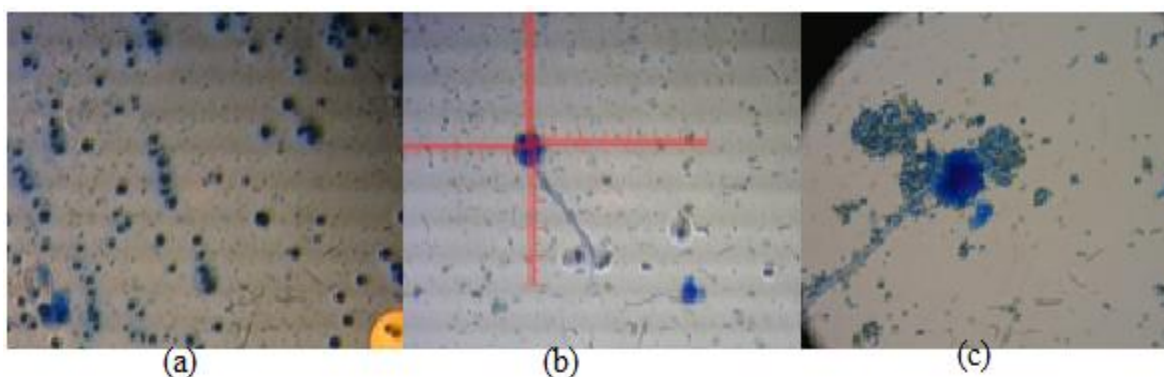


Figure 3 (a) Heavy sporulation of Isolate *Aspergillus niger* (b) Septate and hyaline hyphae of Isolate *Aspergillus niger* and (c) conidial head of Isolate *Aspergillus niger*

### 3.3 Identification of isolate

Isolated fungus strain was identified as *Aspergillus niger* based on morphological observation, cultural, hyphal characteristics and sporulation (Figure 3). This fungus was chosen for further investigation. Initially, the colonies were made up of a compact yellow felt, which later turned brown due to the conidiophores production, which is a characteristic of *A. niger* (Raper and Fennell 1965). The reverse side of the plate ranges from cream to yellow, which aligns with descriptions in the literature (Samson et al. 2010). The hyphal characteristics, including septate and hyaline hyphae, along with the conidial heads that radiate with heavy sporulation, are key identifying features of *A. niger* (Klich 2002). The absence of a teleomorph stage further supports the identification, as *A. niger* is typically known for its asexual reproduction (Gams et al. 1986). The conidia being globose to sub-globose is another hallmark trait corroborating the identification (Pitt and Hocking 2009).

### 3.4 Production of polygalacturonase

In the crude extract (150 ml) obtained using solid-state fermentation involving AT3, AT14, and AT16 strains, the protein content and polygalacturonase enzyme activity were found to be 13.74 mg/ml and 94.6 U/ml, respectively. Hence, the specific activity was 6.89 U/mg. The polygalacturonase activity recorded in the present study was higher than that reported by Alves et al. (2002) in the case of *Mucor genevensis* (5 U/ml) and Thakur et al. (2010) in *M. circinelloides* (9.15 U/ml), while the present study

polygalacturonase activity was lower than the value reported by Gomes et al. (2009) in case of *Penicillium viridicatum* where the activity recorded, was 18 U/ml.

### 3.5 Enzyme purification

Polygalacturonase from the screened *A. niger* was purified from 150 mL of crude extract obtained from solid-state fermentation (Table 3). The polygalacturonase enzyme was initially purified by the salting out procedure, which involves the addition of up to 80% solid ammonium sulphate. Ammonium sulphate precipitation increased the enzyme's specific activity from 6.89 U/mg to 12.42 U/mg. Polygalacturonase can be precipitated with 0 - 90% ammonium sulphate, depending on the source of the enzyme (Buga et al. 2010; Chinedu et al. 2016). Sephadex G-200 column chromatography helped purify the enzyme 3.58 times, resulting in a specific activity of 24.66 U/mg. Finally, Sephacryl S-100 column chromatography increased the specific activity to 68.41 U/mg, which, compared to that of crude extract, was 9.93 times higher. The yield of the enzyme decreased as the purification fold increased.

Previous researchers have found significant variations in the purification fold and yield of polygalacturonase enzymes from various microbial sources. Cheng et al. (2016) isolated an acid-stable endo-polygalacturonase from *P. oxalicum* CZ1028. The purification process involved ammonium sulfate precipitation, hydrophobic interaction chromatography, anion exchange chromatography, and size exclusion chromatography. This resulted

Table 3 Purification of polygalacturonase from *A. niger*

Purification steps	Collected Volume (mL)	Total protein (mg/mL)	Total enzyme Activity (U/mL)	Specific Activity (U/mg)	Purification fold	Yield (%)
Crude extract	150	13.74	94.6	6.89	1	100
(NH <sub>4</sub> ) <sub>2</sub> SO <sub>4</sub> precipitation	80	2.93	36.4	12.42	1.8	38.48
SephadexG-200	12	1.16	28.6	24.66	3.58	30.23
Sephacryl S-100	1	0.29	19.84	68.41	9.93	20.97

in the enzyme purifying 29.9 times, achieving a specific activity of 2320 U/mg, with a final yield of 17.1%. Anand et al. (2016) purified polygalacturonase from *A. fumigatus* MTCC 2584 using acetone precipitation and Sephadex G-100 column, which resulted in 18.43 fold increase in enzyme purity, with a specific activity of 38.9 U/mg. Satapathy et al. (2021) extracted pectinase from *A. parvisclerotigenus* KX928754 using apple pomace as the substrate. The crude filtrate underwent ammonium sulfate precipitation, dialysis, and elution on a Sephadex G-100 column. As a result, the enzyme was purified 2.10-fold, with a yield rate of 2.91% and a specific activity of 1081.66 U/mg. Almowallad et al. (2022) partially purified exo-polygalacturonase from *P. oxalicum* AUMC 4153 using sugar beet manufacturing waste as the sole carbon source. The enzyme purification process included ammonium sulfate precipitation, acetone precipitation, and gel filtration chromatography. This resulted in a 28-fold increase in enzyme purity, with a final yield of 57%.

### 3.6 Characterization of the enzyme

#### 3.6.1 Effect of temperature on the activity of polygalacturonase

Temperature is a critical factor in both microbial growth and product formation. The incubation temperature significantly impacts microbial growth rate, enzyme secretion, enzyme inhibition, and protein denaturation (Adeyefa and Ebuehi 2020). The effect of reaction temperature on polygalacturonase activity is depicted in Figure 4. Enzyme activity was detected at temperatures ranging from 30 to 60°C, with 55°C being the optimal temperature, followed by 50°C and 45°C. This finding demonstrated that polygalacturonase

activity increased with increasing temperature until the optimal temperature was reached. However, polygalacturonase activity dropped dramatically above 55°C. The present study results align with those that Kaur et al. (2004) revealed, who found that exo-polygalacturonase produced from thermophilic mould *Sporotrichum thermophile* was optimally active at 55 °C. The decrease in enzyme activity at very high temperatures is attributed to the denaturation of the enzymes (Almowallad et al. 2022).

#### 3.6.2 Effect of various substrates on the activity of polygalacturonase

The purified enzyme's affinity for different substrates was determined (Figure 5). The best substrates were polygalacturonic acid, pectin, cellulose, xylan, and galactose. Siddiqui et al. (2012) observed a maximal enzyme activity of 8.34 U/ml when polygalacturonic acid was used as a substrate. In the present study, the substrate polygalacturonic acid led to a maximum enzyme activity of 10.1 U/ml.

#### 3.6.3 Effect of pH on the activity of polygalacturonase

The initial pH of the fermentation medium is critical in determining metabolite synthesis levels. The stability of the microbial metabolite is also affected by the medium's hydrogen ion concentration (Adeyefa and Ebuehi 2020). pH is important in polygalacturonase because it promotes and regulates extracellular enzyme synthesis by microorganisms, particularly fungi (Siddiqui et al. 2012). Fungi, particularly *Aspergillus* species, have been shown to thrive in acidic or slightly alkaline environments (Ahmed Olaitan 2019). The present

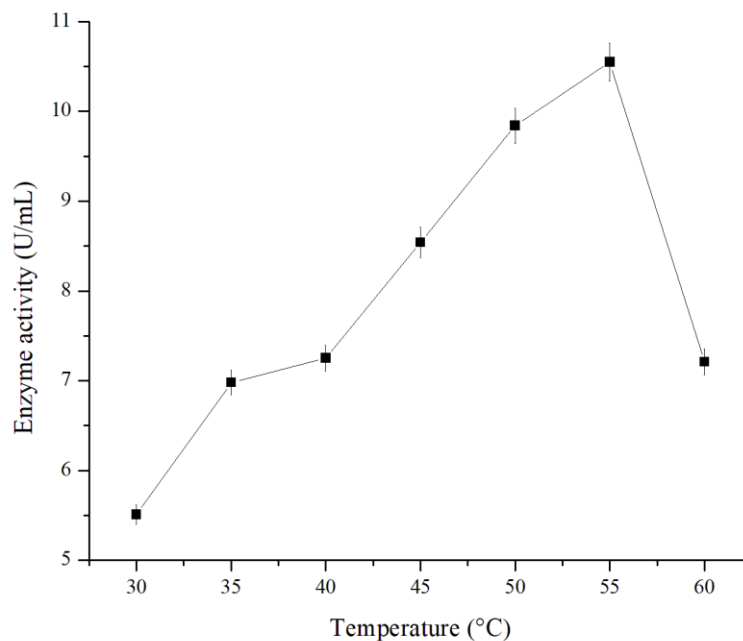


Figure 4 Effect of temperature on polygalacturonase activity from *Aspergillus niger*; values are mean of triplicates; error bar indicates  $\pm$ SE.

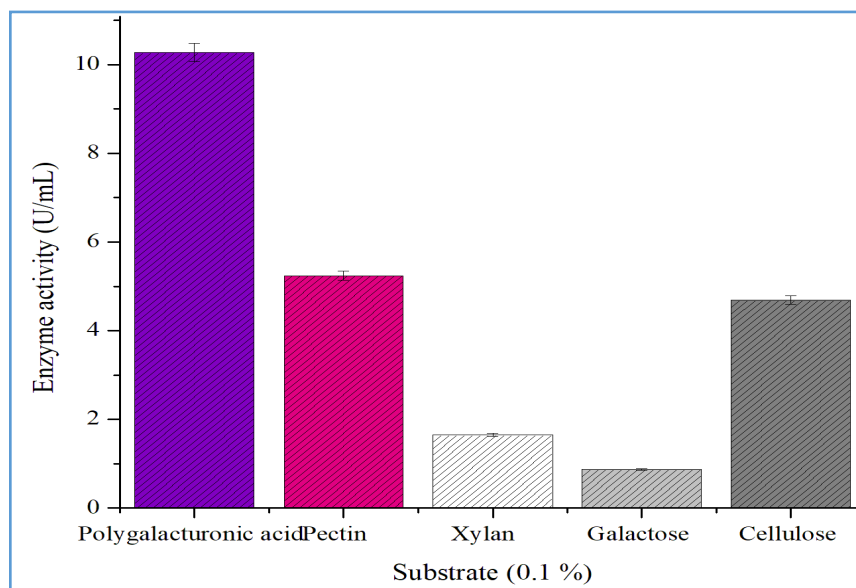


Figure 5 Substrate specificity of polygalacturonase from *Aspergillus niger*; values are mean of triplicates; error bar indicates  $\pm$ SE.

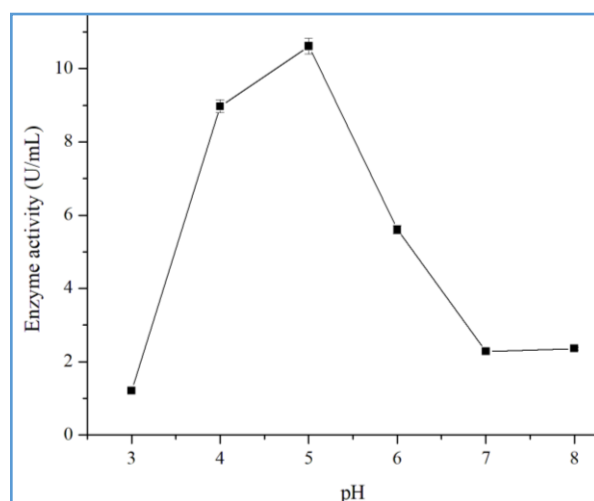


Figure 6 Effect of pH on polygalacturonase activity from *Aspergillus niger*; values are mean of triplicates; error bar indicates  $\pm$ SE.

study found that pH 5 was the optimum for polygalacturonase activity (100% relative activity) produced by *A. niger* (Figure 6). The results agreed with Aminzadeh et al. (2007), who found that polygalacturonase from *Tetracoccusporium* sp. was more active at an acidic pH of 5. Similar observations were reported about the optimum pH for polygalacturonase from *A. fumigatus* (Wang et al. 2015), *P. oxalicum* CZ102 (Cheng et al. 2016), *Thermoascus aurantiacus* (Martins et al. 2012), *P. oxalicum* AUMC 4153 (Almowallad et al. 2022) and *A. tubingensis* (Tai et al. 2013).

### 3.6.4 Effect of divalent cations on enzyme activity

The effects of different metal ions on enzymatic activity were studied using a concentration of 10 mM of each metal ion in the

reaction solution (Figure 7). Among all the divalent cations,  $\text{Ca}^{2+}$  was the optimum for the maximal polygalacturonase activity. On the contrary,  $\text{Zn}^{2+}$  inhibited the enzyme activity. The mechanism behind the increased activity of fungal polygalacturonases in the presence of certain divalent cations is not fully understood, but it is believed to involve several factors. First, divalent cations may help stabilize the enzyme structure, increasing catalytic efficiency (Pedrolli et al. 2009). Additionally, these cations may facilitate the interaction between the enzyme and the pectin substrate, a complex polysaccharide composed of galacturonic acid residues (Balabanova et al. 2018). Furthermore, divalent cations can influence the charge and conformation of the pectin substrate, making it more accessible to the polygalacturonase enzyme (Oumer 2017).

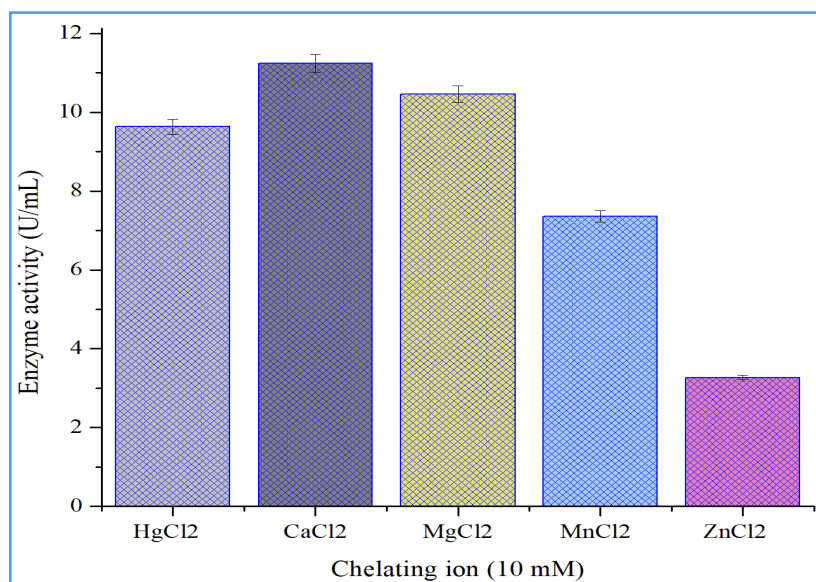


Figure 7 Effect of divalent cations on enzyme activity; values are mean of triplicates; error bar indicates  $\pm$ SE.

## Conclusion

Polygalacturonases are important members of the pectinase enzyme family and have significant biotechnological and commercial potential. In the current study, polygalacturonase was purified from *A. niger* 9.93 times by ammonium sulphate precipitation and column chromatography, resulting in specific activity of 68.41 U/mg protein. The purified polygalacturonase was naturally acidic, with an optimum pH of 5.0. The optimal temperature for maximum enzyme activity was 55°C, indicating that the enzyme is resistant to heat. CaCl<sub>2</sub> was revealed to be the most effective chelating ion for the enzyme. The homogeneity of the enzyme will be investigated using SDS PAGE shortly. Fungi typically produce polygalacturonase, which is essential for producing organic vegetable oil and fruit juice and being used to manufacture easily digestible animal feed.

## Funding

The authors declare that no funds were received for this study.

## Competing interests

The authors have no relevant financial or non-financial interests to disclose.

## Data statement

Data will be made available on reasonable request.

## Authors' contribution

Gebiru S conceived the idea and performed the isolation of fungi, solid state fermentation, and enzyme purification. Jeyaramraja P R

supervised the entire work. Sasikumar J M contributed in manuscript drafting. Abate Ayele performed enzyme assays. All authors have read and approved the final manuscript for publication.

## References

- Acuña-Argüelles, M. E., Gutiérrez-Rojas, M., Viniegra-González, G., & Favela-Torres, E. (1995). Production and properties of three pectinolytic activities produced by *Aspergillus niger* in submerged and solid-state fermentation. *Applied Microbiology and Biotechnology*, 43(5), 808–814. <https://doi.org/10.1007/BF02431912>
- Adedayo, M. R., Mohammed, M. T., Ajiboye, A. E., & Abdulmumini, S. A. (2021). Pectinolytic activity of *Aspergillus niger* and *Aspergillus flavus* grown on grapefruit (citrus Parasidis) peel in solid state fermentation. *Global Journal of Pure and Applied Sciences*, 27(2), 93–105. <https://doi.org/10.4314/gjpas.v27i2.2>
- Adeyefa, O., & Ebuehi, O. (2020). Isolation, Identification and Characterization of Pectinase Producers from Agro Wastes (*Citrus sinensis* and *Ananas comosus*). *World Journal of Agriculture and Soil Science*, 4(3). <https://doi.org/10.33552/WJASS.2020.04.000589>
- Ahmed, J., Thakur, A., & Goyal, A. (2021). Emerging trends on the role of recombinant pectinolytic enzymes in industries- an overview. *Biocatalysis and Agricultural Biotechnology*, 38, 102200. <https://doi.org/10.1016/j.bcab.2021.102200>
- Ahmed Olaitan, Y. (2019). *Characterization and Partial Purification of Pectinase Produced by Aspergillus niger Using Banana Peel as Carbon Source* [Kwara State University]. Retrieved from <https://www.proquest.com/openview/474b6ae1c0692a0a4f9d6ecdae26e885/1?pq-origsite=gscholar&cbl=18750&diss=y>

- Alavi, A., Nia, F. T., & Shariati, F. P. (2020). Polygalacturonase Production by *Aspergillus niger* Solid State Fermentation on Barley Bran and Sugar Beet Pulp Mixture. *Advanced Journal of Chemistry-Section A*, 3(3), 350–357. <https://doi.org/10.33945/SAMI/AJCA.2020.3.13>
- Almowallad, S. A., Alshammari, G. M., Alsayadi, M. M., Aljafer, N., Al-Sanea, E. A., Yahya, M. A., & Al-Harbi, L. N. (2022). Partial Purification and Characterization of Exo-Polygalacturonase Produced by *Penicillium oxalicum* AUMC 4153. *Life*, 12(2), 284. <https://doi.org/10.3390/life12020284>
- Alves, M. H., Campos-Takaki, G. M., Porto, A. L. F., & Milanez, A. I. (2002). Screening of *Mucor* spp. For the production of amylase, lipase, polygalacturonase and protease. *Brazilian Journal of Microbiology*, 33(4). <https://doi.org/10.1590/S1517-83822002000400009>
- Aminzadeh, S., Naderimanesh, H., Khajeh, K., & Sooudi, M. (2007). Isolation and Characterization of Polygalacturonase produced by *Tetracosporium* Sp. *Iranian Journal of Chemistry and Chemical Engineering*, 26(1), 47–54.
- Anand, G., Yadav, S., & Yadav, D. (2016). Purification and characterization of polygalacturonase from *Aspergillus fumigatus* MTCC 2584 and elucidating its application in retting of *Crotalaria juncea* fiber. *3 Biotech*, 6(2), 201. <https://doi.org/10.1007/s13205-016-0517-4>
- Badhan, A., Huang, J., Wang, Y., Abbott, D. W., Di Falco, M., Tsang, A., & McAllister, T. (2018). Saccharification efficiencies of multienzyme complexes produced by aerobic fungi. *New Biotechnology*, 46, 1–6. <https://doi.org/10.1016/j.nbt.2018.05.003>
- Balabanova, L., Slepchenko, L., Son, O., & Tekutyeva, L. (2018). Biotechnology Potential of Marine Fungi Degrading Plant and Algae Polymeric Substrates. *Frontiers in Microbiology*, 9, 1527. <https://doi.org/10.3389/fmicb.2018.01527>
- Bentouhami, N. E., Asehraou, A., Mechri, S., Hasnaoui, I., Moumnassi, S., et al. (2024). Purification and biochemical characterization of a novel thermostable endo-polygalacturonase from *Aspergillus niger* strain HO32 and its suitability for clarification of orange juice. *Process Biochemistry*, 145, 63–73. <https://doi.org/10.1016/j.procbio.2024.06.013>
- Buga, M. L., Ibrahim, S., & Nok, A. J. (2010). Partially purified polygalacturonase from *Aspergillus niger* (SA6). *African Journal of Biotechnology*, 9(52), 8944–8954.
- Cheng, Z., Chen, D., Lu, B., Wei, Y., Xian, L., Li, Y., Luo, Z., & Huang, R. (2016). A Novel Acid-Stable Endo-Polygalacturonase from *Penicillium oxalicum* CZ1028: Purification, Characterization, and Application in the Beverage Industry. *Journal of Microbiology and Biotechnology*, 26(6), 989–998. <https://doi.org/10.4014/jmb.1511.11045>
- Chinedu, S. N., Dayo-Oduko, O. P., & Iheagwam, F. N. (2016). Partial Purification and Kinetic Properties of Polygalacturonase from *Solanum macrocarpum* L. Fruit. *Biotechnology(Faisalabad)*, 16(1), 27–33. <https://doi.org/10.3923/biotech.2017.27.33>
- Cocok, A. M. B., Fahrurrozi, F., & Anja, M. (2017). Pectinase Production and Clarification Treatments of Apple (*Malus Domestica*) Juice. *Annales Bogorienses*, 21(2), 63–68.
- Gams, W., Christensen, M., Onions, A. H., Pitt, J. I., & Samson, R. A. (1986). Infrageneric Taxa of *Aspergillus*. In R. A. Samson & J. I. Pitt (Eds.), *Advances in Penicillium and Aspergillus Systematics* (pp. 55–62). Springer US. [https://doi.org/10.1007/978-1-4757-1856-0\\_5](https://doi.org/10.1007/978-1-4757-1856-0_5)
- Garcia, N. F. L., Santos, F. R. D. S., Bocchini, D. A., Paz, M. F. D., Fonseca, G. G., & Leite, R. S. R. (2018). Catalytic properties of cellulases and hemicellulases produced by *Lichtheimia ramosa*: Potential for sugarcane bagasse saccharification. *Industrial Crops and Products*, 122, 49–56. <https://doi.org/10.1016/j.indcrop.2018.05.049>
- Gomes, E., Leite, R. S. R., Da Silva, R., & Silva, D. (2009). Purification of an Exopolygalacturonase from *Penicillium viridicatum* RFC3 Produced in Submerged Fermentation. *International Journal of Microbiology*, 2009, 1–8. <https://doi.org/10.1155/2009/631942>
- Haile, S., & Ayele, A. (2022). Pectinase from Microorganisms and Its Industrial Applications. *The Scientific World Journal*, 2022, 1–15. <https://doi.org/10.1155/2022/1881305>
- Ikram, M., Ali, N., Jan, G., Jan, F. G., & Khan, N. (2020). Endophytic Fungal Diversity and their Interaction with Plants for Agriculture Sustainability Under Stressful Condition. *Recent Patents on Food, Nutrition & Agriculture*, 11(2), 115–123. <https://doi.org/10.2174/2212798410666190612130139>
- Jayani, R. S., Saxena, S., & Gupta, R. (2005). Microbial pectinolytic enzymes: A review. *Process Biochemistry*, 40(9), 2931–2944. <https://doi.org/10.1016/j.procbio.2005.03.026>
- Jayani, R. S., Shukla, S. K., & Gupta, R. (2010). Screening of Bacterial Strains for Polygalacturonase Activity: Its Production by *Bacillus sphaericus* (MTCC 7542). *Enzyme Research*, 2010, 1–5. <https://doi.org/10.4061/2010/306785>
- Karimi, F., Mazaheri, D., Saei Moghaddam, M., Mataei Moghaddam, A., Sanati, A. L., & Orooji, Y. (2021). Solid-state



- fermentation as an alternative technology for cost-effective production of bioethanol as useful renewable energy: A review. *Biomass Conversion and Biorefinery*. <https://doi.org/10.1007/s13399-021-01875-2>
- Kaur, G., Kumar, S., & Satyanarayana, T. (2004). Production, characterization and application of a thermostable polygalacturonase of a thermophilic mould *Sporotrichum thermophile* Apinis. *Bioresource Technology*, *94*(3), 239–243. <https://doi.org/10.1016/j.biortech.2003.05.003>
- Khatri, B. P., Bhattarai, T., Shrestha, S., & Maharjan, J. (2015). Alkaline thermostable pectinase enzyme from *Aspergillus niger* strain MCAS2 isolated from Manaslu Conservation Area, Gorkha, Nepal. *Springer Plus*, *4*(1), 488. <https://doi.org/10.1186/s40064-015-1286-y>
- Klich, M. A. (2002). *Identification of common Aspergillus species*. Centraalbureau voor Schimmelcultures, Utrecht, The Netherlands.
- Lamounier, K. F. R., Rodrigues, P. O., Pasquini, D., & Baffi, M. A. (2018). Saccharification of Sugarcane Bagasse Using an Enzymatic Extract Produced by *Aspergillus fumigatus*. *Journal of Renewable Materials*, *6*(2), 169–175. <https://doi.org/10.7569/JRM.2017.634151>
- Li, S., Yang, X., Yang, S., Zhu, M., & Wang, X. (2012). Technology Prospecting On Enzymes: Application, Marketing and Engineering. *Computational and Structural Biotechnology Journal*, *2*(3), e201209017. <https://doi.org/10.5936/csbi.201209017>
- Lowry, O. H., Rosebrough, N. J., Farr, A. L., & Randall, R. J. (1951). Protein measurement with the Folin phenol reagent. *The Journal of Biological Chemistry*, *193*(1), 265–275.
- Madamwar, D., Patel, S., & Parikh, H. (1989). Solid state fermentation for cellulases and  $\beta$ -glucosidase production by *Aspergillus niger*. *Journal of Fermentation and Bioengineering*, *67*(6), 424–426. [https://doi.org/10.1016/0922-338X\(89\)90150-5](https://doi.org/10.1016/0922-338X(89)90150-5)
- Majumdar, D. R., Singh, R., Dondilkar, S., Shaikh, N., Pawale, G., Shinde, P., & Sakate, P. (2018). Enzyme array from thermophilic fungal isolate—RSND. *World Journal of Pharmaceutical Research*, *7*(4), 60–70.
- Martins, E. D. S., Leite, R. S. R., Da Silva, R., & Gomes, E. (2012). Production and characterization of polygalacturonase from thermophilic *Thermoascus aurantiacus* on submerged fermentation. *Annals of Microbiology*, *62*(3), 1199–1205. <https://doi.org/10.1007/s13213-011-0360-0>
- Munir, M., Abdullah, R., Haq, I., Kaleem, A., & Iqtedar, M. (2019). Isolation and identification of multi stress tolerant polygalacturonase producing fungi from various fruits. *The Journal of Animal & Plant Sciences*, *29*(3), 825–832.
- Oumer, O. J. (2017). Pectinase: Substrate, Production and their Biotechnological Applications. *International Journal of Environment, Agriculture and Biotechnology*, *2*(3), 1007–1014. <https://doi.org/10.22161/ijeab/2.3.1>
- Paolo, D., Bianchi, G., Scalzo, R. L., Morelli, C. F., Rabuffetti, M., & Speranza, G. (2018). The Chemistry behind Tomato Quality. *Natural Product Communications*, *13*(9), 1934578X1801300. <https://doi.org/10.1177/1934578X1801300927>
- Pedrolli, D. B., Monteiro, A. C., Gomes, E., & Carmona, E. C. (2009). Pectin and Pectinases: Production, Characterization and Industrial Application of Microbial Pectinolytic Enzymes. *The Open Biotechnology Journal*, *3*(1), 9–18. <https://doi.org/10.2174/1874070700903010009>
- Pitt, J. I., & Hocking, A. D. (2009). *Fungi and Food Spoilage*. Springer US. <https://doi.org/10.1007/978-0-387-92207-2>
- Rahman, Md. S., Choi, Y. S., Kim, Y. K., Park, C., & Yoo, J. C. (2019). Production of Novel Polygalacturonase from *Bacillus paralicheniformis* CBS32 and Application to Depolymerization of Ramie Fiber. *Polymers*, *11*(9), 1525. <https://doi.org/10.3390/polym11091525>
- Ramesh, A., Harani Devi, P., Chattopadhyay, S., & Kavitha, M. (2020). Commercial Applications of Microbial Enzymes. In N. K. Arora, J. Mishra, & V. Mishra (Eds.), *Microbial Enzymes: Roles and Applications in Industries* (Vol. 11, pp. 137–184). Springer Singapore. [https://doi.org/10.1007/978-981-15-1710-5\\_6](https://doi.org/10.1007/978-981-15-1710-5_6)
- Ramos-Ibarra, J., Miramontes, C., Arias, A., Arriola, E., Guatemala, G., & Corona-González, R. (2017). Production of hydrolytic enzymes by solid-state fermentation with new fungal strains using orange by-products. *Revista Mexicana de Ingeniería Química*, *16*(1), 19–31.
- Raper, K., & Fennell, D. (1965). *The Genus Aspergillus*. Williams & Wilkins.
- Raveendran, S., Parameswaran, B., Ummalyma, S. B., Abraham, A., Mathew, A. K., Madhavan, A., Rebello, S., & Pandey, A. (2018). Applications of Microbial Enzymes in Food Industry. *Food Technology and Biotechnology*, *56*(1), 16–30. <https://doi.org/10.17113/ftb.56.01.18.5491>
- Ravi, K., & Raghun, R. (2017). Isolation and Screening of Industrially Important Polygalacturonase producing Fungi from the Mangrove Soils of Krishna District Andhra Pradesh. *International Journal of Agricultural Sciences*, *9*(19), 4193–4195.

- Reddy, P., & Sreeramulu, A. (2012). Isolation, identification and screening of pectinolytic fungi from different soil samples of Chittoor district. *International Journal of Life Sciences Biotechnology and Pharma Research*, 1(3), 186–193.
- Ribeiro, D. S., Henrique, S. M. B., Oliveira, L. S., Macedo, G. A., & Fleuri, L. F. (2010). Enzymes in juice processing: A review. *International Journal of Food Science & Technology*, 45(4), 635–641. <https://doi.org/10.1111/j.1365-2621.2010.02177.x>
- Samal, I., Bhoi, T. K., Majhi, P. K., Murmu, S., Pradhan, A. K., et al. (2023). Combatting insects mediated biotic stress through plant associated endophytic entomopathogenic fungi in horticultural crops. *Frontiers in Plant Science*, 13, 1098673. <https://doi.org/10.3389/fpls.2022.1098673>
- Samson, R., Houbraken, J., Thrane, U., Frisvad, J., & Anderson, B. (2010). *Food and indoor fungi: Second Edition. (2nd ed.)* CBS-KNAW Fungal Biodiversity Centre. C B S Laboratory Manual Series No. 2, CBS-KNAW Fungal Biodiversity Centre, Utrecht, The Netherlands
- Satapathy, S., Soren, J. P., Mondal, K. C., Srivastava, S., Pradhan, C., Sahoo, S. L., Thatoi, H., & Rout, J. R. (2021). Industrially relevant pectinase production from *Aspergillus parvisclerotigenus* KX928754 using apple pomace as the promising substrate. *Journal of Taibah University for Science*, 15(1), 347–356. <https://doi.org/10.1080/16583655.2021.1978833>
- Shamly, V., Kali, A., Srirangaraj, S., & Umadevi, S. (2014). Comparison of Microscopic Morphology of Fungi Using Lactophenol Cotton Blue (LPCB), Iodine Glycerol and Congo Red Formaldehyde Staining. *Journal of Clinical and Diagnostic Research*, 8(7), DL01-02. <https://doi.org/10.7860/JCDR/2014/8521.4535>
- Siddiqui, Mohd. A., Pande, V., & Arif, M. (2012). Production, Purification, and Characterization of Polygalacturonase from *Rhizomucor pusillus* Isolated from Decomposing Orange Peels. *Enzyme Research*, 2012, 1–8. <https://doi.org/10.1155/2012/138634>
- Soares, I., Távora, Z., Barcelos, R., & Baroni, S. (2012). Microorganism-produced enzymes in the food industry. In B. Valdez, M. Schorr, & R. Zlatev (Eds.), *Scientific, health and social aspects of the food industry* (pp. 83–94). IntechOpen.
- Tai, E.S., Hsieh, P.C., & Sheu, S.C. (2013). Purification and Characterization of Polygalacturonase from Screened *Aspergillus tubingensis* for Coffee Processing. *Food Science and Technology Research*, 19(5), 813–818. <https://doi.org/10.3136/fstr.19.813>
- Thakur, A., Pahwa, R., Singh, S., & Gupta, R. (2010). Production, Purification, and Characterization of Polygalacturonase from *Mucor circinelloides* ITCC 6025. *Enzyme Research*, 2010, 1–7. <https://doi.org/10.4061/2010/170549>
- Wang, S., Lian, Z., Wang, L., Yang, X., & Liu, Y. (2015). Preliminary investigations on a polygalacturonase from *Aspergillus fumigatus* in Chinese Pu'er tea fermentation. *Bioresources and Bioprocessing*, 2(1), 33. <https://doi.org/10.1186/s40643-015-0061-9>
- Yoon, L. W., Ang, T. N., Ngoh, G. C., & Chua, A. S. M. (2014). Fungal solid-state fermentation and various methods of enhancement in cellulase production. *Biomass and Bioenergy*, 67, 319–338. <https://doi.org/10.1016/j.biombioe.2014.05.013>
- Zhang, S., Amin, F., Xiong, M., Bhatti, H. N., & Bilal, M. (2021). High-yield intracellular production of an exo-polygalacturonase enzyme via heterologous expression of *Penicillium notatum* gene in *Saccharomyces cerevisiae*. *International Food Research Journal*, 28(4), 664–671. <https://doi.org/10.47836/ifrj.28.4.03>



## Journal of Experimental Biology and Agricultural Sciences

<http://www.jebas.org>

ISSN No. 2320 – 8694

### Germination of *Senegalia mellifera* seeds in response to presowing treatments

Fiona Opelo Madisa, Witness Mojeremane\* , Kamogelo Makgobota ,  
Demel Teketay , Topoyame Isaac Makoi

Department of Range and Forest Resources, Faculty of Natural Resources, Botswana University of Agriculture and Natural Resources, Gaborone Botswana

Received – May 07, 2024; Revision – June 22, 2024; Accepted – July 11, 2024

Available Online – July 15, 2024

DOI: [http://dx.doi.org/10.18006/2024.12\(3\).390.398](http://dx.doi.org/10.18006/2024.12(3).390.398)

#### KEYWORDS

Germination

Seed dormancy

Seed dimensions

Pre-sowing treatments

#### ABSTRACT

This study aimed to evaluate the size of *Senegalia mellifera* seeds and determine the most effective scarification techniques to improve germination. The experiment, conducted at Botswana University of Agriculture and Natural Resources, involved ten presowing treatments, including control, nicking, soaking in sulphuric acid for different durations, and boiling water for varying periods. A completely randomized design (CRD) was used for the experiment. Germination data was transformed using arcsine to meet normal distribution requirements and then analyzed using analysis of variance (ANOVA). The results showed that the presowing treatments had a statistically significant effect on germination ( $P < 0.00001$ ). Seeds treated with sulphuric acid, nicking, and those left untreated exhibited the highest germination rates, while seeds treated with boiling water showed the lowest germination percentages. These findings indicate that the seed coats of *S. mellifera* are permeable to water and air, and presowing treatments do not show any significant effect on the successful germination of *S. mellifera* seed.

\* Corresponding author

E-mail: [wmojerem@buan.ac.bw](mailto:wmojerem@buan.ac.bw) (Witness Mojeremane)

Peer review under responsibility of Journal of Experimental Biology and Agricultural Sciences.

Production and Hosting by Horizon Publisher India [HPI]  
(<http://www.horizonpublisherindia.in/>).  
All rights reserved.

All the articles published by [Journal of Experimental Biology and Agricultural Sciences](#) are licensed under a [Creative Commons Attribution-NonCommercial 4.0 International License](#) Based on a work at [www.jebas.org](http://www.jebas.org).



## 1 Introduction

Forests play a crucial role in the environment by providing a wide range of goods and services to both the environment and humans (Opoku et al. 2018; Turner-Skoff and Cavender 2019). Besides offering various environmental services, forests also supply economically important goods such as fruits, traditional medicine, animal feed, charcoal, firewood, and timber for building and household purposes (Cavendish 2000). They also serve as habitats for wildlife, protect water and soil, improve air quality, and store carbon. Anthropogenic activities, particularly deforestation, pose significant conservation issues in tropical regions, leading to a decrease in biodiversity and contributing to poverty in rural areas (Blakesley et al. 2002). This situation has been worsened by forest fires, occasional droughts, and climate change, as noted by Rampart et al. (2021). Deforestation not only endangers the flora and fauna that rely on forests and their resources but also threatens the livelihoods of indigenous people. Moreover, in arid and semi-arid regions, native woody species are extensively harvested without being replaced, despite the essential goods and services they provide.

The lack of attention given to incorporating native woody plants into planting projects and the excessive harvesting of these resources are putting their ongoing existence at risk. Planting initiatives struggle to include these indigenous woody plants due to a lack of knowledge on how to effectively propagate them in tropical areas. Additionally, the use of poor planting materials propagated in tree nurseries also contributes to their exclusion from planting programs (Elliot et al. 2002; McNamara et al. 2006). In recent years, there has been a growing trend towards replanting indigenous woody plants to restore native woodlands (Shono et al. 2007; Raman et al. 2009; Rasebeka et al. 2014; Meli et al. 2014).

Before acacias were renamed, *Senegalia mellifera* (Benth.) Seigler & Ebinger, was known as *Acacia mellifera* (Vahl) Benth. (Kyalangalilwa et al. 2013). *S. mellifera* belongs to the family Fabaceae (Timberlake 1980; Venter and Venter 2012). The tree is also known by several common or vernacular names, such as hook thorn, blackthorn, wait-a-bit, hook thorn, mongana (Timberlake 1980; Smit 2008), and many other names varying from place to place. The species is well-known for its tolerance and is common in arid and semi-arid regions of Africa and the Arabian peninsula (Hagos and Smit 2005; Heuze and Tran 2015). The species thrives in dry conditions and on a variety of soil types, including clayey and sandy Kalahari soils (Timberlake 1980; Tietema et al. 1992; Smit 2008). *S. mellifera* is a thorny shrub that grows up to 4 meters in height with multiple stems (Timberlake 1980) and rarely reaches 6 to 9 meters high (Venter and Venter 2012; Heuze and Tran 2015). The distinguishing feature of *S. mellifera* is a flat, round, or spreading crown with the potential to touch the ground (Venter and

Venter 2012). Furthermore, the *S. mellifera* tree has a robust set of thorns with a sturdy hook at the nodes (Timberlake 1980; Smit 2008; Venter and Venter 2012).

*S. mellifera* is a valuable multipurpose tree species. Different parts of the tree, such as leaves, twigs, pods, shoots, and flowers, are eaten by domestic animals as feed (Palmer and Pitman 1972; Venter and Venter 2012; Abdalkreem et al. 2017). It provides nectar used by honeybees to produce high-quality honey (Bein et al. 1996; Smit 1999; Nonyane 2013). The termite-resistant wood of the tree is also used for making axe and pick handles (Venter and Venter 2012), constructing fences, and producing firewood and charcoal (Orwa et al. 2009; Nonyane 2013; Heuzé and Tran 2015). Local communities utilize the bark, leaves, and roots to treat a variety of illnesses (Hines and Eckman 1993; Mutai et al. 2004; Koch et al. 2005; Fatima and Mamoun 2013). According to Orwa et al. (2009), the tree has been used in agroforestry systems to mark farm boundaries and create live fences.

The purpose of a plant's seed is to establish new plants. However, the process of germination can only occur once because it is essentially a permanent one (Smýkal et al. 2014). Plant seeds have a very long dormancy period, and various mechanisms have evolved to minimize the period of germination and to overcome this dormancy (Foley 2001). Many woody plants, especially legumes, have tough outer seed coats that prevent the entry of water and oxygen to stimulate or initiate germination. Seeds with impermeable or physical dormancy are not able to germinate when conditions are conducive for non-dormant seeds to germinate (Vleeshouwers et al. 1995; Bewley 1997). Seed dormancy influences germination ecology and plant seed ecology (Forbis et al. 2002). Several researchers have used different pre-sowing techniques to crack impermeable seed coats to improve the germination of several plants (Ren and Tao 2004; Anand et al. 2012; Gilani et al. 2019; Botumile et al. 2020; Latiwa et al. 2023; Dasari et al. 2024; Longjam and Kotiya 2024).

The survival of plants depends not only on dormancy but also on seed qualities such as size and weight (Moles et al. 2005). Seed weight and size are critical factors for growth in the early stages of the plant life cycle, particularly in resource-limited areas (Saeed and Shaukat 2000; Moles et al. 2005). Seed size is also crucial for seed germination, dispersal, and the survival rates of plants (Tripathi and Khan 1990; Bonfil 1998; Moles and Westoby 2006). Limited information is available about the seed characteristics, dormancy, and germination requirements of various woody species, including *S. mellifera* in Botswana. This information is crucial for foresters to effectively propagate seedlings of native woody plants for afforestation and replanting initiatives. Therefore, the present study aimed to assess seed characteristics and determine the most effective scarification method for achieving speedy, successful, and consistent

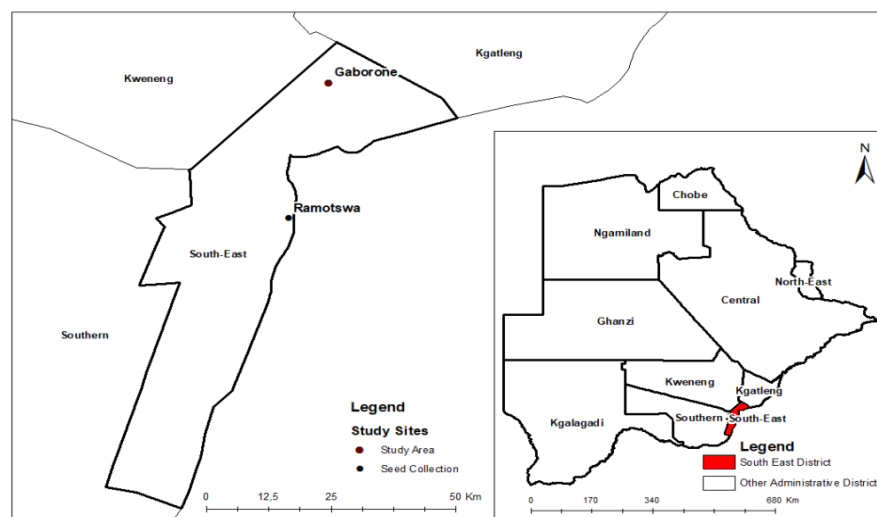


Figure 1 Map of Botswana showing Gaborone, where BUAN is situated, and Ramotswa, in the Southeast, where seeds were gathered (Cartographer T.I. Makoi)



Figure 2 *S. mellifera* pods and seeds (Photographer: F.O. Madisa)

germination in *S. mellifera*. The study's goals included measuring the size and weight of seeds, as well as testing various scarification methods on germination.

## 2 Materials and Methods

### 2.1 The study area description

This study was conducted in 2021 at the Botswana University of Agriculture and Natural Resources (BUAN) in Botswana. The experimental site at BUAN is located at an elevation of 994 meters above sea level, with an altitude of 24° 33'S and a longitude of 25° 54'E. Gaborone has a subtropical, semi-arid climate characterized by warm and wet periods from November to March and dry periods from April to October. The coolest month is July (13.5°C), and the hottest month is January. Gaborone receives approximately 485mm of rainfall each year.

### 2.2 Collection of plant material

Mature fruits were collected from various *S. mellifera* trees in the Disaneng grazing land of Ramotswa, located in the Southeast District of Botswana (Figure 1). Disaneng has semi-arid conditions with consistently sunny summers. The savanna vegetation at Disaneng is primarily composed of shrubs. Dry fruits were manually harvested from randomly chosen trees. Paper bags were used to gather the fruits, which were then transported to BUAN. The seeds were extracted by splitting and opening the fruit, followed by removing the outer covering (Figure 2).

### 2.3 Seed properties

A digital vernier calliper was used to measure the length, width, and thickness of each seed from five sets of ten seeds. Five replicates of ten seeds were weighed on a digital precision scale to determine the



weight of individual seeds. Similarly, the weight of 1000 seeds was determined by weighing five batches of 100 seeds each.

## 2.4 Effect of various seed treatments on germination of *S. mellifera*

In this study, ten treatments were conducted, including control or untreated seeds. The treatments included nicking, soaking in boiling water for one, three, and five minutes, using hot water (cooled for 24 hours), treatment with concentrated sulphuric acid (H<sub>2</sub>SO<sub>4</sub>) for 15, 30, 45, and 60 minutes, as well as untreated seeds. The study used a completely randomized block design (CRB), and each treatment, including the control, was repeated four times. Before starting the experiment, the viability of the seeds was tested by soaking them in water. Viable seeds settled at the bottom of the jar, while those that floated were considered not viable and were discarded. Each replicate contained 25 seeds sown inside 90 mm petri dishes lined with cotton wool, kept moist by adding distilled water as needed. Seeds were considered germinated when the radical had penetrated the seed coat. All germinated seeds were counted and then removed from the petri dish to avoid counting them the next day. The germination study was conducted for 30 days.

### 2.4.1 Nicking treatment

In this treatment, 100 seeds were divided into four groups of 25 seeds for each replication. Each seed underwent a 1-2mm seed coat incision on the curved edge opposite the embryo location to prevent damage or displacement of the embryo.

### 2.4.2 Sulphuric acid treatments

Seeds were treated with concentrated H<sub>2</sub>SO<sub>4</sub> for 15, 30, 45, and 60 minutes using the method described by Teketay (1996b). Each soaking time and treatment involved twenty-five seeds placed in separate heat-resistant beakers. These beakers were filled with enough H<sub>2</sub>SO<sub>4</sub> to soak the seeds and were stirred every five minutes to ensure uniform acid distribution. After each soaking time, an acid-resistant sieve was used to separate the seeds from the acid. The acid was then transferred to a different beaker. The seeds were cleaned and washed with running tap water to eliminate any acidic residues.

### 2.4.3 Boiling water treatment

In this treatment, seeds were subjected to three different boiling water periods: one, three, and five minutes. Each soaking period

comprised of four replicates of 25 seeds enclosed inside coffee filter papers. The seeds were placed in a pot of boiling water on a stove and then removed after one, three, and five minutes. Finally, they were cooled in a small bowl of cold water.

### 2.4.4 Hot water treatment

For this treatment, four coffee filters were filled with 25 seeds each and placed in a 250 ml beaker. After that, boiling water was taken off the heat and poured into the beaker, and the seeds were left for 24 hours to cool down.

### 2.4.5 Control

In this study, each experiment used a control group consisting of four replicates of 25 untreated seeds.

## 2.5 Statistical analyses

The percent germination of the seeds was calculated by directly counting the germinated seeds and using the following formula.

$$\text{Seed germination (\%)} = \frac{\text{Number of seedlings emerged}}{\text{Total number of seeds sown}} \times 100$$

The data was analyzed using Statistix Software, Version 10 (Statistix 10, 1984-2003) for one-way ANOVA and descriptive statistical analysis. The percentage germination data was transformed with arcsine to meet normality requirements before being subjected to analysis of variance (ANOVA) (Zar 1996). The Tukey's Honestly Significant Difference (HSD) Test was utilized to identify significant differences in means at a significance level of  $P < 0.05$ .

## 3 Results

### 3.1 Characteristics of seeds

Each pod contained between 2 and 3 seeds, with 1 to 2 of these being sound seeds. No insect-damaged or aborted seeds were found in the collected samples. The observed measurements for the length, width, and thickness were  $10.32 \pm 0.27$  mm,  $8.52 \pm 0.06$  mm, and  $1.76 \pm 0.08$  mm, respectively (Table 1). The results in Table 1 show that the weight of individual seeds and one thousand seeds were  $0.14 \pm 0.01$  g and  $111.66 \pm 1.11$  g, respectively.

### 3.2 Effect of seed treatment on germination of *S. mellifera*

The influence of pre-sowing treatments on the germination of *S. mellifera* was found to be extremely significant ( $P < 0.00001$ ).

Table 1 Different characteristics of the *Senegalia mellifera* seed samples

Seed length (mm)	Seed width (mm)	Seed breast (mm)	Single seed weight (g)	Thousand seed Wight (g)
$10.32 \pm 0.27$	$8.52 \pm 0.06$	$1.76 \pm 0.08$	$0.14 \pm 0.01$	$111.66 \pm 1.11$

The "±" standard error of mean

Table 2 Effect of various pre-sowing treatments on the cumulative germination of *S. mellifera* seeds

Treatment	Germination percentage	
	Mean germination	Range
Control	79.2± 4.2 <sup>a</sup>	69.7 – 90.0
Nicking	80.8 ± 5.4 <sup>a</sup>	69.7 – 90.0
Sulphuric acid (15 min)	78.5 ± 0.0 <sup>a</sup>	78.5 – 78.5
Sulphuric acid (30 min)	80.1 ± 3.5 <sup>a</sup>	73.6 – 90.0
Sulphuric acid (45 min)	87.1 ± 2.9 <sup>a</sup>	78.5 – 90.0
Sulphuric acid (60 min)	80.1± 3.5 <sup>a</sup>	73.6 – 90.0
Boiling Water (1 min)	27.7 ± 3.0 <sup>c</sup>	20.3 – 34.5
Boiling Water (3 min)	8.0 ± 4.9 <sup>d</sup>	0 – 20
Boiling Water (5 min)	2.9 ± 2.9 <sup>d</sup>	0 – 11
Hot water (allowed to cool for 24 hrs)	54.3 ± 0.70 <sup>b</sup>	53.1–55.6

Values are means ± standard error; Means were separated using Tukey Honestly Significant Differences (HSD) Test at  $p \leq 0.05$ ; Means within columns followed by the same letters are not significantly different.

When compared to untreated seeds, the germination percentage for seeds that were boiled for one, three, and five minutes, as well as those soaked in hot water (and then allowed to cool for 24 hours), was significantly lower (Table 2). Moreover, there were no noteworthy variances in germination percentage between seeds treated with sulphuric acid (for 15, 30, 45, and 60 minutes), nicking, and the control. The seeds that exhibited the highest germination percentage were those treated with sulphuric acid for 45 minutes (87.1%), followed by nicking (80.8%), sulfuric acid treatment for 30 and 60 minutes (80.1%), and the control (79.2%). Conversely, the seeds subjected to the five-minute boiling treatment displayed the lowest germination percentage (2.9%) (Table 2).

#### 4 Discussion

##### 4.1 Seed Properties

The size of a plant's seeds can influence its ability to regenerate and maintain health (Chacon et al. 1998). Larger seeds have been found to have a positive impact on germination and plant survival (Zimmermann and Weis 1983; Chacon et al. 1998; Moles and Westoby 2006). The current study did not observe any damaged or aborted seeds, indicating that these seeds are unlikely to be affected by living or non-living factors. These findings are consistent with a study by Kahaka et al. (2018), which reported no damage or seed abortion in other legume plant species native to Botswana. Table 1 presents the findings on the seed dimensions (length, width, and breadth) of *S. mellifera*. These dimensions are similar to those of other species native to Botswana, particularly *Senegalia erubescens* (Kahaka et al. 2018) and *Senegalia galpini* (Botumile et al. 2020). The length and width of *S. mellifera* seeds are comparable to those of *Vachellia robusta* (Botumile et al.

2020). The weight of a single seed and 1,000 seeds is similar to that of *S. erubescens* (Kahaka et al. 2018) and smaller than that of *Senegalia galpini* (Botumile et al. 2020). The mass of 1,000 seeds is higher compared to *Vachellia rehmanniana* (Mojeremane et al. 2017), *Dichrostachys cineria* (Kahaka et al. 2018), and *Vachellia erioloba* (Odirile et al. 2019). Furthermore, in comparison to small seeds, various studies have indicated that large seeds produce seedlings that are more resistant to drought and have increased survival and/or growth in nutrient-deficient environments (Stock et al. 1990; Milberg et al. 1998; Lloret et al. 1999; Seiwa et al. 2002).

##### 4.2 Effect of seed treatment on *S. mellifera* germination

Leguminous woody plants have impermeable seed coats, which prevent the absorption of water and oxygen, leading to seed dormancy (Considine and Considine 2016). These plants are naturally found in dry environments and have impermeable seed coats to survive tough conditions such as intense heat, animal damage, extreme drought, and physical harm. The low germination rate caused by these impermeable seed coats hinders the use of local species in planting initiatives in dry environments (Smith et al. 2003; Mojeremane et al. 2021).

Based on the data presented in Table 2, *S. mellifera* does not have impermeable seed coats that would prevent water absorption or gas exchange. The results indicate no significant difference in seed germination between seeds treated with sulphuric acid, nicking, and untreated seeds. Untreated seeds showed a germination rate of 79.2%, which is not significantly different from the germination rates of seeds subjected to sulphuric acid and nicking treatments. This suggests that the species lacks the typical hard, impermeable seed coat found in other leguminous woody plants. These findings align with those of Tietema et al. (1992), who reported a 65%

germination rate for untreated *S. mellifera* seeds five days after sowing. Previous reports have indicated that untreated *S. mellifera* seeds can achieve higher germination rates without any prior treatment (Roodt 2008; Venter and Venter 2012; Nonyane 2013) and that soaking the seeds in warm water overnight can expedite their germination process.

Boiling seeds for one, three, or five minutes resulted in the lowest germination rates, ranging from 2.9% to 27.7%. The seeds' sensitivity to high temperatures may explain the low germination rates observed in these treatments (Kahaka et al. 2018). These recent study results are consistent with previous research on various types of trees in Botswana (Kahaka et al. 2018; Odirile et al. 2019; Botumile et al. 2020; Mojeremane et al. 2021; Latiwa et al. 2023). The germination rate of seeds soaked in hot water (allowed to cool for 24 hours) was also found to be lower compared to that of untreated seeds. This finding is supported by studies conducted in Botswana (Mojeremane et al. 2017; Mojeremane et al. 2020) and elsewhere (Diallo et al. 1996; Teketay 1996a, 1996b; Teketay 1998; Fredrick et al. 2017).

## Conclusions

The laboratory germination tests revealed that *S. mellifera* seeds are not impacted by the impermeability of the seed coat, which typically hinders water intake and gaseous exchange necessary for germination. Untreated seeds displayed comparable germination rates to those treated with nicking and sulphuric acid. Consequently, these seeds do not necessitate any prior treatment before planting.

## Acknowledgements

The authors thank the University of Agriculture and Natural Resources for providing facilities for this work.

## Declarations

The authors have no conflicting interests.

## References

Abdalkreem, I.H., & Siam, A.M.J. (2017). Germination responses to water stress and morphometric characteristics of seeds of *Acacia mellifera* and *Acacia laeta*. *Journal of Applied Science*, 9, 65–78.

Anand, B., Devagiri, G.M., Gurav, M., Vasudev, H.S., & Kaple A. K. (2012). Effects of Pre-sowing seed treatments on germination and seedling growth performance of *Melia dubia* CAV: An important multipurpose tree. *International Journal of Life Sciences*, 1(3), 59–63.

Bein, E., Habte, E., Jalber, A., Birnie, A., & Tengnas, B. (1996). *Useful Trees and Shrubs in Eritrea: Technical handbook No 12. Nairobi, Kenya: Regional Soil Conservation Unit.*

Bewley, J.D. (1997). Seed germination and dormancy. *Plant Cell*, 9(7), 1055–1066. <https://doi.org/10.1105/tpc.9.7.1055>

Blakesley, D., Elliott, S., Kuarak, C., Navakitbumrung, P., Zangkum, S., & Anusamsunthorn, V. (2002). Propagating framework tree species to restore seasonally dry tropical forest: implications of seasonal seed dispersal and dormancy. *Forest Ecology and Management*, 164(1-3), 31–38. [https://doi.org/10.1016/S0378-1127\(01\)00609-0](https://doi.org/10.1016/S0378-1127(01)00609-0)

Bonfil, C. (1998). The effect of seed size, cotyledon reserves, and herbivory on seedling survival and growth in *Quercus rugosa* and *Q. laurina* (Fagaceae). *American Journal of Botany*, 85(1), 79–87. <https://doi.org/10.2307/2446557>

Botumile, A., Teketay, D., Mojeremane, W., & Mathowa, T. (2020). Overcoming seed dormancy of *Senegalia galpinii* and *Vachellia robusta* through scarification pre-sowing treatments. *Agriculture and Forestry*, 66(1), 153–169. DOI:10.17707/agricultforest.66.1.15

Cavendish, W. (2000). Empirical regularities in the poverty-environment relationship of rural households: Evidence from Zimbabwe. *World Development*, 28(11), 1979–2003. [https://doi.org/10.1016/S0305-750X\(00\)00066-8](https://doi.org/10.1016/S0305-750X(00)00066-8)

Chacon, P., Bustamante, R., & Henriquez, C. (1998). The effect of seed size on germination and seedling growth of *Cryptocarya alba* (Lauraceae). *Revista Chilena de Historia Natural*, 71(2), 189–197.

Considine, M.J., & Considine, J.A. (2016). On the language and physiology of dormancy and quiescence in plants. *Journal of Experimental Botany*, 67(11), 3189–3203. <https://doi.org/10.1093/jxb/erw138>

Dasari, R., Dharavath, S.B., Yadla, H. & Taduri, S. (2024). Effects of different treatments on seed germination and breaking seed dormancy of *Citrullus colocynthis* an endangered medicinal plant. *Journal of Pharmacognosy and Phytochemistry*, 13 (3), 415-419. <https://doi.org/10.22271/phyto.2024.v13.i3e.14983>

Diallo, I., Danthu, P., Sambou, B., Dione, D., Goudiaby, A.S., & Poulsen, K. (1996). Effects of different pretreatments on germination of *Faidherbia albida* (Del.) A. Chev. seeds. *International Tree Crops Journal*, 9(1), 31–36.

Elliott, S., Kuarak, C., Navakitbumrung, P., Zangkum, S., Anusamsunthorn, V., & Blakesley D. (2002). Propagating framework trees to restore seasonally dry tropical forest in northern Thailand. *New Forests*, 23, 63–70. <https://doi.org/10.1023/A:1015641119271>

Fatima, A.H., & Mamoun, A.M. (2013). The relationship between seed polymorphism and germination of *Acacia mellifera*

- (Vahl)Benth. seeds. *International Journal of Scientific and Research Publications*, 3(5), 1–2.
- Foley, M.E. (2001). Seed dormancy: an update on terminology, physiological genetics and quantitative trait loci regulating germinability. *Weed Science*, 49, 305–317. Doi: 10.1614/0043-1745.
- Forbis, T.A., Floyd, S.K., & de Queiroz, A. (2002). The evolution of embryo size in angiosperms and other seed plants: implication for evolution and seed dormancy. *Evolution*, 56(11), 2112–2125. <https://doi.org/10.1111/j.0014-3820.2002.tb00137.x>
- Fredrick, C., Muthuri, C., Ngamau, K., & Sinclair, F. (2017). Provenance and pre-treatment effect on seed germination of six provenances of *Faidherbia albida* (Delile) A. Chev. *Agroforestry Systems*, 91, 1007–1017. <https://doi.org/10.1007/s10457-016-9974-3>.
- Gilani, M.M., Ahmad, I., Farooq, T.H., FengFei, W., Yousaf, M.S., Khan, M.W., Yousaf, T., & Xiang Qing, M. (2019). Effects of pre-sowing treatments on seed germination and morphological growth of *Acacia nilotica* and *Faidherbia albida*. *Scientia Forestalis*, 122, 374-292.
- Hagos, M.G., & Smit, G.N. (2005). Soil enrichment by *Acacia mellifera* subsp. *deinens* on nutrient poor sandy soil in a semi-arid southern African savanna. *Journal of Arid Environments*, 61(1), 47–59. <https://doi.org/10.1016/j.jaridenv.2004.08.003>
- Heuzé, V., & Tran, G. (2015). *Black thorn (Acacia mellifera) Feedipedia, a programme by INRAE, CIRAD, AFZ and FAO*. Retrieved from <https://www.feedipedia.org/node/347>. Last updated on October 28, 2015,13:20.
- Hines, D.A., & Eckman, K. (1993). Cultural survival Canada. Indigenous multipurpose trees for Tanzaniauses and economic benefits to the people. *Ontario, Canada: Cultural Survival Canada: Development Services Foundation of Tanzania*.
- Kahaka, P., Mojeremane, W., Teketay, D., & Mathowa, T. (2018). Effects of scarification treatments on seed germination of three leguminous species from Botswana. *Silva Lusitana*,26(1-2), 115–131.
- Koch, A., Tamez, P., Pizzuto, J., & Soejarto, D. (2005). Evaluation of plants used for antimalarial treatment by the Maasai of Kenya. *Journal of Ethnopharmacology*, 101(1-3), 95–99. <https://doi.org/10.1016/j.jep.2005.03.011>
- Kyalangalilwa, B., Boatwright J.S., Daru B.H., Maurin, O., & van der Bank, M. (2013). Phylogenetic position and revised classification of *Acacia* s.l. (Fabaceae: Mimosoideae) in Africa, including new combinations in *Vachellia* and *Senegalia*. *Botanical Journal of the Linnean Society*, 172(4), 500–523. <https://doi.org/10.1111/boj.12047>
- Latiwa, A.N., Makgobota, K., Mojeremane, W., & Teketay, D. (2023). Seed characteristics and the influence of scarification treatments on the germination of *Pterocarpus angolensis* in Botswana. *Journal of Experimental Biology and Agricultural Sciences*, 11(6), 1021–1029. [https://doi.org/10.18006/2023.11\(6\).1021.1029](https://doi.org/10.18006/2023.11(6).1021.1029)
- Lloret, F., Casanovas, C., & Penuelas, J. (1999). Seedling survival of Mediterranean shrubland species in relation to root: shoot ratio, seed size and water and nitrogen use. *Functional Ecology*, 13, 210–216.
- Longjam, R., & Kotiya, A. (2024). Different pre-sowing treatments intensify the germination process and the seedling growth of fruit crops. *International Journal of Advanced Biochemistry Research*, 8(5), 541–546. <https://doi.org/10.33545/26174693.2024.v8.i5g.1126>
- McNamara, S., Tinh, D.V., Erskine, P.D., Lamb, D., Yates, D., & Brown, S. (2006). Rehabilitating degraded forest land in Central Vietnam with mixed native species plantings. *Forest Ecology and Management*, 233(2-3), 358–365. <https://doi.org/10.1016/j.foreco.2006.05.033>
- Meli, P., Martinez-Ramos, M., Rey-Benayas, J.M., & Carabias, J. (2014). Combining ecological social and technical criteria to select species for forest restoration. *Applied Vegetation Science*,17(4), 744–753. <https://doi.org/10.1111/avsc.12096>
- Milberg, P., Perez-Fernandez, M., & Lamont, B. (1998) Seedling growth response to added nutrients depends on seed size in three woody genera. *Journal of Ecology*, 86, 624–632.
- Mojeremane, W., Makgobota K., Teketay, D., Rampart, M., et al. (2020). Germination studies on seeds of *Burkea africana* and *Erythrophleum africanum* from Kazuma Forest Reserve, Northern Botswana. *African Journal of Biotechnology*, 19(9), 675–683.
- Mojeremane, W., Makgobota, K., Teketay, D., Rampart, M., et al. (2021). Evaluation of dormancy-breaking treatments on seed germination of two leguminous tree species from Chobe District, Northern Botswana. *Forestry Ideas*, 27(2), 380–395.
- Mojeremane, W., Mathowa, T., Teketay, D., Stimela, T., et al. (2017). Presowing seed treatment methods to overcome *Vachellia rehmanniana* Schinz. *Agriculture and Forestry*, 63(2), 71–181. DOI: 10.17707/AgricultForest.63.2.15
- Moles, A.T., & Westoby, M. (2006). Seed size and plant strategy across the whole life cycle. *Oikos*, 113(1), 91–105. <https://doi.org/10.1111/j.0030-1299.2006.14194.x>
- Moles, A.T., Ackerly, D.D., Webb, C.O., Tweddle, J.C., Dickie, J. B., & Westoby, M. (2005). A brief history of seed size. *Science*, 307(5709), 576–580. DOI: 10.1126/science.1104863

- Mutai, C., Abatis, D., Vagias, C., Moreau, D., Rousakis, C., & Roussis, V. (2004). Cytotoxic lupane-type triterpenoids from *Acacia mellifera*. *Phytochemistry*, 65(8), 1159–1164. <https://doi.org/10.1016/j.phytochem.2004.03.002>
- Nonyane, F. (2013). *Senegalia mellifera* subsp. *detinens*. South Africa National Biodiversity Institute (SANBI). Retrieved from <http://pza.sanbi.org/senegalia-mellifera-subsp-detinens>. Accessed on 29 November 2023.
- Odirile, O., Mojeremane, W., Teketay, D., Kashe, K., & Mathowa, T. (2019). Responses of seeds of *Vachellia erioloba* (E. Mey) in Botswana to different pre-sowing treatment methods. *International Journal of Biology and Biotechnology*, 16(1), 181–188.
- Opoku, J.A., Amissah, J.N., Essilfie, M.E., & Norman J.C. (2018). Effect of pre-sowing treatments on seed germination and seedling growth of silver butterfly tree (*Bauhinia rufescens*). *Current Agriculture Research Journal*, 6(3), 344–354. <http://dx.doi.org/10.12944/CARJ.6.3.13>.
- Orwa, C., Mutua, A., Kindt, R., Jamnadass, R., & Simons A. (2009). Agroforestry Database: a tree reference and selection guide. Version 4. In: Agroforestry Database: a tree reference and selection guide. Version 4. Assessed on 29 November 2023.
- Palmer, E., & Pitman, N. (1972). *Trees of Southern Africa*. Cape Town, South Africa: A. A. Balkema
- Raman, T., Mudappa, D., & Kapoor, V. (2009). Restoring rainforest fragments: Survival of mixed-native seedlings under contrasting site conditions in western Ghats, India. *Restoration Ecology*, 17(1), 137–147. <https://doi.org/10.1111/j.1526-100X.2008.00367.x>
- Rampart, M., Teketay, D., Makgobota, K., Mojeremane, W., et al. (2021). Enhancing germination of seeds of *Cassia abbreviata* and *Senegalia nigrescens* using pre-sowing seed treatments in Botswana. *Current Agriculture Research Journal*, 9(3), 179–187. <http://dx.doi.org/10.12944/CARJ.9.3.05>.
- Rasebeka, L., Mathowa, T., & Mojeremane, W. (2014). Effect of seed pre-sowing treatment on germination of three *Acacia* species indigenous to Botswana. *International Journal of Plant Soil Science*, 3(1), 62–70. <https://doi.org/10.9734/IJPSS/2014/5631>
- Ren, J., & Tao, L. (2004). Effects of different pre-sowing seed treatments on germination of 10 *Calligonum* species. *Forest Ecology and Management*, 195(3), 291–300. <https://doi.org/10.1016/j.foreco.2004.01.046>
- Roodt, V. (2008). *Trees and Shrubs of the Okavango Delta*. Gaborone, Botswana: Shell Oil Botswana (Pty) Ltd.
- Saeed, S., & Shaikat, S.S. (2000). Effect of seed size on germination, emergence, growth, and seedling survival of *Senna occidentalis* Link. *Pakistan Journal of Biological Sciences*, 3(2), 292–295. DOI: 10.3923/pjbs.2000.292.295.
- Seiwa, K., Watanabe, A., Saitoh, T., Kanno, H., & Akasaka, S. (2002). Effects of burying depth and seed size on seedling establishment of Japanese chestnuts, *Castanea crenata*. *Forest Ecology and Management*, 164, 149–156. [https://doi.org/10.1016/S0378-1127\(01\)00607-7](https://doi.org/10.1016/S0378-1127(01)00607-7)
- Shono, K., Cadaweng, E.A., & Durst, P.B. (2007). Application of assisted natural regeneration to restore degraded tropical forestlands. *Restoration Ecology*, 15(4), 620–626. <https://doi.org/10.1111/j.1526-100X.2007.00274.x>
- Smit, N. (1999). *Guide to the Acacias of South Africa*. Pretoria, South Africa: Briza.
- Smit, N. (2008). *Field guide to Acacias of South Africa*. Pretoria, South Africa: Briza.
- Smith, M.T., Wang, B.S.P., & Msanga H.P. (2003). Dormancy and germination. In J.A. Vozzo (Eds.), *Tropical tree seed manual number 1*, Vol. 5 (pp. 149–176). Washington D.C, USA: USDA Forest Service.
- Smykal, P., Vernoud, V., Blair, M.W., Soukup, A., Thompson, R.D. (2014). The role of the testa during development and in the establishment of dormancy of the legume seed. *Frontiers in Plant Science*, 5, 1–19. <https://doi.org/10.3389/fpls.2014.00351>
- Stock, W.D., Pate, J.S., & Delfs, J. (1990). Influence of seed size and quality on seedling development under low nutrient conditions in five Australian and South African members of the Proteaceae. *Journal of Ecology*, 78, 1005–1020. <https://doi.org/10.2307/2260949>
- Teketay, D. (1996a). The effects of different pre-sowing seed treatments, temperature, and light on the germination of five *Senna* species from Ethiopia. *New Forest*, 11, 155–17. <https://doi.org/10.1007/BF00033411>
- Teketay, D. (1996b). Germination ecology of twelve indigenous and eight exotic multipurpose leguminous species from Ethiopia. *Forest Ecology Management*, 80(1-3), 209–223. [https://doi.org/10.1016/0378-1127\(95\)03616-4](https://doi.org/10.1016/0378-1127(95)03616-4).
- Teketay, D. (1998). Germination of *Acacia origena*, *A. pilesipina* and *Pterolobium stellatum* in response to different pre-sowing seed treatments, temperature, and light. *Journal of Arid Environments*, 38(4), 551–560. <https://doi.org/10.1006/jare.1997.0332>



- Tietema, T., Merkesdal, E., & Schroten, J. (1992). *Seed germination of indigenous trees in Botswana*. Nairobi, Kenya: African Centre for Technology Studies Press.
- Timberlake, J. (1980). *Botswana Acacias*. Gaborone, Botswana: Ministry of Agriculture.
- Tripathi, R.S., & Khan, M.L. (1990). Effects of seed weight and microsite characteristics on germination and seedling fitness in two species of *Quercus* in a subtropical wet hill forest. *Oikos*, 57, 289–296. <https://doi.org/10.2307/3565956>
- Turner-Skoff, J.B., & Cavender, N. (2019). The benefits of trees for livable and sustainable communities. *People Plants Planet*, 1(4), 323–335. <https://doi.org/10.1002/ppp3.39>
- Venter, F., & Venter, J.A. (2012). *Making the most of indigenous trees*. Revised ed. Pretoria, South Africa: Briza.
- Vleeshouwers, L.M., Bouwmeester, H.J., & Karssen, C.M. (1995). Redefining seed dormancy: an attempt to integrate physiology and ecology. *Journal of Ecology*, 83(6), 1031–1037. <https://doi.org/10.2307/2261184>
- Zar, J.H. (1996). *Biostatistical Analysis*. 3<sup>rd</sup> ed. Upper Saddle River, New Jersey, USA: Prentice Hall.
- Zimmermann, J.K., & Weis, I.M. (1983). Fruit size variation and its effects on germination and seedling growth in *Xanthium strumarium*. *Canadian Journal of Botany*, 61(9), 2309–2315. <https://doi.org/10.1139/b83-253>








## Journal of Experimental Biology and Agricultural Sciences

<http://www.jebas.org>

ISSN No. 2320 – 8694

### Effect of Preparation and Drying Techniques on the Physicochemical, Functional and Nutritional Properties of products from Beetroot (*Beta Vulgaris L.*) varieties

M. S. Mubajje<sup>2, 4</sup> , M. Lubowa<sup>1,2\*</sup> , S.Y. Yeoh<sup>3</sup> ,  
H. Acham<sup>4</sup> , G. A. Tumuhimbise<sup>4</sup>, M. Matovu<sup>5</sup> 

<sup>1</sup>Department of Food Innovation and Nutrition, Faculty of Agriculture and Environmental Sciences, Mountains of the Moon University, Fort-Portal, Uganda

<sup>2</sup>Department of Food Science and Nutrition, Islamic University in Uganda, Mbale, Uganda

<sup>3</sup>School of Industrial Technology, University Sains Malaysia (USM), 11800 USM, Minden, Penang, Malaysia

<sup>4</sup>Department of Food Technology and Nutrition, Makerere University, Kampala, Uganda

<sup>5</sup>Department of Biosciences, National Agricultural Research Laboratories – NARL Kawanda, Uganda

Received – September 30, 2023; Revision – January 22, 2024; Accepted – May 30, 2024

Available Online – July 15, 2024

DOI: [http://dx.doi.org/10.18006/2024.12\(3\).399.407](http://dx.doi.org/10.18006/2024.12(3).399.407)

#### KEYWORDS

Beetroot powder

Drying techniques

Beetroot phytochemicals

Iron retention

#### ABSTRACT

Beetroot (*Beta vulgaris L.*) is rich in biologically active compounds. This study aimed to assess how different methods of preparation and drying affect the physical, chemical, functional, and nutritional properties of iron-rich beetroot powder. Two beetroot varieties, Detroit Dark Red (DetR) and Crimson Globe (CrimG), were processed using three drying techniques: sun drying (SD), oven drying (OD), and freeze drying (FD), with both boiled and fresh beetroots. The properties evaluated in the study included water activity, color, total phenolics and flavonoids, oxalate content, and mineral content. The results showed significant ( $p < 0.05$ ) differences in these properties between the dried and fresh samples. Notably, drying increased calcium, zinc, and phosphorus levels while decreasing the iron content. Boiling followed by sun drying was the best method for retaining iron, particularly for the CrimG variety. The study suggests that drying can help preserve or even enhance the physicochemical properties and micronutrient content, especially iron while reducing phytochemical levels affecting iron absorption. These findings are important for developing iron-rich beetroot products to improve dietary iron intake, especially for adolescent children.

\* Corresponding author

E-mail: planetlubs@gmail.com (M Lubowa)

Peer review under responsibility of Journal of Experimental Biology and Agricultural Sciences.

Production and Hosting by Horizon Publisher India [HPI]  
(<http://www.horizonpublisherindia.in/>).  
All rights reserved.

All the articles published by [Journal of Experimental Biology and Agricultural Sciences](#) are licensed under a [Creative Commons Attribution-NonCommercial 4.0 International License](#) Based on a work at [www.jebas.org](http://www.jebas.org).



## 1 Introduction

Beetroot (*Beta vulgaris* L.), known for its high fibre and sugar content, is also recognized for its moderate caloric value (Kovarovič et al. 2017). This vegetable, particularly the red beetroot variety (*Beta vulgaris* L. var. *vulgaris*), is appreciated worldwide for its rich composition and numerous health benefits (Székely and Máté 2023). The intense red coloration of beetroot is due to betalains, specifically betacyanins and betaxanthins, which offer significant antioxidant and anti-inflammatory properties (Şeremet and Oana-Viorela 2020). These compounds are noted for their health-promoting effects, such as inhibiting lipid peroxidation and enhancing low-density lipoprotein oxidation resistance (Şeremet and Oana-Viorela 2020).

Furthermore, consuming beetroot is linked to various health benefits, including improved blood circulation, respiratory health, skincare, and immune system support (Şeremet and Oana-Viorela 2020). Additionally, beetroot has shown potential in treating anemia by promoting red blood cell production and boosting hemoglobin levels (Ali and Bilal 2023). In today's market, which favors convenient and nutritious food options, beetroot powder has emerged as a promising product, especially for developing iron-rich supplements to enhance dietary iron intake among school-aged children (Şeremet and Oana-Viorela 2020). The drying techniques used in processing beetroot are crucial for preserving its nutrients, transforming it into powder form, and enhancing its functionality in food preparation or as a beverage ingredient (Şeremet and Oana-Viorela 2020).

However, the impact of these processing methods, including drying and thermal techniques, on the physicochemical, functional, and nutritional properties of beetroot powder needs careful consideration (Hamid and Mohamed Nour 2018). Previous research indicates that various drying techniques substantially influence the chemical composition, mineral content, bioactive compounds, and color characteristics of beetroot slices (Hamid and Mohamed Nour 2018). Various studies have assessed the effects of different drying conditions, such as traditional drying, swell drying, and blanching combined with drying, on the levels and activity of antioxidants in red beetroots (Alonzo-Macías et al. 2020). Moreover, the choice of drying method, including freeze-drying, microwave-assisted drying, or conductive hydro drying, affects the retention of bioactive compounds, phenolics, and antioxidant activity in beetroot products (Preethi et al. 2020; Liu et al. 2022). Drying is a common preservation method, but the effects of these methods on the phytochemicals and antioxidant properties of food products are necessary (Sarkar et al. 2021). Previous studies highlight the importance of evaluating different pre-treatments and temperatures to optimize the drying characteristics of beetroot slices (Mudgal 2023). Additionally, techniques like osmotic dehydration and ultrasound pre-treatments have been

explored to enhance dried beetroot chips' nutritional quality and sensory attributes (Peters et al. 2021). Choosing the right preparation and drying techniques is vital for maintaining the quality, functionality, and nutritional value of beetroot products. Understanding how different processing methods impact the physicochemical properties of beetroot powder can facilitate the development of innovative and nutritious food products. This research aims to produce beetroot powder using various preparation and drying techniques and assess their effects on the physicochemical, functional, and nutritional attributes of dried beetroot products.

## 2 Materials and Methods

### 2.1 Raw materials and sample preparation

This study used two beetroot varieties, Crimson Globe (CrimG) and Detroit Dark Red (DetR). The mature, fresh beetroots were obtained directly from farmers in Kabale, Western Uganda, then transported to the laboratory in Kampala. Upon arrival, the beetroots were sorted, washed under running potable water, peeled using a ceramic knife, and placed in clean water to prevent discoloration.

### 2.2 Processing of samples into powder

The beetroots were peeled, cleaned, and sliced into 1-2 mm thick pieces. The slices were divided into two portions. One portion was boiled at 90°C for 30 minutes in a stainless-steel pan with distilled water, while the other was left unboiled. These portions were further divided into four sub-portions for different drying treatments: (i) Fresh Sample: grated into mash and used as a control, (ii) Oven Drying (OD): dried at 65°C for 48 hours, (iii) Sun Drying (SD): spread on raised plastic mesh using wooden stands, and (iv) Freeze Drying (FD): dried at -80°C for 48 hours. The dried samples were pulverized using a pestle and mortar, passed through a 60 mm plastic mesh sieve, and kept in dark, airtight plastic containers for further analysis.

### 2.3 Estimation of physicochemical and functional characteristics

#### 2.3.1 Water activity

Measurements were conducted using an Aqua Lab water activity meter (Aqualab Series 3, Decagon Devices, Inc., Pullman, WA, USA) with temperature compensation. The measurements were performed in triplicate.

#### 2.3.2 Color measurement

The color was determined using a Minolta CR-10 color reader (Minolta Co. Ltd, Japan), following the method of Youssef and Mokhtar (2014) with some modifications. The chroma meter was

calibrated using a white plate and light trap provided by the manufacturer. Color values were expressed using the CIE Lab\* system.

### 2.3.3 Bulk density

Bulk density was determined using a graduated cylinder following the method described by Roongruangsri and Bronlund (2016).

### 2.3.4 Water solubility and water absorption

The parameters were determined using the methods outlined by Roongruangsri and Bronlund (2016) with necessary adjustments. One gram (1.0 g) of beetroot powder was mixed with 10 milliliters of distilled water and then placed in an incubator at 60°C for 20 minutes. Afterwards, the mixture was centrifuged at 3000 rpm for 15 minutes. The water solubility and absorption were then calculated based on the weights of the remaining solids and precipitates. The following formula was used for the calculation:

$$\text{Water solubility} = \frac{\text{Weight of residue}}{\text{Weight of beetroot powder}} \times 100$$

$$\text{Water absorption} = \frac{\text{Weight of centrifuged precipitate}}{\text{Weight of beetroot powder}}$$

## 2.4 Phytochemical analysis

### 2.4.1 Extraction of phenolic compounds

To extract phenolic compounds, the method described by Wang et al. (2020) and Serna-Vázquez et al. (2021) was followed with some minor adjustments. In summary, 100 mg beetroot sample was blended with a solution of 80% methanol and 2% formic acid (10 mL). This blend was homogenized at room temperature using a Poltron PT 1200E handheld homogenizer. Next, we sonicated the homogenate for 30 minutes at room temperature using a Bandelin Electronic (Germany) sonicator with DT1028. After sonication, the mixture was centrifuged at 3000xg for 25 minutes using an MSE MSB080.CR2.K centrifuge (UK). The supernatant was carefully transferred to a separate container and stored at -18°C. We re-extracted the remaining pellet under the same conditions to ensure maximum extraction efficiency. The supernatants from both extractions were combined and stored in an airtight container in a Sanyo Biomedical Freezer MDF-U333 (Sanyo Electric Biomedical Co. Ltd, Japan) at -18°C. These extracts were subsequently used to determine the total phenolic content (TPC) and total flavonoid content (TFC).

### 2.4.2 Total phenolic content (TPC)

The total phenolic content of the samples was measured using the Folin-Ciocalteu reagent, following the method outlined by Özderin (2024). Briefly, 50.0 µL of beetroot powder extract was added to a

50.0 mL Falcon tube and diluted to 3.0 mL with distilled water. After this, 250 µL of Folin-Ciocalteu reagent (diluted 2-fold before use) was added to the mixture and allowed to react for 5 minutes. Subsequently, 250 µL of 7% (w/v) sodium carbonate solution was added, and the mixture was topped up to 5 mL with distilled water. This mixture was then incubated at ambient temperature for 90 minutes to develop the color. Absorbance was then measured at 765 nm using a UV/Vis spectrophotometer (Jenway 6405 UV/Vis, UK). A calibration curve with gallic acid standards (0, 20, 40, 60, 80, and 100 mg/mL) was used to quantify the total phenolic content. Results were expressed as milligrams of gallic acid equivalent (GAE) per 100 mL on a dry weight basis (DW).

### 2.4.3 Total flavonoid measurement

The total flavonoid content was measured using a method adapted from Sinurat et al. (2022). To summarize, 125 µL of either catechin standard solution or beetroot powder extract was placed in a 5 mL disposable test tube and mixed with 0.625 mL of deionized water and 37.5 µL of 5% (w/v) sodium nitrite solution. The reaction proceeded at room temperature for 6 minutes, after which 75 µL of 10% (w/v) aluminium chloride was added. The mixture was left to react for another 6 minutes before adding 0.25 mL of 4.0M sodium hydroxide. Finally, 0.4 mL of distilled water was added, and the absorbance was recorded at 510 nm using a UV/Vis spectrophotometer (Jenway 6405 UV/Vis, UK). A standard calibration curve was created using varying concentrations of catechin (ranging from 0.2 to 1.00 mg/mL). The total flavonoid content was expressed as milligrams of catechin equivalents per 100 mL of beetroot extract (mg CE/100 mL) on a dry weight basis (DW).

### 2.4.4 Measurement of Oxalates

The oxalate content of the samples was determined using a method similar to the classical titrimetric method described by Karamad et al. (2019). For one hour, 2.0 g of beetroot sample was digested with 10 mL of 6M hydrochloric acid. After cooling, the mixture was brought to a final volume of 250 mL with distilled water and filtered. Two portions of 125 mL were taken from this filtrate and placed in beakers. 3-4 drops of methyl red indicator were added to each portion. Concentrated ammonium hydroxide was added drop by drop until the solution changed from salmon pink to pale yellow, and the pH was recorded. Each portion was then heated to 90°C, cooled, and filtered to remove any precipitate. The filtrate was reheated to 90°C, and 10 mL of 5% calcium chloride solution was added while stirring continuously. The resulting solution was decanted, and the precipitate was dissolved entirely in 10 mL of 20% (v/v) sulfuric acid solution. This solution was then topped up to 300 mL with distilled water. An aliquot of 125 mL of this filtrate was heated until near boiling and titrated against 0.05 M standardized potassium permanganate until a pink color persisted

for 30 seconds at the endpoint. The oxalate content was calculated using a specific formula.

$$\text{Oxalate content} = \frac{T \times V_{me} \times Df \times 105}{ME \times Mf}$$

Where: T = Titer value of Potassium permanganate,  $V_{me}$  = volume- mass equivalent (that is, 1 ml of 0.05 m Potassium permanganate, = 0.00228 g of anhydrous oxalic acid), Df= dilute factor ( $V_t/A$  that is, total volume of titrate/ Aliquot used), Mf= mass of sample used, ME = molar equivalence of Potassium permanganate in oxalate concentration in  $g/dm^3$ .

## 2.5 Nutritional analysis

### 2.5.1 Digestion and Mineral Content Analysis

The dried, ground beetroot sample underwent complete digestion using a solution composed of 50% nitric acid ( $HNO_3$ ) and 30% hydrogen peroxide ( $H_2O_2$ ), following a modified version of the method described by He et al. (2013). Briefly, 1.0 g of the ground sample was placed in a 50 mL grainer falcon tube. Approximately 0.5 mL of 50%  $HNO_3$  and 0.2 mL of 30%  $H_2O_2$  were added to the sample. The mixture was left overnight to allow for cold digestion. The next day, the samples were subjected to warm digestion on a heating block, initially at 80°C for 30 minutes, then increasing to 125°C for 2 hours. Once the solution became clear with a slightly yellowish tint, digestion was halted, and the volume was brought up to 25 mL with deionized water. The samples were then stored at room temperature in preparation for further analysis.

The digested samples were transferred into vials and placed in an autosampler (SPS 4 Autosampler, Agilent Technologies). Mineral content and control samples were analyzed using microwave plasma atomic emission spectroscopy (4200 MP-AES, Agilent Technologies). The concentration of each analyte was calculated in parts per million (PPM). The final concentration in mg/kg was determined using the formula:

Final Concentration (mg/kg) =

$$\text{Sample Concentration (PPM)} \times \frac{\text{Total Dilution}}{\text{Weight of Sample}}$$

## 2.6 Data analysis

Experimental data were presented as mean  $\pm$  standard deviation of triplicate measurements and analyzed using IBM SPSS Statistics version 16 (IBM Corporation, New York, USA). Statistical significance was determined at  $p \leq 0.05$  using Student's t-test and one-way ANOVA, followed by Fisher's Least Significant Difference test (LSD) for post hoc analysis.

## 3 Results and Discussion

### 3.1 Functional and physicochemical properties

Table 1 illustrates the significant influence of preparation and drying methods on beetroot powder's functional and physicochemical properties.

#### 3.1.1 Water Activity

The water activity of beetroot samples decreased significantly ( $p < 0.05$ ) with boiling and drying methods. The highest values were observed in boiled freeze-dried samples ( $0.54 \pm 0.00$  for Detroit Dark Red and  $0.52 \pm 0.00$  for Crimson Globe). The lowest water activity values were reported in boiled sun-dried ( $0.25 \pm 0.01$ ) and sun-dried ( $0.23 \pm 0.01$ ) samples for the Crimson Globe variety. This reduction in water activity improves shelf-life stability by inhibiting microbial growth, which aligns with the findings of Stavropoulou and Bezirtzoglou (2019), who emphasized the importance of low water activity in food preservation.

#### 3.1.2 Bulk Density

The bulk density varied significantly ( $p < 0.05$ ) depending on the preparation and drying methods. The boiled oven-dried samples exhibited the highest bulk density ( $0.86 \pm 0.01$  for Detroit Dark

Table 1 Functional and physicochemical properties of crimson globe and detroit dark red beetroot powders

Treatment	Bulk Density(g/mL)		WaterAbsorptivity index		Water Solubility Index (%)		Water activity ( $a_w$ )	
	DetR	CrimG	DetR	CrimG	DetR	CrimG	DetR	CrimG
FDR	$0.18 \pm 0.03^c$	$0.22 \pm 0.02^d$	$4.59 \pm 0.08^c$	$5.09 \pm 0.36^c$	$39.00 \pm 8.00^f$	$41.00 \pm 4.00^d$	$0.52 \pm 0.02^b$	$0.52 \pm 0.01^b$
FDB	$0.27 \pm 0.01^c$	$0.26 \pm 0.04^d$	$8.84 \pm 0.50^a$	$8.40 \pm 0.48^a$	$64.00 \pm 10.00^d$	$44.00 \pm 6.00^d$	$0.54 \pm 0.03^b$	$0.52 \pm 0.02^b$
ODR	$0.66 \pm 0.02^b$	$0.69 \pm 0.01^c$	$3.35 \pm 0.07^d$	$6.49 \pm 0.57^b$	$77.00 \pm 6.00^b$	$78.00 \pm 5.00^a$	$0.29 \pm 0.01^{cd}$	$0.31 \pm 0.03^c$
ODB	$0.86 \pm 0.02^a$	$0.79 \pm 0.02^b$	$4.73 \pm 0.17^c$	$4.74 \pm 0.08^d$	$67.00 \pm 11.00^d$	$72.00 \pm 4.00^b$	$0.33 \pm 0.02^c$	$0.37 \pm 0.02^c$
SDR	$0.68 \pm 0.01^b$	$0.74 \pm 0.01^b$	$5.34 \pm 0.12^b$	$5.44 \pm 0.10^c$	$78.00 \pm 5.00^a$	$75.00 \pm 4.00^b$	$0.26 \pm 0.01^d$	$0.23 \pm 0.01^d$
SDB	$0.82 \pm 0.02^a$	$0.90 \pm 0.02^a$	$5.26 \pm 0.19^b$	$4.03 \pm 0.03^f$	$71.00 \pm 8.00^c$	$60.00 \pm 6.00^c$	$0.25 \pm 0.01^d$	$0.26 \pm 0.02^f$

Values represent means  $\pm$  standard deviation from three separate experiments, different superscript letters in the same column indicate significant differences ( $P < 0.05$ ); here DetR (Detroit Dark Red), CrimG (Crimson Globe), FDR (Freeze-Dried Raw), FDB (Freeze-Dried Boiled), ODR (Oven-Dried Raw), ODB (Oven-Dried Boiled), SDB (Sun-Dried Boiled), SDR (Sun-Dried Raw)



Red and  $0.90 \pm 0.02$  for Crimson Globe), while the boiled freeze-dried samples had lower bulk densities. The higher bulk densities in the boiled samples indicate a more compact structure, which is in line with the findings of Hamid and Mohamed Nour (2018), who observed that drying methods significantly impact the physical properties of beetroot slices.

### 3.1.3 Water Absorption and Solubility

The highest water absorption index was found in the boiled freeze-dried samples for both varieties, while the lowest was observed in the oven-dried Detroit Dark Red and boiled sun-dried Crimson Globe samples. On the other hand, the water solubility index was highest in the sun-dried Detroit Dark Red and oven-dried Crimson Globe samples, with the lowest values in freeze-dried samples. The porous structure of freeze-dried products allows for higher water uptake, which is beneficial for rehydration (Razzak 2024). This is crucial due to the impact of the speed at which a powder dissolves in water on its rehydration properties and the quality of the finished product (Grabowski et al. 2006; Kim et al. 2012).

### 3.2 Color

Table 2 shows the color characteristics of beetroot powders based on different processing methods. The lightness (L) values increased when the beetroot was boiled and dried, with the highest values reported in oven-dried and freeze-dried boiled samples. The redness (a) values were highest in the freeze-dried samples, while sun-dried and oven-dried samples showed a significant reduction. The yellowness (b) values increased significantly with sun and oven drying, indicating a relationship with drying temperature. The pigment analysis revealed that the betacyanin content in freeze-dried samples was similar to that of fresh samples but decreased as the temperature increased. Conversely, the betaxanthin content increased with higher drying

temperatures. This suggests that betacyanin, the red pigment, is sensitive to heat and degrades with increased temperature, possibly converting into betaxanthin (Gokhale and Lele 2011). The increase in yellow betaxanthin could be due to the chemical transformation of betacyanin or enhanced extractability at higher temperatures. These findings are consistent with the observation that freeze-drying preserves texture and minimizes shrinkage, unlike sun and oven drying, which cause considerable shrinkage (Hamid and Mohamed Nour 2018).

### 3.3 Nutritional Characteristics

The assessed nutrients included mineral levels, oxalates, and the total contents of phenolics and flavonoids in various dried samples of beetroots. The results of these analyses are presented in Tables 3, 4, and 5.

#### 3.3.1 Mineral Content

Table 3 shows the mineral content of fresh and dried beetroot samples (calcium, iron, magnesium, zinc, and phosphorus). The study found a significant increase ( $p < 0.05$ ) in the calcium content after drying, with the highest level of calcium reported in oven-dried boiled Crimson Globe and sun-dried boiled Detroit Dark Red samples. These results are supported by Asante et al. (2024), who found that boiling before drying enhanced calcium content. Iron also significantly increased ( $p < 0.05$ ) in boiled-dried samples, with the highest levels in boiled and sun-dried samples, consistent with the findings of Joshi and Mehta (2010). Additionally, there was a significant increase in the levels of magnesium and zinc in boiled dried samples, particularly in oven-dried boiled samples, which aligns with the results of Alassane et al. (2022). Furthermore, fresh samples had higher phosphorus content than dried samples ( $p < 0.05$ ), contrary to the findings of Asante et al. (2024).

Table 2 Colour characteristics of the crimson globe and detroit dark red beetroot varieties

Treatment	L* (Lightness)		a* (Redness)		b* (Yellowness)	
	DetR	CrimG	DetR	CrimG	DetR	CrimG
FB	34.55±0.07 <sup>b</sup>	35.65±0.35 <sup>b</sup>	7.0±0.42 <sup>c</sup>	8.55±0.42 <sup>b</sup>	8.2±0.14 <sup>c</sup>	9.25±0.70 <sup>b</sup>
FDR	35.40±0.40 <sup>a</sup>	38.10±0.20 <sup>a</sup>	11.50±0.40 <sup>b</sup>	12.40±0.00 <sup>a</sup>	7.80±0.10 <sup>f</sup>	8.85±0.10 <sup>c</sup>
FDB	34.40±0.20 <sup>b</sup>	38.70±0.20 <sup>a</sup>	15.10±0.40 <sup>a</sup>	14.80±0.10 <sup>a</sup>	7.65±0.10 <sup>f</sup>	9.15±0.10 <sup>b</sup>
ODR	36.00±0.11 <sup>a</sup>	38.60±0.20 <sup>a</sup>	6.50±0.00 <sup>c</sup>	6.20±0.30 <sup>c</sup>	10.30±0.00 <sup>a</sup>	11.65±0.20 <sup>a</sup>
ODB	34.60±0.20 <sup>b</sup>	37.40±0.10 <sup>a</sup>	2.70±0.10 <sup>f</sup>	2.70±0.20 <sup>g</sup>	8.60±0.00 <sup>c</sup>	11.40±0.00 <sup>a</sup>
SDR	35.60±0.10 <sup>a</sup>	35.50±0.10 <sup>b</sup>	7.20±0.40 <sup>c</sup>	6.90±0.30 <sup>c</sup>	9.70±0.00 <sup>b</sup>	10.30±0.10 <sup>a</sup>
SDB	32.50±0.20 <sup>c</sup>	32.80±0.08 <sup>c</sup>	4.70±0.20 <sup>d</sup>	4.40±0.00 <sup>f</sup>	8.05±0.10 <sup>c</sup>	8.30±0.00 <sup>c</sup>

Values are presented as means ± standard deviation from three independent experiments, different superscript letters in the same column denote significant differences ( $p < 0.05$ ), here DetR (Detroit Dark Red), CrimG (Crimson Globe), FDR (Freeze-Dried Raw), FDB (Freeze-Dried Boiled), ODR (Oven-Dried Raw), ODB (Oven-Dried Boiled), SDB (Sun-Dried Boiled), SDR (Sun-Dried Raw), FB (Fresh Beetroot)

Table 3 Mineral content of the processed crimson globe and Detroit dark red beetroot products

Treatment	Ca mg/100gDW		Fe mg/100gDW		Mg mg/100gDW		Zn mg/100gDW		P mg/100gDW	
	DetR	CrimG	DetR	CrimG	DetR	CrimG	DetR	CrimG	DetR	CrimG
FDR	72.65±2.55 <sup>f</sup>	103.89±6.5 <sup>d</sup>	2.94±0.9 <sup>d</sup>	5.71±0.5 <sup>d</sup>	144.36±2.8 <sup>c</sup>	130.23±10.8 <sup>d</sup>	4.62±0.92 <sup>c</sup>	6.63±0.4 <sup>b</sup>	146.02±1.9 <sup>f</sup>	105.56±4.5 <sup>f</sup>
FDB	117.97±1.3 <sup>c</sup>	105.31±5.9 <sup>d</sup>	5.72±0.6 <sup>b</sup>	5.10±1.0 <sup>f</sup>	171.35±27.4 <sup>b</sup>	147.96±5.28 <sup>c</sup>	6.21±0.2 <sup>b</sup>	5.90±0.1 <sup>c</sup>	167.68±4.8 <sup>c</sup>	149.92±1.6 <sup>d</sup>
F	100.74±3.3 <sup>d</sup>	124.24±1.4 <sup>a</sup>	4.19±0.2 <sup>c</sup>	7.23±0.8 <sup>b</sup>	183.03±17.8 <sup>a</sup>	183.73±11.9 <sup>a</sup>	3.83±0.7 <sup>d</sup>	4.58±0.2 <sup>d</sup>	213.24±5.1 <sup>a</sup>	240.69±13.9 <sup>a</sup>
FB	118.74±9.9 <sup>c</sup>	110.52±5.1 <sup>c</sup>	6.36±2.0 <sup>b</sup>	5.47±0.3 <sup>d</sup>	154.12±1.4 <sup>c</sup>	143.72±2.7 <sup>c</sup>	6.26±0.4 <sup>b</sup>	4.35±0.6 <sup>d</sup>	217.09±1.7 <sup>a</sup>	184.92±6.4 <sup>b</sup>
ODR	117.35±2.4 <sup>c</sup>	98.81±3.6 <sup>f</sup>	4.55±0.3 <sup>c</sup>	5.72±0.4 <sup>d</sup>	166.31±21.4 <sup>b</sup>	154.43±23.2 <sup>b</sup>	5.23±0.1 <sup>b</sup>	5.77±0.1 <sup>c</sup>	211.19±4.4 <sup>a</sup>	148.37±1.2 <sup>a</sup>
ODB	143.89±4.1 <sup>a</sup>	227.25±8.5 <sup>a</sup>	6.10±0.1 <sup>b</sup>	6.68±0.7 <sup>c</sup>	195.50±18.9 <sup>a</sup>	190.10±29.3 <sup>a</sup>	6.83±0.3 <sup>a</sup>	8.72±0.3 <sup>a</sup>	192.55±4.58 <sup>b</sup>	197.72±9.46 <sup>b</sup>
SDR	126.10±4.8 <sup>b</sup>	118.64±7.5 <sup>b</sup>	8.49±0.3 <sup>a</sup>	7.54±0.3 <sup>b</sup>	131.58±22.8 <sup>d</sup>	113.10±6.9 <sup>f</sup>	6.14±0.3 <sup>b</sup>	5.35±0.2 <sup>c</sup>	168.97±7.85 <sup>c</sup>	153.01±0.4 <sup>c</sup>
SDB	165.19±3.8 <sup>a</sup>	128.10±8.4 <sup>a</sup>	9.25±0.7 <sup>a</sup>	9.51±0.7 <sup>a</sup>	153.17±18.1 <sup>c</sup>	129.63±20.1 <sup>d</sup>	5.95±0.1 <sup>b</sup>	4.61±0.1 <sup>d</sup>	166.80±5.6 <sup>c</sup>	158.86±2.7 <sup>c</sup>

Values are presented as means ± standard deviation from three independent experiments, different superscript letters in the same column denote significant differences ( $p < 0.05$ ), DetR (Detroit Dark Red), CrimG (Crimson Globe), FDR (Freeze-Dried Raw), FDB (Freeze-Dried Boiled), ODR (Oven-Dried Raw), ODB (Oven-Dried Boiled), SDB (Sun-Dried Boiled), SDR (Sun-Dried Raw), F (Fresh Non-Boiled Beetroot), FB (Fresh Boiled Beetroot)

Table 4 Total phenolic and flavonoid content of the crimson globe and detroit dark red beetroot powder

Treatment	Total phenolic content mg GAE 100mg <sup>-1</sup> DW		Flavonoid content (mg CE 100 mg <sup>-1</sup> ) DW	
	DetR	CrimG	DetR	CrimG
FDR	0.53±0.00 <sup>b</sup>	0.41± 0.01 <sup>d</sup>	0.46±0.01 <sup>e</sup>	0.42±0.01 <sup>f</sup>
FDB	0.74±0.08 <sup>a</sup>	0.68±0.02 <sup>b</sup>	1.84±0.02 <sup>a</sup>	1.00±0.02 <sup>a</sup>
ODR	0.78±0.01 <sup>a</sup>	0.56±0.02 <sup>c</sup>	0.98±0.02 <sup>c</sup>	0.75±0.02 <sup>d</sup>
ODB	0.55±0.02 <sup>b</sup>	0.48±0.01 <sup>d</sup>	0.56±0.01 <sup>d</sup>	0.88±0.01 <sup>c</sup>
SDR	0.50±0.03 <sup>b</sup>	0.35±0.03 <sup>f</sup>	0.57±0.04 <sup>d</sup>	0.45±0.03 <sup>f</sup>
SDB	0.51±0.02 <sup>b</sup>	0.80±0.04 <sup>a</sup>	0.63±0.03 <sup>f</sup>	1.01±0.02 <sup>a</sup>

Values are presented as means ± standard deviation from three independent experiments, different superscript letters in the same column denote significant differences ( $p < 0.05$ ), here DetR (Detroit Dark Red), CrimG (Crimson Globe), FDR (Freeze-Dried Raw), FDB (Freeze-Dried Boiled), ODR (Oven-Dried Raw), ODB (Oven-Dried Boiled), SDB (Sun-Dried Boiled), SDR (Sun-Dried Raw), F (Fresh Non-Boiled Beetroot)

Table 5 Oxalate content of the crimson globe and detroit dark red beetroot powder

Treatment	Oxalate content (calcium oxalate) mg/100g					
	Insoluble		Soluble		Total	
	DetR	CrimG	DetR	CrimG	DetR	CrimG
FDR	13333.30±721.70 <sup>a</sup>	9583.30±721.70 <sup>a</sup>	5833.30±721.70 <sup>a</sup>	5416.70±721.70 <sup>a</sup>	19166.70±721.70 <sup>a</sup>	15000.00±1250.00 <sup>a</sup>
FDB	10833.30±721.70 <sup>b</sup>	5416.70±721.70 <sup>b</sup>	4166.70±721.70 <sup>b</sup>	5416.70±721.70 <sup>a</sup>	15000.00±1250.00 <sup>b</sup>	10833.30±721.70 <sup>b</sup>
F	7083.33±721.70 <sup>c</sup>	7500±721.00 <sup>b</sup>	2500±0.7210 <sup>c</sup>	1666.67±721.70 <sup>c</sup>	9583.33±721.69 <sup>c</sup>	9166.67±721.69 <sup>c</sup>
FB	5000±721.70 <sup>g</sup>	4166.67±721.67 <sup>d</sup>	1666.67±721.70 <sup>f</sup>	1250.00±721.00 <sup>b</sup>	6666.67±721.67 <sup>f</sup>	5416.67±721.69 <sup>f</sup>
ODR	6666.70±721.70 <sup>d</sup>	4583.30±721.70 <sup>f</sup>	1666.70±721.70 <sup>f</sup>	1666.70±721.70 <sup>c</sup>	8333.30±1443.40 <sup>d</sup>	6250.00±721.70 <sup>d</sup>
ODB	7083.30±721.70 <sup>c</sup>	6666.70±721.70 <sup>c</sup>	2500.00±0.00 <sup>c</sup>	2500.00±721.70 <sup>b</sup>	9583.30±721.70 <sup>c</sup>	9166.70±721.70 <sup>c</sup>
SDR	7083.30±721.70 <sup>c</sup>	7500.00±721.70 <sup>b</sup>	2083.30±721.70 <sup>d</sup>	1666.70±721.70 <sup>c</sup>	9166.70±721.70 <sup>c</sup>	9166.70±721.70 <sup>c</sup>
SDB	5416.70±721.70 <sup>f</sup>	5000.00±721.70 <sup>b</sup>	2500.00±721.60 <sup>c</sup>	1666.7±721.70 <sup>c</sup>	7916.70±721.70 <sup>b</sup>	6666.70±721.70 <sup>b</sup>

Values are presented as means ± standard deviation from three independent experiments, different superscript letters in the same column denote significant differences ( $p < 0.05$ ), here DetR (Detroit Dark Red), CrimG (Crimson Globe), FDR (Freeze-Dried Raw), FDB (Freeze-Dried Boiled), ODR (Oven-Dried Raw), ODB (Oven-Dried Boiled), SDB (Sun-Dried Boiled), SDR (Sun-Dried Raw), F (Fresh Non-Boiled Beetroot), FB (Fresh Boiled Beetroot)

### 3.3.2 Total Phenolic Content (TPC)

The processing methods significantly impacted the total phenolic content (TPC), with the highest levels of TPC reported in raw oven-dried beetroot powder for dark red and boiled sun-dried samples for light red beetroot powder (Table 4). These findings are consistent with those of Guldiken et al. (2016), who observed a 36% increase in TPC in dried red beetroot compared to fresh samples. However, it differs from the results of Youssef and Mokhtar (2014), who noted a reduction in TPC during drying.

### 3.3.3 Total Flavonoid Content (TFC)

The treatment methods significantly affected TF content ( $p < 0.05$ ). The highest TF content was found in boiled freeze-dried dark red samples and boiled sun-dried crimson globe samples (Table 4). The influence of drying methods on flavonoid content has been extensively researched. Mandale et al. (2023) underscored the importance of drying methods in preserving nutritional quality; these findings are also consistent with those of Liu et al. (2021).

### 3.3.4 Oxalates

Table 5 displays the oxalate content of beetroot powders. The total oxalate content varied significantly among treatments and varieties, with the highest levels found in raw freeze-dried samples. Oxalic acid, known to chelate metal cations, can contribute to the formation of kidney stones (Holmes and Assimos 2004; Weaver et al. 2006). The observed oxalate levels are higher than those reported by Wruss et al. (2015), which aligns with the typically high oxalic acid content found in beetroots (Duke 2001).

### Conclusion

The study showed that beetroot is a rich source of essential minerals such as iron, zinc, phosphorus, magnesium, calcium, phenolic compounds, and flavonoids. These nutrients are important for physiological functions and overall health. The research also found that how beetroot powder is prepared and dried significantly affects these properties. Specifically, the treatment methods can protect or enhance the physical and micronutrient properties, especially iron, while potentially reducing phytochemicals affecting iron bioavailability. This understanding is crucial for developing iron-rich beetroot products that can effectively supplement dietary iron intake, especially for adolescent school children.

### Conflict of interest

The authors declare that there is no conflict of interest concerning the publication of this research.

### References

- Alassane, C. T., Touré, A., Fabrice, Z. A., Claude, K. A. L., Souleymane, M., & Adama, C. (2022). Effect of three drying modes on nutritive and antinutritive properties of leafy vegetables consumed in Northern Côte d'Ivoire. *EAS Journal of Nutrition and Food Sciences*, 4(4), 102-111. <https://doi.org/10.36349/easjnfs.2022.v04i04.001>
- Ali, Z., & Bilal, A. (2023). Efficacy assessment of beetroot extract in regulating iron deficiency anemia in anemic rats. *Pakistan Journal of Science*, 75(1), 88-93. <https://doi.org/10.57041/pjs.v75i1.826>

- Alonzo-Macías, M., Cardador-Martínez, A., Besombes, C., Allaf, K., Tejada-Ortigoza, V., Soria-Mejía, M., & Téllez-Pérez, C. (2020). Instant controlled pressure drops as blanching and texturing pre-treatment to preserve the antioxidant compounds of red dried beetroot (*Beta vulgaris* L.). *Molecules*, 25(18), 4132. <https://doi.org/10.3390/molecules25184132>
- Asante, J. M., Amaglo, N., & Tandoh, P. K. (2024). Effect of different drying methods on the mineral composition of three indigenous leafy vegetables. *International Journal of Plant & Soil Science*, 36(5), 621-632. <https://doi.org/10.9734/ijps/2024/v36i54560>
- Duke, J. A. (2001). *Handbook of Phytochemical Constituents of GRAS Herbs and Other Economic Plants* (2nd ed.). Routledge. <https://doi.org/10.1201/9780203752623>
- Gokhale, S. V., & Lele, S. S. (2011). Dehydration of red beet root (*Beta vulgaris*) by hot air drying: Process optimization and mathematical modeling. *Food Science and Biotechnology*, 20(4), 955. <https://doi.org/10.1007/s10068-011-0132-4>
- Grabowski, J., Truong, B., & Daubert, C. (2006). Spray-drying of amylase hydrolyzed sweet potato puree and physicochemical properties of powder. *Journal of Food Science*, 71(5) E209-E217. <https://doi.org/10.1111/j.1750-3841.2006.00036.x>
- Guldiken, B., Toydemir, G., Nur Memis, K., Okur, S., Boyacioglu, D., & Capanoglu, E. (2016). Home-processed red beetroot (*Beta vulgaris* L.) products: Changes in antioxidant properties and bioaccessibility. *International Journal of Molecular Sciences*, 17(6), 858. <https://doi.org/10.3390/ijms17060858>
- Hamid, M. G., & Mohamed Nour, A. A. A. (2018). Effect of different drying methods on quality attributes of beetroot (*Beta vulgaris*) slices. *World Journal of Science, Technology and Sustainable Development*, 15(3), 287-298. <https://doi.org/10.1108/WJSTSD-11-2017-0043>
- He, Z., Lan, M., Lu, D., Zhao, H., & Yuan, H. (2013). Antioxidant activity of 50 traditional chinese medicinal materials varies with total phenolics. *Chinese Medicine*, 04(04), 148-156. <https://doi.org/10.4236/cm.2013.44018>
- Holmes, R. P., & Assimios, D. G. (2004). The impact of dietary oxalate on kidney stone formation. *Urological Research*, 32(5), 311-316. <https://doi.org/10.1007/s00240-004-0437-3>
- Joshi, P., & Mehta, D. (2010). Effect of dehydration on the nutritive value of drumstick leaves. *Journal of Metabolomics and Systems Biology*, 1(1), 5-9. <https://doi.org/10.5897/JMSB.9000003>
- Karamad, D., Khosravi-Darani, K., Hosseini, H., & Tavasoli, S. (2019). Analytical procedures and methods validation for oxalate content estimation. *Biointerface Research in Applied Chemistry*, 9(5), 4305-4310. <https://doi.org/10.33263/briac95.305310>
- Kim, S., Choi, Y., Lee, H., Lee, S., Ahn, J., Noh, B., & Min, S. (2012). Physicochemical properties of jujube powder from air, vacuum, and freeze drying and their correlations. *Journal of the Korean Society for Applied Biological Chemistry*, 55(2), 271-279. <https://doi.org/10.1007/s13765-012-1039-3>
- Kovarovič, J., Bystrická, J., Tomáš, J., & Lenková, M. (2017). The influence of variety on the content of bioactive compounds in beetroot (*Beta vulgaris* L.). *Potravinarstvo Slovak Journal of Food Sciences*, 11(1), 106-112. <https://doi.org/10.5219/702>
- Liu, Y., Sabadash, S., & Duan, Z. (2021). Research of physicochemical properties and antioxidant activity of beetroots as affected by vacuum microwave drying conditions. *Technology Audit and Production Reserves*, 5(3(61)), 40-45. <https://doi.org/10.15587/2706-5448.2021.243069>
- Liu, Y., Sabadash, S., Duan, Z., & Gao, D. (2022). Influence of different microwave-assisted drying methods on the physical properties, bioactive compounds and antioxidant activity of beetroots. *Eastern-European Journal of Enterprise Technologies*, 1(11(115)), 15-25. <https://doi.org/10.15587/1729-4061.2022.251942>
- Mandale, N., Atkan, A., Kumar, S., & Kumar, N. (2023). Drying kinetics and quality assessment of refractance window dried beetroot. *Journal of Food Process Engineering*, 46(7) e14332. <https://doi.org/10.1111/jfpe.14332>
- Mudgal, D. (2023). Effect of different pre-treatments and temperatures on drying characteristics of beetroot slices. *Current Journal of Applied Science and Technology*, 42(28), 1-10. <https://doi.org/10.9734/cjast/2023/v42i284196>
- Özderin, S. (2024). Chemical properties, antioxidant, and antimicrobial activities of fruit extracts of *Crataegus monogyna* var. *odensisii*. *Bioresources*, 19(1), 1542-1557. <https://doi.org/10.15376/biores.19.1.1542-1557>
- Peters, A., Tullio, L., Lima, R., Carvalho, C., Barros, Z., Neta, E., & Ferreira, S. (2021). Physicochemical properties and sensory acceptability of beetroot chips pre-treated by osmotic dehydration and ultrasound. *Brazilian Journal of Food Technology*, 24, e2020068. <https://doi.org/10.1590/1981-6723.06820>
- Preethi, R., Deotale, S., Moses, J., & Anandharamakrishnan, C. (2020). Conductive hydro drying of beetroot (*Beta vulgaris* L) pulp: Insights for natural food colorant applications. *Journal of Food Process Engineering*, 43(12), e13557. <https://doi.org/10.1111/jfpe.13557>

- Razzak, M. (2024). Evaluating the bioactive compounds of beetroot and their pharmacological activities in promoting health. *European Journal of Health Sciences*, 10(1), 13-30. <https://doi.org/10.47672/ejhs.1802>
- Roongruangsri, W., & Bronlund, J. E. (2016). Effect of air-drying temperature on physicochemical, powder properties and sorption characteristics of pumpkin powders. *International Food Research Journal*, 23(3), 962-972.
- Sarkar, A., Rashid, M., Musarrat, M., & Billah, M. (2021). Drying effects on phytochemicals and antioxidant properties of ginger powder undergoing different drying techniques. *European Journal of Agriculture and Food Sciences*, 3(1), 128-131. <https://doi.org/10.24018/ejfood.2021.3.1.236>
- Şeremet, L., & Oana-Viorela, N. (2020). Red beetroot: Composition and health effects - A review. *Journal of Nutritional Medicine and Diet Care*, 6, 043. <https://doi.org/10.23937/2572-3278.1510043>
- Serna-Vázquez, J., Ahmad, M., Boczkaj, G., & Castro-Muñoz, R. (2021). Latest insights on novel deep eutectic solvents (des) for sustainable Extraction of phenolic compounds from natural sources. *Molecules*, 26(16), 5037. <https://doi.org/10.3390/molecules26165037>
- Sinurat, J., Karo, R., & Berutu, R. (2022). Determination of total flavonoid content of saputangan leaves (*Maniltoa grandiflora* (a. gray) scheff) and its ability as antioxidant. *Jurnal Sains Dan Kesehatan*, 4(3), 275-279. <https://doi.org/10.25026/jsk.v4i3.1042>
- Stavropoulou, E., & Bezirtzoglou, E. (2019). Predictive Modeling of Microbial Behavior in Food. *Foods* (Basel, Switzerland), 8(12), 654. <https://doi.org/10.3390/foods8120654>
- Székely, D., & Máté, M. (2023). Red beetroot (*Beta vulgaris* L.). *IntechOpen*. <https://doi.org/10.5772/intechopen.106692>
- Wang, J., Jayaprakasha, G., & Patil, B. (2020). Uplc-qtof-ms fingerprinting combined with chemometrics to assess the solvent extraction efficiency, phytochemical variation, and antioxidant activities of *Beta vulgaris* L. *Journal of Food and Drug Analysis*, 28(2), 217-230. <https://doi.org/10.38212/2224-6614.1056>
- Weaver, C. M., Heaney, R. P., & Nickel, P. I. (2006). Calcium bioavailability from high oxalate vegetables: Chinese vegetables, sweet potatoes and rhubarb. *Journal of Food Science*, 62(3), 524-525. <https://doi.org/10.1111/j.1365-2621.1997.tb04421.x>
- Wruss, J., Waldenberger, G., Huemer, S., Uygun, P., Lanzerstorfer, P., Müller, U., Höglinger, O., & Weghuber, J. (2015). Compositional characteristics of commercial beetroot products and beetroot juice prepared from seven beetroot varieties grown in Upper Austria. *Journal of Food Composition and Analysis*, 42, 46-55. <https://doi.org/10.1016/j.jfca.2015.03.005>
- Youssef, K. M., & Mokhtar, S. M. (2014). Effect of drying methods on the antioxidant capacity, color and phytochemicals of *Portulaca oleracea* L. leaves. *Journal of Nutrition and Food Science*, 4(6), 322. <https://doi.org/10.4172/2155-9600.1000322>





## Journal of Experimental Biology and Agricultural Sciences

<http://www.jebas.org>

ISSN No. 2320 – 8694

### Clonal propagated 'Ek Pothi Lehsun' as a potential antifungal agent against *Candida* sp.

Ankita Sharma, Shardulya Shukla, Manoj Kumar Patel, Om Prakash Chaurasia, Shweta Saxena\*

Defence Institute of High Altitude Research (DIHAR), Defence Research and Development Organization, C/o 56 APO, Leh-Ladakh-194101, India

Received – January 31, 2024; Revision – May 19, 2024; Accepted – June 05, 2024

Available Online – July 15, 2024

DOI: [http://dx.doi.org/10.18006/2024.12\(3\).408.418](http://dx.doi.org/10.18006/2024.12(3).408.418)

#### KEYWORDS

Ek Pothi Lehsun

Micropropagation

Antifungal activity

#### ABSTRACT

'Ek Pothi Lehsun', also known as snow mountain garlic, is a type of garlic grown in the high mountainous region of Jammu and Kashmir state of India. The present study aimed to develop a protocol for propagating snow mountain garlic *in-vitro* using corm seed as an explant. The study also assessed the antifungal potential of *in vitro*-grown bulbils against different *Candida* species. Four different concentrations of NAA and 2,4-D were tested for their effectiveness in promoting root formation, and eighteen different combinations of BAP ( $\mu\text{M}$ ), KN ( $\mu\text{M}$ ) and TDZ ( $\mu\text{M}$ ) were investigated for effective proliferation of shoots with varied lengths. Shoot with maximum length ( $5.03\pm 1.40$ ) was obtained in MS medium containing  $1.0 \mu\text{M}$  TDZ after 24 days of inoculation, whereas MS basal media was found effective for rooting plantlets. Rooted micro shoots were acclimatized successfully in hardening trays with a percent survival of nearly 80%. Seven different concentrations of Sucrose, i.e. 5%, 7%, 10%, 15%, 17%, 20%, and 25% were investigated for effective bulbil formation. Bulbil with a maximum diameter of 0.86 cm was obtained in 20% sucrose-containing MS media in 5 days. Further, the antifungal potential of aqueous extract (TC-SMG) of *in vitro* grown bulbils was investigated against three *Candida* sp. A zone of inhibition of  $22.30\pm 0.33$  mm,  $17.3\pm 0.33$  mm and  $19.3\pm 0.33$  mm was observed against *C. albicans*, *C. tropicalis* and *C. glabrata* respectively, by using 200 mg/mL extract after 24 hrs depicting the remarkable potential of TC-SMG as an antifungal agent. *In vitro* culture of snow mountain garlic has demonstrated promising antifungal properties against *Candida* species.

\* Corresponding author

E-mail: [drshwetaxena.dihar@gov.in](mailto:drshwetaxena.dihar@gov.in) (Shweta Saxena)

Peer review under responsibility of Journal of Experimental Biology and Agricultural Sciences.

Production and Hosting by Horizon Publisher India [HPI]  
(<http://www.horizonpublisherindia.in/>).  
All rights reserved.

All the articles published by [Journal of Experimental Biology and Agricultural Sciences](#) are licensed under a [Creative Commons Attribution-NonCommercial 4.0 International License](#) Based on a work at [www.jebas.org](http://www.jebas.org).



## 1 Introduction

For millennia, plants have served humanity as sources of beneficial drugs, food, flavouring agents, colourants, binders and lubricants. They have been used to develop and maintain various communities and cultures' physical, psychological and spiritual health (Davis and Choicy 2024). *Allium* is one such plant genera with many valuable medicinal properties. Several health benefits of this plant species have already been documented in Charaka Samhita, one of the oldest Indian medicinal treatises (Devi et al. 2014). *Allium* has been recognized as one of the initial instances of the plant to be utilized for medicinal purposes. This genus includes many economically important crops like garlic, onion, and other ornamental species (Devi et al. 2014). *Allium sativum* (garlic) is a valuable bulbous crop of this genus, widely used as a spice/condiment throughout India. It is a natural antibiotic and a remedy for various physical ailments (Parekh and Chanda 2007; Papu et al. 2014). Earlier, various civilizations, viz., Egyptian, Phoenicians, Greek, Indian, Roman, Babylonian, and Chinese, have demonstrated this plant species to be used for curing many ailments such as heart disorders, arthritis, pulmonary disorders, uterine growths, skin disease, symptoms of ageing, diarrhoea, headache, worms and tumours. Egyptians have been demonstrated to provide garlic to the labour force involved in heavy pyramid construction work (Woodward 1996; Sasi et al. 2021).

'Ek pothi lehsun', commonly known as snow mountain garlic or 'Kashmiri garlic', is a type of garlic found to grow in mountainous regions of the Himalayas at an altitude of 1800 meters from MSL. Solid cloves of snow mountain garlic are the cold, hardy corm seeds developed from the elephant garlic, planted in September or October and harvested in the summers. If left in the field, each clove miraculously transforms into complete elephant garlic in the following year. Earlier, mountaineers were found to use it to enhance their energy levels and remove toxins in extreme environmental conditions ([https://specialtyproduce.com/produce/Kashmiri\\_Garlic\\_13356.php](https://specialtyproduce.com/produce/Kashmiri_Garlic_13356.php)).

*Candida* sp. is an opportunistic fungal pathogen of the human oral-gastrointestinal tract. These pathogenic species have been recognized as one of the most prevalent reasons for nosocomial infections in patients (Lemar et al. 2002). Therefore, it is also known as "the disease of the diseased" (Al-Dorzi et al. 2020). Antifungal agents such as flucytosine and amphotericin B (AmB) are conventionally used to treat such infections (Kim et al. 2012). However, with the increase in fungal resistance to conventional medicines and the side effects of using these medicines, especially in immune-compromised patients, there is an urgent necessity to hunt for new sources of alternative medicines. Various studies have indicated the hidden power of garlic (*A. sativum*) as an alternative source of antimicrobial properties (Bayan et al. 2020). It has been found to contain a compound named 'allicin' containing

diallylsulphide and thiosulfinate, which has been responsible for its antimicrobial potential (Rounds et al. 2012; Heshmati et al. 2010). Elephant garlic extracts, like other *Allium* species, have also been found to contain eight different thiosulfates responsible for their antimicrobial activity (Huang and Ren 2013). Snow mountain garlic is a variant species of *Allium*. It has been considered a survival strategy for elephant garlic in various abiotic and biotic stress conditions. Therefore, it might be reasonable to systematically study the effectiveness of snow mountain garlic against various *Candida* sp.

However, the long life cycle and low productivity have made this plant species less acceptable among the farmers. Further, the necessity of environmental stress conditions has restricted this crop plant to the farmers of particular habitats. Therefore, in the present study, an attempt has been made to establish an *in vitro* propagation protocol of this plant species to reduce its life cycle so that increased commercial demand can be satisfied without the requirement of environmental stress conditions followed by an assessment of the effectiveness of water extract of *in vitro* grown bulb (TC-SMG) against different *Candida* species.

## 2 Materials and Methods

### 2.1 Collection of plant material and sterilization

Certified snow mountain garlic corm seeds were obtained from Srinagar, Jammu & Kashmir, India. Collected seeds were kept in running tap water for three hours followed by surface sterilization in three steps for establishment of *in vitro* tissue culture of snow mountain garlic which involved sterilization of corm seeds with ethanol (70% (v/v)) for 120 seconds, mercuric chloride (0.04% (w/v, 60 seconds)) followed by extensive washing for 4–5 times, with autoclaved distilled water in order to remove the remaining traces of sterilizing agents and then transferred to MS medium having 3% sucrose as carbon source (Morales et al. 2006).

### 2.2 Establishment of aseptic culture of snow mountain garlic using corm bud as explant

In-vitro culture of snow mountain garlic was established using corm seeds containing axillary bud as a source of explants (Figure 1). For this, the thick coat of each of these seeds was removed using a scalpel blade to expose the bud. After this, seeds were shifted to MS medium augmented with 3.00% (w/v) sucrose, 0.78% agar, and numeral concentrations of plant growth regulators, i.e., 6-benzylaminopurine (BAP), thidiazuron (TDZ) and kinetin (KN) for effective shoot multiplication. Agar-agar was added to the culture medium after setting the pH (5.80). The medium thus prepared was transferred to various culture vessels for effective sterilization in an autoclave at a pressure of 15 psi for 15 min. A Laminar air chamber was used to inoculate explants on a sterilized medium under aseptic conditions. All the inoculated cultures were then kept at a



Figure 1 A) Cloves of Snow Mountain Garlic B) Peeled cloves exposing the axillary bud

temperature of  $22 \pm 2^\circ\text{C}$ , humidity of 70–80%, and in photoperiod of 16/8 h light/dark in the culture room containing optimal light intensity ( $40 \mu\text{molm}^{-2}\text{s}^{-1}$ ) using white fluorescent lamps (cool). Data was recorded 25 days after inoculation.

### 2.3 Effect of different auxins on root induction from explant

Four different concentrations of NAA (1, 1.5, 3.0, 4.0  $\mu\text{M}$ ) and 2,4 D (1, 1.5, 3.0, 4.0  $\mu\text{M}$ ) were investigated for effective root formation. For this, shoots in the early stages of development were transferred to MS medium containing different concentrations of NAA and 2,4 D.

### 2.4 Effect of different concentrations of Sucrose on bulb formation

Seven different Sucrose concentrations, 5%, 7%, 10%, 15%, 17%, 20%, and 25%, were studied for effective bulb formation, keeping the standard 3% sucrose concentration as control.

### 2.5 Hardening and acclimatization of *in vitro* grown plants

Hardening of *in vitro* grown plants of snow Mountain Garlic was carried out in hardening trays. For this, *in vitro* grown plants of 80 days were taken out from tubes and inoculated into hardening media consisting of a mixture of cocopeat and vermicompost in the ratio of 1:1. Before transferring, the plants were given treatment of a fungicide bavistin (0.04%), followed by thorough washing to remove traces of bavistin. Plants were kept in a hardening chamber. Frequent water sprays were given to maintain humidity.

### 2.6 Preparation of aqueous extract of *in vitro* grown garlic bulbils

Aqueous extract of *in vitro* developed garlic bulbils was prepared using the method given by Suleria et al. (2012). Seed bulbils from *in vitro* grown plants were collected and weighed (5.0 g), followed by their thorough homogenization with double distilled water to obtain fine garlic juice. The homogenized mixture was filtered

through 2-3 layers of muslin cloth. The resultant aqueous garlic extract was passed through Whatman™ grade 1 filter paper. The recovered filtrate was freeze-dried and stored at  $4^\circ\text{C}$  until further use. Different concentrations of garlic extract were prepared by diluting it with sterile water (Suleria et al. 2012). Prior to each antifungal assay, aqueous extract was filtered through a Whatman™ 0.22 $\mu\text{m}$  PVDF membrane filter.

### 2.7 Analysis of the antifungal activity of aqueous extract of Snow Mountain Garlic against different *Candida* species

Antifungal potential of aqueous extract of *in vitro* grown snow mountain garlic was assessed through agar well diffusion assay. Three species of *Candida* viz., *Candida glabrata*, *C. tropicalis*, and *C. albicans* were obtained from MTCC (Microbial type culture collection), CSIR- IMTECH, Chandigarh, India. Procured fungal cells were grown on Yeast Malt Agar (YMA) at  $30^\circ\text{C}$  and sub-cultured 2-3 times to confirm the purity and viability of cells. Single colony of each species was activated in YM broth for 4-5 hrs (OD was 0.4- 0.5). Each activated pathogen inoculum was spread on YM agar containing petridishes using a sterile L-shaped spreader and allowed to dry at room temperature for 2-3 minutes. Wells of 6mm diameter were made by using a cork borer. Six different concentrations (200, 100, 80, 60, 40, 20 mg/mL) of garlic extract were dispensed in the holes, followed by incubation at  $30^\circ\text{C}$  for 24 and 48 hrs, respectively. The negative control well was poured with sterile MQ water. The zone of inhibition diameter was measured with an antibiotic zone scale after 24 and 48 hrs for each selected pathogenic strain, respectively.

### 2.8 Minimum Inhibitory Concentration (MIC)

The MIC value of TC-SMG (aqueous extract) was analyzed using the Tholen et al. (2004) protocol with slight modifications. This study used six different concentrations viz., 0.8, 1.6, 3.2, 6.4, 12.8, and 25.6 mg/mL of *in vitro* grown tissue culture (TC-SMG extract were prepared by serial dilution). Twenty microliters of each concentration was dispersed in 80  $\mu\text{L}$  of YM broth, followed by

100 µL of cell suspension inoculums with 0.003-0.004 OD at 600 nm, which was added to the 96-well plate. Two wells of 100 µL of YM broth and fungal cell suspension were kept as a positive control. Plates were incubated at 30 °C, and OD was measured at 600 nm at 24 and 48 hours using an ELISA microplate reader (Thermofischer, USA).

### 2.9 Statistical analysis

All the experimental results were presented as the mean ± standard error (SE), and all experiments were performed in triplicate. Independent t-test was used in SPSS 17.0 (Statistical Program for Social Sciences, SPSS Corporation, Chicago, IL) to determine the significance of the results. A probability (p) value of ≤ 0.05 was treated significantly for ANOVA and the marked correlations between the numeral assays.

### 3 Results

Sterilized cloves of snow mountain garlic were transferred to MS medium supplemented with different combinations of auxins and cytokinins. Germination started within 10-12 days in explants of snow mountain garlic.

### 3.1 Effect of different cytokinins on shoot induction from explant

Hard coat of sterilized cloves of Kashmiri garlic was removed carefully and transferred to MS medium containing distinct concentrations of BAP (µM), KN (µM), and TDZ (µM). A total of 18 various compositions of three selected cytokinins were studied to assess their effect on shoot proliferation of varied lengths. MS basal without the addition of any growth hormones was used as a control. Single shoot was found to develop in all the investigated hormones. In the case of BAP and KN, the highest length of shoot, i.e., 1.36±0.23 cm and 1.43±0.133 cm, was witnessed in a medium containing 5.0 µM concentration of each respective hormone. However, the maximum length of the shoot (5.03±1.40) was observed in MS medium supplemented with 1.0 µM TDZ by direct organogenesis after 24 days of inoculation, whereas no shoot formation was observed in control. A sudden increase in shoot length was observed in shoots after 15 days of inoculation, which showed further enhancement in length with time. Thus, basal medium (MS) containing 1.0 µM TDZ was selected as the optimum medium for effective shoot proliferation compared to BAP and KN supplemented medium (Table 1).

Table 1 Effect of different concentrations of cytokinins on shoot development

S. N.	Medium Code	Medium composition	No of Shoots	Length of shoots
1.	SMGK0A	MSBM	0.00 <sup>a</sup>	0.00 <sup>a</sup>
2.	SMGK1	MSBM + 1.0 µM KN	0.67±0.33 <sup>c</sup>	0.50±0.05 <sup>ab</sup>
3.	SMGK2	MSBM + 2.0 µM KN	1.00±0.00 <sup>d</sup>	1.43±0.14 <sup>bc</sup>
4.	SMGK3	MSBM + 3.0 µM KN	1.00±0.00 <sup>d</sup>	1.00±0.15 <sup>b</sup>
5.	SMGK5	MSBM + 5.0 µM KN	1.00±0.00 <sup>d</sup>	1.43±0.13 <sup>bc</sup>
6.	SMGK7	MSBM + 7.0 µM KN	0.67±0.33 <sup>c</sup>	0.80±0.44 <sup>ab</sup>
7.	SMGB1	MSBM + 1.0 µM BAP	1.00±0.00 <sup>d</sup>	1.00±0.19 <sup>b</sup>
8.	SMGB3	MSBM + 3.0 µM BAP	1.00±0.00 <sup>d</sup>	1.03±0.08 <sup>b</sup>
9.	SMGB5	MSBM + 5.0 µM BAP	0.67±0.33 <sup>c</sup>	1.36±0.23 <sup>bc</sup>
10.	SMGB7	MSBM + 7.0 µM BAP	0.33±0.33 <sup>b</sup>	0.32±0.33 <sup>a</sup>
11.	SMGT0.5	MSBM + 0.5 µM TDZ	1.00±0.0 <sup>d</sup>	3.77±0.89 <sup>d</sup>
12.	SMGT1	MSBM + 1.0 µM TDZ	1.00±0.0 <sup>d</sup>	5.03±1.40 <sup>e</sup>
13.	SMGT3	MSBM + 3.0 µM TDZ	1.00±0.0 <sup>d</sup>	4.87±0.73 <sup>e</sup>
14.	SMGT5	MSBM + 5.0 µM TDZ	1.00±0.0 <sup>d</sup>	2.30±0.05 <sup>c</sup>
15.	SMGG0.5	MSBM + 5.0 µM TDZ+ 0.5 µM GA3	1.00±0.0 <sup>d</sup>	2.06±0.08 <sup>c</sup>
16.	SMGG1	MSBM + 1.0 µM TDZ+ 1.0 µM GA3	1.00±0.0 <sup>d</sup>	3.17±0.07 <sup>d</sup>
17.	SMGG3	MSBM + 3.0 µM TDZ+ 1.0 µM GA3	1.00±0.0 <sup>d</sup>	3.20±0.52 <sup>d</sup>
18.	SMGG5	MSBM + 5.0 µM TDZ+ 1.0 µM GA3	1.00±0.0 <sup>d</sup>	2.63±0.06 <sup>cd</sup>

MSBM - MS basal medium; Values are in means ± SEM of three determinations; Values with distinctive superscript (little letter set) letters inside a column were altogether distinctive ( $p \leq 0.05$ )



Table 2 Effect of different concentrations of auxins on root development

S. N.	Medium Code	Concentration of NAA ( $\mu\text{M}$ )	No of roots (cm)	Length of roots (cm)
1.	SMG0	0.0 $\mu\text{M}$ NAA	4.33 $\pm$ 0.33 <sup>a</sup>	1.43 $\pm$ 0.14 <sup>a</sup>
2.	SMG1	1.0 $\mu\text{M}$ NAA	4.00 $\pm$ 0.57 <sup>a</sup>	1.50 $\pm$ 0.11 <sup>a</sup>
3.	SMG2	1.5 $\mu\text{M}$ NAA	2.33 $\pm$ 0.33 <sup>b</sup>	1.27 $\pm$ 0.03 <sup>ab</sup>
4.	SMG3	3.0 $\mu\text{M}$ NAA	1.33 $\pm$ 0.33 <sup>c</sup>	0.91 $\pm$ 0.02 <sup>b</sup>
5.	SMG4	4.0 $\mu\text{M}$ NAA	0.67 $\pm$ 0.33 <sup>d</sup>	0.58 $\pm$ 0.11 <sup>c</sup>

Values are means  $\pm$  SEM of three determinations. The values having distinctive superscript (little letter set) letters inside a column were altogether distinctive ( $p \leq 0.05$ ).

### 3.2 Effect of different auxins on root and callus induction from explants

Four different concentrations of NAA ( $\mu\text{M}$ ) were studied for effective root formation. Initiation of root development was observed after 10 days of inoculation. A significant variation in the number of roots was observed in a medium supplemented with different concentrations of NAA ( $\mu\text{M}$ ). Among all the studied concentrations of NAA, the highest no of roots (4.0 $\pm$ 0.578) with the highest length (1.5 $\pm$ 0.11 cm) were found to develop in 1.0  $\mu\text{M}$  concentration of NAA. However, the maximum no of roots

(4.33 $\pm$ 0.33) was found to develop in the MS basal medium (control) (Table 2).

In the case of 2,4 D, callus formation was observed in all the studied concentrations of 2,4D viz. 1  $\mu\text{M}$ , 1.5  $\mu\text{M}$ , 3  $\mu\text{M}$  and 4  $\mu\text{M}$  (Figure 2).

Based on the above results, MS medium supplemented with 1.0  $\mu\text{M}$  TDZ was selected as the optimum medium for effective shoot and root development and selected further for effective multiplication of plants (Figure 3).

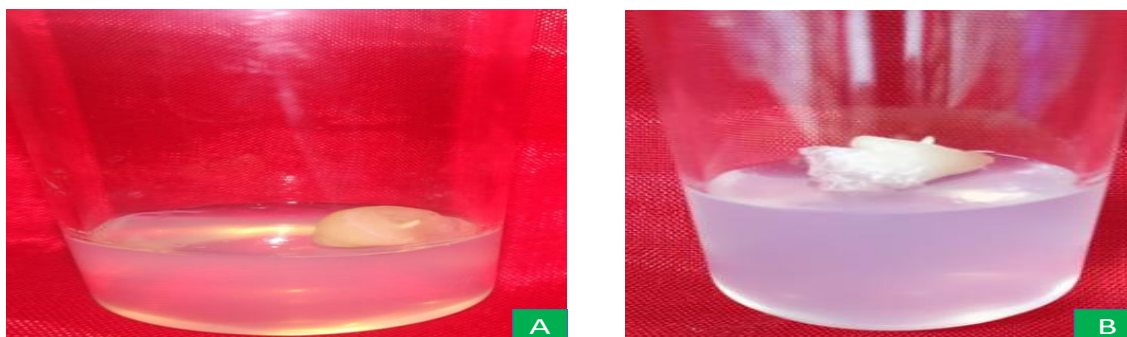


Figure 2 A) Inoculation of explant on MS medium containing 2, 4 D B) Formation of callus (15 days)

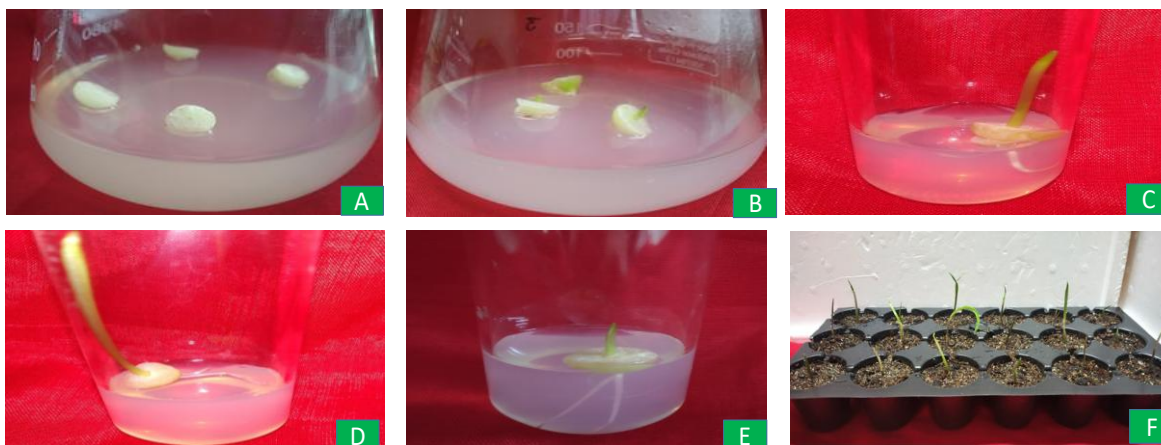


Figure 3 A) Explant transferred to MS medium supplemented with different concentrations of growth hormones B) Initiation of germination (10-12 days) C) Initiation of shoot formation on MS medium supplemented with 1.0  $\mu\text{M}$  TDZ D) Elongation of shoot (15 days) E) Development of roots in MS basal medium F) Hardening of plants in controlled conditions



Table 3 Effect of various sucrose concentrations on bulb formation

S. N.			
1.	3.0	25.33±0.88 <sup>d</sup>	0.27±0.008 <sup>a</sup>
2.	5.0	14.67±0.67 <sup>c</sup>	0.28±0.011 <sup>a</sup>
3.	7.0	14.00±0.58 <sup>c</sup>	0.49±0.052 <sup>b</sup>
4.	10.0	12.33±0.33 <sup>b</sup>	0.55±0.014 <sup>b</sup>
5.	15.0	5.00±0.58 <sup>a</sup>	0.74±0.015 <sup>c</sup>
6.	17.0	4.67±0.33 <sup>a</sup>	0.84±0.012 <sup>d</sup>
7.	20.0	5.00±0.00 <sup>a</sup>	0.89±0.012 <sup>d</sup>
8.	25.0	5.00±0.00 <sup>a</sup>	0.88±0.008 <sup>d</sup>

Values are as means ± SEM of three determinations. Values with distinctive superscript (little letter set) letters inside a column were altogether distinctive ( $p \leq 0.05$ ).

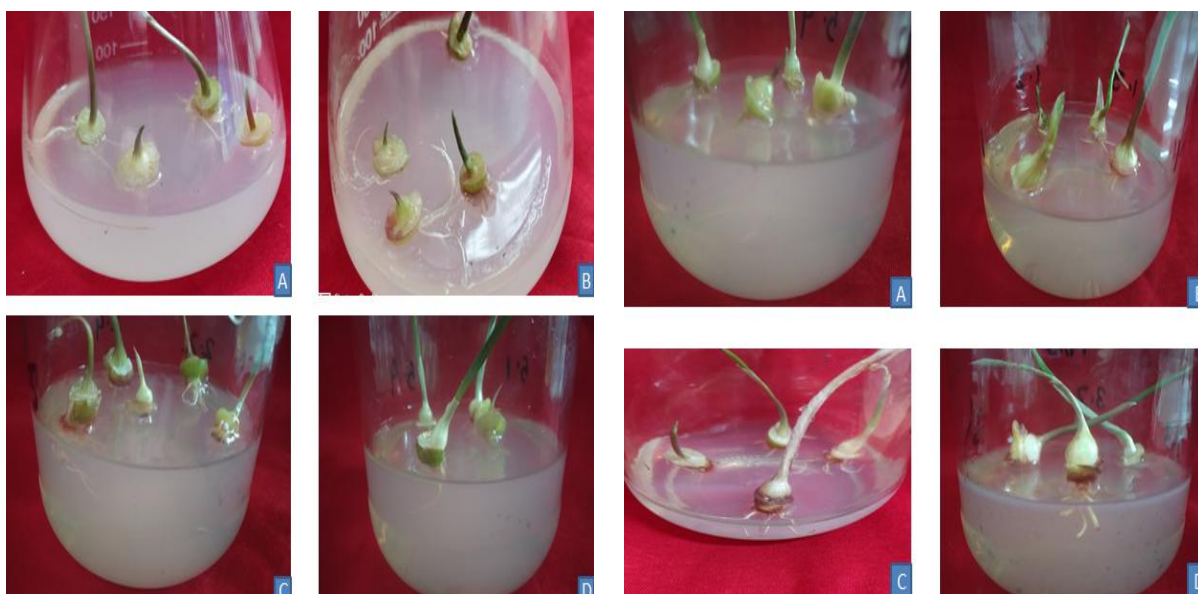


Figure 4A: A) Explant in 3% sucrose B) Explant in 5% sucrose C) Explant in 7% sucrose D) Explant in 9% sucrose

Figure 4B: A) Explant in 15% sucrose B) Explant in 17% sucrose C) Explant in 19% sucrose D) Explant in 20% sucrose

### 3.3 Effect of different concentrations of Sucrose on bulb formation

Development of corms from shoots can play an important role in their successful acclimatization and *in vitro* mass cultivation. Corms formed under *in vitro* conditions are better adapted to storage conditions. Thus, in this study, six different concentrations of Sucrose in MS medium, i.e., 5, 7, 10, 15, 17, 20, and 25%, were investigated for *in vitro* corm development while 3% sucrose concentration was used as control. The average diameter of bulb was noticed to enlarge with the increment in concentration of Sucrose, whereas the duration of bulb development was found to decrease with the increase of sucrose concentration. A maximum diameter of 0.86 cm was obtained in MS medium supplemented with 20% sucrose in 5 days, while further increase in the

concentration of Sucrose has left no further impact on the increase of diameter as well as on-time duration. Further, a diameter of 0.25 cm was observed in MS medium supplemented with 3.0% sucrose (control) after an average duration of 25.33 days (Table 3, Figure 4A-B). Investigation of liquid medium containing optimized concentration of Sucrose, i.e., 20% for effective bulbil formation, has resulted in a further decrease in time duration (3 days) of bulb formation (Figure 5).

### 3.4 Hardening and acclimatization of *in vitro* grown plants

Rooted plants were hardened and acclimatized in plastic trays in a hardening chamber. A frequent sprinkling of water was carried out to ensure humidity maintenance. Approximately 80% survival of plantlets was observed after 3 weeks of transplantation (Figure 3).



Figure 5 Development of bulbil in liquid MS media supplemented with 20% sucrose (3 days)

### 3.5 Analysis of the antifungal activity of aqueous extract of Snow Mountain Garlic against different *Candida* species

The agar well diffusion method evaluated the effectiveness of TC-SMG aqueous extract against 3 selected *Candida* species. Six different concentrations of TC-SMG viz., 20, 40, 60, 80, 100, and 200 mg/mL were tested against all the selected pathogens at 24 and 48 hrs, respectively. In the case of *C. albicans*, the maximum zone of inhibition ( $22.30 \pm 0.33$  mm) was observed using 200 mg/ml extract after 24 hrs. Further, a non-significant inhibition zone

reduction was observed after 48 hrs (Table 4). In the case of *C. tropicalis*, no inhibition was observed by using 20 mg/mL concentration at both time intervals (Table 4). However, the zone of inhibition was found to increase by further increasing the concentration, whereas the maximum zone of inhibition was achieved by using 200 mg/mL of TC-SMG after 24 ( $17.3 \pm 0.33$  mm) and 48 hrs ( $16.3 \pm 0.88$  mm). Similarly, in the case of *C. glabrata*, no zone of inhibition was observed using 20 mg/mL TC-SMG aqueous extract, and the highest zone of inhibition ( $19.30 \pm 0.33$  mm) was reported after 24 hrs (Table 4). In all three

Table 4 Antifungal activity of various concentrations of TC-SMG extracts against selected *Candida* sps

S. N.	TC-SMG Concentration (mg/mL)	Zone of Inhibition (mm) at 24 hours			Zone of Inhibition (mm) at 48 hours			Positive control
		<i>C. albicans</i>	<i>C. tropicalis</i>	<i>C. glabrata</i>	<i>C. albicans</i>	<i>C. tropicalis</i>	<i>C. glabrata</i>	
1.	20	$13.70 \pm 0.33^a$	$0.00 \pm 0.00^a$	$0.00 \pm 0.00^a$	$7.00 \pm 3.51^a$	$0.00 \pm 0.00^a$	$0.00 \pm 0.00^a$	Growth
2.	40	$16.70 \pm 0.33^b$	$12.00 \pm 0.00^b$	$4.00 \pm 4.00^b$	$14.70 \pm 0.33^b$	$6.70 \pm 3.33^b$	$4.00 \pm 4.00^b$	Growth
3.	60	$18.70 \pm 0.33^c$	$14.30 \pm 0.33^c$	$8.30 \pm 4.26^c$	$16.70 \pm 0.33^{bc}$	$12.30 \pm 0.33^c$	$7.70 \pm 3.93^b$	Growth
4.	80	$19.70 \pm 0.33^c$	$15.70 \pm 0.33^d$	$15.00 \pm 0.58^d$	$17.70 \pm 0.33^{bc}$	$14.30 \pm 0.33^d$	$13.30 \pm 1.33^c$	Growth
5.	100	$20.70 \pm 0.33^d$	$16.30 \pm 0.33^d$	$16.70 \pm 0.67^{de}$	$18.70 \pm 0.33^c$	$14.70 \pm 0.33^d$	$15.00 \pm 1.00^d$	Growth
6.	200	$22.30 \pm 0.33^e$	$17.30 \pm 0.33^e$	$19.30 \pm 0.33^e$	$21.00 \pm 0.58^d$	$16.30 \pm 0.88^e$	$18.70 \pm 0.67^e$	Growth

Values are as means  $\pm$  SEM of three determinations. Values with distinctive superscript (little letter set) letters inside a column were altogether distinctive ( $p \leq 0.05$ ).

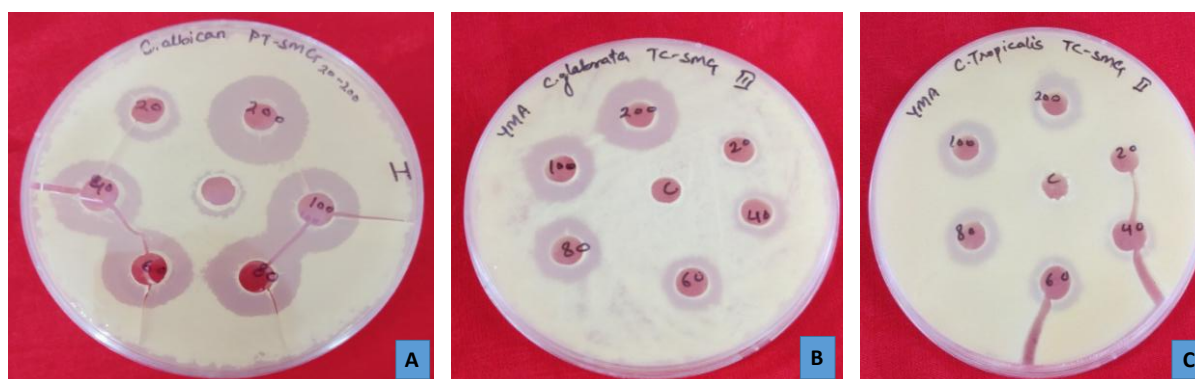


Figure 6 Antifungal effect of different concentrations of TC-SMG after 24 hrs on A) *Candida albicans*, B) *C. glabrata*, C) *C. tropicalis*

cases, depicting its remarkable potential to be used as an antifungal agent, a non-significant reduction in the size inhibition zone was observed after 48 hrs (Figure 6).

### 3.6 Minimum Inhibitory Concentration (MIC)

Minimum inhibitory concentration (MIC) against all the test pathogens was also evaluated in the range of 0.8, 1.6, 3.2, 6.4, 12.8, and 25.6 mg/ml. A MIC<sub>99</sub> value of 3.2 mg/mL was observed for *C. albicans* at 24 and 48 hrs. For *C. tropicalis*, a MIC<sub>99</sub> value of 1.6mg/mL was observed at 24 hrs, whereas at 48 hrs, it was observed to be 3.2 mg/mL. Further, in the case of *C. glabrata*, MIC<sub>99</sub> of 6.4 mg/mL was obtained at both 24 and 48 hrs. From these results, it is visible that *C. tropicalis* has more susceptibility towards TC- SMG aqueous extract than the other two pathogens. On the other hand, *C. glabrata* was found more resistant to TC-SMG extract as it has shown the highest MIC amongst all three *Candida* spp.

### 4 Discussion

For thousands of years, garlic has remained an important herb for human consumption. When antibiotics and other pharmaceutical products did not exist, a bulb of garlic was used to represent the pharmaceutical industry due to its broad spectrum effects (Petrovska and Cekovska 2010). Various clinical investigations have revealed many beneficial effects of garlic, such as (i) reduced risk factors towards cardiovascular disorders, (ii) cancer risk, (iii) enhanced antioxidant and antimicrobial activity, and (v) detoxification of foreign components and liver protection (Aviello et al. 2009; Colín-González et al. 2012). These therapeutical properties of garlic and other members of the genera *Allium* have been attributed to various organosulfur compounds, and the most important sulfurous compound present in intact bulbs is allicin (S-allylcysteine sulfoxide). In addition to this, whole bulbs have also been found to contain several other sulphur compounds such as  $\gamma$ -glutamyl-S-allylcysteine (GSAC), S-methylcysteine sulfoxide (methiin), S-trans-1-propenylcysteine sulfoxide, S-2-carboxypropylglutathione and S-allylcysteine (SAC), though some of these are available in much smaller amounts (Amagase 2006). These sulphur-rich compounds have been suggested to be responsible for the various medicinal properties of garlic (Iciek et al. 2009).

Snow mountain garlic is one of the variants found to grow in the mountainous region of Jammu & Kashmir state of India. In ancient times, snow mountain garlic has been observed to be used by various mountain climbers to regain energy and by Greeks to increase the efficiency of athletes participating in Olympics (Sasi et al. 2021). In literature, very little information is available regarding snow mountain garlic. However, for the last few years, an increment in commercial demand for snow mountain garlic has been observed. This increased demand in the market can be

attributed to its reduced pungent flavor and beneficial medicinal properties, such as anti-inflammatory, antioxidant, and arthritic properties (Kaur et al. 2024). This garlic is a good source of various minerals, viz., manganese, copper, selenium, phosphorus, and vitamins B6 and C (Kaur et al. 2022).

However, the long life cycle, low productivity, and requirement of long, cold winters have restricted this species to specific areas of the country. A single seed bulb can grow into one plant only, so the availability of a large stock of seed corms is another limitation of its large-scale propagation. Thus, *in vitro* propagation and the development of seed bulbs are important approaches to quickly producing many propagules. In the present study, corm seeds containing axillary bud were used as a source of explant and inoculated on MS medium containing eighteen different concentrations of three selected cytokinins viz., BAP ( $\mu$ M), KN, and TDZ ( $\mu$ M) for efficient shoot proliferation, whereas, basal MS medium was used as control. Maximum shoot length was observed in MS medium supplemented with 1.0  $\mu$ M TDZ, whereas BAP and KN were less efficient for shoot proliferation. Similarly, Mahajan et al. (2013) reported the lower efficiency of the combinations of BAP and KN for *in vitro* shoot proliferation compared to individual concentration. However, for the first time, the effect of TDZ has been studied in our investigation, and it has been found more promising than BAP and KN for *in vitro* shoot development.

The long life cycle and development of fewer seed propagules are the key limitations of large-scale cultivation of this species. Therefore, an attempt has been made to develop *in vitro* corm seeds that can be distributed to farmers and can be utilized to satisfy increased commercial demands. For this, different concentrations of Sucrose were applied in MS media. An increase in the bulb's diameter was found with the increase in sucrose concentration. This increase in bulb size with the increase in sucrose concentration can be attributed to the enhancement in the starch and total carbohydrate content (Khokhar 2022). Further, a liquid medium containing an optimized concentration of Sucrose was found to develop corm seed using less medium quantity, depicting the cost-effective *in vitro* development of bulb. It can be attributed to the ease of nutrient uptake resulting in bulbs' development. *Candida* sp has been observed to be able to switch between yeast and hyphae forms, ultimately leading to the formation of biofilms and developing resistance to various antifungal agents (Brand 2012). Since ancient times, plants have been renowned as natural sources of medicine. Several plant species viz., *Osmium sanctum* (Khan et al. 2010); *Glycyrrhiza glabra* (Martins et al., 2016); *Euphorbia hirta* (Rajeh et al., 2010); *Terminalia bellerica* (Valsaraj et al. 1997) have been tested against various *Candida* sp. However, none of these plant products has reached the marketing stage due to insufficient information and efficacy. Therefore, hunting for new plant species with antifungal properties is an alternative to solve these problems.

In the present investigation, aqueous extract of *in vitro* grown Snow Mountain garlic bulbs (TC-SMG) were studied for their efficacy against three *Candida* sp. viz., *C. albicans*, *C. glabrata*, and *C. tropicalis* after 24 and 48 hrs by agar well diffusion method. Six different concentrations were studied against all the selected pathogens. The diameter of the zone of inhibition was found to increase with the increase in extract concentration in all three cases at both time durations. Further, a non-significant reduction in the diameter of the zone of inhibition was observed after 48 hrs, depicting the remarkable potential of this extract to be used as an antifungal agent against different *Candida* sp, specifically in *C. albicans* where the zone of inhibition was found in all concentrations. *Candida* cidal activity of snow mountain garlic has also been investigated by Kaur et al. (2022). It has been suggested that allicin, the major compound found in garlic, can inhibit the thiol-containing amino acids and proteins, thus resulting in the interference in cell metabolism and ultimately leading to the death of the organism (Ankri and Mirelman 1999; Soliman et al. 2017, Kaur et al. 2023).

### Conclusion

Food commodities with medicinal properties have remained popular for curing many health problems since immemorial and are being continued until today. Snow mountain garlic is one such plant with several medicinal properties but with a long life cycle and limited productivity. In the present investigation, an effective micropropagation protocol for multiplication of this plant followed by the development of bulbils under *in vitro* conditions for a reduction in its life cycle in order to their usage as seeds have been investigated and found that 1.0  $\mu$ M TDZ and 20gm Sucrose can be a best suitable combination for the *in-vitro* micropropagation of this garlic. Further, water extract at the 200 mg/ml concentration was found fully effective in suppressing *Candida* species growth completely. It will be interesting to determine the effect of this extract on the molecular level of *Candida* proteins targeted by the extract. Further, this protocol could be used to commercialize the cultivation of this snow mountain garlic. To our knowledge, this is the first investigation of antifungal properties of aqueous extract of *in vitro* grown bulbs of snow mountain garlic against different *Candida* sp., depicting its strong rationale for industrial applications.

### Acknowledgement

The authors are highly grateful to DRDO for providing a platform for financial assistance to carry out this work.

### Author Contributions

AS wrote draft preparation and carried out experiments, SS performed the tissue culture experiments, MKP contributed to the

collection of samples, OPC supervised project administration and funding acquisition, and SSa supervised the work and edited the manuscript. All authors have seen the draft copy and approved the final version.

### Funding

The Defence Institute of High Altitude Research (DIHAR)-DRDO, Ministry of Defence, C/o 56 APO Leh-Ladakh-194101, India, funded this research.

### Competing of Interest

There is no competing interest among the authors.

### Ethics approval

There is no need for ethics approval as this investigation was unrelated to any animal or human subject.

### Consent for publication

All authors have approved the manuscript and agree with its submission to JEBAS.

### Availability of data and material

The datasets generated during and/or analyzed during the current study are available from the corresponding author upon reasonable request.

### References

- Al-Dorzi, H. M., Sakkijha, H., Khan, R., Aldabbagh, T., Toledo, A., Ntinika, P., Al Johani, S. M., & Arabi, Y. M. (2020). Invasive Candidiasis in Critically Ill Patients: A Prospective Cohort Study in Two Tertiary Care Centers. *Journal of intensive care medicine*, 35(6), 542–553. <https://doi.org/10.1177/0885066618767835>.
- Amagase, H. (2006). Clarifying the real bioactive constituents of garlic. *The Journal of Nutrition*, 136(3), 716-725.
- Ankri, S., & Mirelman, D. (1999). Antimicrobial properties of allicin from garlic. *Microbes and infection*, 1(2), 125-129.
- Aviello, G., Abenavoli, L., Borrelli, F., Capasso, R., Izzo, A. A., Lembo, F., & Capasso, F. (2009). Garlic: empiricism or science?. *Natural Product Communications*, 4(12), 1785–1796.
- Bayan, L., Koulivand, P. H., & Gorji, A. (2014). Garlic: a review of potential therapeutic effects. *Avicenna journal of phytomedicine*, 4(1), 1–14.
- Brand, A. (2012). Hyphal growth in human fungal pathogens and its role in virulence. *International journal of microbiology*, 2012, 517529. <https://doi.org/10.1155/2012/517529>.



- Colín-González, A. L., Santana, R. A., Silva-Islas, C. A., Cháñez-Cárdenas, M. E., Santamaría, A., & Maldonado, P. D. (2012). The antioxidant mechanisms underlying the aged garlic extract- and S-allylcysteine-induced protection. *Oxidative medicine and cellular longevity*, 2012, 907162. <https://doi.org/10.1155/2012/907162>
- Davis, C. C., & Choisy, P. (2024). Medicinal plants meet modern biodiversity science. *Current biology : CB*, 34(4), R158–R173. <https://doi.org/10.1016/j.cub.2023.12.038>.
- Devi, A., Rakshit, K., & Sarania, B. (2014). Ethnobotanical notes on *Allium* species of Arunachal Pradesh. *India Journal of Traditional Knowledge*, 13(3), 606-612.
- Heshmati, M., Delshad, A. A., & Gheini, M. (2010). Garlic Extract can Induce apoptotic death in the Human colon adenocarcinoma HT29 Cell Line. *Iranian Journal of Pathology*, 5(3), 126-131.
- Huang, Z., & Ren, J. (2013). Antibacterial activity of elephant garlic and its effect against U2OS human osteosarcoma cells. *Iranian Journal of Basic Medical Sciences*, 16(10), 1088-1094.
- Iciek, M., Kwiecień, I., & Włodek, L. (2009). Biological properties of garlic and garlic-derived organosulfur compounds. *Environmental and molecular mutagenesis*, 50(3), 247-265.
- Kaur, B., Kumar, N., Chawla, S., Sharma, D., Korpole, S., et al. (2022). A comparative study of in-vitro and in-silico anti-candidal activity and GC-MS profiles of snow mountain garlic vs. normal garlic. *Journal of applied microbiology*, 133(3), 1308–1321. <https://doi.org/10.1111/jam.15537>
- Kaur, B., Kumar, N., Kumari, L., Gupta, A.P., Sharma, R., Chopra, K., & Saxena, S. (2024) In-vitro antioxidant and anti-inflammatory potential along with p.o. pharmacokinetic profile of key bioactive phytochemicals of Snow Mountain Garlic: a comparative analysis vis-à-vis normal garlic. *Inflammopharmacology*, 32(3), 1871-1886.
- Kaur, B., Kumar, N., Patel, M. K., Chopra, K., & Saxena, S. (2023). Validation of traditional claims of anti-arthritic efficacy of trans-Himalayan snow mountain garlic (*Allium ampeloprasum* L.) extract using adjuvant-induced arthritis rat model: A comparative evaluation with normal garlic (*Allium sativum* L.) and dexamethasone. *Journal of ethnopharmacology*, 303, 115939. <https://doi.org/10.1016/j.jep.2022.115939> .
- Khan, A., Ahmad, A., Akhtar, F., Yousuf, S., Xess, I., Khan, L. A., & Manzoor, N. (2010). Ocimum sanctum essential oil and its active principles exert their antifungal activity by disrupting ergosterol biosynthesis and membrane integrity. *Research in microbiology*, 161(10), 816–823. <https://doi.org/10.1016/j.resmic.2010.09.008>.
- Khokhar, K. M. (2022). Bulb development in garlic – a review. *The Journal of Horticultural Science and Biotechnology*, 98(4), 432–442.
- Kim, Y. S., Kim, K. S., Han, I., Kim, M. H., Jung, M. H., & Park, H. K. (2012). Quantitative and qualitative analysis of the antifungal activity of allicin alone and in combination with antifungal drugs. *PLoS One*, 7(6), e38242.
- Lemar, K. M., Turner, M. P., & Lloyd, D. (2002). Garlic (*Allium sativum*) as an anti-Candida agent: a comparison of the efficacy of fresh garlic and freeze-dried extracts. *Journal of Applied Microbiology*, 93(3), 398-405.
- Mahajan, R., Sharma, K., Bandryal, S., Jamwal, P., & Billowria, P. (2013). In vitro propagation and cryopreservation of snow mountain garlic endemic to Himalayan region. *International Journal of Advanced Biotechnology and Research*, 4(3), 372-379.
- Martins, N., Ferreira, I.C., Henriques, M., & Silva, S. (2016). In vitro anti-Candida activity of *Glycyrrhiza glabra* L. *Industrial Crops and Products*, 83, 81-85.
- Morales, S., Milaneze, M.A.G., Maria de Fatima PSM (2006) Effect of activated charcoal for seedlings development of *Catasetum fimbriatum* (Orchidaceae). *Journal of Plant Sciences*, 1, 384-391.
- Papu, S., Jaivir, S., Sweta, S., & Singh, B. R. (2014). Medicinal values of garlic (*Allium sativum* L.) in human life: an overview. *Greener Journal of Agricultural Sciences*, 4(6), 265-280.
- Parekh, J., & Chanda, S. (2007). In vitro antimicrobial activity of *Trapa natans* L. fruit rind extracted in different solvents. *African Journal of Biotechnology*, 6(6), 766-770.
- Petrovska, B.B., & Cekovska, S. (2010). Extracts from the history and medical properties of garlic. *Pharmacognosy reviews*, 4(7), 106-110.
- Rajeh, M.A.B., Zuraini, Z., Sasidharan, S., Latha, LY, & Amutha, S. (2010). Assessment of *Euphorbia hirta* L. leaf, flower, stem and root extracts for their antibacterial and antifungal activity and brine shrimp lethality. *Molecules*, 15(9), 6008-6018.
- Rounds, L., Havens, C. M., Feinstein, Y., Friedman, M., & Ravishanker, S. (2012). Plant extracts, spices, and essential oils inactivate *Escherichia coli* O157: H7 and reduce formation of potentially carcinogenic heterocyclic amines in cooked beef patties. *Journal of agricultural and food chemistry*, 60(14), 3792-3799.
- Sasi, M., Kumar, S., Kumar, M., Thapa, S., Prajapati, U., et al. (2021). Garlic (*Allium sativum* L.) Bioactives and Its Role in



- Alleviating Oral Pathologies. *Antioxidants (Basel, Switzerland)*, 10(11), 1847. <https://doi.org/10.3390/antiox10111847>
- Soliman, S., Alnajdy, D., El-Keblawy, A.A., Mosa, K.A., Khoder, G., & Noreddin, A.M. (2017). Plants' natural products as alternative promising anti-Candida drugs. *Pharmacognosy reviews*, 11(22), 104-122.
- Suleria, R., Sadiq Butt, H.A., Muhammad Anjum, M., Saeed, F., Batool, R., & Nisar Ahmad, A. (2012). Aqueous garlic extract and its phytochemical profile; special reference to antioxidant status. *International Journal of Food Sciences and Nutrition*, 63(4), 431-439.
- Tholen, D. W., Linnet, K., Kondratovich, M., Armbruster, D. A., Garrett, P. E., et al. (2004). Clinical and Laboratory Standards Institute (CLSI). Protocols for Determination of Limits of Detection and Limits of Quantitation, Approved Guideline. *CLSI document EP17-A*. CLSI, Wayne, PA.
- Valsaraj, R., Pushpangadan, P., Smitt, U. W., Adsersen, A., Christensen, S. B., et al. (1997). New anti-HIV-1, antimalarial, and antifungal compounds from *Terminalia bellerica*. *Journal of natural products*, 60(7), 739-742.
- Woodward P.W. (1996). *Garlic and Friends: The History, Growth and Use of Edible Alliums*, Volume 2 (pp. 248-276). Hyland House; Melbourne, Australia.



# Journal of Experimental Biology and Agricultural Sciences

<http://www.jebas.org>

ISSN No. 2320 – 8694

## Principal component analysis of morpho-floral traits in *Oryza sativa* × *Oryza longistaminata* advanced backcross lines of rice

Madhu Choudhary\* , Ravi P Singh, PK Singh, Jayasudha S

Institute of Agricultural Sciences, Banaras Hindu University, Varanasi, Uttar Pradesh, India

Received – March 24, 2024; Revision – June 07, 2024; Accepted – July 04, 2024

Available Online – July 15, 2024

DOI: [http://dx.doi.org/10.18006/2024.12\(3\).419.425](http://dx.doi.org/10.18006/2024.12(3).419.425)

### KEYWORDS

Hybrid rice  
Morpho-floral  
Principal component analysis  
Out-crossing  
Stigma exertion

### ABSTRACT

Hybrid rice technology substantially improves the food security of South Asian countries where rice (*Oryza sativa* L.) is a staple food. Several traits contribute to hybrid seed production efficiency, among which stigma exertion is crucial for enhancing production by facilitating out-crossing pollination. This study evaluated the variation patterns and relative impact of 12 morpho-floral traits on overall variability in advanced backcross lines derived from crosses CRMS 32B cv. *Oryza sativa* and *Oryza longistaminata*. For this study, 290 BC<sub>4</sub>F<sub>2</sub> lines were grown during Kharif 2019 in 3 replications using a randomized complete block design (RCBD). Principle component analysis (PCA) was performed on all traits, and the findings revealed 11 principal components (PCs). Out of 11 PCs, the first five displayed eigenvalues exceeding 1, collectively explaining 78.78% of the total variability. PC1, PC2, PC3, PC4, and PC5 contributed 26.36%, 19.94%, 14.22%, 9.81%, and 8.44% of the variation, with eigenvalues of 3.16, 2.39, 1.71, 1.18 and 1.01, respectively. PC1 was predominantly associated with yield-related traits such as panicle length, plant height, grain yield per plant, grains per panicle, and effective tillers per plant. On the other hand, PC2 was mainly associated with outcrossing-related floral traits such as total stigma exertion percentage, dual stigma exertion percentage, and single stigma exertion percentage. However, PC3 and PC4 were associated with both floral and yield-related traits, i.e., days to 50% flowering (DF), days to maturity (DM), plant height (PH), effective tillers per plant (ETPP), spikelet fertility percentage (SFP), grain yield per plant (GYPP) and grains per panicle (GPP). Therefore, PC1, PC2, PC3, and PC4 were major contributors to rice hybrid seed production.

\* Corresponding author

E-mail: [anamikaz0129@gmail.com](mailto:anamikaz0129@gmail.com) (Madhu Choudhary)

Peer review under responsibility of Journal of Experimental Biology and Agricultural Sciences.

Production and Hosting by Horizon Publisher India [HPI]  
[\(http://www.horizonpublisherindia.in/\)](http://www.horizonpublisherindia.in/).  
 All rights reserved.

All the articles published by [Journal of Experimental Biology and Agricultural Sciences](#) are licensed under a [Creative Commons Attribution-NonCommercial 4.0 International License](#) Based on a work at [www.jebas.org](http://www.jebas.org).



## 1 Introduction

Rice (*Oryza sativa* L.) is a major staple crop, serving as the primary food source for over half of the global population and fulfilling more than 21% of the world's caloric requirements (Sathe et al. 2021). The world's population is increasing and is estimated to reach 9.7 billion people by 2050; thus, increasing the productivity of major cereal crops such as rice is urgently needed to keep pace with the population surge (Kumar et al. 2022). Although increased rice yields were successfully achieved by integrating semidwarf genes, the limited genetic diversity among breeding lines has decreased the yield of released rice varieties. It is now crucial to expand the genetic diversity of rice varieties to surpass the yield limit and satisfy the rising demand for rice. Hybrid rice technology has emerged as the most feasible and adaptable option to address this situation, providing a yield advantage of 15-20% over conventional varieties (Qian et al. 2016). However, the major challenge hindering the widespread adoption of hybrid rice is the low seed yield ( $\leq 2.5$  ton ha<sup>-1</sup>), which consequently leads to high seed costs, and farmers often purchase hybrid seeds at a relatively high price for every cropping season (Xie 2009). Rice is an autogamous plant that prevents it from being naturally out-crossing; therefore, the most efficient strategy for enhancing hybrid seed production is to create male sterile lines with a high out-crossing rate. The out-crossing rate is affected by multiple traits, including both parents' flowering behavior and morphological traits (Marathi and Jena 2015). Among these traits, the stigma exertion rate is critical for enhancing out-crossing and ensuring efficient hybrid rice seed production (Zhang et al. 2018). It is a genetic trait that varies among male sterile lines and can be improved through targeted breeding efforts with appropriate donor varieties. Wild rice species serve as valuable repositories for revealing novel variations in flowering and morphological traits and could be utilized to increase the genetic background of elite cultivars (Ramos et al. 2016). Furthermore, these wild rice species exhibit a higher out-crossing rate than cultivated rice, ranging from 3.2% to 70.0%, while some wild rice species, such as *Oryza longistaminata* and *O. rufipogon* exhibit out-crossing rates of up to 100% (Prahalada et al. 2021). Incorporating favorable traits from wild species into elite breeding materials through wide hybridization has been a longstanding strategy (Zeliang and Pattanayak 2013). Although backcross introgression is also a feasible method for incorporating favorable traits from wild species, this method primarily involves the genome of recurrent parents with minimal donor segments and offers advantages for accurately estimating novel genes or QTLs and diversifying existing germplasms (Todorovska et al. 2013; Balakrishnan et al. 2016).

The effectiveness of any breeding program relies on understanding genetic variability to determine appropriate selection strategies for improving targeted traits. Multivariate analysis aids plant breeders

in devising these selection approaches (Ravindra et al. 2012). Principal component analysis (PCA) is a widely utilized multivariate statistical tool for compressing, reducing, and transforming data. This approach aims to simplify complex datasets by reducing their dimensionality to a minimum number of components while retaining most of the variance (Rahangdale et al. 2021). Through orthogonal transformation, PCA transforms a set of possibly related variables into a fresh set of linearly unrelated variables, facilitating data simplification and interpretation. PCA is extensively used to assess morphological and physiological traits by analyzing multiple parameters of each individual simultaneously. The eigenvalue of a given principal component signifies the extent of variance in attributes explained by that principal component, making it crucial for trait selection (Singh et al. 2020). Hence, the present research aimed to explore the genetic variations and to identify key factors contributing to the overall variance among selected morpho-floral traits of rice advanced backcross lines using PCA.

## 2 Materials and Methods

The plant material utilized in this study consisted of 290 BC<sub>4</sub>F<sub>2</sub> lines with recurrent parents. These advanced backcross lines (BC<sub>4</sub>F<sub>2</sub>) were developed through interspecific crossing between the recurrent parent CRMS 32B (maintainer of male sterile line with low stigma exertion) cv. *O. sativa* and the donor parent *O. longistaminata* (wild rice with high stigma exertion). The BC<sub>4</sub>F<sub>2</sub> lines were evaluated during *Kharif* 2019 at the Research Farm of the Institute of Agricultural Sciences, Banaras Hindu University, Varanasi, Uttar Pradesh. This study site is located in northern India's northern Gangetic Alluvial Plain zone, at latitude 25.18° N and longitude 83.03° E. The material was planted with three replications using a randomized complete block design (RCBD), with each row 3.0 meters long and a 20 × 15 cm spacing. Standard packages and practices were implemented to ensure optimal crop growth and quality. Observations were taken for 12 quantitative traits, which included days to 50% flowering (DF), days to maturity (DM), plant height (PH), effective tillers per plant (ETPP), panicle length (PL), grains per panicle (GPP), spikelet fertility percentage (SFP), grain yield per plant (GYPP), test weight (TW), single stigma exertion percentage (SSE%), dual stigma exertion percentage (DSE%) and total stigma exertion percentage (TSE%). These traits were measured on five randomly selected plants from each line in every replicate. Morphological characterization followed the standard evaluation system (SES) for rice, as the IRRI (2013) outlined. After the data were collected, the mean values for each trait were calculated and subjected to further statistical analysis. PCA was performed to identify key traits that significantly impacted the overall variability, and biplots were generated to visually represent the data effectively. The analysis, including PCA and biplot, was carried out using R software version 4.3.2.

### 3 Results and Discussion

Principal component analysis is pivotal for identifying the primary contributors to overall variability. It reduces the dimensionality of large datasets by extracting a small set of major independent variables that encapsulate the original variability without sacrificing its integrity (Sharma et al. 2022). PCA was performed on a set of 12 morpho-floral traits observed in 290 advanced backcross lines of rice, and the findings revealed 11 principal components (PCs). The eigenvalues, percentage of variability, and cumulative percentage are provided in Table 1. Eigenvalues represent the variance explained by each principal component, with higher values indicating more significant contributions to variability. Generally, components with eigenvalues >1 are considered essential because they capture more variance than does a single original variable (Brejda et al. 2000). Out of 11 PCs, five PCs displayed eigenvalues exceeding 1, and these PCs collectively explained 78.78% of the total variability. The first principal component (PC1) explained 26.36% of the overall variation with an eigenvalue of 3.16, whereas PC2, PC3, PC4, and PC5 individually accounted for 19.94%, 14.22%, 9.81%, and 8.44% of the variation with eigenvalues of 2.39, 1.71, 1.18 and 1.01, respectively. The results demonstrated that the first five principal

components captured a substantial portion of the total variability (78.78%), effectively summarizing the information in the original set of traits. This reduction in dimensionality while retaining most of the variance proved valuable for identifying key traits that influenced the genetic variation among the rice lines. Similarly, Sheela et al. (2020) reported four principal components that explained 72.24% of the total observed variability in rice germplasm.

The analysis of factor loadings revealed that the phenotypic traits having the most significant impact on variation displayed high positive loadings across various principal components (Table 1). In PC1, traits such as PL, PH, GYPP, GPP, and ETPP exhibited positive loadings, indicating that these traits were positively correlated and contributed significantly to the variation explained by PC1. Conversely, the remaining traits displayed negative loadings in PC1, suggesting an inverse relationship with this principal component. Thus, lines with high values of PC1 tended to have longer panicles, taller plants, greater grain yield, more grains per panicle, and more effective tillers. In PC2, the TSE%, DSE%, SSE%, GYPP, and PL traits had more positive loadings than did the other traits, suggesting that these traits, particularly those related to stigma exertion, were significant contributors to the

Table 1 Eigenvalues, variability percentages, cumulative percentages, and factor loadings of different morph-floral traits across principal components

Principal Components	PC1	PC2	PC3	PC4	PC5	PC6	PC7	PC8	PC9	PC10	PC11
Eigenvalues	3.163	2.393	1.707	1.177	1.013	0.889	0.494	0.456	0.262	0.234	0.211
Variability Percentage	26.362	19.940	14.224	9.808	8.445	7.405	4.121	3.799	2.187	1.953	1.758
Cumulative Percentage	26.362	46.302	60.526	70.333	78.778	86.183	90.304	94.102	96.289	98.242	100.000
Component matrix	Factor loadings										
DF	-0.556	-0.070	0.666	-0.088	-0.086	-0.320	-0.032	0.006	-0.201	-0.280	0.066
DM	-0.562	-0.104	0.624	-0.023	0.001	-0.400	0.083	-0.020	0.222	0.256	-0.031
PH	0.669	0.203	0.072	-0.415	-0.032	-0.249	-0.129	0.491	0.005	0.003	-0.111
ETPP	0.469	0.245	0.327	0.723	-0.048	-0.026	-0.013	-0.021	0.091	-0.124	-0.250
PL	0.755	0.301	0.107	-0.342	0.023	-0.133	-0.003	-0.261	0.280	-0.172	0.131
GPP	0.564	0.256	0.499	-0.383	-0.064	0.207	0.137	-0.260	-0.222	0.134	-0.145
SFP	-0.255	-0.113	0.587	-0.104	0.098	0.696	0.024	0.210	0.150	-0.063	0.041
GYPP	0.641	0.343	0.356	0.435	0.156	-0.030	-0.076	0.095	-0.116	0.139	0.289
TW	0.005	-0.163	0.008	-0.059	0.976	-0.088	-0.009	-0.038	-0.031	-0.032	-0.073
SSE%	-0.483	0.756	-0.009	-0.068	0.037	0.078	-0.416	-0.084	0.009	0.035	-0.036
DSE%	-0.256	0.785	-0.158	0.020	0.075	-0.044	0.516	0.128	-0.002	-0.046	0.022
TSE%	-0.455	0.881	-0.076	-0.040	0.059	0.036	-0.070	-0.004	0.005	0.005	-0.016

PC- principal component; DF-days to 50% flowering (days); DM-days to maturity (days); PH-plant height (cm); ETPP-effective tillers per plant (no.); PL-panicle length (cm); GPP-grains per panicle (no.); SFP-spikelet fertility%; GYPP-grain yield per plant (g); TW-test weight (g); SSE%- single stigma exertion%; DSE%- dual stigma exertion%; TSE%- total stigma exertion%

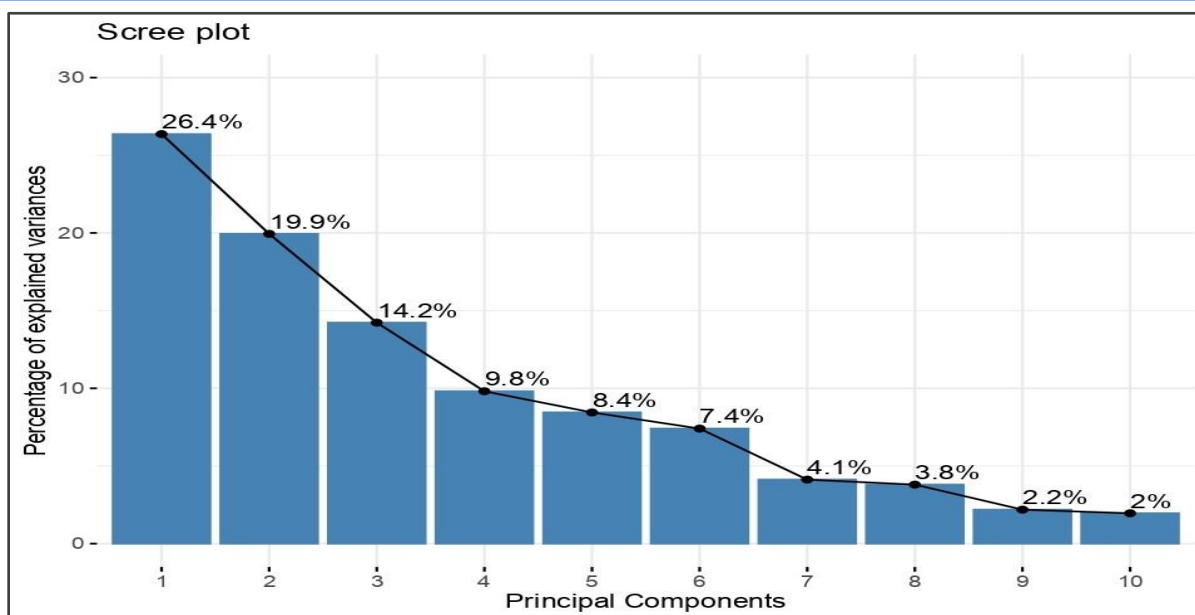


Figure 1 Scree plot visually representing the distribution of variance among principal components.

variability explained by PC2. The DF, DM, SFP, and GPP traits showed high positive loadings in PC3, indicating that these traits were important for the variability captured by PC3. On the other hand, the ETTP, GYPP, and TW traits showed substantial positive loadings in PC4 and PC5, respectively. This suggests that the ETTP and GYPP traits were key contributors to the variability explained by PC4, whereas TW was the primary contributor to the variability explained by PC5. These results demonstrated the complex interplay of various morpho-floral traits contributing to the overall genetic variability among the rice advanced backcross lines. The scree plot in Figure 1 illustrates the variance distribution across principal components, with PC1 displaying the highest variability (26.36%), followed by a decreasing trend in variability for the subsequent PCs. This indicates that PC1 captured the most significant variation in the dataset, followed by diminishing contributions from the subsequent principal components.

The interpretation of the rotated component matrix demonstrated that every principal component is distinctly loaded with various morphological and floral characteristics. The contributions of 12 traits to the first five PCs are detailed in Table 2. PC1 was primarily influenced by yield-related morphological traits, notably PL (17.998%), PH (14.163%), and GYPP (12.970%). On the other hand, PC2 was primarily contributed by outcrossing-related floral traits, particularly the stigma exertion traits TSE% (32.402%), DSE% (25.739%), and SSE% (23.884%). PC3 contributed to both floral and yield-related traits, *viz.*, DF (26.019%), DM (22.791%), SFP (20.164%), and GPP (14.562%).

In PC4, the traits ETTP (44.402%), GYPP (16.082%), PH (14.637%), and GPP (12.455%) were prominent contributors.

Therefore, PC1, PC2, PC3, and PC4 were key contributors to rice hybrid seed production. PC5 was mainly driven by the TW (94.083%) trait, and similar findings were reported by Bhargava et al. (2023). Overall, the results suggested that yield-related morphological traits played a significant role in PC1, highlighting their potential for increased productivity. Conversely, outcrossing-related floral traits were the major contributors to PC2, reflecting their role in reproductive success and potential for genetic diversity. PC3 and PC4 were influenced by a combination of flowering time-related and panicle characteristics, indicating their importance in determining the developmental and yield-related aspects of the plants. PC5 was influenced mainly by TW, indicating its role in determining grain size and weight. These results are consistent with Riaz et al. (2018), who reported that PC1 and PC2 were predominantly associated with yield-contributing traits, while flowering time-related traits, such as DF and DM, were clustered within the PC3 component.

The biplot is a powerful graphical tool that integrates information from both variables and observations into a single plot, offering a visual representation of the relationships between variables (traits) and observations (advanced backcross lines) in the reduced-dimensional space defined by the principal components. In the biplot, the length and direction of the vectors representing variables indicate the magnitude and direction of their contributions to the principal components, respectively. The clustering of variables in the biplot revealed the patterns of correlation or covariance among traits, while the positioning of observations relative to variable vectors provides insights into the performance of individual lines across various traits. A biplot between PC1 and PC2 was created using different morpho-floral



Table 2 Contribution of morpho-floral traits to the variation observed in the first five principal components

Traits	PC1	PC2	PC3	PC4	PC5
DF	9.784	0.203	26.019	0.651	0.726
DM	10.000	0.450	22.791	0.047	0.000
PH	14.163	1.730	0.304	14.637	0.104
ETPP	6.965	2.511	6.276	44.402	0.229
PL	17.998	3.790	0.666	9.949	0.051
GPP	10.057	2.737	14.562	12.455	0.403
SFP	2.050	0.535	20.164	0.925	0.953
GYPP	12.970	4.908	7.415	16.082	2.415
TW	0.001	1.111	0.003	0.292	94.083
SSE%	7.377	23.884	0.005	0.394	0.134
DSE%	2.079	25.739	1.459	0.034	0.557
TSE%	6.556	32.402	0.336	0.133	0.344

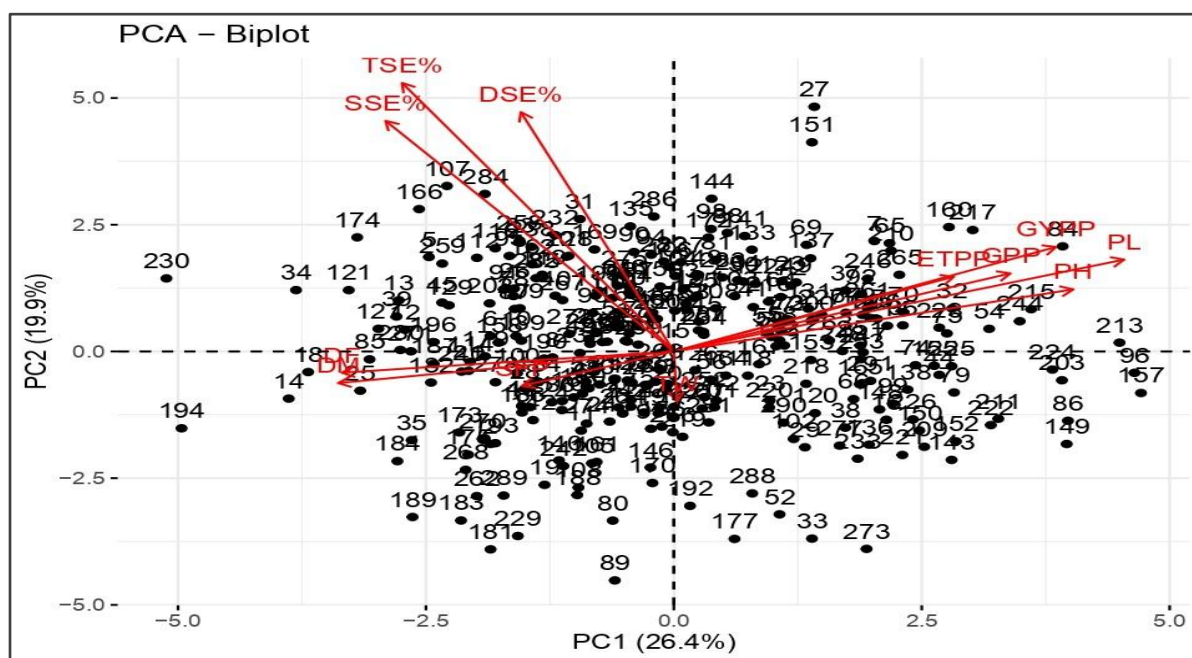


Figure 2 Biplot between PC1 and PC2 using different morpho-floral traits of rice advanced lines

traits, as depicted in Figure 2. The results indicated that traits showing positive correlations were clustered together, while those with negative correlations were positioned on opposite sides of the plot origin. The PL, GYPP, and PH traits had greater vector lengths (distance from the origin) in PC1, while the TSE%, DSE%, and SSE% traits had greater vector lengths in PC2, indicating a good representation of these traits compared to other traits. Figure 2 also illustrates the distribution and diversity of both variables in the advanced backcross lines. Overall, PC1 and PC2 accounted for 46.30% of the total variability. Among the traits, TSE% exhibited

the greatest vector length, suggesting its substantial contribution to the overall divergence, followed by SSE%, DSE%, PL, GYPP, PH, and GPP. Advanced backcross lines adjacent to the trait vector within the same quadrant were more likely to exhibit favorable performance for the corresponding traits. Lines 27, 151, 107, 284, 213, 84, 230, 157, 96, 194, and 89 significantly contributed to the overall diversity, owing to their high PC scores and considerable distance from the origin of axes. Therefore, rigorous selection methods can be devised to expedite the enhancement of the aforementioned morpho-floral traits in advanced backcross

populations of rice. Similarly, Rahangdale et al. (2021) identified superior genotypes for yield and quality traits by focusing on high PC scores in their PCA.

### Conclusion

PCA was employed to assess the contribution of different morpho-floral traits to overall variability. The analysis revealed that the first five PCs collectively accounted for an average of 78.78% of the total variability. The important traits (PL, PH, GYPP, TSE%, DSE%, and SSE%) grouped within PC1 and PC2 helped explain maximum variability and displayed a tendency to cooccur consistently. Therefore, this study provides valuable insights into identifying parameters contributing to variability and selecting suitable lines for breeding, facilitating crop improvement for morpho-floral traits. Furthermore, the investigated advanced backcross population exhibited notable segregation and diversity in morphological and floral characteristics, suggesting its potential for mapping genomic regions associated with yield and out-crossing (stigma exertion) traits.

### Acknowledgment

The authors would like to convey their gratitude to Dr. R.L. Verma, Crop Improvement Division, National Rice Research Institute, Cuttack, Odisha, for providing the essential materials to accomplish this research work. Furthermore, the authors wish to express their gratitude to the Department of Science and Technology (DST), Ministry of Science and Technology, Government of India, for providing partial funding support through a DST INSPIRE fellowship to the first author for pursuing a doctoral degree program at Banaras Hindu University, Varanasi.

### Declaration of competing interest

The authors declare that they have no competing interests related to this study.

### References

Balakrishnan, D., Subrahmanyam, D., Badri, J., Raju, A. K., Rao, Y. V., et al. (2016). Genotype × environment interactions of yield traits in backcross introgression lines derived from *Oryza sativa* cv. Swarna/*Oryza nivara*. *Frontiers in Plant Science*, 7, 1530.

Bhargava, K., Sreedhar, M., Lakshmi, V. J., Rathod, R., Parimala, K., & Vanisri, S. (2023). Genetic analysis of backcross derived lines for yield and yield attributing traits in rice (*Oryza sativa* L.). *Theoretical Biology Forum*, 12(2), 51-59.

Brejda, J. J., Moorman, T. B., Karlen, D. L., & Dao, T. H. (2000). Identification of regional soil quality factors and indicators. I. Central and Southern High Plains. *Soil Science Society of America Journal*, 64, 2115-2124.

IRRI. (2013). *Standard evaluation system (SES) for rice* (5<sup>th</sup> ed.). IRRI, Philippines.

Kumar, L., Chhogyel, N., Gopalakrishnan, T., Hasan, M. K., Jayasinghe, S. L., et al. (2022). Climate change and future of agri-food production. In *Future Foods: Global Trends, Opportunities, and Sustainability Challenges* (pp. 49-79). Cambridge, MA, USA: Academic Press. DOI: <https://doi.org/10.1016/B978-0-323-91001-9.00009-8>.

Marathi, B., & Jena, K. K. (2015). Floral traits to enhance out-crossing for higher hybrid seed production in rice: present status and future prospects. *Euphytica*, 201, 1-14.

Prahalada, G. D., Marathi, B., Vinarao, R., Kim, S. R., Diocton, R., 4th, Ramos, J., & Jena, K. K. (2021). QTL Mapping of a Novel Genomic Region Associated with High Out-Crossing Rate Derived from *Oryza longistaminata* and Development of New CMS Lines in Rice, *O. sativa* L. *Rice (New York, N.Y.)*, 14(1), 80. <https://doi.org/10.1186/s12284-021-00521-9>.

Qian, Q., Guo, L. B., Smith, S. M., & Li, J. Y. (2016). Breeding high-yield superior quality hybrid super rice by rational design. *National Science Review*, 3(3), 283-294.

Rahangdale, S., Singh, Y., Upadhyay, P. K., & Koutu, G. K. (2021). Principal component analysis of JNPT lines of rice for the important traits responsible for yield and quality. *Indian Journal of Genetics and Plant Breeding*, 81(01), 127-131.

Ramos, J. M., Furuta, T., Uehara, T. K., Chihiro, N., Angeles-Shim, R. B., et al. (2016). Development of chromosome segment substitution lines (CSSLs) of *Oryza longistaminata* A. Chev. & Röhr in the background of the elite japonica rice cultivar, Taichung 65 and their evaluation for yield traits. *Euphytica*, 210, 151-163.

Ravindra, B. V., Sherya, K., Dangi, K. S., Usharani, G., & Shankar, A. S. (2012). Correlation and path analysis studies in popular rice hybrids of India. *International Journal of Scientific and Research Publications*, 2, 1-5.

Riaz, A., Bibi, T., Raza, Q., Sabar, M., & Akhter, M. (2018). Evaluation of rice (*Oryza sativa* L.) advance uniform lines using multivariate analysis. *African Journal of Plant Science*, 12(11), 284-289.

Sathe, A. P., Kumar, A., Mandlik, R., Raturi, G., Yadav, H., et al. (2021). Role of silicon in elevating resistance against sheath blight and blast diseases in rice (*Oryza sativa* L.). *Plant Physiology and Biochemistry*, 166, 128-139.

Sharma, N., Bandyopadhyay, B. B., Chand, S., Pandey, P. K., Baskheti, D. C., Malik, A., & Chaudhary, R. (2022). Determining

- selection criteria in finger millet (*Eleusine coracana*) genotypes using multivariate analysis. *Indian Journal of Agricultural Sciences*, 92(6), 763-768.
- Sheela, K. R. V. S., Robin, S., & Manonmani, S. (2020). Principal component analysis for grain quality characters in rice germplasm. *Electronic Journal of Plant Breeding*, 11(01), 127-131.
- Singh, P., Jain, P. K., & Tiwari, A. (2020). Principal component analysis approach for yield attributing traits in chilli (*Capsicum annum* L.) genotypes. *Chemical Science Review and Letters*, 9(33), 87-91.
- Todorovska, E., Hadjiivanova, B., Bozhanova, V., Dechev, D., Muhovski, Y., Panchev, I., & Ivanova, A. (2013). Molecular and phenotypic characterization of advanced backcross lines derived from interspecific hybridization of durum wheat. *Biotechnology & Biotechnological Equipment*, 27(3), 3760-3771.
- Xie, F. (2009). Priorities of IRRI hybrid rice breeding. In F. Xie & B. Hardy (Eds.), *Accelerating hybrid rice development* (pp. 49-62). International Rice Research Institute, Los Baños.
- Zeliang, P. K., & Pattanayak, A. (2013). Wide Hybridization in the Genus *Oryza*: Aspects and Prospects. *Indian Journal of Hill Farming*, 26(2), 71-77.
- Zhang, K., Zhang, Y., Wu, W., Zhan, X., BakrAnis, G., et al. (2018). qSE7 is a major quantitative trait locus (QTL) influencing stigma exertion rate in rice (*Oryza sativa* L.). *Scientific Reports*, 8(1), 14523.



# Journal of Experimental Biology and Agricultural Sciences

<http://www.jebas.org>

ISSN No. 2320 – 8694

## Exploring intra-allelic and inter-allelic gene interactions influencing seed yield and its components in inter-varietal crosses of Mungbean (*Vigna radiata* (L.) Wilczek)

T Nivethitha<sup>1\*</sup> , C Babu<sup>2</sup>, P Jayamani<sup>1</sup>

<sup>1</sup>Department of Pulses, Centre for Plant Breeding and Genetics, Tamil Nadu Agricultural University, Coimbatore, India

<sup>2</sup>Directorate of Research, Tamil Nadu Agricultural University, Coimbatore, India

Received – May 07, 2024; Revision – June 18, 2024; Accepted – June 24, 2024

Available Online – July 15, 2024

DOI: [http://dx.doi.org/10.18006/2024.12\(3\).426.434](http://dx.doi.org/10.18006/2024.12(3).426.434)

### KEYWORDS

Epistasis

Gene action

Generation mean analysis

Mungbean

Non-allelic interaction

### ABSTRACT

Mungbean (*Vigna radiata* (L.) Wilczek) is a versatile legume widely cultivated for its nutritional value and adaptability. Meeting the increasing global demand for nutritious food requires the development of high-yielding varieties. Therefore, understanding the inheritance of yield and component traits is crucial for defining effective breeding strategies. In the present study, we aimed to investigate the genetic effects and interactions governing inheritance through generation mean analysis. The four crosses viz., IPM409-4×VGG18-002, IPM409-4×WGG42, COGG13-39×VGG16-058 and COGG13-39×VGG18-002 and their five generations (P<sub>1</sub>, P<sub>2</sub>, F<sub>1</sub>, F<sub>2</sub> and F<sub>3</sub>) were evaluated for nine yield and yield component traits during 2023 summer season. The significance of additive, dominance, and epistatic components viz., additive×additive [*i*] and dominance×dominance [*I*] of each trait was found to be different among all the crosses. Mungbean is a self-pollinated crop, so only fixable gene effects can be exploited for trait improvement. In the IPM409-4×VGG18-002 cross, all the traits exhibited additive or additive × additive gene action except for plant height and seed yield per plant (dominance). The scaling test was significant in IPM409-4×WGG42 cross for all the traits, except for the number of pods per cluster. Except for the number of branches per plant in which the dominance effect was evident, additive or additive×additive gene effects were observed for the other traits. In COGG13-39×VGG16-058 and COGG13-39×VGG18-002 crosses, all the yield traits recorded fixable (additive and additive×additive) gene effects except for number of pods per plant in COGG13-39×VGG18-002. Considering the results of all four crosses, gene actions that exhibit consistency across crosses revealed that epistatic interaction (additive×additive) significantly influenced the expression of various mung bean traits. Therefore, the

\* Corresponding author

E-mail: [nivethitha120897@gmail.com](mailto:nivethitha120897@gmail.com) (T Nivethitha)

Peer review under responsibility of Journal of Experimental Biology and Agricultural Sciences.

Production and Hosting by Horizon Publisher India [HPI]  
 (<http://www.horizonpublisherindia.in/>).  
 All rights reserved.

All the articles published by [Journal of Experimental Biology and Agricultural Sciences](#) are licensed under a [Creative Commons Attribution-NonCommercial 4.0 International License](#) Based on a work at [www.jebas.org](http://www.jebas.org).



later generation selection of short-duration segregants with high yield, bold seeds, and resistance to yellow mosaic disease from the above populations can be carried out to develop commercially valuable mung bean varieties.

## 1 Introduction

Mungbean (*Vigna radiata* (L.) Wilczek) is a dynamic crop in Asia, serving significant roles as a food and economic resource. It is consumed in various forms, including whole or split seeds, flour, or sprouts, and serves as a valuable protein source (24 %). Additionally, mungbean offers substantial amounts of dietary fiber (64%), calcium (13%), magnesium (47%), and other vitamins and minerals (Shanthala et al. 2020). Despite its nutritional and economic value, the yield and productivity of mungbean in India remain unstable and volatile, leading to a broadening gap between demand and supply (Varma and Vishwanath 2023). Consequently, developing high-yielding varieties is crucial to meet the growing demands.

Conventional breeding methods in mungbean primarily involve hybridization followed by selection. Adopting an appropriate breeding strategy to enhance selection efficiency is essential based on understanding the gene action related to the yield and yield component traits. These traits are governed by complex gene actions, viz., intra-allelic (additive and dominance) and inter-allelic interactions (epistasis), which are strongly influenced by environmental factors. Additive gene action resulting from the cumulative effects of many alleles can be effectively fixed through selection (Singh and Mahama 2023). Conversely, exploiting dominant gene action through hybrid development is impractical in mungbean due to the self-pollinating nature of the crop and the challenges in maintaining heterosis. Epistasis, or the interaction between genes at different loci, can significantly influence trait expression and complicate the estimation of additive and dominance effects. Although the epistatic component is of low magnitude, it should not be overlooked, as it can lead to biased

estimates of additive and dominance variance. The presence or absence of epistasis can be identified through scaling tests. The application of the biometrical tool, generation mean analysis, is crucial for accurately delineating the nature of gene effects and the types of epistasis involved in the trait expression (Yadav et al. 2017). This method involves evaluating parents,  $F_1$ , and segregating generations to partition the genetic variance into its constituent components. By doing so, researchers can identify the contributions of additive, dominance, and epistatic effects to the overall phenotype. This approach assists in determining the most appropriate breeding strategy for enhancing various yield-contributing traits in mungbean.

Therefore, the present investigation uses generation mean analysis to estimate the additive, dominance, and epistatic effects of the yield and yield contributing traits in the intra-specific crosses of mungbean. This knowledge will enable the development of mungbean varieties with stable and enhanced yields, ultimately bridging the gap between demand and supply.

## 2 Materials and Methods

Five mungbean genotypes including IPM 409-4, COGG 13-39, VGG 16-058, VGG 18-002 and WGG 42 were used to generate four segregating populations viz., IPM 409-4  $\times$  VGG 18-002, IPM 409-4  $\times$  WGG 42, COGG 13-39  $\times$  VGG 16-058 and COGG 13-39  $\times$  VGG 18-002. These crosses were decided based on the contrasting nature of the parents for duration and yield attributes. Details of the parental source and characteristics are presented in Table 1. The field experiment was conducted at the Department of Pulses, Centre for Plant Breeding and Genetics, Tamil Nadu Agricultural University, Coimbatore, Tamil Nadu, India. The

Table 1 Parent materials involved in the study with their characteristic features

S. No.	Genotypes	Source	Special Characteristics
Female parents			
1.	IPM 409-4	ICAR-Indian Institute of Pulses Research, Kanpur	Variety: Early duration (<28 days to 50 % flowering), Shiny seeds, short pod (pod length < 8 cm)
2.	COGG 13- 39	Department of Pulses, Tamil Nadu Agricultural University, Coimbatore	Breeding line: Shiny seeds, high yield
Male parents			
3.	VGG 16-058	National Pulses Research Centre, Vamban, Tamil Nadu Agricultural University, Coimbatore	Breeding line: Shiny, bold seeds (test weight > 5g/100 seeds) and resistant to yellow mosaic disease
4.	VGG 18-002	National Pulses Research Centre, Vamban, Tamil Nadu Agricultural University, Coimbatore	Breeding line: Shiny, bold seeds (test weight > 5g/100 seeds), long pod (pod length > 10 cm)
5.	WGG 42	Regional Agricultural Research Station, Warangal, Professor Jayashankar Telangana State Agricultural University, Hyderabad	Variety: Shiny seeds, bold seeds (test weight > 5g/100 seeds), long pod (pod length > 10 cm)



Table 2 Details of population size of all the generations of four crosses

S. No.	Crosses	Population size				
		P <sub>1</sub>	P <sub>2</sub>	F <sub>1</sub>	F <sub>2</sub>	F <sub>3</sub>
1.	IPM 409-4 × VGG 18-002	10	10	10	48	89
2.	IPM 409-4 × WGG 42	10	10	10	99	253
3.	COGG 13- 39× VGG 16-058	10	10	10	84	210
4.	COGG 13- 39× VGG 18-002	10	10	10	152	179

crossing program was carried out in 2022 summer to synthesize hybrids of the above four crosses. During *Kharif* 2022, F<sub>1</sub>s were raised, and the true hybrids were morphologically confirmed based on contrasting traits between parents. The true hybrid plants of F<sub>1</sub>s were harvested individually, and the F<sub>2</sub> populations were raised during *rabi* 2022 to procure the seeds for F<sub>3</sub> generation.

### 2.1 Evaluation of Genetic Materials

The four crosses' five generations (P<sub>1</sub>, P<sub>2</sub>, F<sub>1</sub>, F<sub>2</sub>, and F<sub>3</sub>) were raised during the summer of 2023 in a row length of 4 m at a 30 × 10 cm spacing. Standard cultivation practices were strictly adhered to ensure a healthy crop. Nine biometrical traits, *viz.*, plant height, number of branches, number of clusters, number of pods per cluster, number of pods per plant, pod length, number of seeds per pod, hundred seed weight, and seed yield per plant were recorded in all five generations of four crosses (Table 2). The mean values of five generations were used to derive the gene effects.

### 2.2 Statistical analysis

The scaling test (Mather 1949) was used to test the adequacy of a simple additive-dominance model. The simple additive-dominance model was considered inadequate when either of the scales, *viz.*, C or D, were significant, indicating the presence of epistasis. The generation means analysis with a five-parameter model (Hayman 1960) was performed to estimate residual effect [*m*], additive [*d*], dominance [*h*], and epistatic components, *i.e.*, additive × additive [*i*] and dominance × dominance [*l*]. The five-parameter model lacks insights into additive × dominance [*j*] interactions, and data analysis was conducted using the TNAU-STAT statistical package (Manivannan 2014).

### 3 Results and Discussion

The precise knowledge of gene effects governing the expression of yield and yield-contributing traits is essential for formulating an efficient breeding and selection strategy. The generation mean analysis was carried out in the four inter-varietal crosses *viz.*, IPM 409-4 × VGG 18-002, IPM 409-4 × WGG 42, COGG 13-39 × VGG 16-058 and COGG 13-39 × VGG 18-002 to estimate the additive, dominant and epistatic effects influencing yield and yield

components. Each parent exhibited distinctive characteristics, such as IPM 409-4 with early duration (<28 days for 50 % flowering), COGG 13-39 being high-yielding (>20 g/singe plant), and male parents *viz.*, VGG 18-002, VGG 16-058 and WGG 42 with bold seeds (test weight >5 g/100 seeds) (Table 3). This indicates that variability in mean performance exists for yield components, suggesting the potential for further improvement.

Among the parents, COGG 13-39 outperformed for traits such as number of branches (2.70), number of clusters (15.70), number of pods per cluster (5.00), number of pods per plant (49.90), and seed yield per plant (23.09 g) (Table 3). The male parent, VGG 18-002 was found to be superior for pod length (10.15 cm), number of seeds per pod (12.40), and hundred seed weight (5.54 g) (Table 3). In F<sub>1</sub> generation, mean performance surpassed that of the parental mean value in IPM 409-4 × VGG 18-002 cross for seed yield per plant (18.85 g) and in IPM 409-4 × WGG 42 cross for number of branches (3.50) indicating potential vigor for yield and branching (Table 3). However, major yield components *viz.*, number of clusters, number of pods per plant, pod length and hundred seed weight in all the four crosses (IPM 409-4 × VGG 18-002, IPM 409-4 × WGG 42, COGG 13-39 × VGG 16-058 and COGG 13-39 × VGG 18-002) exhibited intermittent values within the range of parental values (Table 3). In F<sub>2</sub> to F<sub>3</sub> generations, an upward trend was observed in the expression of all traits in IPM 409-4 × VGG 18-002 and COGG 13-39 × VGG 18-002 populations except for number of clusters in IPM 409-4 × VGG 18-002 and number of branches, pod length and number of seeds per pod in COGG 13-39 × VGG 18-002 (Table 3).

In all the four inter-varietal crosses evaluated for nine biometrical traits through scaling tests, at least one of the two scales (C and D) consistently exhibited statistical significance except the number of pods per cluster in IPM 409-4 × WGG 42 and the number of pods per plant in COGG 13-39 × VGG 16-058 (Table 4). The significant deviation of scales from zero indicated the presence of epistasis (non-allelic interaction). The presence of epistatic interactions in mungbean for yield and yield-related traits has been substantiated through various studies and research findings. In mungbean, Lenka et al. (2022) and Nainu et al. (2023) have observed complex genetic interactions influencing traits such as yield per plant, number of pods per plant, seed weight, and other

productivity-related parameters. These interactions play a are critical considerations in breeding programs aimed at significant role in shaping the phenotypic expression of traits and enhancing yield in mungbean varieties.

Table 3 Mean and standard errors for yield and yield component traits in various generations of mungbean crosses

Cross	Traits	Generation				
		P <sub>1</sub>	P <sub>2</sub>	F <sub>1</sub>	F <sub>2</sub>	F <sub>3</sub>
IPM 409-4 × VGG 18-002	Plant height (cm)	60.69±0.97	58.39±0.80	52.16±1.31	32.33±0.72	40.68±0.98
	Number of branches	2.20 ± 0.13	2.40 ± 0.16	2.40 ± 0.24	2.71 ± 0.12	2.88 ± 0.09
	Number of clusters	14.90 ± 0.72	8.40 ± 0.62	11.60 ± 0.93	10.04 ± 0.42	8.38 ± 0.34
	Number of pods per clusters	4.10 ± 0.28	4.20 ± 0.25	3.60 ± 0.24	3.25 ± 0.08	4.07 ± 0.10
	Number of pods per plant	50.50 ± 4.01	29.80 ± 1.05	31.80 ± 1.11	27.31 ± 1.22	31.78 ± 1.54
	Pod length (cm)	7.05 ± 0.11	10.15 ± 0.13	7.88 ± 0.11	7.65 ± 0.12	7.95 ± 0.08
	Number of seeds per pod	11.50 ± 0.29	12.40 ± 0.29	12.20 ± 0.27	10.74 ± 0.12	10.95 ± 0.10
	Hundred seed weight (g)	3.53 ± 0.11	5.54 ± 0.09	4.71 ± 0.07	4.17 ± 0.07	4.25 ± 0.05
	Seed yield per plant (g)	16.48 ± 1.13	15.97 ± 0.84	18.85 ± 0.86	12.55 ± 0.41	14.39 ± 0.42
IPM 409-4 × WGG 42	Plant height (cm)	60.69 ± 0.97	66.76 ± 2.46	48.67 ± 2.32	30.32 ± 0.60	39.11 ± 0.35
	Number of branches	2.20 ± 0.13	2.10 ± 0.10	3.50 ± 0.22	2.33 ± 0.06	2.29 ± 0.03
	Number of clusters	14.90 ± 0.72	12.90 ± 0.5	14.83 ± 1.62	11.01 ± 0.30	9.28 ± 0.2
	Number of pods per clusters	4.10 ± 0.28	4.40 ± 0.37	4.00 ± 0.37	3.79 ± 0.09	3.92 ± 0.05
	Number of pods per plant	50.50 ± 4.01	30.60 ± 0.69	38.00 ± 4.18	35.61 ± 1.18	29.78 ± 0.81
	Pod length (cm)	7.05 ± 0.11	9.56 ± 0.14	7.18 ± 0.16	7.75 ± 0.07	6.80 ± 0.03
	Number of seeds per pod	11.50 ± 0.29	12.73 ± 0.24	10.06 ± 0.23	10.67 ± 0.09	11.26 ± 0.05
	Hundred seed weight (g)	3.53 ± 0.11	5.02 ± 0.17	4.27 ± 0.10	4.09 ± 0.05	3.44 ± 0.02
	Seed yield per plant (g)	16.48 ± 1.13	15.96 ± 0.75	11.30 ± 2.34	15.42 ± 0.53	13.95 ± 0.22
COGG 13-39 × VGG 16-058	Plant height (cm)	66.54 ± 1.60	58.10 ± 0.74	52.34 ± 1.15	54.99 ± 0.63	54.51 ± 0.51
	Number of branches	2.70 ± 0.26	1.70 ± 0.26	2.10 ± 0.10	3.17 ± 0.09	2.76 ± 0.07
	Number of clusters	15.70 ± 0.98	9.00 ± 0.47	8.10 ± 0.60	9.99 ± 0.48	8.44 ± 0.21
	Number of pods per clusters	5.00 ± 0.15	4.00 ± 0.26	5.00 ± 0.26	4.08 ± 0.09	4.03 ± 0.06
	Number of pods per plant	49.90 ± 2.51	28.80 ± 0.71	29.20 ± 1.70	33.95 ± 2.14	33.88 ± 0.96
	Pod length (cm)	8.04 ± 0.1331	8.84 ± 0.147	8.07 ± 0.22	8.55 ± 0.06	8.41 ± 0.05
	Number of seeds per pod	11.63 ± 0.3	11.53 ± 0.14	11.12 ± 0.29	11.37 ± 0.10	11.19 ± 0.06
	Hundred seed weight (g)	4.13 ± 0.03	5.03 ± 0.05	4.28 ± 0.14	4.51 ± 0.05	4.37 ± 0.04
	Seed yield per plant (g)	23.09 ± 0.9	14.24 ± 0.35	15.47 ± 1.22	15.79 ± 0.38	14.32 ± 0.28
COGG 13-39 × VGG 18-002	Plant height (cm)	66.54 ± 1.6	58.39 ± 0.77	53.50 ± 1.79	64.29 ± 1.02	65.13 ± 0.81
	Number of branches	2.70 ± 0.26	2.40 ± 0.16	2.60 ± 0.22	3.11 ± 0.08	3.42 ± 0.08
	Number of clusters	15.70 ± 0.98	8.40 ± 0.62	14.00 ± 0.63	10.55 ± 0.37	12.14 ± 0.38
	Number of pods per clusters	5.00 ± 0.15	4.20 ± 0.25	3.60 ± 0.22	4.15 ± 0.07	4.96 ± 0.07
	Number of pods per plant	49.90 ± 2.51	29.80 ± 1.05	45.30 ± 3.12	37.45 ± 1.31	45.56 ± 1.25
	Pod length (cm)	8.04 ± 0.13	10.15 ± 0.13	8.60 ± 0.12	8.24 ± 0.04	7.85 ± 0.04
	Number of seeds per pod	11.63 ± 0.30	12.40 ± 0.29	11.87 ± 0.16	11.40 ± 0.06	11.24 ± 0.05
	Hundred seed weight (g)	4.13 ± 0.030	5.54 ± 0.09	4.66 ± 0.09	4.21 ± 0.03	3.96 ± 0.02
	Seed yield per plant (g)	23.09 ± 0.90	15.97 ± 0.48	20.97 ± 0.77	16.35 ± 0.53	16.50 ± 0.39

Mean ± Standard error

Table 4 Scaling test and estimates of genetic parameters for yield and yield contributing traits of mungbean crosses

Cross	Trait	Scale				Parameter			
		C	D	<i>m</i>	[ <i>d</i> ]	[ <i>h</i> ]	[ <i>i</i> ]	[ <i>l</i> ]	
IPM 409-4 × VGG 18-002	Plant height	-94.39** ± 4.09	-21.32** ± 4.38	32.33** ± 0.72	1.00 ± 0.63	-9.05** ± 3.12	0.48 ± 2.97	97.42** ± 8.53	
	Number of branches	1.43* ± 0.72	1.49** ± 0.49	2.71** ± 0.12	-0.10 ± 0.11	-0.65 ± 0.38	-0.95* ± 0.42	0.07 ± 1.26	
	Number of clusters	-6.33* ± 2.68	-9.86** ± 1.87	10.04** ± 0.42	3.25** ± 0.48	5.46** ± 1.39	12.01** ± 1.65	-4.70 ± 4.56	
	Number of pods per clusters	-2.50** ± 0.70	1.47** ± 0.56	3.25** ± 0.08	-0.05 ± 0.19	-1.95** ± 0.34	-1.50** ± 0.47	5.29** ± 1.05	
	Number of pods per plant	-34.65** ± 6.78	-7.82 ± 7.82	27.31** ± 1.22	10.35** ± 2.08	-8.91 ± 4.84	20.14** ± 6.2	35.77** ± 13.10	
	Pod length	-2.35** ± 0.54	-0.70 ± 0.44	7.65** ± 0.12	-1.55** ± 0.08	-0.65 ± 0.33	-3.03** ± 0.36	2.20* ± 1.07	
	Number of seeds per pod	-5.32** ± 0.85	-1.60* ± 0.63	10.74** ± 0.12	-0.45* ± 0.21	0.42 ± 0.41	-0.72 ± 0.55	4.97** ± 1.34	
	Hundred seed weight	-1.82** ± 0.35	-0.39 ± 0.30	4.17** ± 0.07	-1.01** ± 0.07	0.14 ± 0.21	-2.06** ± 0.25	1.90** ± 0.66	
	Seed yield per plant	-21.44** ± 2.77	-1.49 ± 2.35	12.55** ± 0.41	-0.5 ± 0.70	-0.71 ± 1.51	-3.57 ± 1.96	26.59** ± 4.62	
IPM 409-4 × WGG 42	Plant height	-103.53** ± 5.85	-31.64** ± 3.23	30.32** ± 0.6	-3.04* ± 1.32	-11.22** ± 2.17	-2.23 ± 2.88	95.84** ± 8.04	
	Number of branches	-1.97** ± 0.53	0.19 ± 0.24	2.33** ± 0.06	0.05 ± 0.08	0.90** ± 0.21	-0.35 ± 0.28	2.87** ± 0.77	
	Number of clusters	-13.43** ± 3.57	-12.71** ± 1.33	11.01** ± 0.3	1.00* ± 0.44	7.17** ± 1.34	8.24** ± 1.69	0.95 ± 5.05	
	Number of pods per clusters	-1.35 ± 0.94	-0.39 ± 0.54	3.79** ± 0.09	-1.15* ± 0.23	-0.21 ± 0.34	-	-	
	Number of pods per plant	-14.68 ± 10.43	-33.18** ± 5.71	35.61** ± 1.18	9.95** ± 2.04	17.13** ± 4.24	39.58** ± 6.37	-24.67 ± 15.23	
	Pod length	0.02 ± 0.48	-4.88** ± 0.27	7.75** ± 0.07	-1.26** ± 0.09	2.13** ± 0.20	0.74** ± 0.27	-6.54** ± 0.75	
	Number of seeds per pod	-1.65* ± 0.71	-0.54 ± 0.48	10.67** ± 0.09	-0.62** ± 0.19	-1.98** ± 0.28	-1.15* ± 0.46	1.48 ± 1.01	
	Hundred seed weight	-0.73* ± 0.34	-2.97** ± 0.23	4.09** ± 0.05	-0.75** ± 0.10	1.85** ± 0.13	0.36 ± 0.21	-2.99** ± 0.48	
	Seed yield per plant	4.61 ± 5.31	-9.55** ± 1.94	15.42** ± 0.53	-0.77 ± 0.68	1.19 ± 1.98	5.60* ± 2.58	-18.88* ± 7.64	

Cross	Trait	Scale				Parameter			
		C	D	<i>m</i>	[ <i>d</i> ]	[ <i>h</i> ]	[ <i>i</i> ]	[ <i>l</i> ]	
COGG 13-39 × VGG 16-058	Plant height	-9.36* ± 3.84	-16.59** ± 2.97	54.99** ± 0.63	4.22** ± 0.88	-0.48 ± 2.00	17.94** ± 2.71	-9.64 ± 6.49	
	Number of branches	4.07** ± 0.54	0.31 ± 0.50	3.17** ± 0.09	0.50* ± 0.18	0.37 ± 0.27	1.47** ± 0.41	-5.00** ± 0.83	
	Number of clusters	-0.95 ± 2.5	-10.92** ± 1.67	9.99** ± 0.48	3.35** ± 0.54	2.87* ± 1.18	13.82** ± 1.72	-13.30** ± 4.29	
	Number of pods per clusters	-2.67** ± 0.71	-1.03* ± 0.43	4.08** ± 0.09	0.50** ± 0.15	0.74* ± 0.31	1.24** ± 0.39	2.18* ± 1.08	
	Number of pods per plant	-1.29 ± 9.59	-11.10 ± 6.32	33.95** ± 2.14	10.55** ± 1.30	-2.97 ± 5.12	-	-	
	Pod length	1.17* ± 0.55	-0.33 ± 0.31	8.55** ± 0.06	-0.40** ± 0.10	0.05 ± 0.23	-0.39 ± 0.30	-2.00* ± 0.82	
	Number of seeds per pod	0.10 ± 0.78	-1.17* ± 0.46	11.37** ± 0.10	0.05 ± 0.17	0.33 ± 0.32	1.89* ± 0.49	-1.68 ± 1.16	
	Hundred seed weight	0.32 ± 0.34	-0.70** ± 0.19	4.51** ± 0.05	-0.45** ± 0.03	0.22 ± 0.17	-0.37* ± 0.18	-1.36* ± 0.56	
	Seed yield per plant	-5.12 ± 3.03	-11.60** ± 1.67	15.79** ± 0.38	4.43** ± 0.48	3.69** ± 1.35	15.73** ± 1.74	-8.64 ± 4.70	
COGG 13-39 × VGG 18-002	Plant height	25.24** ± 5.71	7.01 ± 4.22	64.29** ± 1.02	4.08** ± 0.89	-9.43** ± 3.2	7.68* ± 3.70	-24.31* ± 10.39	
	Number of branches	2.15** ± 0.63	2.37** ± 0.46	3.11** ± 0.08	0.15 ± 0.15	-1.18** ± 0.3	-0.93* ± 0.42	0.30 ± 0.97	
	Number of clusters	-9.89** ± 2.27	3.35 ± 2.04	10.55** ± 0.37	3.65** ± 0.58	-1.93 ± 1.32	3.42* ± 1.69	17.66** ± 3.97	
	Number of pods per clusters	0.21 ± 0.60	2.34** ± 0.42	4.15** ± 0.07	0.4* ± 0.15	-2.53** ± 0.27	-0.73* ± 0.34	2.85** ± 0.90	
	Number of pods per plant	-20.51* ± 8.59	27.66** ± 6.27	37.45** ± 1.31	10.05** ± 1.36	-16.41** ± 4.72	-1.76 ± 5.42	64.23** ± 14.95	
	Pod length	-2.42** ± 0.36	-3.29** ± 0.25	8.24** ± 0.04	-1.06** ± 0.09	1.3** ± 0.16	-0.32 ± 0.23	-1.16* ± 0.53	
	Number of seeds per pod	-2.18** ± 0.58	-1.87** ± 0.48	11.4** ± 0.06	-0.38 ± 0.21	0.73** ± 0.21	0.12 ± 0.42	0.41 ± 0.71	
	Hundred seed weight	-2.17** ± 0.24	-2.25** ± 0.16	4.21** ± 0.03	-0.7** ± 0.05	0.96** ± 0.11	-0.27* ± 0.13	-0.10 ± 0.39	
	Seed yield per plant	-15.59** ± 2.82	-5.76** ± 2.15	16.35** ± 0.53	3.56** ± 0.51	2.69 ± 1.58	8.36** ± 1.91	13.11* ± 5.16	

\* & \*\* Significance at 0.05 and 0.01 probability levels, respectively; C- Scale C; D- Scale D; m- Residual; [d]- Additive; [h]- Dominance; [i]- Additive × Additive; [l]- Dominance × Dominance; (-)- Absence of epistasis

### 3.1 Gene action

On dissection of the generation mean into five different genetic components, the effect of residual mean was highly significant, indicating variation across the generations in all crosses. For each trait, the significance and relative strength of additive, dominance, and epistatic components *viz.*, additive  $\times$  additive [*i*] and dominance  $\times$  dominance [*l*] were different from each other in all four crosses (Table 4). The observed disparity can be attributed to the involvement of genes with varying frequencies and contrasting or synergistic effects in the parental genotypes. Therefore, a targeted selection strategy tailored to specific crosses could be developed for trait improvement, followed by a more generalized strategy. However, as a highly self-pollinated crop, mungbean, only the fixable gene effects, *viz.*, additive and additive  $\times$  additive, could be exploited for trait improvement. Therefore, in the present study, for deciding the selection criteria, the non-fixable gene effects (dominance and dominance  $\times$  dominance) were ignored when the fixable gene effects for the traits were significant.

In IPM 409-4  $\times$  VGG 18-002 population, various traits such as number of clusters, number of pods per plant, pod length, and hundred seed weight displayed additive and additive  $\times$  additive gene actions (Table 4). This indicates that the expression of these traits is influenced by individual gene effects (additive) and interactions between genes (epistasis), specifically additive  $\times$  additive interactions. In contrast, traits like the number of seeds per pod exhibited additive gene action, and the number of branches and pods per cluster exhibited additive  $\times$  additive gene action (Table 4). These findings suggest that selection strategies for traits exhibiting epistatic interactions should be deferred to later generations to harness these interactions for trait improvement effectively. Previous studies by Latha et al. (2018) and Kanwade et al. (2019) have reported similar genetic findings in mungbean, corroborating the presence of fixable gene effects for traits such as number of branches, number of clusters, number of pods per cluster, number of pods per plant and hundred seed weight. This implies that these traits can be improved through selective breeding efforts targeting additive and epistatic gene interactions. Conversely, plant height and seed yield per plant displayed nonfixable gene effects (dominance and dominance  $\times$  dominance) (Table 4). Latha et al. (2019) and Lenka et al. (2022) have also reported the predominance of dominance  $\times$  dominance gene interaction for plant height and Kanwade et al. (2019) and Patel et al. (2012) for seed yield per plant in mungbean. However, in mungbean, non-fixable gene effects cannot be exploited through selection.

The outcomes of the scaling test in the IPM 409-4  $\times$  WGG 42 population revealed that epistasis was significant for all the traits except for the number of pods per cluster (Table 4). Notably,

additive gene action was observed for the number of pods per cluster, indicating the feasibility of early-generation selection for trait improvement. The additive gene action for the number of pods per cluster corroborates with the findings of Pathak et al. (2014) in mungbean, validating the role of additive effects in shaping this trait. Simultaneously, additive and additive  $\times$  additive gene effects influenced the inheritance of the number of clusters, number of pods per plant, pod length, number of seeds per pod, and hundred seed weight, while the predominance of additive gene effect for plant height and additive  $\times$  additive gene effects for seed yield per plant were observed (Table 4) underscoring their complex genetic inheritance. With fixable gene effects and epistasis, the above traits can be improved through selection in later generations. The results of fixable gene effects were reported for plant height, number of clusters, and number of pods per plant by Latha et al. (2018), for pod length by Lenka et al. (2022), and number of seeds per pod and hundred seed weight by Yadav et al. (2017) and Narasimhulu et al. (2018) in mungbean. On the other hand, the absence of significant fixable gene effects for the number of branches indicated that trait improvement through selection is not feasible in this population.

In this study, COGG 13-39  $\times$  VGG 16-058 population of mungbean, we investigated the genetic effects influencing various agronomic traits (Table 4). Epistasis was notably present in all traits except for the number of pods per plant, which displayed primarily additive gene action, suggesting its suitability for early-generation selection. This finding is consistent with previous research by Kumar et al. (2015), further supporting the role of additive genetic effects in influencing the number of pods per plant. Whereas, for most traits *viz.*, plant height, number of branches, number of clusters, number of pods per cluster, hundred seed weight, and seed yield per plant were recorded as additive and additive  $\times$  additive gene effects (Table 4). Further, pod length and number of seeds per pod exhibited additive and additive  $\times$  additive gene actions, respectively (Table 4). Consequently, the above traits with fixable epistatic gene effects can be effectively improved by postponing the selection process to later generations. This indicates a complex genetic architecture where trait expression is influenced by interactions between alleles at different loci, highlighting the need for strategic breeding approaches. The findings of Pathak et al. (2014) suggested a selection procedure involving delayed selection that fixes the additive  $\times$  additive genetic effect for the above traits in later generations. The selection procedure of delayed selection, which fixes the additive  $\times$  additive genetic effect for the number of branches, number of clusters, number of pods per cluster, and hundred seed weight, was also reported by Narasimhulu et al. (2018) and for pod length and number of seeds per pod by Lenka et al. (2022) in mungbean. Kumar et al. (2015) have also reported additive and additive  $\times$  additive gene actions for seed yield per plant in mungbean. These studies advocate for a



delayed selection strategy that stabilizes additive  $\times$  additive genetic effects in subsequent generations, providing insights for optimizing breeding programs to improve mungbean productivity traits through genetic manipulation and selection strategies tailored to trait-specific genetic architectures.

In COGG 13-39  $\times$  VGG 18-002 population, additive, and additive  $\times$  additive gene effects were reported for plant height, number of clusters, number of pods per cluster, hundred seed weight, and seed yield per plant (Table 4). The findings of significant fixable genetic components for the above traits in mungbean were in accordance with Latha et al. (2018), Narasimhulu et al. (2018), and Nainu et al. (2023). Whereas, additive gene action was prevalent for expressing the number of pods per plant and pod length, and additive  $\times$  additive gene action was prevalent for the number of branches (Table 4). Additive  $\times$  additive gene action for the number of branches (Kumar et al. 2015; Narasimhulu et al. 2018) and additive gene effects for the number of pods per plant and pod length (Alam et al. 2014) were reported in mungbean. The presence of significant additive and additive  $\times$  additive gene actions suggests that selecting for these traits should be deferred to later generations to exploit their genetic potential fully. This strategic selection delay aligns with current literature recommendations, ensuring stabilization and enhancement of desired traits through cumulative genetic effects over generations. On the contrary, the predominance of dominance gene action in the expression of the number of seeds per pod indicates that trait improvement is not achievable through selection. This finding is corroborated by recent studies of Narasimhulu et al. (2018) and Latha et al. (2019), highlighting the challenge of improving number of seeds per pod through traditional selection approaches due to the nature of non-fixable genetic effects. The complex interplay of additive, additive  $\times$  additive, and dominance gene actions in trait inheritance is evident. These insights underscore the importance of tailored breeding strategies that leverage genetic interactions to optimize mungbean cultivars for enhanced productivity.

## Conclusion

For formulating a selection program for mungbean, emphasis was placed on identifying gene actions that exhibit consistency in most of the crosses. Epistatic interactions played a crucial role in the inheritance of the number of branches, number of clusters, number of pods per cluster, hundred seed weight, and seed yield per plant. However, these traits were under the influence of additive  $\times$  additive (fixable) gene effects, and hence, improvement through selection in later generations is feasible when desirable recombinants become available. As these populations were derived from early-maturing, bold-seeded, and high-yielding parents, selecting high-yielding segregants, combined with traits such as early maturity and bold seeds, becomes feasible in

subsequent generations. In addition, due to the involvement of MYMV-resistant male parents (VGG 16-058), the selection strategy coupled with MYMV screening will be rewarding.

## Acknowledgment

The first author expresses heartfelt gratitude to the Department of Science and Technology, Government of India, for the invaluable support granted through the DST INSPIRE Fellowship.

## Conflict of Interest

The authors declare no conflict of interest

## References

- Alam, A. M., Somta, P., & Srinives, P. (2014). Generation mean and path analyses of reaction to mungbean yellow mosaic virus (MYMV) and yield-related traits in mungbean (*Vigna radiata* (L.) Wilczek). *SABRAO Journal of Breeding & Genetics*, 46(1), 152-159.
- Hayman, B. (1960). The separation of epistatic from additive and dominance variation in generation means. II. *Genetica*, 31(1), 133-146.
- Kanwade, D., Kute, N., Jaybhaye, C., Deshmukh, S., Giri, M., & Pawar, V. (2019). Gene action for seed yield and maturity traits in mungbean (*Vigna radiata* (L.) R. Wilczek). *Frontiers in Crop Improvement*, 7(2), 142-144.
- Kumar, B. S., Prakash, M., & Gokulakrishnan, J. (2015). Genetic studies on biometric, biochemical, biophysical and morpho-physiological traits in mungbean [*Vigna radiata* (L.) Wilczek]. *Legume Research-An International Journal*, 38(4), 457-460.
- Latha, V. S., Eswari, K., & Kumar, S. S. (2018). Scaling and Joint Scaling tests for Quantitative Characters in Greengram (*Vigna radiata* (L.) Wilczek.). *Journal of Pharmacognosy and Phytochemistry*, 7(2), 185-190.
- Latha, V. S., Eswari, K., & Kumar, S. S. (2019). Heterosis and inbreeding depression in greengram (*Vigna radiata* (L.) Wilczek.). *Journal of Pharmacognosy and Phytochemistry*, 8(6), 798-802.
- Lenka, B., Baisakh, B., Dash, M., Lenka, D., & Tripathy, S. K. (2022). Gene action studies for yield and its related traits by using generation mean analysis in mungbean [*Vigna radiata* (L.) wilczek]. *Legume Research-An International Journal*, 45(2), 149-153.
- Manivannan N. (2014). TNAU STAT- Statistical package. Retrieved from <https://sites.google.com/site/tnaustat>.

- Mather, K. (1949). Biometrical genetics. The study of continuous variation. *Biometrical genetics. The study of continuous variation*. Methuen and Co., Ltd, London.
- Narasimhulu, R., Naidu, N., & Reddy, K. (2018). Genetic analysis for yield and yield attributes in greengram (*Vigna radiata* L. Wilczek). *Legume Research-An International Journal*, 41(3), 349-355.
- Nainu, A. J., Vadivel, K., Murugan, S., & Kumar, N. S. (2023). Generation Mean Analysis for Yield, its Components and MYMV Disease Resistance in Greengram [*Vigna radiata* (L.) Wilczek]. *Legume Research*, 46(11), 1541-1546.
- Patel, M., Vachhani, J., Jivani, L., Patel, B., & Kelaiya, D. (2012). Inheritance of quantitative traits and yellow mosaic virus in mungbean [*Vigna radiata* (L.) Wilczek]. *International Journal of Agricultural Sciences*, 8(2), 400-402.
- Pathak, N., Singh, M., Mishra, M., & Saroj, S. (2014). Estimates of gene effects and detection of epistasis for yield characters in mungbean [*Vigna radiata* (L.) Wilczek]. *Journal of Food Legumes*, 27(4), 289-292.
- Shanthala, J., Savithamma, D.L., Gazala, P., Jambagi, B.K., Desai, S.K.P. (2020). Genomics-Assisted Breeding Green Gram (*Vigna radiata* (L.) Wilczek) for Accelerating Genetic Gain. In S.S. Gosal, & S.H. Wani, (Eds.) *Accelerated Plant Breeding* (pp. 143-171). Springer, Cham Publishers. [https://doi.org/10.1007/978-3-030-47306-8\\_5](https://doi.org/10.1007/978-3-030-47306-8_5)
- Singh, A., & Mahama, A. A. (2023). Refresher on Population and Quantitative Genetics. *Crop Improvement*. Iowa State University Digital Press. Retrieved from <https://iastate.pressbooks.pub/cropimprovement/chapter/refresher-on-population-and-quantitative-genetics/>.
- Varma, P., & Vishwanath, D. (2023). Self Sufficiency in Pulses Production in India: An Analysis Based on the Successful Performance of Pulse Production and its Export from Myanmar. Retrieved from <https://www.iima.ac.in>
- Yadav, S., Prakash, V., & Khedar, O. (2017). Generation mean analysis for yield and its components in green gram [*Vigna radiata* (L.) Wilczek]. *Plant Archives*, 17(2), 1361-1367.




## Journal of Experimental Biology and Agricultural Sciences

<http://www.jebas.org>

ISSN No. 2320 – 8694

### Inheritance pattern of Qualitative traits, Genetic analysis and association of yield attributes in F<sub>2</sub> populations of Rice (*Oryza sativa*)

Santhiya S<sup>1</sup> , Pushpam R<sup>1\*</sup> , Subramanian A<sup>1</sup> , John Joel A<sup>2</sup> , Senthil A<sup>3</sup> ,  
Suresh R<sup>1</sup> , Manonmani S<sup>1</sup> , Pravin Kumar K<sup>1</sup> 

<sup>1</sup>Centre for Plant Breeding and Genetics, TNAU, Coimbatore, India

<sup>2</sup>Centre for Plant Molecular Biology and Biotechnology, TNAU, Coimbatore, India

<sup>3</sup>Department of Crop Physiology, TNAU, Coimbatore, India

Received – March 18, 2024; Revision – June 09, 2024; Accepted – June 29, 2024

Available Online – July 15, 2024

DOI: [http://dx.doi.org/10.18006/2024.12\(3\).435.445](http://dx.doi.org/10.18006/2024.12(3).435.445)

#### KEYWORDS

Rice

F<sub>2</sub> segregants

Inheritance

Skewness and Kurtosis

Genetic estimates

#### ABSTRACT

Understanding the extent of genetic variability within the segregating generations is crucial for identifying superior segregants with high yield and better market acceptability. Thus, the present study was carried out to quantify the extent of genetic variation available in the segregating population of rice. Three crosses, viz., CO 55 × IC 457996, CO 55 × IC 464685, and CO 55 × IC 115439 were evaluated using a non-randomized experimental design for six yield attributing and two physical grain quality traits in F<sub>2</sub> generation. The inheritance pattern of basal leaf sheath colour and grain colour in CO 55 × IC 115439 indicate digenic complementary gene interaction (9:7), whereas grain colour in CO 55 × IC 464685 exhibits inhibitory gene action (13:3). The positively skewed nature of productive tillers per plant and single-plant yield in the F<sub>2</sub> segregants emphasizes the need for intensive selection to facilitate rapid improvement due to the influence of complementary gene action. Moderate to high GCV with high heritability and GAM for traits such as plant height, productive tillers per plant, hundred seed weight, grain width, and single-plant yield in the F<sub>2</sub> segregants underscore the prevalence of additive gene action and thus provide the most effective condition for simple phenotypic selection. Moreover, productive tillers per plant and single-plant yield showed a strong positive association in all the crosses. Therefore, productive tillers per plant can be considered an indicator trait when selecting high-yielding segregants for grain yield improvement.

\* Corresponding author

E-mail: [pushpamtau@gmail.com](mailto:pushpamtau@gmail.com) (Pushpam R)

Peer review under responsibility of Journal of Experimental Biology and Agricultural Sciences.

Production and Hosting by Horizon Publisher India [HPI]  
(<http://www.horizonpublisherindia.in/>).  
All rights reserved.

All the articles published by [Journal of Experimental Biology and Agricultural Sciences](#) are licensed under a [Creative Commons Attribution-NonCommercial 4.0 International License](#) Based on a work at [www.jebas.org](http://www.jebas.org).



## 1 Introduction

Rice (*Oryza sativa* L.) is a primary dietary food source that sustains half of the world's population. As the world's population is projected to reach approximately 9.7 billion in 2050, the demand for food is expected to surge by 70% (Bin Rahman and Zhang 2021). However, to keep pace with the growing population, the current annual rice production levels are expected to increase by approximately 5.8 million tons (Santhiya et al. 2024). Over the past decades, the annual growth rate of rice yield remained  $\leq 1\%$ , failing to keep pace with the escalating demand due to various constraints (Khush 2013). In the present era, the importance of quality parameters is increasingly recognized, particularly in areas where rice production is self-sustaining. This underscores the importance of developing rice cultivars that yield high and exhibit superior quality. In light of the presently recognized resource limitations and changing climatic conditions, boosting rice production through sustainable practices remains a significant challenge. Thus, creating new variability through hybridization is one among several genetic approaches aimed at overcoming the yield barrier and enhancing rice productivity.

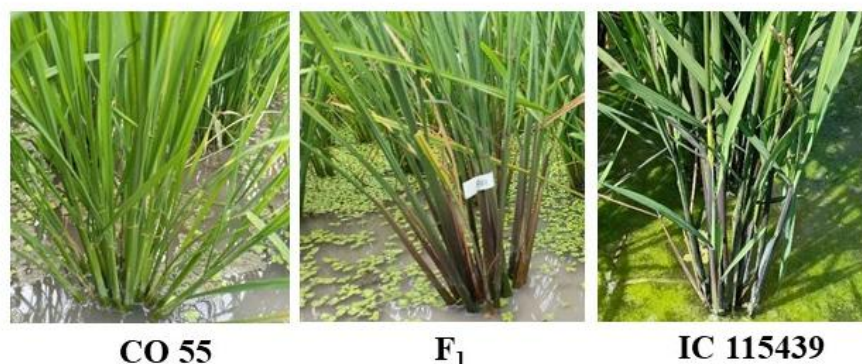
Genetic variability is crucial for effectively selecting superior segregants from the segregating population (Thúy et al. 2022). The genetic variability parameters, such as genotypic and phenotypic coefficient of variation, provide an insight into the relative amount of variation present in the segregating generations. However, the knowledge of the degree of heritable proportion of variation from the parent to its progeny is of paramount importance in deciding the traits to be selected (Bassuony et al. 2022). Third and fourth-degree statistics, specifically skewness and kurtosis, offer valuable insights into the type of gene action and the number of genes influencing traits within segregating generations (Fisher et al. 1932; Robson 1956). Therefore, understanding the extent of genetic variability and the distribution pattern of the  $F_2$  segregates would be effective tools to identify superior segregates with high yield and better market acceptability (Bassuony et al. 2022). Grain yield is a complex trait governed by polygenic loci, which in turn depends upon many independent contributing characteristics such as the number of productive tillers (Kalaivani et al. 2023), panicle length (Muthuvijayaragavan and Jebaraj, 2022), panicle weight (Nofal et al. 2024), thousand seed weight (Kalaivani et al. 2023), and filled grains per panicle (Bassuony et al. 2022). Therefore, direct selection for yield is often not effective. A better understanding of their association with single plant yield would be essential for formulating an effective breeding strategy, attributing traits as effective indicators in selection. In this context, the present study was designed to analyze the statistics and quantify the level of genetic variation present within the  $F_2$  (segregating) generation for yield, yield-attributing, and grain quality traits.

## 2 Materials and Methods

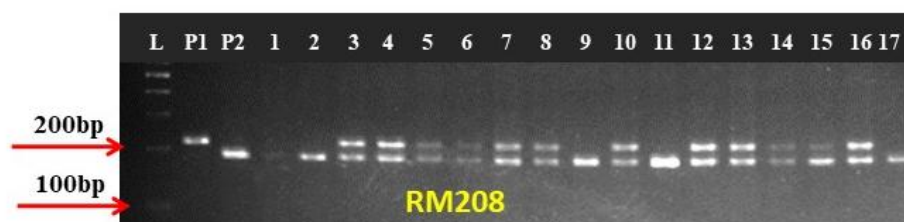
The study was conducted at the Department of Rice, TNAU, Coimbatore, Tamil Nadu, India ( $11^\circ$  N latitude and  $77^\circ$  E longitude). Hybridization was carried out between a popular high-yielding fine grain rice variety, CO 55, with three drought-tolerant landraces viz., IC 457996, IC 464685, and IC 115439 during *Rabi* 2022, and the resulting  $F_1$ s were evaluated during Summer 2023. True hybrids were distinguished based on their distinct morphological characteristics, such as the pigmentation of basal leaf sheath in CO 55 (green)  $\times$  IC 115439 (purple) (Figure 1), as well as grain colour in CO 55 (white)  $\times$  IC 464685 (red) and CO 55 (white)  $\times$  IC 115439 (red). Subsequently, all identified hybrids were further subjected to molecular confirmation using polymorphic marker RM1 between CO 55 and IC 464685 and RM3412 between CO 55 and IC 115439. Due to the lack of a visual morphological marker in CO 55  $\times$  IC 457996, polymorphic marker RM208 was used for identifying the true  $F_1$ s between CO 55 and IC 457996 (Figure 1). The heterozygous plants obtained from each cross CO 55  $\times$  IC 457996 (cross I), CO 55  $\times$  IC 464685 (cross II), and CO 55  $\times$  IC 115439 (cross III) were advanced to  $F_2$  generation during *Kharif* 2023. Seedlings were transplanted on twenty-one days, with a single seedling per hill, while maintaining a spacing of 30 cm between the rows and 20 cm between the plants. The crop was grown adopting recommended agronomic practices. Qualitative characteristics like basal leaf sheath colour were individually assessed in the  $F_2$  segregants of cross III. Likewise, grain colour was observed in crosses II and III using a single panicle from each plant. Six yield attributing traits viz., days to first flowering (DFP in days), plant height (PH in cm), productive tillers per plant (NPT), panicle length (PL in cm), hundred seed weight (HSW in g) and single plant yield (GYPP in g) along with two physical grain quality traits, grain length (KL in mm) and grain width (KB in mm) were recorded from 380, 391 and 217  $F_2$  plants in crosses I, II and III, respectively.

The inheritance pattern for qualitative traits was assessed through the  $\chi^2$  (Chi-square) test (Fisher 1936). Shapiro-Wilks' W test was carried out to test the normality of the  $F_2$  populations using R software (Shapiro et al. 1968). Skewness and kurtosis were computed to understand the extent of the distribution pattern for yield and quality attributes in the segregating population by using SPSS Statistics version 29.0.2.0 (Snedecor and Cochran 1989). The Genotypic and Phenotypic Coefficient of Variation (GCV and PCV) were calculated as per the formula given by Burton, 1952. The broad sense heritability ( $h^2$ ) and genetic advance as a percentage of the mean (GAM) were calculated as per Lush (1940) and Johnson et al. (1955). Pearson's pairwise correlation among variables was computed to analyze their mutual linear relationship using the 'corrplot' statistical package in R software.

## Morphological confirmation



## Molecular confirmation



Note: L - Ladder (100bp); P1 - CO 55; P2 - IC 457996;

True F1s - 3,4,5,6,7,8,10,12,12,14,14,16

Figure 1 Hybrid confirmation using morphological and molecular markers

Table 1 Segregation pattern of the progenies for qualitative traits in F<sub>2</sub> generation

Basal leaf sheath colour							
Name of the cross	P <sub>1</sub> /P <sub>2</sub>	F <sub>1</sub> Phenotypes	Number of F <sub>2</sub> plants		$\chi^2$ ratio	$\chi^2$ value	p-value
			Purple	Green			
CO 55 × IC 115439	Green/Purple	Purple	119	98	9:7	0.18	0.6752
Grain colour							
Name of the cross	P <sub>1</sub> /P <sub>2</sub>	F <sub>1</sub> Phenotypes	Number F <sub>2</sub> plants		$\chi^2$ ratio	$\chi^2$ value	p-value
			Red	White			
CO 55 × IC 115439	White/Red	Red	175	42	13:3	0.05	0.8194
CO 55 × IC 464685	White/Red	Red	208	183	9:7	1.48	0.2236

## 3 Results and Discussion

### 3.1 Inheritance pattern of qualitative traits

True hybrids were identified by their distinct morphological characteristics, such as the pigmentation of basal leaf sheath in CO 55 × IC 115439 and grain colour in CO 55 × IC 464685 and CO 55

× IC 115439. All true F<sub>1</sub>s resulting from CO 55 × IC 115439 exhibited red grain colour and purple pigmentation in their leaf sheath (Figure 1). Likewise, in CO 55 × IC 464685 the true F<sub>1</sub>s had red grain colour. Besides conferring disease resistance, basal leaf sheath colour is an important morphological marker for distinguishing off types at an early stage. The segregation pattern of the progenies of the cross between green and purple pigmented



leaf sheath in the F<sub>2</sub> generation closely fitted to the 9:7 ratio ( $\chi^2 = 0.68$ ) (Table 1). The result herein emphasizes that two genes with complementary gene interaction jointly govern the expression of basal leaf sheath colour in rice (Pandey et al. 2016). Likewise, the proportion of plants exhibiting red and white grain colour in F<sub>2</sub> generation of the cross CO 55 × IC 464685 closely followed a 9:7 ratio ( $\chi^2 = 0.22$ ) (Table 1). Thus, it confirms that the red grain colour in rice is determined by digenic complementary gene interaction. Meanwhile, a segregation ratio of 13:3 (red:white) gave the best fit for grain colour in the cross CO 55 × IC 115439 ( $\chi^2 = 0.82$ ) (Table 1). This indicates that the red grain colour in the cross CO 55 × IC 115439 might be due to dominant suppression epistasis, i.e., two genes with an inhibitory effect jointly govern the expression of the trait (Waghmode et al. 2017).

### 3.2 *Per se* performance of yield-attributing traits

The *per se* performance of the studied traits in the F<sub>2</sub> segregants indicated a wide range of variation (Table 2, 3, and 4), providing ample opportunities to identify and utilize the most promising

segregants in future breeding programs. Days to first flowering in the F<sub>2</sub> segregants of the cross I (CO 55 × IC 457996) ranged from 75.00 to 114.00 days (Table 2), while it was from 76.00 to 105.00 days in cross II (CO 55 × IC 464685) (Table 3) and 79.00 to 117.00 days in cross III (CO 55 × IC 115439) (Table 4). Transgressive segregants with lower values than the early parent are desirable for days to first flowering. Nearly 20% of plants in cross I, 27.59% in cross II, and 5.53% in cross III were identified as early flowering compared to their parent CO 55 (86.4 days). Transgressive segregants with higher values than the high-yielding parent are desirable for yield-attributing traits. The transgressive segregants with higher value of productive tillers per plant were more in the F<sub>2</sub> generation of cross I (93 plants) followed by cross III (55 plants) and cross II (23 plants). Similarly, single plant yield in the F<sub>2</sub> segregants of cross I, varied from 8.97 to 74.52 g, while in cross II, it ranged from 8.11 to 61.96g and in cross III, it ranged from 10.08 to 61.86 g. The wide range of variation for these traits in all three crosses underscores the presence of transgressive segregation. The number of plants in F<sub>2</sub> that outperformed the mean single plant yield of parents was 176 in cross I, 116 in cross II, and 96 in cross III. Koide et al. (2019) indicated

Table 2 Genetic variability estimates of yield and quality attributes in the F<sub>2</sub> population of CO 55 × IC 457996

Traits	W-test	Probability	Mean	Range	Skewness	Kurtosis	PCV	GCV	h <sup>2</sup>	GAM
DFE	0.981	0.001	95.26	75.00 - 114.00	-0.08	-0.74	9.68	9.59	97.96	19.54
PH	0.968	0.000	147.11	70.00 - 200.00	-0.51	-0.26	15.23	14.81	94.56	29.66
NPT	0.968	0.000	14.15	5.00 - 28.00	0.55**	-0.12	35.18	30.99	77.61	56.24
PL	0.992	0.039	27.27	20.00 - 35.60	-0.03	-0.02	9.82	8.62	76.94	15.57
HSW	0.996	0.501	2.07	1.43 - 2.84	0.09	-0.05	11.96	11.22	87.97	21.68
KL	0.805	0.000	8.40	7.20 - 9.80	0.17	-0.28	6.61	6.54	97.74	13.31
KB	0.247	0.000	2.44	1.90 - 3.80	0.60**	1.52**	10.45	10.08	92.97	20.02
GYPP	0.963	0.000	34.27	8.97 - 74.52	0.70**	0.12	37.39	34.75	86.35	66.52

\*\*1% level of significance; \*5% level of significance; DFE - Days to First Flowering; PH - Plant Height (cm); NPT - Productive Tillers per plant; PL - Panicle Length (cm); HSW - Hundred Seed Weight (g); GYPP - Single Plant Yield (g); KL - Grain Length (mm); KB - Grain Breadth (mm); PCV - Phenotypic Coefficient of Variation; GCV - Genotypic Coefficient of Variation; h<sup>2</sup> - Heritability in broad sense; GAM - Genetic Advance as per cent of Mean

Table 3 Genetic variability estimates for yield and quality attributes in the F<sub>2</sub> population of CO 55 × IC 464685

Traits	W-test	Probability	Mean	Range	Skewness	Kurtosis	PCV	GCV	h <sup>2</sup>	GAM
DFE	0.965	0.000	91.30	76.00 - 105.00	-0.27	-0.22	6.21	6.01	93.82	11.99
PH	0.936	0.000	122.43	80.00 - 184.00	0.43**	-0.98	19.02	18.39	93.50	36.63
NPT	0.960	0.000	12.53	4.00 - 35.00	0.80**	1.77**	36.77	28.81	61.40	46.51
PL	0.973	0.000	26.08	19.00 - 37.00	0.52**	0.99**	10.17	8.32	67.05	14.04
HSW	0.939	0.000	1.76	1.26 - 2.55	0.99**	0.35	17.64	17.05	93.46	33.96
KL	0.972	0.000	8.41	7.00 - 9.60	-0.58	0.38	5.55	5.44	96.36	11.01
KB	0.984	0.000	2.35	1.40 - 3.50	0.11	-0.54	16.48	16.07	95.07	32.28
GYPP	0.908	0.000	28.78	8.11 - 61.96	0.52**	-0.76	38.53	34.06	78.14	62.03

\*\*Significance at 1% level; \*Significance at 5% level

Table 4 Genetic variability estimates for yield and quality attributes in the F<sub>2</sub> population of CO 55 × IC 115439

Traits	W-test	Probability	Mean	Range	Skewness	Kurtosis	PCV	GCV	h <sup>2</sup>	GAM
DFP	0.981	0.005	100.65	79.00 - 117.00	-0.34	-0.12	7.32	7.19	96.50	14.56
PH	0.976	0.001	138.82	90.00 - 184.00	-0.39	-0.40	13.99	12.70	82.38	23.75
NPT	0.972	0.000	12.28	4.00 - 28.00	0.58**	0.72*	34.73	30.18	75.52	54.04
PL	0.972	0.000	26.76	18.00 - 32.00	-0.40	0.48	8.42	6.75	64.24	11.14
HSW	0.972	0.000	2.05	1.12 - 2.95	0.18	1.40**	14.18	13.70	93.30	27.26
KL	0.980	0.004	8.29	7.10 - 9.80	0.33	0.37	5.04	4.97	97.37	10.10
KB	0.970	0.000	2.90	2.20 - 3.80	0.37*	-0.25	10.77	10.39	93.18	20.67
GYPP	0.980	0.004	31.01	10.08 - 61.86	0.45**	0.47	32.05	26.90	70.43	46.50

\*\*Significance at 1% level; \*Significance at 5% level

that transgressive segregation is more common in the F<sub>2</sub> population derived from parents with more proximal phenotypes. Among the obtained high-yielding F<sub>2</sub> segregants, 28 plants in cross I, 16 in cross II, and 4 in cross III were found to be high-yielding and early flowering. Therefore, the promising transgressive segregants thus identified offer significant potential for employing them in breeding programs for evolving short-duration high-yielding rice cultivars.

### 3.3 Skewness and Kurtosis

Shapiro-Wilks test (W-test) revealed that except for hundred seed weight in Cross I, none of the traits exhibited a normal distribution, suggesting the skewed nature of the segregating population (Table 2, 3, and 4). The nature of gene action governing any trait can be identified based on the sign of skewness and its distribution pattern (Fisher et al. 1932; Robson 1956). Cross I noticed significant positive skewness for productive tillers per plant, grain width, and single plant yield (Table 2). Similarly, in cross II, the traits productive tillers per plant, plant height, panicle length, hundred seed weight, and single plant yield (Table 3) were positively skewed (Figure 2, 3). Likewise, productive tillers per plant, grain width, and single plant yield in cross III were identified to have significant positive skewness (Table 4 and Figure 4). The skewed nature underscores the significance of complementary gene action in determining the expression of these traits. Thus, intensive selection is needed to improve the genetic gain of these traits, as mild selection could lead to slow progress (Riyanto et al. 2021; Bassuony et al. 2022). However, the non-significant values for skewness for the remaining traits in the crosses indicate the existence of additive gene action, implying that early-generation selection will be more effective for these traits. Kurtosis indicates the shape of the distribution curve, and it helps determine the number of genes governing the traits. The significant and positive kurtosis observed for traits such as grain width (in cross I), productive tillers per plant, panicle length (in cross II) as well as productive tillers per plant and hundred seed weight (in cross III) indicate their leptokurtic distribution. This suggests that only a few genes are involved in governing their expression. However, the

non-significant kurtosis values for the remaining traits in the crosses suggest a mesokurtic distribution, implying that a larger number of genes will likely determine these traits.

### 3.4 Estimation of variance component

Understanding the extent of genetic variability within breeding materials is essential for optimizing selection processes in any breeding program. Thus, understanding genetic parameters allows breeders to enhance the effectiveness of selection. For all traits investigated across the three crosses, the Phenotypic Coefficient of Variation (PCV) was consistently higher than the Genotypic Coefficient of Variation (GCV) (Tables 2, 3, and 4). However, a narrow difference between PCV and GCV in the F<sub>2</sub> segregants for all the studied traits signifies a pronounced genetic influence on the phenotypic expression with minimal environmental impact. In cross I, PCV values ranged from 6.61% (grain length) to 37.39% (single plant yield), while in cross II, it varied from 5.55% (grain length) to 38.53% (single plant yield). Likewise, in cross III, PCV values ranged from 5.04% (grain length) to 34.73% (productive tillers per plant). Similarly, GCV values in cross I varied from 6.54% (grain length) to 34.75% (single plant yield), while in cross II, they varied from 5.44% (grain length) to 34.06% (single plant yield). Further, GCV values in cross III varied from 4.97% (grain length) to 30.18% (productive tillers per plant). High GCV estimate (>20%) was observed for productive tillers per plant and single-plant yield in all the crosses. High GCV estimates indicate these traits' inherent high degree of variability, which could augur well for rice improvement programs (Riyanto et al. 2021; Kumar et al. 2023). Plant height, hundred seed weight, and grain width in all crosses displayed moderate GCV estimates (10% to 20%). Conversely, the low estimate of GCV (<10%) was observed for days to first flowering, panicle length, and grain length across all crosses. Low GCV estimates indicate the presence of a limited range of variability for these traits within the population (Thúy et al. 2022; Kalaivani et al. 2023; Kumar et al. 2023). Therefore, selection based on these traits is expected to be less effective.

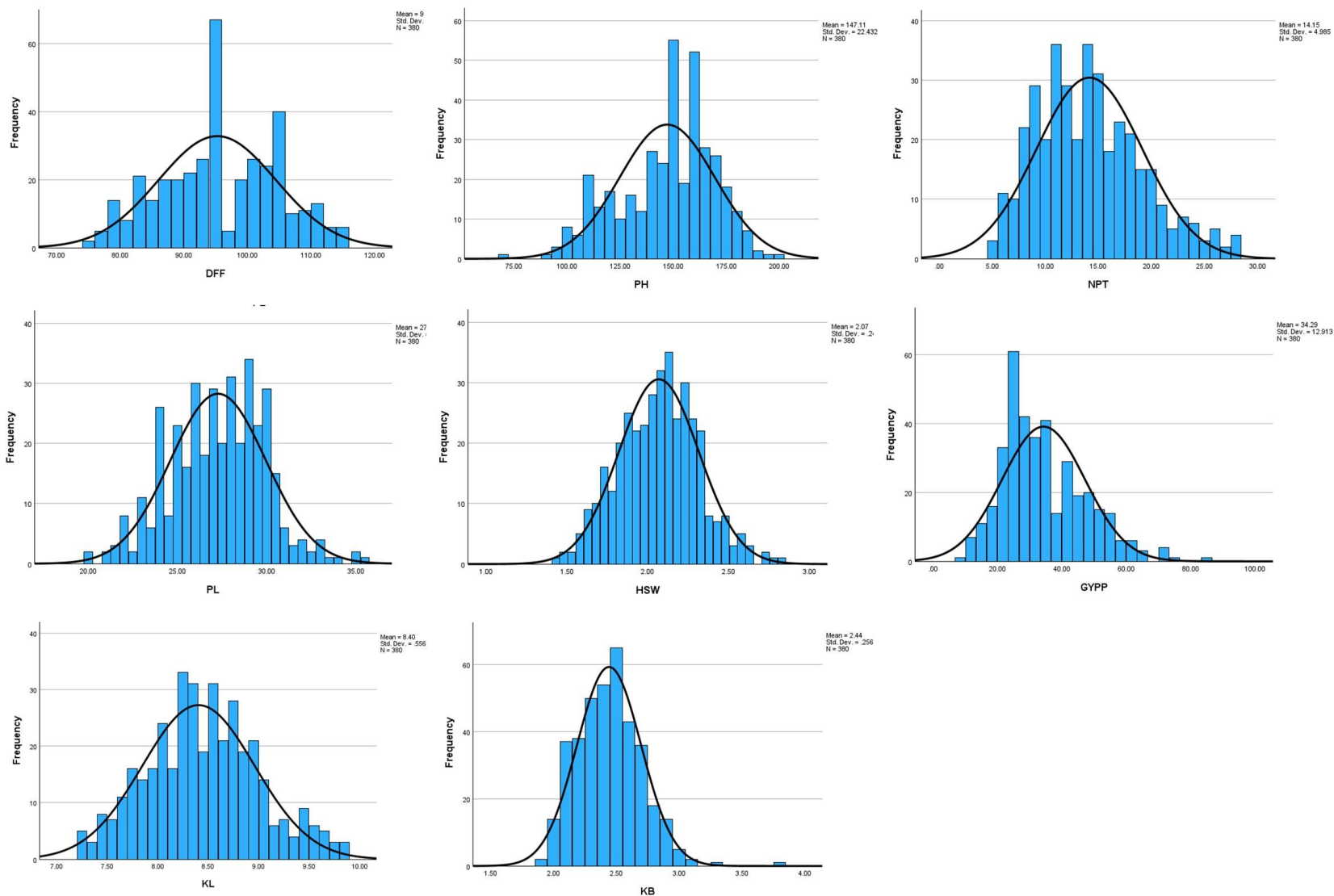


Figure 2 Distribution pattern of yield and quality attributes in the segregating population of CO 55 × IC 457996

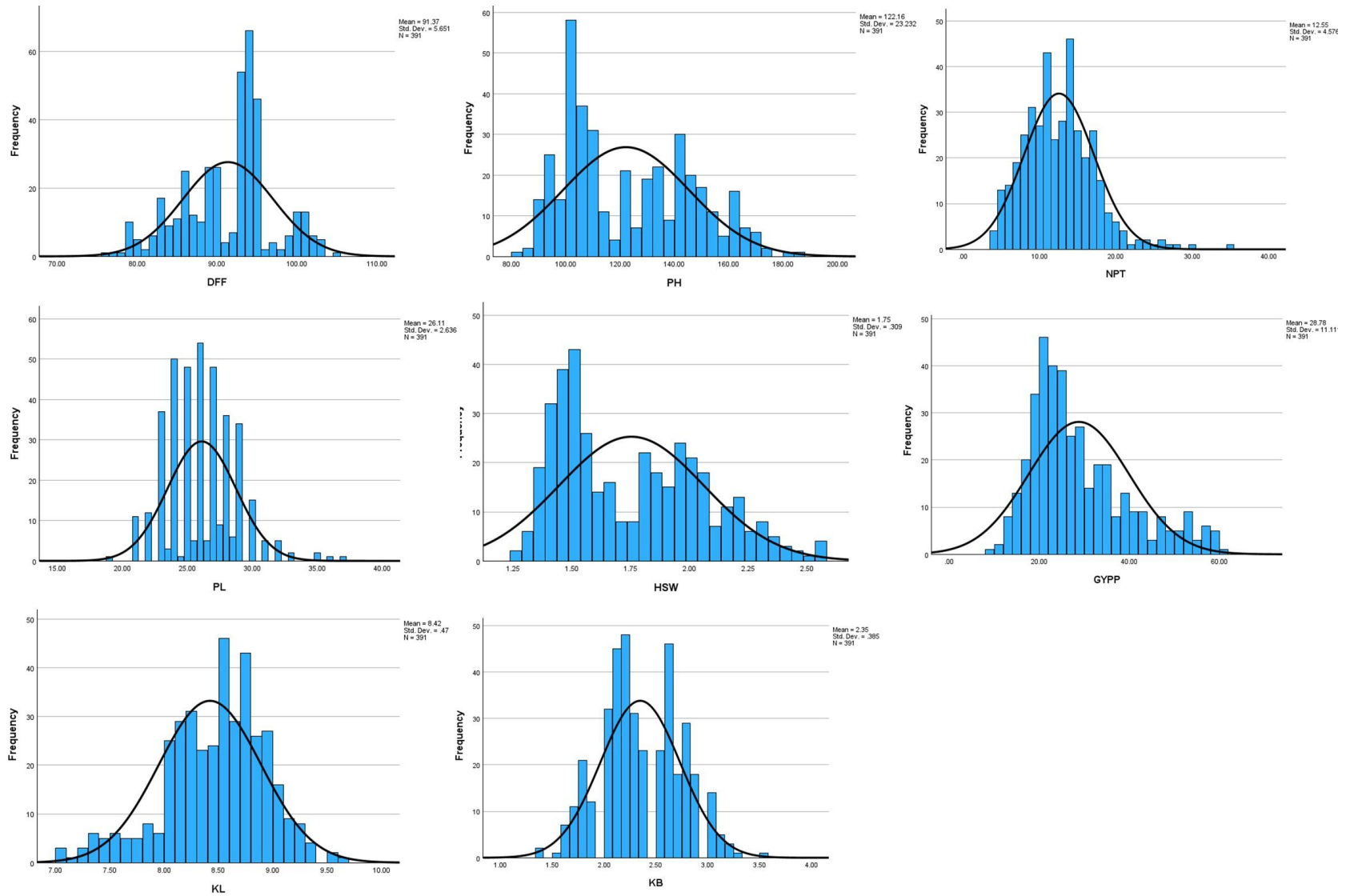


Figure 3 Segregation pattern of yield and quality attributes in the segregating population of CO 55 × IC 464685

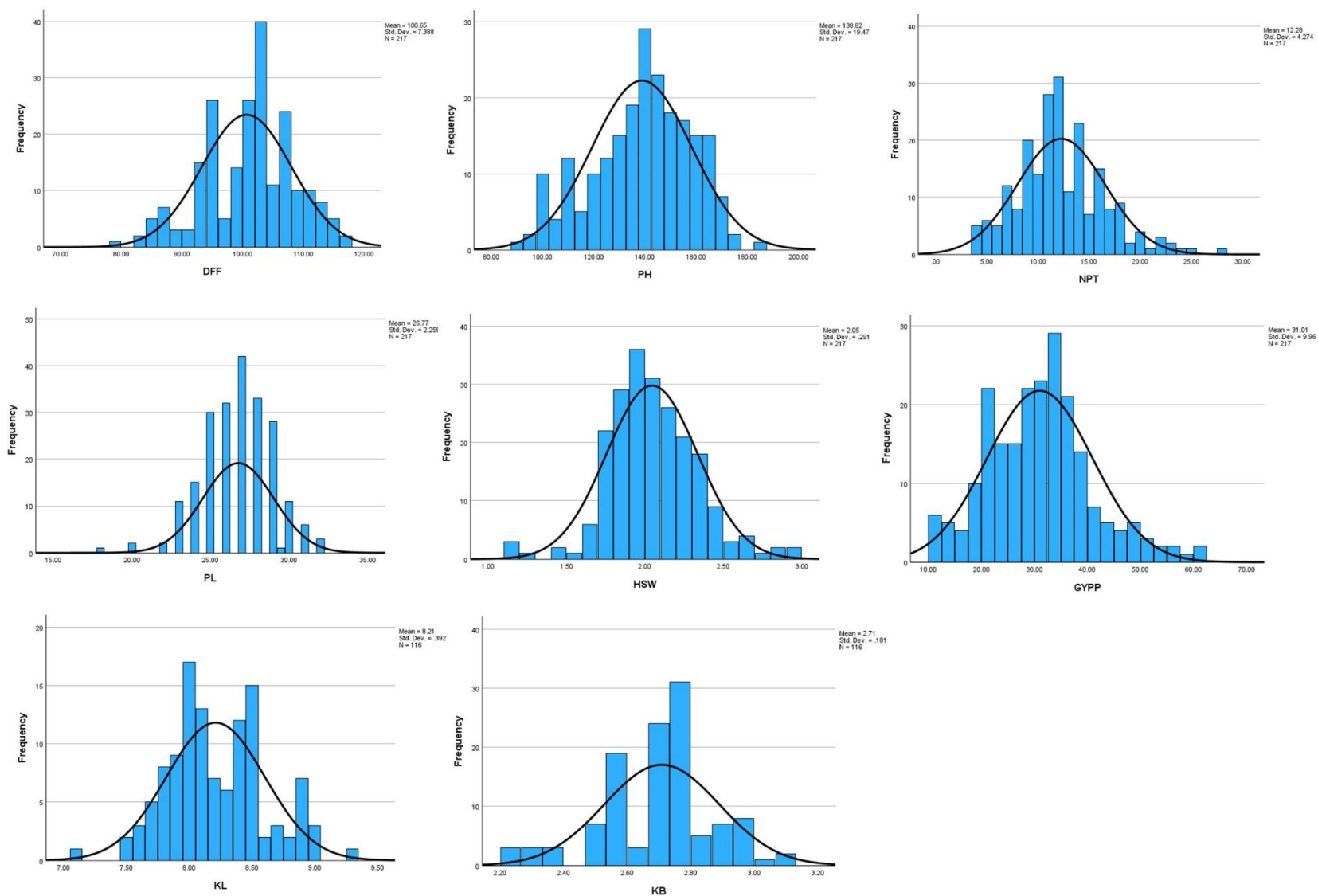


Figure 4 Segregation pattern of yield and quality attributes in the segregating population of CO 55 × IC 115439



### 3.5 Broad sense heritability and Genetic advance as percent of mean

Although GCV provides insights into the genetic variability present within the population, it alone does not suffice to ascertain the heritable portion of the variation. The efficiency of exploiting the residing genetic variability through selection depends upon the heritability of individual traits. In cross I (Table 2), broad sense heritability ranged from 76.94% (panicle length) to 97.96% (days to first flowering), with genetic advance as a percent of the mean (GAM) varying from 13.31% (grain length) to 66.52% (single plant yield). Similarly, in cross II (Table 3), heritability ranged from 61.40% (productive tillers per plant) to 96.36% (grain length), with GAM ranging from 11.01% (grain length) to 62.03% (single plant yield). In cross III (Table 4), heritability ranged from 64.24% (panicle length) to 97.37% (grain length), with GAM ranging from 11.14% (panicle length) to 54.04% (productive tillers per plant). High broad sense heritability ( $H^2$ ) observed for all the examined traits across three crosses suggests that environmental factors have minimal influence, with genetic factors predominantly governing these traits. Lestari et al. (2015) suggested that early-generation selection is possible for traits with high heritability as

genetic factors predominantly influence the plant phenotype. For effective selection, heritability in consonance with GAM could be useful in predicting the genetic gain under selection (Bassuony et al. 2022). Across all the crosses, high  $H^2$  (>60%) and GAM (>20%) were noticed for single plant yield, productive tillers per plant, plant height, hundred seed weight, and grain width. High broad sense heritability coupled with high GAM emphasizes that these traits are predominantly controlled by additive gene action, making them highly amenable to simple phenotypic selection (Prajapati et al. 2022; Kalaivani et al. 2023; Kumar et al. 2023). Furthermore, traits like days to first flowering, panicle length, and grain length exhibited high  $H^2$  (>60%) and moderate GAM (10% to 20%) across all the  $F_2$  segregants. High broad sense heritability coupled with moderate GAM emphasizes that both additive and non-additive gene action play a major role in determining their expression (Yaseen et al. 2020; Prathiksha et al. 2022; Kumar et al. 2023). However, the high heritability in these crosses might be due to environmental factors rather than genotype, rendering selection less rewarding. Consequently, enhancing the genetic gain of these traits can be achieved by intermating superior genotypes within the segregating population.

Table 5 Phenotypic correlation among yield and quality attributes in the segregating population

Traits	Cross	DFP	PH	NPT	PL	HSW	KL	KB
PH	1	0.33**						
	2	0.26**						
	3	0.24**						
NPT	1	0.01	0.24**					
	2	0.11	0.36**					
	3	0.03	0.08					
PL	1	0.37**	0.42**	0.01				
	2	0.23**	0.38**	0.23**				
	3	0.22**	0.38**	0.18**				
HSW	1	0.08	0.11*	-0.01	0.08			
	2	0.15**	0.50**	0.23**	0.11*			
	3	0.00	0.17**	-0.18**	-0.01			
KL	1	0.06	0.03	0.01	0.05	0.29**		
	2	0.06	-0.26**	-0.11*	0.05	-0.27**		
	3	0.13*	-0.08	0.05	-0.02	0.15*		
KB	1	0.04	0.02	-0.07	0.05	0.10	-0.54**	
	2	0.02	0.44**	0.20**	0.03	0.64**	-0.29**	
	3	0.04	0.04	0.04	0.04	0.02	0.13*	
GYPP	1	0.19**	0.42**	0.65**	0.21**	0.12*	0.07	-0.12*
	2	0.15**	0.49**	0.66**	0.20**	0.38**	-0.22**	0.34**
	3	0.43**	0.17**	0.87**	0.27**	0.18**	0.09	0.01

### 3.6 Correlation analysis

Correlation provides a better insight into the mutual relationship among the traits. Thus, a better understanding of their association with grain yield would make the selection more precise and accurate with the attributing traits as effective indicators in selection. Across all crosses, productive tillers plants (0.65, 0.66, and 0.87) exhibited a strong positive correlation with single plant yield (Table 5). Similarly, the traits *viz.*, plant height (0.42, 0.49 and 0.17), panicle length (0.21, 0.20 and 0.27), and hundred seed weight (0.12, 0.38 and 0.18) showed a positive significant association with single plant yield across all the crosses. These results herein show that more tillers might produce more panicles and increased synthesis and translocation of photo-assimilates from the source to sink could significantly improve yield through enhanced grain filling and seed set (Thúy et al. 2022; Kalaivani et al. 2023). In crosses I and II, days to first flowering and single plant yield showed a positive association (0.19 and 0.15). Likewise, within cross II, single plant yield positively correlated with grain width (0.34) while negatively correlated with grain length (-0.22). In general, selecting indicator traits can target high yield through potential traits directly. The results herein show that productive tillers per plant, panicle length, and hundred-seed weight can be indicator traits while selecting high-yielding segregants for grain yield improvement.

### Conclusion

The findings of this study emphasize that productive tillers per plant can be used as a reliable trait for direct selection when identifying high-yielding segregants for enhancing grain yield in rice as it exhibits high estimates for PCV and GCV, heritability, and GAM. The positively skewed distribution and leptokurtic nature of the productive tillers per plant suggests the involvement of a limited number of genes governing its expression, and thus, an intense selection from existing genetic variability could significantly enhance the genetic gain of this trait. Moreover, correlation analysis emphasizes that grain yield improvement in rice can be attained by indirectly selecting F<sub>2</sub> segregants with more productive tillers and longer panicles with high hundred seed weights.

### Conflict of interest

The authors declare no conflict of interest.

### References

Bassuony, N. N., Zsembeli, J., Juhász, C., & Elshenawy, M. M. (2022). Estimation of genetic variability and frequency distribution in F<sub>2</sub> generation of rice under normal and deficit water supply. *Cereal Research Communications*, 50, 489-500. <https://doi.org/10.1007/s42976-021-00185-7>

Bin Rahman, A. R., & Zhang, J. (2023). Trends in rice research: 2030 and beyond. *Food and Energy Security*, 12(2), e390. <https://doi.org/10.1002/fes3.390>

Burton, G. W. (1952). Quantitative inheritance in grasses. *Proceedings of Sixth International Grassland Congress, 1*, 277-283.

Fisher, R. A. (1936). The use of multiple measurements in taxonomic problems. *Annals of eugenics*, 7(2), 179-188. <https://doi.org/10.1111/j.1469-1809.1936.tb02137.x>

Fisher, R. A., Immer, F. R., & Tedin, O. (1932). The genetical interpretation of statistics of the third degree in the study of quantitative inheritance. *Genetics*, 17(2), 107. <https://doi.org/10.1093/genetics/17.2.107>

Johnson, H. W., Robinson, H. F., & Comstock, R. E. (1955). Estimates of genetic and environmental variability in soybeans. *Agronomy Journal*, 47, 314-318.

Kalaivani, A., Pushpam, R., Suresh, R., Raveendran, M., & Senthil, A. (2023). Genetic variability and association studies for yield and quality characters in BC<sub>3</sub>F<sub>2</sub> generation of rice (*Oryza sativa* L.). *Electronic Journal of Plant Breeding*, 14(3), 1118-1126. <https://doi.org/10.37992/2023.1403.134>

Khush, G.S. (2013). Strategies for increasing the yield potential of cereals: case of rice as an example. *Plant Breeding*, 132 (5), 433-436.

Koide, Y., Sakaguchi, S., Uchiyama, T., Ota, Y., Tezuka, A., et al. (2019). Genetic properties responsible for the transgressive segregation of days to heading in rice. *G3: Genes, Genomes, Genetics*, 9(5), 1655-1662. <https://doi.org/10.1534/g3.119.201011>

Kumar, M. B., Vidyadhar, B., Anuradha, C., Chary, D. S., Aravind, A., et al. (2023). Genetic Variability, Heritability and Genetic Advance in F<sub>2</sub> Segregating Population of Cross RNR-15048 x Dokra-Dokri in Rice (*Oryza sativa* L.). *International Journal of Environment and Climate Change*, 13(12), 965-972. <https://doi.org/10.9734/ijec/2023/v13i123760>

Lestari, A. P., Sopandie, D., & Aswidinnoor, H. (2015). Panicle length and weight performance of F<sub>3</sub> population from local and introduction hybridization of rice varieties. *Hayati Journal of Biosciences*, 22(2), 87-92. <https://doi.org/10.4308/hjb.22.2.87>

Lush, J. L. (1940). Intra-sire correlations or regressions of offspring on dam as a method of estimating heritability of characteristics. *Journal of Animal Science*, 1940(1), 293-301. <https://doi.org/10.2527/jas1940.19401293x>

Muthuvijayaragavan, R., & Jebaraj, S. (2022). Correlation and path coefficient analysis in F<sub>2</sub> families of rice (*Oryza sativa* L.) under

- direct seeded condition. *Journal of Genetics, Genomics and Plant Breeding*, 6(2), 44-53.
- Nofal, R. S., Bassuony, N. N., & Gaballah, M. M. (2024). Genetic Analysis to Improve Rice (*Oryza sativa* L) Grain Yield Attributes and Quality Traits. *Journal of Plant Production*, 15(4), 197-206. <https://doi.org/10.21608/jpp.2024.282761.1327>
- Pandey, D., Subedi, L. P., & Sharma, R.C. (2016). Inheritance of anthocyanin pigmentation in interspecific cross of rice (*Oryza sativa* L. × *O. rufipogon* Griff). *Azarian Journal of Agriculture*, 3(1), 17-21.
- Prajapati, M. R., Bala, M., Patel, V. P., Patel, R. K., Sushmitha, et al. (2022). Analysis of genetic variability and correlation for yield and its attributing traits in F<sub>2</sub> population of rice (*Oryza sativa* L.). *Electronic Journal of Plant Breeding*, 13(3), 983-990. <https://doi.org/10.37992/2022.1303.127>
- Prathiksha, R., Pushpam, R., Amudha, K., & Raveendran, M. (2022). Estimation of genetic parameters and character association for yield and quality traits in BC<sub>1</sub>F<sub>2</sub> population of rice (*Oryza sativa* L.). *Electronic Journal of Plant Breeding*, 13(2), 498-505. <https://doi.org/10.37992/2022.1302.091>
- Riyanto, A., Haryanto, T. A. D., & Hidayat, P. (2021). Genetic parameter and analysis of traits interrelationship in F<sub>2</sub> rice generation of Inpago Unsoed 1 X Basmati Delta 9. *American-Eurasian Journal of Sustainable Agriculture*, 15(1), 15-28.
- Robson, D. S. (1956). Applications of the k 4 statistic to genetic variance component analyses. *Biometrics*, 12(4), 433-444.
- Santhiya, S., Pushpam, R., Subramanian, A., Joel, A. J., & Senthil, A. (2024). Nature of gene action and combining ability effects for grain yield and quality traits in rice (*Oryza sativa* L.). *Electronic Journal of Plant Breeding*, 15(1), 11-20. <https://doi.org/10.37992/2024.1501.003>
- Shapiro, S. S., Wilk, M. B., & Chen, H. J. (1968). A comparative study of various tests for normality. *Journal of the American Statistical Association*, 63(324), 1343-1372.
- Snedecor, G. W., & Cochran, W. G. (1989). *Statistical methods*, Ames, IA: Iowa State University.
- Thúy, L. T., Vu, T. N., Pham, V. T., Nguyen, A. D., & Nguyen, T. K. (2022). Variability, correlation and path analysis for several quantitative traits derived multi-parent advanced generation inter-cross (Magic) F<sub>2</sub> population of rice (*Oryza sativa* L.). *International Journal of Scientific Research and Management*, 10(11), 356-363. <https://doi.org/10.18535/ijstrm/v10i11.ah01>
- Waghmode, B.D., Kore, A.B., Navhale, V.C., Sonone, N.G., & Thaware, B.L. (2017). Genetic Analysis of Promising Crosses and Good Combiners for Developing New Genotypes in Groundnut (*Arachis hypogaea* L.). *International Journal of Current Microbiology and Applied Sciences*, 6 (7), 324-331. DOI: <http://dx.doi.org/10.20546/ijcmas.2016.501.038>.
- Yaseen, S. M., Aananthi, N., Pillai, M. A., Shoba, D., Manikandan, K., et al. (2020). Genetic variability and frequency distribution studies for yield in OsPSTOL1 gene introgressed segregating populations of rice (*Oryza sativa* L.). *Journal of Pharmacognosy and Phytochemistry*, 9(3), 810-815.